INVESTIGATIONS INTO THE ANATOMICAL STRUCTURE AND DIFFERENTIATION RELATED GENE EXPRESSION IN THE DOG CLAW

by

Hayley Henderson (BSc Hons)

Doctoral thesis submitted in partial fulfilment of the requirements of the award

Doctor of Philosophy

Awarded by De Montfort University

Sponsored by IAMS

August 2007

ABSTRACT

The canine claw is a complex structure consisting of several cell types that undergo tissue specific differentiation. The aim was to study the anatomy and keratin expression within the canine claw. These studies showed that proximal canine claw was comparable to human nail and hair follicle. The claw fold contained several layers similar to hair follicle: outer root sheath (termed outer claw sheath: OCS), inner root sheath (inner claw sheath: ICS) companion layer (CL) and inner root sheath cuticle (ICS cuticle: ICScu). A thin cellular layer comparable to the hair and nail cuticle coated the surface of the claw plate was termed stratum externum (SE). Immunohistochemistry studies using human and mouse antibodies (K5, K6, K14, K16 and K17) showed that the OCS was K5, K6, K14, K16 and K17 positive and K6, K16 and K17 defined the CL. The claw plate comprised two macroscopic layers: stratum medium (SM) and stratum internum (SI). The SM was sub-divided into four layers (SM1-4), each generated from a different germinative region (GR) protected within the bony ungual groove of the distal phalanx. SM2 contained epithelial tubules, generated from the apex of GR2 papillae and ran the entire length of SM2. Tubule cells were K6 and K16 positive and provided the hard claw plate with plasticity. GR3 (expressing K5, K6, K14, K16 and K17 positive) and GR4 (K6 and K17 positive) lay over a thick mesenchyme (lunula) and produced SM3 and SM4 horn respectively. The SM4 produced a large K6 positive eosinophillic strip within the claw plate providing it with further flexibility which may allow independent movement between two 'hard' claw plate layers. The bony ungual process and longitudinal ridge (LR) decreased in size and shape in a distal direction and two additional layers (SI1 and SI2) were generated (GR5 and GR6 respectively) and filled the gap between claw plate and bone. GR5 cells were K6 positive but no keratin expression was found in GR6. Over the medial and lateral walls, the laminar GR9 produced a soft epithelium (termed sole 2: S2) to which the hard claw plate adhered. Three further sole layers (S1, S3 and S4) were identified and all expressed K5, K6, K14, K16 and K17. SDS-PAGE analysis of the claw plate showed protein bands within the hair-specific keratin (HSK) molecular weight range but HSK antibodies did not cross-react with canine tissue so the presence of these keratins within SM1-4 and SI1 and SI2 could not be confirmed.

ACKNOWLEDGEMENTS

I would like to thank Dr Paul E. Bowden (Department of Dermatology, Cardiff University) for his constant support all throughout my PhD. I am completely indebted to him for supervising this project and for the invaluable help that he unselfishly provided during my studies. He is a great friend and mentor. Also to his wife, Diana, who fed and watered me during my final week of the project and to whom I am extremely grateful.

I would like to thank the all the staff and students at the Department of Dermatology (Cardiff University) who were extremely friendly and helpful during my stay. Special thanks go to Dr Rebecca Porter for help with immunoblotting and Mr Steve Gaskell, who sadly and suddenly died during the course of this study, for his help with immunohistochemistry and imaging. He will be greatly missed.

I would like to thank Dr John Reilly for providing a veterinary opinion, a link to the canine samples required for the project and for organising the sponsorship to make this project possible. I also thank IAMS for their sponsorship money.

I would especially like to thank my parents, John and Lynne, for all the financial support and endless encouragement and understanding that they have provided me over the years. They are wonderful parents and I will always be extremely grateful for everything that they have done for me.

Finally, to all my friends and family who believed that I would finish this, especially my partner, Simon. I love you.

CONTENTS

LIST OF FIGURES

LIST OF TABLES

ABBREVIATIONS

ABC	**A**vidin **B**iotin **C**omplex
APES	3-**A**mino**P**ropyltri**E**thoxy**S**ilane
βME	**B**eta-**M**ercaptoethanol
BMZ	**B**asement **M**embrane **Z**one
BSA	**B**ovine **S**erum **A**lbumin
CASC	**C**itric **A**cid **S**odium **C**itrate
CE	**C**ornified **E**nvelope
CL	**C**ompanion **L**ayer
CTL	**C**onnective **T**issue **L**ayer
DAB	**Di**amino**b**enzidine
DP	**D**ermal **P**apilla
EBS	**E**pidermolysis **B**ullosa **S**implex
ECL	**E**lectrochemi**l**uminescence
EDTA	**E**thylene**d**iaminetetra**a**cetic Acid
DTT	**D**i**t**hiothreitol
GR	**G**erminative **R**egion
GM	**G**erminative **M**atrix
Ha	**H**air-Specific **A**cidic Keratin
Hb	**H**air-Specific **B**asic Keratin
HC	**H**air **C**uticle
He	**He**nley's Layer
H&E	**H**aemotoxylin and **E**osin
HF	**H**air **F**ollicle
HM	**H**air **M**atrix
HRP	**H**orse **R**adish **P**eroxidase
Hu	**Hu**xley's Layer
HSK	**H**air **S**pecific **K**eratin
ICS	**I**nner **C**law **S**heath
ICScu	**I**nner **C**law **S**heath **Cu**ticle
IF	**I**ntermediate **F**ilament
IHC	**I**mmuno**h**istochemistry

IFAP	**I**ntermediate **F**ilament **A**ssociated **P**rotein
IMF	**Im**munofluorescence
IRS	**I**nner **R**ooth **S**heath
IRScu	**I**nner **R**ooth **S**heath **Cu**ticle
K	**K**eratin
KDa	**K**ilodalton
LSAB	**L**abelled **S**trept**a**vidin **B**iotin
OCS	**O**uter **C**law **S**heath
ORS	**O**uter **R**oot **S**heath
PAGE	**P**olyacryl**a**mide **G**el **E**lectrophoresis
PEL	**P**rimary **E**pidermal **L**aminae
PVDF	**P**oly**v**inylidene **Di**fluoride
SDS	**S**odium **D**odecyl **S**ulphate
SEL	**S**econdary **E**pidermal **L**aminae
SEM	**S**canning **E**lectron **M**icroscopy
SM	**S**tratum **M**edium
SI	**S**tratum **I**nternum
S	**S**ole
TBS-T	**T**ris **B**uffered **S**aline – **T**ween 20
TEMED	N,N,N',N'-**Te**tra**me**thyleth**yle**ne**di**amine
TEM	**T**ransmission **E**lectron **M**icroscopy
TGRB	**T**op **G**el **R**unning **B**uffer

CHAPTER 1

1 REVIEW OF LITERATURE

1.1 INTRODUCTION

Skin appendages (hair, nail, hoof and claw) are derived from specialised epithelia that arise by targeted differentiation of cutaneous epidermal cells during development. The process of keratinisation in these epithelia is characterised by complex keratin expression combined with the expression of specific junctional and envelope proteins. Consequently, any disruption of this complex process can give rise to disorders of the skin and its appendages, leading to pathological disease.

Recently, advances in bioinformatics and biostatistics combined with information from the human and mouse genome projects have aided discovery of the molecular events underlying many genetic and metabolic disorders. This has ultimately accelerated drug therapy research (Van Ommen, 2002), leading to the development of new therapies and aided a better understanding of several dermatological diseases such as epidermolysis bullosa simplex (EBS) in humans (Sagoo *et al*, 2004; Schuilenga-Hut *et al*, 2002). The dog genome project is also underway and this will aid the development of better diagnosis and improved treatment of canine diseases and may also help to understand the genetic basis of diseases common to both humans and dogs.

Many of the major skin problems in dogs, including claw diseases, have been fairly well documented clinically (Boord *et al*, 1997; Bergvall, 1998; Olivery *et al*, 1998; Auxilia and Hill, 2000; Faergemann *et al*, 2001; Senter *et al*, 2002). However, the diagnostic approaches to claw diseases have still not been thoroughly investigated (Mueller *et al*, 2000; Scott *et al*, 1995) and a detailed molecular analysis of the claw is still absent from the literature. One reason may be due to a lack of detailed macro- and micro-anatomy of the canine claw. Furthermore, the publications that do exist, present a conflicting story regarding the anatomy of the claw and a uniform nomenclature of canine claw anatomy is

still elusive. With this in mind, the aim of this study is to provide a detailed analysis of the macro- and micro-anatomy of the canine claw using histological techniques and using the equine hoof, human nail and human hair follicle as comparable reference tools; the anatomy of which has been discussed in the review of literature. This knowledge will then be used to identify differentiation related gene expression within the dog claw, focussing principally on keratins. This will provide a basis for future canine claw disease research and ultimately lead to the development of new therapies for many canine skin and claw diseases.

1.2 Structure of Normal Skin and its Appendages

1.2.1 Skin Anatomy

The 'integument' or skin, is the largest and perhaps most complex organ of the body. Depending on the species and age, skin represents 12-24% of total body weight (Davenport and Reinhart, 2000; Tortora and Grabowski, 2000). Furthermore, the skin has many important functions, including forming a barrier to protect the organism from the environment, regulating temperature, producing protective pigment, synthesising vitamin D and playing a role in sensory perception (Galvin *et al*, 1989; Rao *et al*, 1996; Suter *et al*, 1997; Davenport and Reinhart, 2000). Anatomically, the skin consists of six structures (Figure 1.1): hypodermis, adipose fat, appendages (hair follicles, nails/claws, sebaceous and sweat glands), dermis, basement membrane and epidermis (Dyce *et al*, 1987; Watt, 1988; Suter *et al*, 1997). While some discussion of the dermis and basement membrane has been included, the epidermis and its appendages (hair, nail and claw) are presented in greater detail, as they are the focus of this thesis.

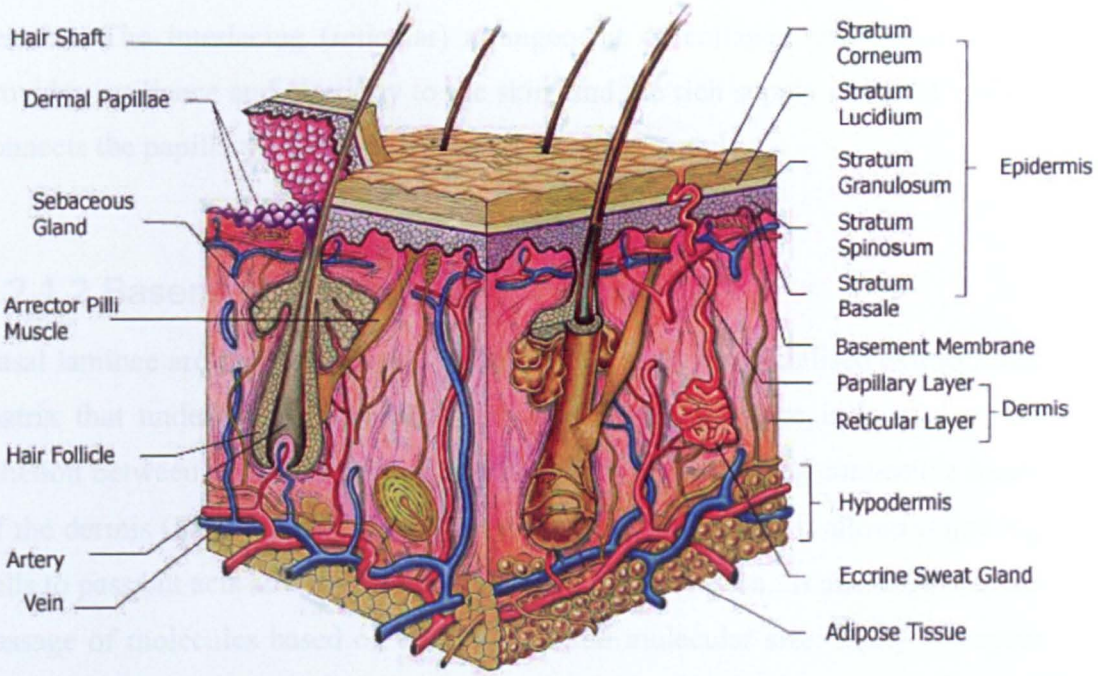

Figure 1.1: Structure of Human Skin

The general structure of skin is that of a stratified tissue comprising of four layers: The **epidermis** (which consists of a further five sub-layers: the stratum corneum, stratum lucidum (only observed in palmar-plantar skin), stratum granulosum, stratum spinosum and stratum basale). Beneath, the **basement membrane** attaches the epidermis to the underlying **dermis.** The dermis and **hypodermis** contain a complex combination of connective tissue (collagen and elastin) blood vessels, hair follicles, sebaceous and eccrine sweat glands as well as the deep lying adipose tissue which is a specialized connective tissue that functions as the major storage site for fat (adapted from url source: http://www.tarleton.edu/~anatomy/integpix1.html).

1.2.1.1 Dermis

The dermis, sometimes called the corium, is a connective tissue (mesenchyme structure) which supports, nourishes, and to some degree, regulates the rate of proliferation and differentiation of both the epidermis and its appendages (Suter *et al*, 1997; Hsieh and Lin, 1999). The dermis consists of a collagen and elastin matrix secreted by the fibroblasts contained within this matrix. It also contains an extensive vascular system necessary for the metabolic support of the avascular epidermis and for thermoregulation (Mulling, *et al*, 1999). The papillary dermis assists in the metabolic support of the epidermis by increasing the surface area, and therefore allowing greater exchange of nutrients with the epidermis which

occurs entirely by diffusion (Mulling *et al*, 1999; Aughey and Frye, 2001). The underlying papillary layer is reticular in nature and forms the major part of the dermis. The interlacing (reticular) arrangement of collagen and elastin fibres provides resilience and elasticity to the skin, and the rich supply of blood vessels connects the papillary layer to the network of blood vessels.

1.2.1.2 Basement Membrane

Basal laminae are flexible thin (40-120nm thick) mats of specialised extracellular matrix that underly all epithelia. This specialized structure is located at the junction between epithelial cells (epidermis) and the underlying connective tissue of the dermis (Figure 1.2A). Under physiological conditions, it allows migrating cells to pass but acts as a barrier against tumour cell invasion. It also regulates the passage of molecules based on their charge and molecular size. Many basement membrane ligands interact with cell surface receptors, influencing epithelial cell behaviour during morphogenesis, foetal development, and wound healing by regulating cell shape, proliferation, differentiation, and motility as well as gene expression and apoptosis (Timpl, 1996, Burgeson & Christiano, 1997, Smola *et al*, 1998; Erickson and Couchman, 2000; Ghohestani *et al*, 2001).

The basal lamina is largely synthesised by the cells that rest on it. Most basal laminae consist of two distinct layers: an electron-lucent layer (*lamina lucida* or *rara*) adjacent to the basal plasma membrane of cells that rest on the lamina (typically epithelial cells) and an electron-dense layer (*lamina densa*) just below. In some cases a third layer containing collagen fibrils (*lamina fibroreticularis*) connects the basal lamina to the underlying connective tissue. The term basement membrane is commonly used by some cell biologists to describe the composite of all three layers, which is usually thick enough to be seen in the light microscope.

The basement membrane also contains a specialised structure (Figure 1.2B), the hemidesmosome-anchoring filament complex, which ensures a stable connection between the dermis and epidermis (McMillan *et al*, 1998; Smola *et al*, 1998). Hemidesmosomes, or half desmosomes, resemble desmosomes morphologically but are both functionally and chemically distinct. Instead of joining adjacent

epithelial cell membranes, they connect the basal surface of epithelial cells to the underlying basement membrane. Moreover, whereas keratin filaments which associate with desmosomes make lateral attachments to the demosomal plaque, those that associate with hemidesmosomes appear to have their ends buried in the plaque. The hemidesmosome anchoring complex provides links between the intracellular cytoskeletal proteins of epidermal keratinocytes (keratins) and the connective tissue proteins of the dermis (collagen).

The internal plaque of the hemidesmosome consists of two plakin family proteins, plectin and BP230 (Favre *et al,* 2001). On the cytoplasmic side of the plaque, plectin and BP230 function as cross-linkers of the cytoskeletal filament network, binding them to the hemidesmosome plaque. On the plasma membrane side, the plaque proteins bind to transmembrane proteins, collagen XVII (BP180) and α6β4 integrin (Figure 1.2B), which anchors the plaque to the cell membrane.

The thread-like anchoring filaments of laminin 5 also connect to α6β4 integrin and BP180 on the other side of the cell membrane, anchoring them to the lamina densa, which is composed largely of collagen type IV and perlecan (Figure 1.2B). Anchoring fibrils composed of collagen VII then connect the lamina densa to the connective tissue of the dermis (collagen types I and III). Therefore, this structure physically connects keratin filaments in epidermal keratinocytes to the collagen fibres in the dermis.

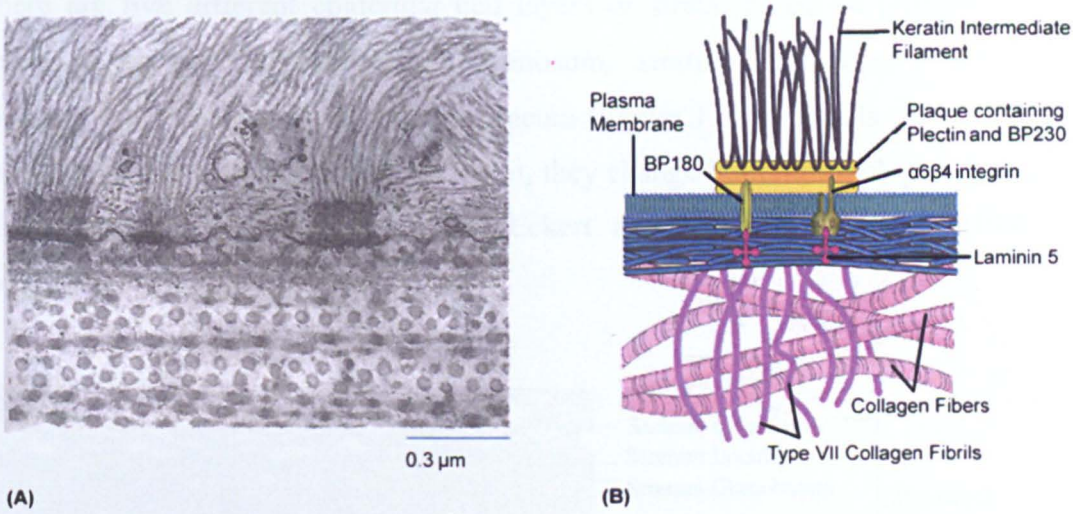

Figure 1.2: Hemidesmosomal anchoring complex and basement membrane zone.

(A) SEM of basement membrane showing the hemidesmosome anchoring epithelial cells to the basement membrane. **(B)** Cartoon of hemidesmosomal adhesion complex and basement membrane zone showing the different proteins which comprise it (adapted from url source: www.hykim.chungbuk.ac.kr).

1.2.1.3 Epidermis

The epidermis is a stratified squamous epithelium composed of several cell layers. The majority of cells forming the epidermis are keratinocytes, but melanocytes, Langerhans cells and Merkel cells are also present in small numbers (Galvin *et al*, 1989). The function of each cell type is detailed in Table 1.1.

Table 1.1: The Function of Different Cell Types in the Epidermis

Cell Type	Function
Keratinocytes	Protective barrier from environment
Langerhans Cells	Immune surveillance
Melanocytes	UV protection by production of pigment (melanin)
Merkel Cells	Transducer of fine touch stimuli

There are five different epidermal cell layers or strata, based on position and structure: stratum basale, stratum spinosum, stratum granulosum, stratum lucidum, and the superficial stratum corneum (Figure 1.3). As cells transit from the stratum basale to the stratum corneum, they change both morphologically and biochemically (Bowden *et al*, 1984; Eckert and Rorke, 1989; Watt, 1989; Wilkinson *et al*, 1989; Gibbs *et al*, 2000).

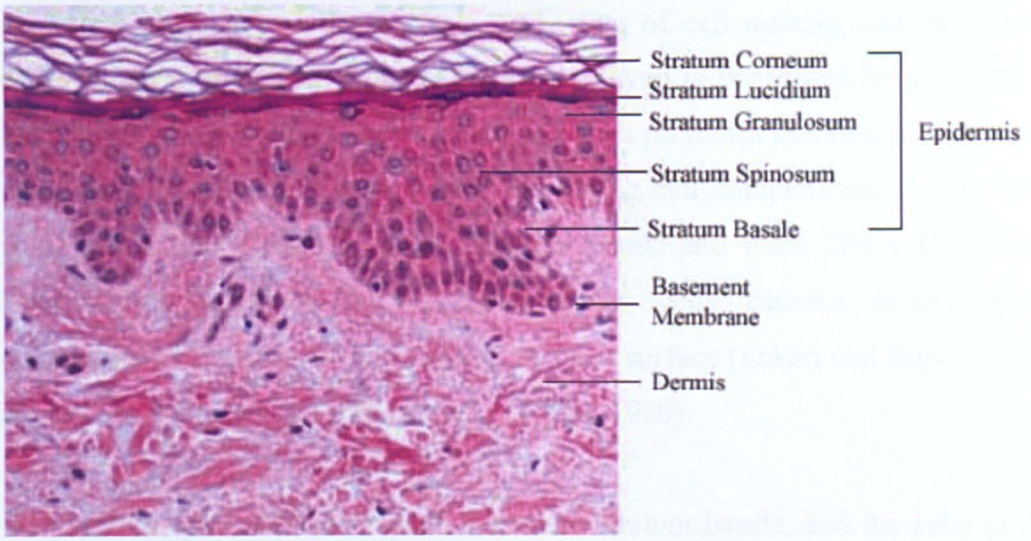

Figure 1.3: Layers of the Epidermis

Basal cells of the epidermis undergo morphological and biological changes during terminal differentiation. As a result, the epidermis can be divided into several layers depending on the cells location and structure; **Stratum Basale**, **Stratum Spinosum**, **Stratum Granulosum**, **Stratum Lucidum** (generally only seen in thickened skin), and the superficial **Stratum Corneum**.

Keratinocytes are the predominant epidermal cell type within the epidermis suggesting that their function within this structure is significant (Watt, 1989; Wilkinson *et al*, 1989; Suter *et al*, 1997). Keratinocytes synthesise structural proteins (keratins) which form an internal cellular cytoskeleton. This not only provides the keratinocyte with strength and rigidity but ultimately forms the body's first line of defence, the protective surface layer of the skin (Gibbs *et al*, 2000).

Basal cells are attached to the basement membrane via hemidesmosomes and have the capacity for DNA synthesis and mitosis (Fuchs, 1990). The basal layer contains two types of proliferative keratinocyte: stem cells, which have unlimited

self-renewal capacity and transit amplifying cells, which are destined to withdraw from the cell cycle and differentiate after a few rounds of division. Their attachment to the dermis is important, not only for the physical and mechanical integration of the epidermis, but also as a regulatory signal to restrain or trigger proliferation (Watt, 1989; Suter *et al*, 1997). The balance between proliferation and differentiation (homeostasis) is such that, for every new cell that is produced in the basal layer, a terminally differentiated cell is shed from the surface of the epidermis (Arnold and Watt, 2001). The rate of cell mitosis, and subsequent differentiation and maturation of the keratinocyte, is controlled by a variety of factors including c-Myc, a protooncogene, which promotes mobilisation of human epidermal stem cells into the transit amplifying cell compartment (Watt, 1988; Bikle and Pillai, 1993; Ponec *et al*, 1997; Arnold and Watt, 2001). Once basal keratinocytes have divided, some daughter cells become committed to differentiation and migrate outwards to the skin surface (Eckert and Rorke, 1989), a process called terminal differentiation (Watt, 1988).

The stratum spinosum lies superficial to the stratum basale, and the cells in this layer are larger than basal cells. Spinous cells are firmly bound to each other by desmosomes (junctional complexes that form between adjacent cells maintaining structure and rigidity). When the tissue is prepared for microscopy the cells shrink and the plasma membrane at these points stretches but remains firmly attached to its neighboring cell's membrane and the resulting morphology is said to be spinous; hence the name, stratum spinosum. Keratins interact with desmosomes in a similar way to their interaction with hemidesmosomes (Chu and Weiss, 2002). Such a highly interconnected type of cellular arrangement provides cohesion between epidermal cells, which serves to resist the effects of friction and abrasion and to minimise mechanical pressure by distributing such stresses over a larger area.

The stratum granulosum, so named because of abundant cytoplasmic keratohyalin granules and membrane coating granules, is intermediate in position between the stratum spinosum and the stratum corneum. Anatomically, keratinocytes in this layer are larger and still attached to surrounding cells by numerous desmosomes.

The stratum lucidum is only apparent in thick epidermis and represents a transition from the stratum granulosum to the stratum corneum. It is a translucent layer of extremely flattened cells that have no nucleus or cellular organelles. The epidermis varies in thickness throughout the body mainly due to frictional forces and is thickest on the palms of the hands and soles of the feet. As a result, the stratum lucidum is observed on the foot pads of dogs, but is insignificant or absent elsewhere on the body (Adam *et al*, 1970).

The stratum corneum consists of several layers of dead keratinocytes referred to as corneocytes (Gimeno *et al*, 2000). The corneocyte is not totally inactive metabolically but lacks a nucleus and cellular organelles (Watt, 1989). Elias (1991) likened corneocytes to bricks, which are bound by mortar in a model of stratum corneum structure. This connotation not only describes the protective function of the corneocyte, but also describes the extracellular lipid (mortar) which surrounds the corneocyte and provides a water resistant seal between the environment and the living cells of the organism. The corneocyte is further strengthened by a protein cornified envelope bound to the plasma membrane and this surrounds and protects the cell. The cornified envelope (CE) is an insoluble proteinaceous layer approximately 10nm thick and of uniform density (Jarnik *et al*, 1998) deposited subjacent to the plasma membrane. The constituent proteins become cross-linked by transglutaminase, which forms γ-glutamyl-ε-lysine isopeptide bonds and ultimately creates a permanent, stable, insoluble macromolecular protein complex. Cell biological, biochemical and protein sequencing studies have revealed that at least 20 proteins are used to assemble the CE but the two major components are involucrin and loricrin (Steinert and Marekov, 1997). The CE ultimately forms a uniform layer that serves as a template or scaffold for subsequent maturation or reinforcement stages of CE assembly (Steinert and Marekov, 1995 & 1999).

Once fully matured a combination of enzyme activity (trypsin and chymotrypsin like) and environmental wear and tear releases corneocytes from the surface of the skin (desquamation) and these are replaced by proliferating basal cells. This cycle of cell division, migration and desquamation forms the basis of epidermal homeostasis and this takes 21 days in the dog (Baker, 1974) and 28 days in man.

1.3 HAIR

Hair research has received much attention over the past 10 years after a period of very little progress. Advances in understanding hair structure and growth using murine hair growth models have helped define the mechanisms of hair growth control (Stenn, 1991; Stenn *et al*, 1996; 1998; Hardy, 1992; Paus, 1996; Philpott and Paus, 1998; Paus and Cotsarchis, 1999; McElwee *et al*, 2003; Porter *et al*, 2004). In particular, an ever increasing number of spontaneous or experimentally generated mouse mutations have provided invaluable insights into the functional significance of selected gene products in the control of hair follicle (HF) morphogenesis and cycling (Sundberg, 1994; Stenn *et al*, 1996; Paus and Cotsarchis, 1999; Philpott and Paus, 1998; Paus *et al*, 1999; Porter *et al*, 2004).

1.3.1 Hair Anatomy

The hair follicle develops from an ectodermal bud that grows into the underlying mesenchyme during embryogenesis (Dyce *et al*, 1987; Stark *et al*, 1987).

The major structural components of the hair follicle include the connective tissue layer or sheath (CTL), the dermal papilla (DP), the germinative epithelium (GE), the epithelial hair matrix (HM), the hair cortex (HC), the hair medulla (HM), the hair cuticle (HC), the inner root sheath (IRS) and the outer root sheath (ORS). The IRS has a further three sub-layers: Henle's and Huxley's layer and the IRS cuticle (Figure 1.4).

Hair production originates from proliferating germinative epithelial cells located in the hair follicle bulb, under control of the dermal papilla (Philpott *et al*, 1990). Complex cell signalling within the germinative cells of the hair follicle bulb undergo lineage restricted differentiation to give rise to at least six concentric rings of cells (Figure 1.4) which form the cortex and cuticle of the hair fibre as well as the cuticle, Henle's layer and Huxley's layer of the inner root sheath (Porter *et al*, 2004).

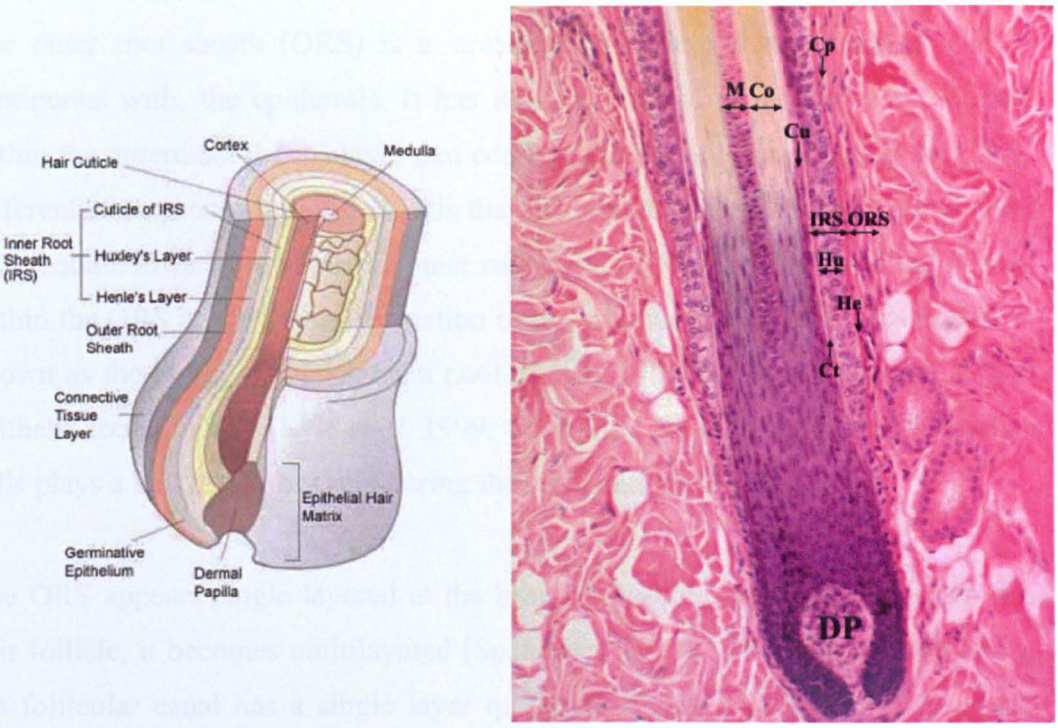

Figure 1.4: Structure of the Hair Follicle.

Cartoon of adult hair follicle structure (left), and a haematoxylin/eosin-stained section of the layers of the hair follicle (right): ORS, outer root sheath; IRS, inner root sheath; M, medulla of the hair shaft; Co, cortex of the hair shaft; He, Henle's layer of the IRS; Hu, Huxley's layer of the IRS; Cu, cuticle of the IRS; Ct, cuticle of the hair shaft; Cp, companion layer (cartoon adapted from url source: http://www.texascollaborative.org/hildasustaita/hairstructure.gif).

1.3.1.1 The Dermal Papilla (DP)

Located at the base of the mature hair follicle is the hair bulb, an expanded region containing rapidly proliferating epithelial-derived matrix cells. Associated directly below this is a cluster of mesenchyme-derived cells, which become surrounded by the expanded hair follicle bulb epithelium. This highly specialised fibroblast population, known as the dermal papilla (DP), controls production of the concentric cylindrical layers of the hair fibre via differentiation of matrix daughter cells (Paus and Cotsarelis, 1999). This mesenchymal structure is essential for hair growth and is probably involved in signalling the end of telogen and the induction of early anagen during the hair growth cycle (Paus and Cotsareus, 1999; Dewplewski and Rosenfield, 2000).

1.3.1.2 The Outer Root Sheath (ORS)

The outer root sheath (ORS) is a stratified epithelium that resembles, and is contiguous with, the epidermis. It has its own pool of progenitor cells located within the outermost (basal) layer that contacts the basal lamina. Within the ORS, differentiation proceeds along an axis that is parallel to the skin surface and cells differentiate inwards towards the inner root sheath (IRS). A local swelling occurs within the ORS at the point of insertion of the arrector pili muscle. This region is known as the bulge, and contains a pool of stem cells that can regenerate all the epithelia found in skin (Lyle *et al*, 1999, Costarelis, 2006). This pool of epithelial cells plays a key regulatory role during the adult hair cycle.

The ORS appears single layered at the base of the bulb, whereas further up the hair follicle, it becomes multilayered (Spearman, 1977). The region surrounding the follicular canal has a single layer of flattened cells located at the interface between the ORS and the IRS (Wang *et al*, 2003). These cells comprise the companion layer and are morphologically and biochemically distinct from both the IRS and ORS between which it lies. The companion layer was once considered part of the ORS, but the cells of the companion layer appeared to have more in common with the IRS than the ORS, as they contain gap junctions and desmosomes (Ito, 1986). Nonetheless, more recent data indicates that the companion layer is derived from hair bulb progenitor cells (Winter *et al*, 1998), confirming that the companion layer should be considered as the outermost layer of the IRS rather than part of the ORS (Porter, 2003).

The multi-layered structure of the ORS surrounds the IRS and an exchange of metabolites between the dermis and the growing hair fibre occurs, through these layers (Rogers *et al*, 1998).

1.3.1.3 The Inner Root Sheath (IRS)

The IRS is recognised as a three layer compartment located between the companion layer and hair shaft (Wang *et al*, 2003). Its keratinsed rigid tube structure not only protects the developing hair cuticle and cortical cells but it is

also thought to permit the smooth passage of the hair shaft by controlling the growth rate of the cortex and allowing clean separation of the IRS from the hair cuticle (Hashimoto, 1988). The IRS is made up of three concentric cellular layers. The outer most is Henle's layer, then Huxley's layer followed by the IRS cuticle which is physically interlocks with and supports the growing hair fibre. Henle's layer is usually one cell thick whereas Huxley's layer can be two or even three cells thick in larger hair follicles (Hashimoto, 1988). These layers of the IRS originate from the cells of the germinative matrix at the base of the hair follicle (Rogers, 1964).

The interaction between the IRS and growing hair fibre requires that the two structures must grow together inside the surrounding ORS. However, the cells of the IRS become degraded and dissociate into the hair follicle canal above the level of the sebaceous gland, leaving the hair fibre to emerge at the skin surface. As the IRS cells move up the follicular canal they differentiate forming a hardened filament matrix complex and all the cellular protein becomes insoluble. As keratinisation proceeds, the cell volume of the IRS is reduced by dehydration and degradation of the nucleus occurs. The cells start to form round granules of the protein trichohyalin which disperse throughout the cytoplasm. Trichohyalin is a structural protein found in the IRS and in the medulla of the hair fibre (Rothangel and Rogers, 1986) as well as in the granular layer of the epidermis, nail matrix and filiform ridges of the tongue (O'Keefe *et al.* 1993; Steinert *et al.* 2003). Due to its expression in many epithelial tissues which are hardened or toughened, it is thought that the role of trichohyalin is to provide mechanical strength to cells that need to withstand intense abrasion through physical stress (Steinert *et al.* 2003).

1.3.1.4 The Hair Shaft

The hair shaft is comprised of the hair cuticle, the hair matrix and cortex, and the medulla (Figure 1.5). A single type of progenitor cell, the matrix epithelial cell gives rise to all layers of both the IRS and the hair shaft; a significant occurrence given that each layer is the result of a distinct program of terminal differentiation. It is thought that the position of a matrix cell relative to the dermal papilla may

play a role in the choice of specific differentiation program under the control of various developmental genes and cell signalling pathways.

The cortex forms the bulk of the hair shaft and the component trichocytes (hair shaft epithelial cells) synthesise a complex mixture of structural proteins. The majority consist of keratin intermediate filaments (IF) proteins and keratin IF associated proteins (IFAPs). Wool research has provided much information concerning the keratinisation and ultrastructural organisation of hair (wool) fibres leading to the identification of two different types of cortical cells: paracortical and orthocortical (Rogers and Powell, 1993, Robbins, 2002). The difference between the two types of cortical cells can be distinguished by their morphology, as paracortical cells have a hexagonal pattern of intermediate filament packing whilst orthocortical cells adopt a cylindrical lattice formation.

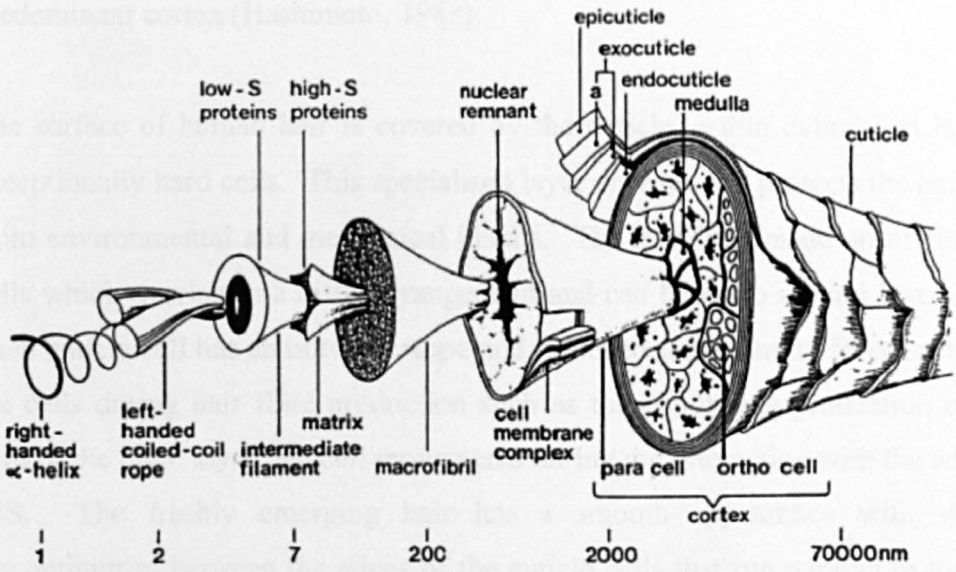

Figure 1.5: Schematic of a Human Hair Fibre

(Adapted from Marshall *et al*, 1991)

Cortical cells contain abundant keratin IF proteins that are spaced about 10 nm apart and occur in a matrix consisting of smaller keratin IF-associated proteins (IFAPs) which fill the spaces between them. Within the cortical cells, long fibrillar aggregates of IFs, termed macrofibrils, are orientated with the direction of growth and increase in size and abundance as the cells differentiate. The transverse sections of head hairs contain a ring of orthocortical-type cells, about

two or three cells thick, surrounding a core of paracortical-type cells. The spindle-shaped macrofibrils in human hair are approximately 40 to 200nm in diameter and extend the full length of a cortical cell. Each macrofibril consists of keratin IF's (originally called macrofibrils), with a diameter of approximately 7.5 nm.

The medulla consists of a column of cells centrally placed within the cortex of the hair fibre. In humans, the medulla is absent in vellus hairs where it appears to be only one cell thick, and is discontinuous in terminal scalp hairs. However, the medulla is much broader in thicker hair, such as human beard hair. After keratinisation, or degeneration of the hair shaft, a central air canal is left in the absence of the medulla which provides an insulating effect more often seen in animal fur. In human hair, this space is often very small and eventually disappears in the distal hair shaft or is interrupted under the pressure of the predominant cortex (Hashimoto, 1988).

The surface of human hair is covered by the cuticle, a thin cylindrical layer of exceptionally hard cells. This specialised layer encases and protects the hair fibre from environmental and mechanical insults. The cuticle is made up of flattened cells which overlap in a distal arrangement and can be up to several layers thick. Each cuticle cell has an outward slope and flattened shape due to forces acting on the cells during hair fibre production such as the continuing production of new cells at the basal layer and cell movements during the interaction with the adjacent IRS. The freshly emerging hair has a smooth appearance with shallow discontinuities between the edges of the cuticle cells that run parallel to the fibre axis. Environmental and mechanical processes (e.g. washing, brushing and combing) damage the hair and cause small fragments to chip away from the cuticle edges revealing a scaling pattern. This continual wearing process leads to a reduction in the number of cuticular cell layers and can eventually lead to exposure of the underlying cortex and fracture of the hair fibre.

1.3.1.5 Structure of Canine Hair

In many species, including mature dogs and cats, several hairs share a single follicle opening (Figure 1.6). The central (primary) hair is longest, while the surrounding (secondary) hairs are shorter and softer (Baker, 1974; Dyce *et al*, 1987). These compound hair follicles are slanted in relation to the surface of the skin. Al-Bagdadi (1979) reported that the primary and secondary hair follicles extend to different depths into the dermis. The larger hairs tend to extend more deeply than do smaller hairs (Figure 1.6).

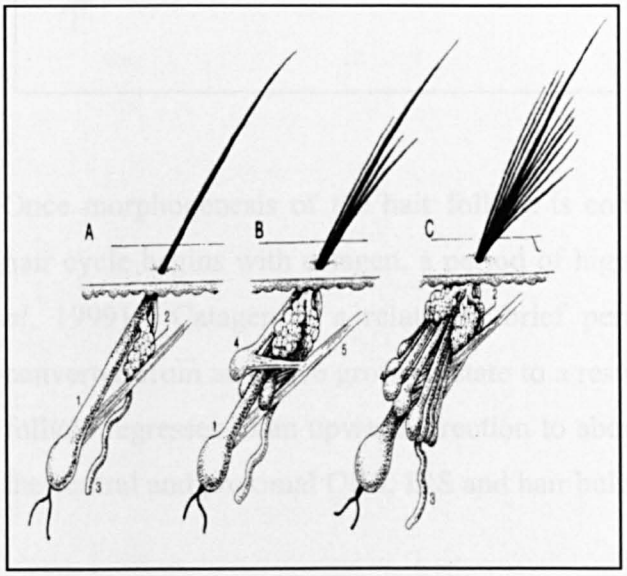

Figure 1.6: Hair Follicles of the Dog

A, Simple follicle present after birth. **B,** Follicle present during the first few months following birth. **C**, Complex follicle present in the adult; the primary hair is surrounded by several secondary hairs.

1, primary hair follice; **2**, sebaceous gland; **3**, duct of sweat gland; **4**, secondary hair follicle; **5**, arrector pilli muscle (adapted from Dyce *et al*, 1987).

1.3.2 Hair Growth

Three distinct stages of hair growth can be identified (Figure 1.7): an active phase (anagen) during which hair growth occurs, an intermediate phase (catagen) where the hair follicle regresses, and a resting phase (telogen) during which no cell proliferation occurs (Stark *et al*, 1987).

During anagen, the hair follicle is at its largest and the epithelial matrix (germ) cells surrounding the dermal papilla (DP), a specialised mesenchymal tissue, increase in number through epithelial-mesenchymal interactions. These epithelial cells then begin a complex program of proliferation and differentiation forming the different cell layers of the hair fibre and IRS.

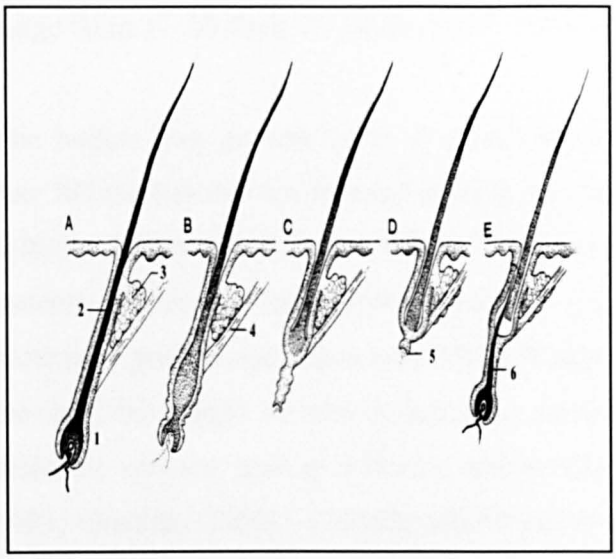

Figure 1.7: Stages of the Hair Cycle

A, Fully functional hair follicle, anagen phase. **B**, Follicle begins to atrophy, early catagen phase. **C**, Further atrophy of follicle, late catagen phase. **D**, Atrophied follice. Hair is displaced distally and new hair matrix begins to form, telogen phase. **E**, New hair matrix established and new hair begins to grow, early anagen phase. **1**- hair follicle; **2**- hair fibre; **3**- sebaceous gland; **4**- arrector pilli muscle; **5**- new hair matrix; **6**- new hair fibre (adapted from Dyce *et al,* 1987).

Once morphogenesis of the hair follicle is completed, initiation of the intrinsic hair cycle begins with catagen, a period of highly controlled involution (Stenn *et al*, 1999). Catagen is a relatively brief period during which the follicle is converted from an active growing state to a resting state. During this process, the follicle regresses in an upward direction to about one third of its full length with the central and proximal ORS, IRS and hair bulb matrix being lost.

After catagen, hair follicles enter a stable resting phase (telogen) during which no cell proliferation occurs (Stark *et al*, 1987). The telogen hair follicle is a complex mix of highly differentiated mesenchymal and epithelial cells comprising the secondary hair germ and epithelial stem cells from which a new anagen follicle develops. The rapid regression of anagen hair follicles can be thought of as a mechanism akin to entering an embryonic state capable of regeneration. Furthermore, a periodic return to the telogen state can be considered a defence against abnormal hair shaft production and may help to prevent derived skin cancers (Koch *et al*, 1998).

These phases are repeated continuously throughout life and the dynamics of each hair growth cycle can vary between different species and depend on follicle position and type. Thus, the duration of active growth (anagen) varies from

animal to animal. For example, in mouse, rat and human scalp hair, anagen can range from 17-20 days, 21-26 days and 7-8 years respectively (Butcher, 1951).

The human hair growth cycle is asynchronous, suggesting that each individual hair follicle has its own internal cycling mechanism, independent of adjacent hair follicles (Philpott and Paus, 1998). This is unlike many other mammals, such as rodents, where the hair growth cycle is synchronised and follows a specific pattern of growth and regression (Philpott and Paus, 1998; Paus *et al*, 1999). In the dog, the length of time required to complete the hair cycle varies between different species, and is different among breeds (Gunaratnam and Wilkinson, 1983; Credille, 2000). Credille (2000) stated that canine hair generally tends to grow to a preordained length and then enters a long period of telogen activity in which the hair follicle firmly retains the hair shaft. However, the length of time that the hair follicle remains in telogen appears to be a breed specific phenomenon (Credille, 2000). In some Nordic breeds, the hair appears to be held in a telogen state for years. In other breeds, such as Poodles, the hair cycle has a long anagen phase, and like humans, these dogs require haircuts. Gunaratnam and Wilkinson (1983) also noted that the rate of hair growth not only varied between individual dogs but also between different regions on the same dog. For example, growth rate was most rapid in the shoulder region followed by the flank and then the forehead region and was slightly more rapid in the shoulder and flank regions of some of the dogs tested during summer compared to winter, suggesting that seasonal variations in hair growth also occur.

1.4 CANINE CLAW

The hard, keratinised structure of the claw, which covers and protects the entire distal phalanx, has prehensile, offensive and defensive functions (Hamrick, 2002). It has been reported that nails have evolved from claws (Le Gros Clark, 1936; Thorndike, 1968; Schummer, 1981; Hamrick, 2001) but, unlike the human nail, the canine claw has received very little attention with regard to its structure and composition. In addition to this, the literature available on the canine claw is often conflicting and sometimes unreliable, often due to translation errors from foreign language papers. A review of the current canine claw literature is reported

below, and a detailed analysis of the macro- and micro- anatomy of the canine claw is described in Chapter 3.

1.4.1 Distal Limb of the Dog

The distal limb of the dog has developed through evolution to serve as part of the locomotor apparatus. The foot comprises four weight-bearing toes, each of which has a claw and a (digital) foot pad. There is, in addition to this, a metacarpal or metatarsal pad (Adam *et al*, 1970; Dyce *et al*, 1987). On the forepaw, a carpal pad and a fifth claw are seen, known as the dew claw but both structures have lost their use through evolution (Dyce *et al*, 1987). The digits are numbered in a lateral to medial direction, the forepaw digits numbered I to V and the hindpaw digits I to IV (Figure 1.8).

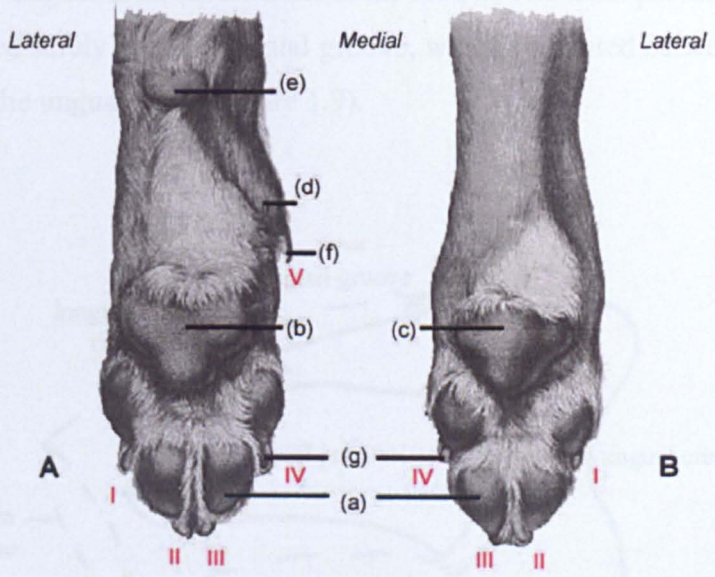

Figure 1.8: The Distal Limb of the Dog

Palmar and plantar views of the left fore (A) and left hind (B) distal limbs of a German Shepherd dog. (a) digital pad (b) metacarpal pad (c) metatarsal pad (d) digital pad of the dew claw (e) carpal pad (f) dew claw (g) claw (adapted from Schummer *et al*, 1981).

1.4.2 Canine Digit

1.4.2.1 Distal Phalanx

The distal phalanx is the bone which lies inside the horny part of the claw and the pointed, cone shaped part is known as the ungual process. This bone is curved along its long axis and generally resembles the claw in shape. Schummer *et al* (1981) reported that in dogs and cats, the dorsal convexity of the ungual process carries a longitudinal groove. This structure is known as the ruckenwulst (Budras and Seidel, 1992) or longitunal ridge (Bragulla *et al*, 2001). Bragulla *et al* (2001) suggested that the longitudinal ridge could be interpreted as the projection of one major bony lamina that acts to enhance the fastening of the horny claw to the dermal surface.

A thin shelf of bone forms a collar round the base of the ungual process. This is known as the ungual crest (Schummer *et al*, 1981). The most proximal part of the claw is housed safely into the ungual groove, which is located between the ungual process and the ungual crest (Figure 1.9).

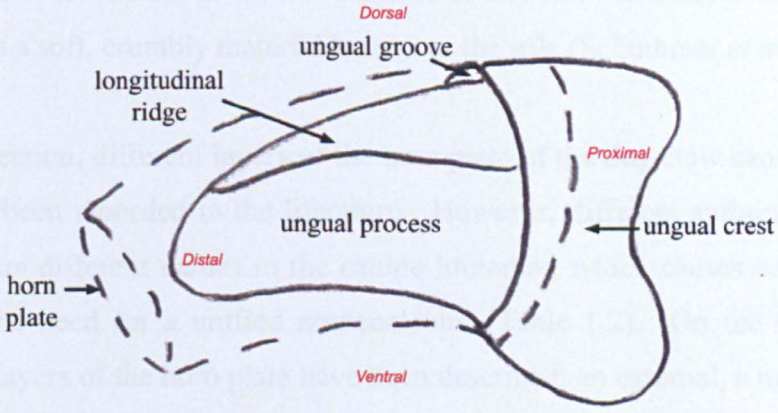

Figure 1.9: Distal Phalanx of the Canine Claw

The canine distal phalanx comprises of a long, pointed bone (ungual process) which sits inside a bone collar (ungual crest). The ungual groove is the gap created between the ungual process and the ungual crest. This houses the germinative region of the horn plate and protects it from external damage. The longitudinal ridge lies along the dorsal part of the ungual process and is thicker at the proximal end of the ungual process and narrows further down the bone. This structure is thought to provide an effective anchoring mechanism for the horn plate to the underlying phalanx and also to prevent rotation of the horn plate over the bone.

1.4.2.2 Claw Fold

The claw fold or vallum (Budras and Seidel, 1992) is where the skin attaches firmly to the ungual crest and to the base of the claw. The outer surface of the claw fold has hair bearing skin but the inner aspect of the claw fold is generally hair and gland free (Schummer *et al*, 1981).

1.4.2.3 Horn Plate

The hard, keratinised portion of the dog claw is the horn plate (Mueller, 1999). This has a smooth shiny surface and can be either darkly pigmented or bare little pigmentation at all (Schummer *et al*, 1981). Literature on the macro-anatomy of the horn plate is confusing with many different terms defining the same structure. For example, the horn plate has been referred to as the crown plate (Schummer *et al*, 1981), or wall (Dyce *et al*, 1987). Miller *et al* (1992) went a step further and broke down the horn plate into three different areas, the medial and lateral walls and the dorsal ridge. However, for the purpose of this thesis, this region of the claw will be referred to as the horn plate as this term best describes the properties of this structure. The horn plate does not entirely enclose the underlying distal phalanx and terminates on the ventral side of the claw forming a narrow fissure filled with a soft, crumbly material known as the sole (Schummer *et al*, 1981).

In cross section, different layers of the horn plate of the dog claw can be observed and have been recorded in the literature. However, different authors have given these layers different names in the canine literature, which causes confusion and stresses the need for a unified nomenclature (Table 1.2). On the whole, three different layers of the horn plate have been described: an external, a middle and an internal portion. The external layer covering the claw has been defined by various researchers and given at least four different names: periople or seam horn (Budras and Seidel, 1992), stratum externum (Schummer *et al*, 1981) and stratum tectorium (Mueller *et al*, 1993). It is understood that this layer forms a protective covering over the whole horn plate but is thought to be worn down and lost as the claw is used. Lying immediately beneath this is the middle layer which has been termed the superficial stratum (Le Gros Clark, 1936; Soligo and Muller, 1999),

crown horn (Budras and Seidel, 1992) and horny shell (Fowler, 1980). This layer makes up the bulk of the visible claw. The internal layer, which has been described as lying deep within the claw next to the distal phalanx, has been recognised by some authors and termed the wall segment (Budras and Seidel, 1992) or deep stratum/layer (Le Gros Clark, 1936; Soligo and Muller, 1999).

A more uniform nomenclature describing similar segments in the equine hoof has been suggested (Leach and Oliphant, 1983; Pollitt, 1992; Reilly, *et al*, 1996). Different segments of the equine hoof wall have been defined as stratum externum, stratum medium, and stratum internum. As similar structures have been recorded within the canine claw these terms have been adopted in this thesis to describe the different segments of the canine claw in an attempt to unify the equine and canine terminology.

Each of these different strata is thought to be produced from different germinative cells within the claw. Le Gros Clark (1936) and Schummer *et al* (1981) reported that the bed of the horn plate is comprised of two areas, the germinative matrix or proximal coronary bed, and the distal, extensive plate bed termed the sterile matrix (Figure 1.10).

The germinative matrix (GM), located at the proximal end of the claw, has been divided into a proximal region, housed within the ungual groove of the distal phalanx, and a distal region, located further down the claw (Figure 1.10). These have been termed basal and terminal matrix respectively (Le Gros Clark, 1936; Clark, 1971). The basal and terminal matrices have both been reported to consist of proliferative epithelial cells that produce a variety of differentiation products. For example, Clark (1971) proposed that the basal matrix produces the stratum externum whereas others believe that it generates the superficial layer (Le Gros Clark, 1936; Soligo and Muller, 1999). On the other hand, Schummer *et al* (1981) stated that the function of the claw fold consisted not only to protect the base of the claw, but where the "epidermal layer" is in direct contact with the horn plate it produces the stratum externum. Budras and Seidel (1992) imply that the basal matrix produces the stratum medium (or crown horn), but Clark (1971) proposed that the terminal matrix produced the stratum medium.

Le Gros Clark (1936) argued that distal to the terminal matrix, the claw rests on the sterile matrix, over the surface of which it glides forwards as growth occurs and new horn is produced in the proximal germinative matrix. Le Gros Clark (1936) also added that the sterile matrix is a thin epithelium no more than two cells thick and only produces a small amount of horn. This theory was supported by both claw and equine hoof scientists who state that the majority of horn plate is produced from the coronary region with only a small contribution of horn plate from the sterile matrix (Butler, 1992; Grosenbaugh and Hood, 1993 and Pollitt, 1998). Controversially, Budras and Seidel (1992) noted in their observations that the sterile matrix within the canine claw produced a large amount of horn and that the description of 'sterile matrix' is therefore groundless.

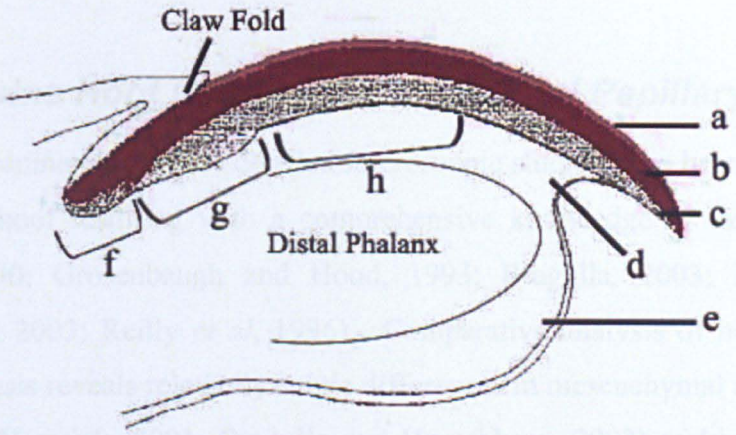

Figure 1.10: Old Terminology of Claw Anatomy

Schematic representation of a parasaggital section of claw. (a) stratum externum (b) stratum medium (c) stratum internum (d) sole (e) digital foot pad (f) basal matrix (g) terminal matrix (h) sterile matrix. Table 1.2 shows the differences in terminology between authors regarding the gross anatomical structures of the canine horn plate (adapted from Soligo and Muller, 1999).

Table 1.2: Various Terms for the Different Layers of the Canine Claw Horn Plate

Author	Stratum Externum (a)	Stratum Medium (b)	Stratum Internum (c)
Budras and Seidel (1992)	Perioplic Segment	Crown Segment	Wall Segment
Fowler (1980)	Periople	Horny Shell	-
Le Gros Clark (1936)	-	Superficial Stratum	Deep Stratum
Mueller *et al* (1989)	Stratum Tectorium	Medial/Lateral Walls and Dorsal Ridge	-
Schummer *et al* (1981)	Stratum Externum	Wall	-
Soligo and Muller (1999)	-	Superficial Layer	Deep Layer

1.4.3 Equine Hoof Comparisons – Dermal Papillary Body

Unlike the canine claw, more detailed microscopic studies have been achieved on the equine hoof resulting with a comprehensive knowledge of this appendage (Pollitt, 1990; Grosenbaugh and Hood, 1993; Bragulla, 2003; Bragulla and Hurschberg, 2003; Reilly *et al*, 1996). Comparative analysis of hoof and claw morphogenesis reveals relatively subtle differences in mesenchymal and epithelial patterning (Hamrick, 2001; Bragulla and Hurschberg, 2003) making the equine hoof a good comparative tool when studying microscopic detail of the canine claw.

The final shape and internal structure of the integumentary organs such as the claw and hoof are largely defined by the configuration of the dermo-epidermal interface which determines the three-dimensional arrangement of the overlying epidermal cells (Budras and Seidel, 1992; Bragulla and Hirschberg, 2003). This interface has an important influence on the mechanical properties of corneous structures, such as surface smoothness or roughness, pliability, resilience, resistance to abrasion, or transmissibility of mechanical stimuli. Papillae and laminae (collectively known as the papillary body) are dermal modifications that

provide a greater area for attachment of the horn plate to the underlying subcutaneous and bony structures as well as increase the dermal surface area in order to provide a better nutritional supply to the adjacent epidermal structures (Mulling, 1993).

Development of a dermal papillary body in the hoof/claw is segment specific meaning that different dermal regions of the digit form before others during foetal development and may adopt different dermal structures such as papillae or laminae (for review see Bragulla, 2003). The equine hoof has been divided segmentally into periople, coronet, wall and sole (Bragulla, 2003), which are homologous to those in the hooves of even-hoofed mammals like pigs or cows, in the feline and canine claw, and to those in the primate nail (Budras and Seidel, 1992; Hamrick, 2001; Bragulla, 2003).

Development of the segment-specific papillary body is initiated by an increase in mitotic activity within basal cells which invaginate the dermal surface, thus forming dermal micro-ridges. These micro-ridges can be transformed into single dermal papillae, which are arranged in rows, or enlarged to become primary and secondary laminae (Budras and Seidel, 1992; Bragulla *et al*, 2001; Bragulla, 2003).

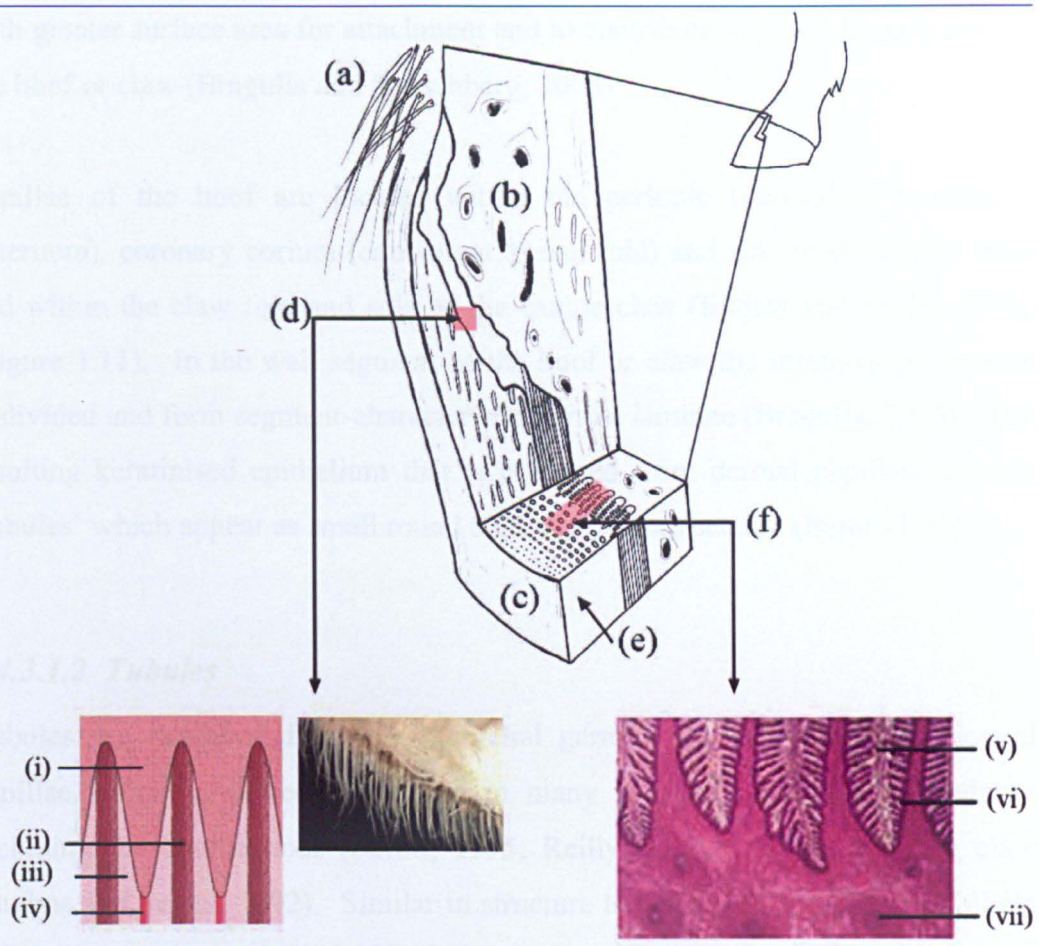

Figure 1.11: Papillae, Tubules, Laminae Structures in the Equine Hoof

Dermal papillae are finger like projections which bring about small tubular structures within the hard keratinised horn of hooves and claw. They aid in increasing the surface area of the mesenchyme for hoof attachment and allow penetration of nutrients in the growing hoof/claw. On the inner aspect of the hoof, leaf like structures known as laminae create a larger surface for contact between the horn plate and the underlying distal phalanx. Secondary laminae are added modifications to the primary laminae which also aid in increasing the surface area of the 'nail bed' of the claw/hoof. (a) hair at coronary border (b) bone of distal phalanx (c) external surface of hoof wall (stratum externum) (d) papillated germinative region in proximal hoof (e) stratum medium containing tubules (f) primary and secondary laminae (stratum internum) (i) dermal papillae (ii) intertubular horn (iii) cortex of tubular horn (iv) medulla of tubular horn (v) primary dermal lamina (v) secondary dermal lamina (vii) transverse section of horn tubule (adapted from Pollitt 1998).

1.4.3.1.1 Papillae

Embryonic formation of the dermal papillae starts on the dermal micro-ridges where distinct swellings occur. These swellings enlarge to form small dome-shaped papillae, which develop into cone shaped structures before forming finger like projections. As papillae originate on low dermal ridges (the remnants of the initial micro-ridges), they are arranged in rows to provide the resulting epithelia

with greater surface area for attachment and to contribute to pressure resistance in the hoof or claw (Bragulla and Hurschberg, 2003).

Papillae of the hoof are located within the periople (equivalent to stratum externum), coronary corium (equivalent to nail fold) and sole of the equine hoof and within the claw fold and sole of the canine claw (Budras and Seidel, 1992; (Figure 1.11). In the wall segment of the hoof or claw the micro-ridges remain undivided and form segment-characteristic dermal laminae (Bragulla, 2003). The resulting keratinised epithelium that is produced from dermal papillae contains 'tubules' which appear as small round artefacts in cross section (Figure 1.11).

1.4.3.1.2 Tubules

Tubules are produced from the epithelial germinative cells overlying dermal papillae which have been identified in many mammalian digital appendages including the equine hoof (Pollitt, 1995; Reilly *et al*, 1996) and canine claw (Budras and Seidel, 1992). Similar in structure to the medulla of the hair follicle (Pers. Observation), equine hoof tubules consist of a central medullary cavity that extends the length of the hoof wall. In the proximal hoof, the central medullary cavity of the horny tubule accommodates the dermal papillae (Figure 1.11). The cortex of the tubule is surrounded by keratinised epithelial cells, which gradually merge with the keratinised cells of the intertubular horn. The cells of the intertubular horn are continous with the epidermal cells between the papillae of the corium at the cornary band. The horn tubules are generated by the germinal layer of the coronary epidermis underlying the long papillae of the corium, whereas the intertubular horn is formed from the germinal epithelium, located between the tubular projections of the coronet. The relative density of the tubules within the hoof seems to vary across the inner hoof wall. This differential density in hoof wall tubules may be related to the different mechanical properties of the hoof wall, which vary according to the demands across the hoof wall and the pressure placed on different hoof regions. The tubules of the stratum medium have long been thought to contribute to significant mechanical dampening of the hoof wall during locomotion (Reilly, *et al*, 1996,). However, the mechanical functioning of the hoof wall may not be as simple as the "load bearing elements"

of the hoof, but may be related to the ability of the fibres to reinforce the hoof wall against propagation of any cracks in the long axis of the hoof. Other functions of the hoof wall tubules, such as water conduction and temperature insulation, may also be important.

In the canine claw, tubules may not be an important feature with respect to the weight bearing potential of the claw. The foot pads of the paw are the main weight bearing structures in the dog and therefore, a loss in tubular structure within the claw may have occurred through evolution. The tip of the claw is essential during digging and for break-over, where the claw is in intermittent contact with ground during locomotion and this can put a high load on the tip of the claw (Mattheck and Reuss, 1991). Dissipation of this load is needed in order to avoid damage to the proliferative region of the claw and it has been suggested that the horn tubules are constructed in such a way that they offer strong resistance to compressive and bending forces. The tubules within the stratum medium may act to dissipate such forces induced through break-over or digging.

Budras and Seidel (1992) state that there is development of horn tubuli produced from the terminal matrix within the crown horn of canine claw, but no tubular structure is present within the stratum internum. They also observed that the tubular structure within the stratum medium of the canine claw was not apparent at the distal tip. They observed transverse claw sections and found that tubules in the proximal part of the claw are large and round, but as the horn plate grows distally the tubules become more triangular, then oval and finally become indistinct before disappearing completely.

1.4.3.1.3 Laminae

In the equine hoof the innermost layer, the stratum internum is non-pigmented and tubule free consisting of keratinised laminae and non-keratinised secondary laminae that interdigitate with congruent structures of the corium in a plane perpendicular to the papillae. These primary epidermal laminae (PEL) serve to unite the inner hoof/claw wall and the distal phalanx through collagen fibres, and supply the hoof with tensile properties (Bragulla and Hirschberg, 2003). There

are approximately 600 PEL around the perimeter of the equine hoof wall that suspend the distal phalanx, and each PEL has about 100 secondary epidermal laminae (SEL). This arrangement increases the surface area immensely, which in turn, may serve to reduce the tension per unit area on the inner hoof.

Laminae have been observed on the inner aspect of the horn plate in the canine claw and were described as ridge like depressions (Schummer *et al*, 1981; Budras and Seidel, 1992).

1.4.3.1.4 White Line

Where the sole and horn meet in distal hoof and claw (Figure 1.12), papillae (terminal papillae) arise from the distal ridge of the primary dermal laminae (Budras and Seidel, 1992; Budras *et al*, 1998). The stratum basale of the terminal papillae differentiates to form an epithelium known as terminal horn (tubules and inter-tubular horn) which fills the space between neighbouring epidermal laminae. This epithelium contributes to a thin layer within the hoof known as the white line, or *zona alba* due to its non-pigmented appearance. It can be observed on the weight bearing surface of the equine hoof as a thin pale strip between the horn plate (stratum internum) and the sole. According to Bolliger (1991), terminal horn tubules contribute to approximately 85% of the white line in the equine hoof. Another zone (called cap horn) is situated peripheral to the terminal horn and adjacent to the stratum internum. Cap horn is derived from horn production along the laminar region of the hoof wall (Figure 1.12). Bolliger (1991) stated that both terminal horn and cap horn be used to describe the white line which would make for easier comparative studies in other species. Thus, the white line should not be viewed as a narrow line or a completely white structure.

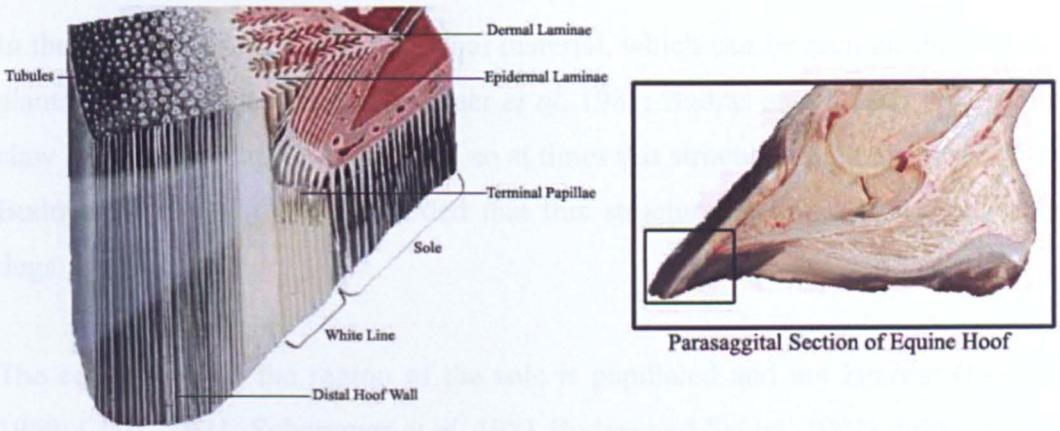

Figure 1.12: Location of the White Line in the Equine Hoof

The white line lies on the ventral surface of the hoof between both horn plate and sole material. **Terminal papillae** arise from the distal ridge of the primary dermal laminae and generate an epithelium known as **terminal horn.** This horn consists of tubules and inter-tubular horn and is also non-pigmented giving rise to the term 'white line'. **Cap horn** also comprises approximately 15% of the white line structure and is situated peripheral to the terminal horn and adjacent to the Stratum Internum. Cap horn is derived from horn production along the laminar region of the hoof wall and is not always non-pigmented (Adapted from Pollitt, 1996).

The function of the white line is thought to provide some independent movement between the wall of the hoof and the sole (Reilly *et al*, 1997; Bragulla *et al*, 1998). It is of great clinical significance as a barrier against ascending bacterial invasion of the hoof, as observed in white line diseases. Although Budras and Seidel (1992) did refer to the '*zona alba*' in their canine claw studies there is still very little literature on whether the white line exists in the canine claw and if this structure is comparable to that in the equine hoof.

A similar structure has been identified within the human nail as a pale line traversing the nail near the tip and has been termed onychocorneal band or junction (Sonnex *et al*, 1991). Clinical and histoloigical studies have revealed that this band is present in more than 90% of normal adult fingernails and represents the most proximal point of attachment of the fingertip stratum corneum to the nail plate. It is thought that is has the same purpose as the white line of the canine claw and equine hoof by providing a major barrier to foreign material passing proximally beneath the nail plate (Sonnex *et al*, 1991).

1.4.3.2 Sole

In the dog, the sole is a soft epithelial material, which can be seen on the palmar-plantar aspect of the claw (Schummer *et al*, 1981; Budras and Seidel, 1992). The claw horn may encapsulate the sole, so at times this structure is not always visible. Budras and Seidel (1992) recorded that this structure was soft and crumbly in dogs.

The corium within the region of the sole is papillated and not laminar (Dobler, 1969; Clark, 1971; Schummer *et al*, 1981 Budras and Seidel, 1992) unlike that of the feline claw (Bragulla *et al*, 2001). However, it has also been suggested that no tubular structures are produced within the keratinised sole material of the canine claw (Budras and Seidel, 1992; Scummer *et al*, 1981) whereas, tubules have been identified within sole material of the equine hoof (Pollitt, 1998).

1.4.3.3 Foot Pads

The foot pads of the dog are characterised macroscopically as having a thick but soft and elastic keratinous layer and a tall papillary body (Schummer *et al*, 1981; Lansdown, 1985), providing the foot pad with shock-absorbing properties.

Histological examination of the foot pad reveals the dermis to be extremely undulating so the surface of the foot pad is covered in small finger like ridges. A similar profile is also seen in human palmar-plantar skin such as the heel but their undulations are not as great. Hamrick (1998) stated that the papillary ridges serve not only to improve the frictional properties of the digital skin but also to increase the skin's sensitivity to tactile stimuli.

Numerous apocrine tubular glands can be observed in histological sections of the foot pad, which are thought to act as additional scent or marker organs (Schummer *et al.* 1981) but there are no hair follicles present in the foot pad making this structure free of hair.

1.4.4 Human Nail, Human Hair and Canine Claw Comparisons

One of the characteristic features of primates is the possession of fingernails and toenails (Le Gros Clark, 1936). These are homologous to the claws of most other mammals, but unlike claws, nails are flattened, almost straight in their longitudinal axis and camber transversely (Figure 1.13). The evolution of the nail seems to have been associated with changes in the locomotor habits of primates away from movement along large diameter trunks and branches where claws provide excellent grip, to locomotion along smaller diameter branches and twigs (Hamrick, 1998). Grip on such supports was improved by the development of broad apical pads and epidermal ridging (fingerprints) and the change from claw to nail probably happened at the same time. Thus, anatomically, the human nail appears as a very basic form of the claw and past research on the nail will be used in this study for comparative work.

Similar to the hoof and claw it is thought that human nail is composed of three layers of keratinous tissue: dorsal, intermediate and ventral layer (Zook, 1980; Reardon *et al.* 1999; Bragulla, 2003, Farren *et al.* 2004). The narrow dorsal layer is positioned along the surface of the nail plate and is also positioned along the lateral fold. The harder intermediate layer is located along the proximal nail bed up to the end of the lunula, while the narrow ventral layer can be observed towards the middle of the nail bed/sterile matrix (Reardon *et al.* 1999). Towards the tip of the nail bed the protective hyponychium, which seals off the gap between the nail and finger, is produced (Farren *et al.* 2004). Laminae have also been identified within the human nail, existing post lunula and extending to the nail tip, confirming the presence of micro-ridges during foetal development and supporting the theory that nails may have evolved from claws (Bragulla, 2003).

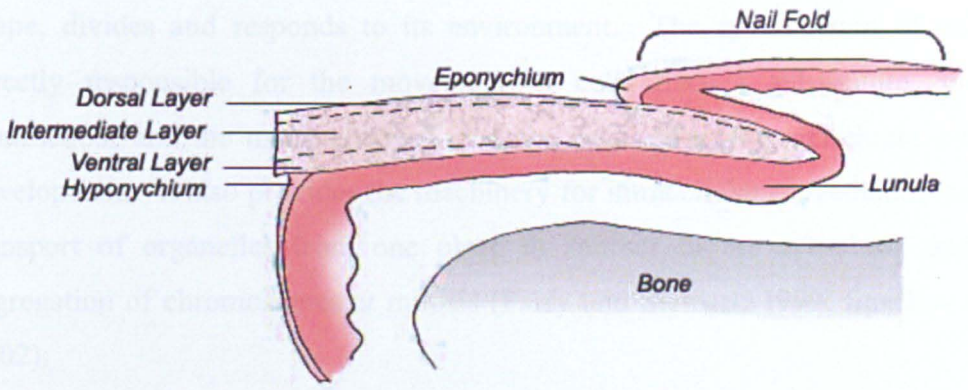

Figure 1.13: Anatomy of Human Nail

The human nail plate is thought to have three layers; Dosral layer, intermediate layer and ventral layer. In the proximal part of the nail, the nail plate rests on a thickened dermal layer known as the lunula. The eponychium acts as a skin plug in the region of the nail fold whereas the hyponychium acts to fill in the gap between the nail plate and the digit pad of the finger.

A similarity between hair and nails has been suggested as they are both derived from the embryonic ectoderm. Achten (1968) noted that the nail unit was comparable in some respects to a hair follicle, sectioned longitudinally and observed on its side. The hair bulb was considered analogous to the intermediate nail matrix and the cortex to the nail plate. The nail unit could be seen as an unfolded form of the hair follicle producing a hair with no cortex, just a hard cuticle. Scanning electron microscopy (SEM) of the nail confirms that its structure is more similar to compacted cuticular cells than cortical fibres.

1.5 The Cytoskelton

The diverse activities of the cytoskeleton depend on three types of protein filament (Steinert *et al*, 1993) composed of actin containing microfilaments, tubulin containing microtubules, and intermediate filaments (IFs), so named because their 10-15 nm diameter is intermediate between that of microfilaments (6nm) and microtubules (23nm).

The ability of eukaryotic cells to adopt a variety of shapes and carry out coordinated and directed movements depends on a complex network of protein filaments that extend throughout the cytoplasm. This network is called the

cytoskeleton, which has the ability to reorganise continuously as the cell change shape, divides and responds to its environment. The cytoskeleton of cells is directly responsible for the movement of cells over a substratum, muscle contraction, and the many changes in shape required during vertebrate embryo development. It also provides the machinery for intracellular movements, such as transport of organelles from one place to another in the cytoplasm and the segregation of chromosomes at mitosis (Parry and Steinert, 1999; Strelkov *et al.* 2002).

The IF superfamily comprises of more than 50 proteins that are expressed in a cell type specific fashion (Yoon *et al*, 2001). Based on information about gene structure, protein structure and primary sequence, IF proteins have been divided into six-sub types shown in Table 1.3 (Bowden, *et al*, 1987; Parry and Steinert, 1999; Rao *et al*, 1996).

The largest group within this multigene family are the keratins (Type I and Type II intermediate filament proteins) which are expressed specifically in the cytoplasm of epithelial cells where they form a dense network of 10nm filaments.

Table 1.3: Intermediate Filament Types in Vertebrate Cells

Classification (Type)	Protein Name	Cellular Expression
Type I	Keratins (Acidic)	Epithelial cells and their derivatives (e.g. hair and nail)
Type II	Keratins (Neutral-Basic)	Epithelial cells and their derivatives (e.g hair and nail)
Type III	Vimentin, peripherin, desmin, GFAP and plasticin	Mesenchymal (fibroblasts), peripheral nerves, myogenic cells, astrocytes
Type IV	α-internexin, Neurofilaments L, H & M and Nestin	Neurones, glial scars, early neurons and muscle
Type V	Lamins (A and C)	Nuclear lamina

1.6 KERATIN

The term keratin was coined from the Greek word *keratos* meaning horn. Keratin has also been referred to in some literature as cytokeratin but this is no longer used. Also, keratin has been used as a general term to describe the material substance found in skin, hair, nail, horn, scale and feather. Thus, keratin has been referred to as "soft keratin" in the context of soft tissues such as skin and other epithelia, or as "hard keratin" when referring to hardened epithelial structures such as hair, nail, claws and hooves. It has also been established that some keratins are α-helical in structure whereas others adopt a β-pleated sheet structure (Astbury and Marwick, 1932; Pauling and Corey, 1953). This gave rise to the use of the terms α-keratin and β-keratin in the early literature, referring to protein X-ray diffraction patterns. Bird feathers and reptilian scales are composed of β-keratins and have a β-type X-ray diffraction pattern (Astbury and Marwick, 1932) while Pauling and Corey (1953) demonstrated that skin and wool keratins have an α-type diffraction pattern.

1.6.1 Keratin Proteins

1.6.1.1 Nomenclature of Epithelial and Hair Keratins

The epithelial cell-specific keratins are the most diverse class of IF proteins and have a narrow molecular weight range between 40-70 kilodaltons (kDa) and have been catalogued individually using two-dimensional polyacrylamide gel electrophoresis (2D-PAGE), which separates proteins by both charge and size. Immunoblotting using specific monoclonal, or polyclonal antibodies has also been used in conjunction with 1-dimensional or 2-dimensional electrophoresis to identify specific keratins (Kitahara and Ogawa, 1991; Wattle, 2000). The epithelial keratin intermediate filament proteins were characterised initially (Moll *et al*, 1982a) and placed into two groups depending on their molecular weight and the gene they were expressed from. Thus, the basic-neutral type II keratins were termed K1-K8 and the acidic type I keratins, K9-K19.

As this system of naming keratins was not open ended for the type II keratins the naming of new type II keratin proteins resulted in the addition of suffix letters to keratin proteins that demonstrated similar properties. For example, two different keratin genes (KRT2a and KRT2b) were found to encode keratin 2 (K2,) a type II keratin that was first identified in skin and oral epithelia as a polypeptide of molecular mass 65.5 KDa (Langbein *et al*, 1993; Moll *et al*, 1987). The two resulting K2 gene products are expressed in different tissues; K2e, predominantly in epidermis and a marker for late differentiation, and K2p, in the oral epithelia such as hard palate and gingiva (Collin *et al*, 1992). Around the same time, it was also noted that K6, a human type II keratin had two functional genes (KRT6a and KRT6b) encoding different protein isoforms termed K6a and K6b (Tyner and Fuchs, 1986). Later, Takahashi *et al* (1995) identified at least six K6 isoforms (K6a-f) after screening human genomic and skin cDNA libraries with probes derived from the K6b gene. However, this has recently been disputed and now there appears to be only three functional protein isoforms of K6 (K6a, K6b and K6h) and four of the originally designated genes (K6c, K6d, K6e and K6f) do not exist in the human genome (Rogers *et al*, 2005).

In addition, "hard" α-keratins belonging to hair and nail were not incorporated into the epithelial nomenclature resulting in a plethora of different terms for the "hard" keratins over the years which led to a lot of confusion. Sheep wool keratins were named according to a completely different system and no relationship between human epidermal and sheep wool keratin proteins was apparent. Furthermore, the protein extraction and analytical methods employed by the wool researchers was different to that used by Moll *et al* (1982) which made comparison even more difficult. As wool proteins are considerably more insoluble than skin proteins, different reagents were used to break down the abundant disulphide bridges found in wool proteins. Iodoacetate was a reducing reagent commonly used as it cleaved and permanently blocked disulphide bonds. The proteins were converted to more stable derivatives by reaction with iodoacetic acid which forms S-carboxymethylcysteine. However, it was found that the use of this reagent altered the size of the extracted proteins making comparisons between epidermal and wool keratins difficult at the protein level (Heid *et al*, 1986; Powell and Rogers, 1986). The reduced and alkylated proteins of wool

were fractioned into two major classes (Steinert and Rogers, 1973): one of a lower S-carboxymethylcysteine content than the total protein (low-sulphur keratins) and the other of higher S-carboxymethylcysteine content (high-sulphur keratins). Further fractionation also revealed two other classes of molecule in wool, the ultra high-sulphur and high glycine-tyrosine proteins.

Further research revealed that at the level of cDNA and genomic DNA that human hair, mouse hair and sheep wool keratin intermediate filament protein and gene sequences were closely related to epidermal keratins (Powell *et al*, 1982; Heid *et al*, 1986; Heid *et* al, 1988; Bowden *et al*, 1994) and a further nomenclature was introduced (Ha= Hair acidic and Hb= Hair basic). The hair specific keratins that were identified initially were numbered Ha1-4 and Hb1-4 (Heid *et al*, 1986) and these were the proteins that were originally termed "low-sulphur keratins". The high-sulphur keratins, ultra high-sulphur keratins and high glycine-tyrosine proteins were not IF-keratins and were re-assigned initially as matrix proteins and then as IF-associated proteins (IFAP).

More recently, a catalogue of human type I hair specific keratins was compiled increasing the total to nine (Ha1-Ha9), including two highly related Ha3 genes (Rogers *et al*, 1996; Rogers *et al*, 1998; Langbein *et al*, 1999). The number of type II hair specific genes has also risen to six, Hb1-6 (Rogers *et al*, 1997; Bowden *et al*, 1998).

Later studies identified a cluster of four keratin genes on chromosome 12q13.1 which encoded new human type II keratins, K6irs-K6irs4, which were all specifically expressed in the three layers of the hair follicle IRS (Langbein *et al*, 2002 & 2003). However, characterisation of the type I equivalents of human K6irs1-K6irs4 was more complicated. Simultaneous studies between research groups reported on the identification of four type I keratin gene orthologs in sheep, mice and humans. This gave rise to a number of different terms for the same protein which led to confusion and highlighted a need to update and unify the keratin nomencalture (Aoki *et al,* 2001; Bawden *et al*, 2001; Hesse *et al,* 2001 & 2004; Porter *et al,* 2001 & 2004; Rogers *et al,* 2004). An overview of different terms used to identify type I IRS keratins has been provided in Table 1.4.

Table 1.4 The different terms used for the type I IRS keratins and their genes

Keratin IRS proteins are highlighted in bold and its gene in italics. Human *Gene 4* is not the ortholog of the *oIRSa3.2* gene and its sequence is more related to *hIRSa3.1* (adapted from Langbein *et al*, 2006).

Species	Reference	Type I IRS keratin proteins and their genes			
Sheep	Bawden *et al* (2001)	oIRSa1	oIRSa3.2	oIRS3.1	OIRSa2
Human	Bawden *et al* (2001)	**hIRSa1** *hIRSa1*	- Gene 4	hIRSa3.1 hIRSa3.1	HIRSa2 hIRSa2
	Hesse *et al* (2001)	**K10C** KRT10C	K10D KRT10D	K12 KRT12B	Not identified -
	Rogers *et al* (2004)	**K25irs1** *KRT25A*	**K25irs2** *KRT25B*	**K25irs3** *KRT25C*	**K25irs4** KRT25irs4
	Schweizer *et al* (2006)	**K25** KRT25	**K26** KRT26	**K27** KRT27	K28 KRT28
Mouse	Porter *et al* (2004)	**mIRSa1** *mIRSa1*	Not identified -	**mIRSa3.1** *mIRSa3.1*	**mIRSa2** *mIRSa2*

Due to the complexity of keratin protein terminology, a more systematic nomenclature has come to fruition which is an extension from the original nomenclature produced by Moll *et al* (1982a). The new system of naming keratin proteins incorporates human epithelial and hair keratins but also allows for the inclusion of keratin pseudogenes as well as epithelial and hair-specific keratins from other mammalian species whose genes are either absent or occur as pseudogenes in the human genome (for review see Schweizer *et al*, 2006). The new designated keratin nomenclature will be used in this thesis (Table 1.5).

Table 1.5: Keratin Nomenclature

Type I		Type II	
New Term	Old Term	New Term	Old Term
K1	K1	**K9**	K9
K2	K2e	**K10**	K10
K3	K3	**K12**	K12
K4	K4	**K13**	K13
K5	K5	**K14**	K14
K6a	K6a	**K15**	K15
K6b	K6b	**K16**	K16
K6c	K6e-h	**K17**	K17
K7	K7	**K18**	K18
K8	K8	**K19**	K19
K71	K6irs1	**K20**	K20
K72	K6irs2	**K23**	K23
K73	K6irs3	**K24**	K24
K74	K6irs4	**K25**	K25irs1
K75	K6hf	**K26**	K25irs2
K76	K2p	**K27**	K25irs3
K77	K1b	**K28**	K25irs4
K78	K5b	**K31**	Ha1
K79	K6l	**K32**	Ha2
K80	Kb20	**K33a**	Ha3-1
K81	Hb1	**K33b**	Ha3-11
K82	Hb2	**K34**	Ha4
K83	Hb3	**K35**	Ka5
K84	Hb4	**K36**	Ha6
K85	Hb5	**K37**	Ha7
K86	Hb6	**K39**	Ka35
		K40	Ka36

There is no evidence for the existence of K11, although the Moll *et al* catalogue did include K11. No gene has ever been identified which encodes this protein, and it was shown to be the same size as a post-transitional modification of K10 (Bowden *et al*, 1984).

1.6.1.2 Structure of Intermediate Filament (IF) Proteins

The major structural characteristic of all IF proteins is the central α-helical rod domain, which is highly conserved both in size (310-315 amino acid residues for types I-IV and 355 residues for type V) and structure (Figure 1.14). The central domain is flanked by the 'head' and 'tail' domains at the N-terminal and C-terminal ends respectively (Geisler and Weber, 1982; Struman *et al*, 1996; Parry and Steinert, 1999; Strelkov *et al*. 2002). The rod domain reveals a quasi heptad repeat pattern $(a\text{-}b\text{-}c\text{-}d\text{-}e\text{-}f\text{-}g)_n$, where positions *a* and *d* are usually occupied by apolar amino acid residues (e.g. leucine) and the other positions are occupied by polar or charged residues. This gives rise to an α-helical twist in the polypeptide chain favouring the formation of a coiled-coil structure, and producing a characteristic surface pattern of charged and hydrophobic residues making IF water insoluble. The heptad periodicity within the rod domain is interrupted in several places, resulting in four consecutive α-helical segments (1A, 1B, 2A and 2B) that are connected by short non α-helical linkers (L1, L12 and L2). The non α-helical N- and C-terminal domains of hair-specific keratins have a high content of cysteine and proline residues allowing them to form disulphide bridges with the high-sulphur matrix proteins (IFAPs) within the hair fibre which ultimately produces a tougher, more durable structure (Dowling *et al*, 1986; Powell and Rogers, 1986; Heid *et al*, 1988).

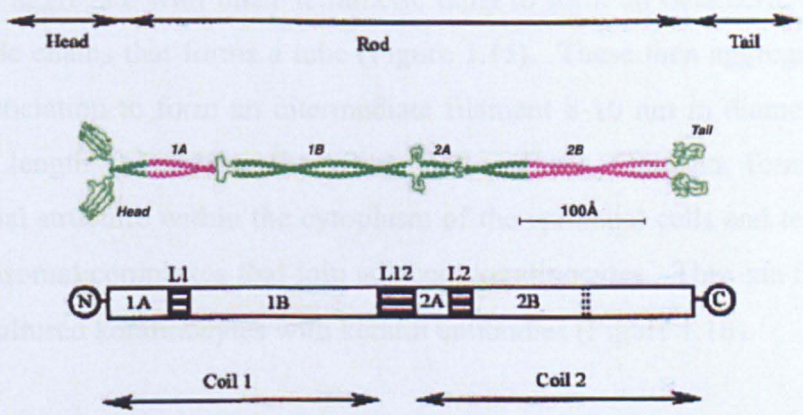

Figure 1.14: Basic Protein Structure of Keratin Monomer and Dimer Formation

The individual polypeptide chain is divided into four α-helical domains (1A, 1B, 2A, 2B) separated by three non-helical linkers (L1, L12, L2). An amino terminal domain (Head) and a carboxyl terminal domain (Tail) flank the central domain. The coiled-coil dimer shown is the result of hydrophobic interactions between the 'in register' α-helical domains of the two component polypeptide chains (adapted from Bowden, 1993).

1.6.1.3 Keratin Intermediate Filament Assembly

The first step of keratin intermediate filament assembly is formation of a dimer comprised of two keratin polypeptides. Hatzfield and Franke (1985), and Steinert (1990) agreed that dimers are composed of a 1:1 ratio of type I and type II subunits, referred to as a heterodimer, which form a coiled-coil structure. However, more recently, Suter *et al* (1997) reported that through evaluation of spatial configuration of known amino acid sequences of keratin filaments, homodimer formation can be demonstrated, in addition to heterodimer formation.

The next step towards intermediate filament formation is the condensation of two dimers to form a tetramer. There are two opposing views. In the case of a homodimer, two different types of dimer (type I homodimer plus type II homodimer) condense to form a hetrotetramer (Suter *et al*, 1997). In the case of heterodimers, two identical dimers form the tetramer. Early studies suggested that the tetramers are aligned antiparallel to each other, however confusion does exist as to whether they lie in register or are staggered. More recent studies showed that the staggered mode of alignment is the thermodynamically most stable form in solution (Steinert, 1991; Steinert and Parry, 1993).

Tetramers aggregate with other tetrameric units to form an octameric unit of 32 polypeptide chains that forms a tube (Figure 1.15). These then aggregate by end to end association to form an intermediate filament 8-10 nm in diameter and of sufficient length to traverse the whole cell. These filaments form a three-dimensional structure within the cytoplasm of the epithelial cells and terminate at the desmosomal complexes that join adjacent keratinocytes. This can be seen by staining cultured keratinocytes with keratin antibodies (Figure 1.16).

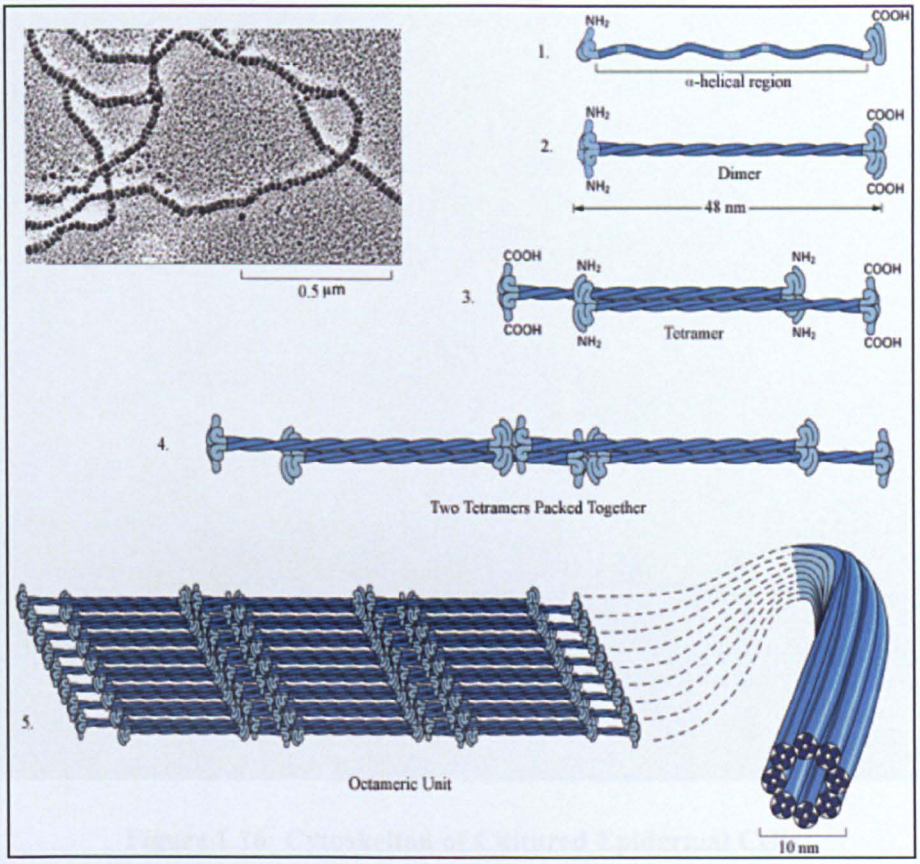

Figure 1.15: Steps in the Formation of Keratin Intermediate Filaments

The monomer shown in (1) pairs with another monomer to form a dimer (2) in which the conserved α-helical central regions are aligned in parallel and are wound together into a coiled coil. Two dimers then line up side by side to form a 48-nm by 3-nm protofilament containing four polypeptide chains (3). These protofilaments then associate in a staggered manner to form successively larger structures (4 and 5). An electron micrograph of the final filament is shown above left (adapted from Alberts *et al*, 1994).

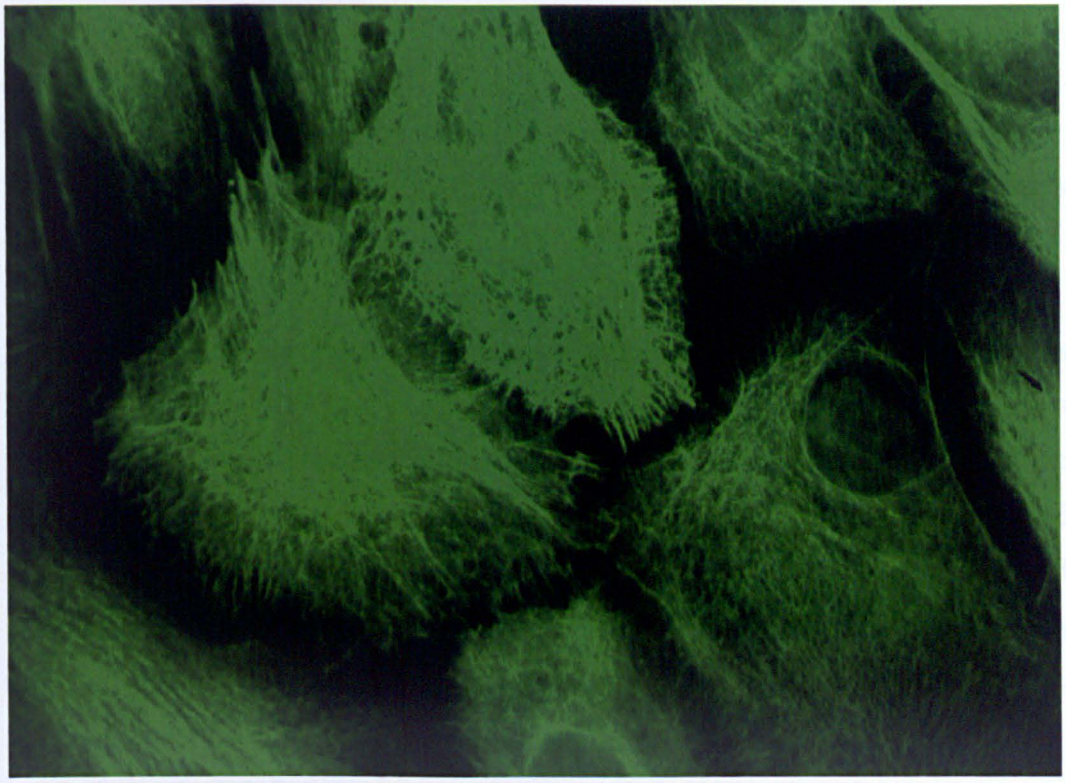

Figure 1.16: Cytoskelton of Cultured Epidermal Cells

Primary keratinocytes treated with anti-keratin antibody and detected by immunofluorescence microscopy with FITC. The three-dimensional keratin IF network is clearly visible throughout the cells cytoplasm (courtesy of Dr. P.E Bowden, Cardiff University).

1.6.2 Intermediate Filaments

The past two decades have seen a tremendous increase in the understanding of intermediate filament structure and function, due to the application of molecular genetic techniques and advances in biochemistry, molecular biology, cell biology and electron microscopy. While some protein sequences were available for wool keratins, a rapid increase in sequence information has allowed a more detailed comparison of the diverse members of the IF multigene family.

The IF genes of types I-III are remarkably conserved in structure and show common intron/exon boundaries. Human keratin gene (KRT) structure demonstrates a considerable amount of homology and is conserved in a type-specific manner. Generally, genes encoding type I keratin proteins have eight exons and seven introns, while type II and type III genes (vimentin, desmin,

GFAP) have nine exons and eight introns (Li *et al*, 1989). However, there are exceptions where type II K8 gene only contains seven introns in total as intron V, located at the beginning of the 2B helix, is lacking. Both type I keratin genes, K18 and K19 lack one intron at the C-terminal however, K19 lacks a further intron towards the end of the 2B helix resulting in it only containing 5 introns (Bowden, 1993).

The different types of IF genes are spread throughout the genome and have been localised to several different chromosomes. Desmin, vimentin and GFAP genes are all on different chromosomes (2, 10 and 17 respectively) and the neurofilament genes have been localised to two chromosomes (NF-L and NF-M on 8; NF-H on 22). However, all type I keratin genes except KRT18 are localised to two clusters: on one on the short arm (17p12) and the other on the long arm (17q11.2) of chromosome 17 (Rosenberg *et al*, 1998). All type II keratin genes and one type I gene (KRT18) have been localised in a single cluster (12q13-13) on the long arm of chromosome 12 (Popescu *et al*, 1989). As only chromosomes 1-21 have been standardised in the canine karyotype (Switonski *et al*, 1996), the type I keratin genes in the dog have been localised to chromosome 20 while the type II keratin genes were thought to be on a small autosome not yet included in the partial canine standard karyotype (Keller *et al*, 1998a). Since then, the identification of the remaining canine chromosomes (22-38), have since been standardised (Breen *et al*, 1999) and using fluorescence in situ hybridisation (FISH) experiments with clones isolated from a canine genomic library it has now thought that the basic Type II canine keratin gene cluster is localised on chromosome 27 (Miller *et al*, 1999).

The idea that the gene encoding K18 (KRT18), a type I keratin, located on chromosome 12 instead of the expected chromosome 17 was initially controversial. K8 (KRT8), the type II keratin with which it is co-expressed is also located on chromosome 12 as expected. Waseem *et al* (1990) stated that these findings are consistent with the hypothesis that K8 and K18, which are expressed in simple epithelia, may be closer to an ancestral keratin gene than the keratins of more highly differentiated epithelia.

1.6.3 Keratin Expression in the Epidermis

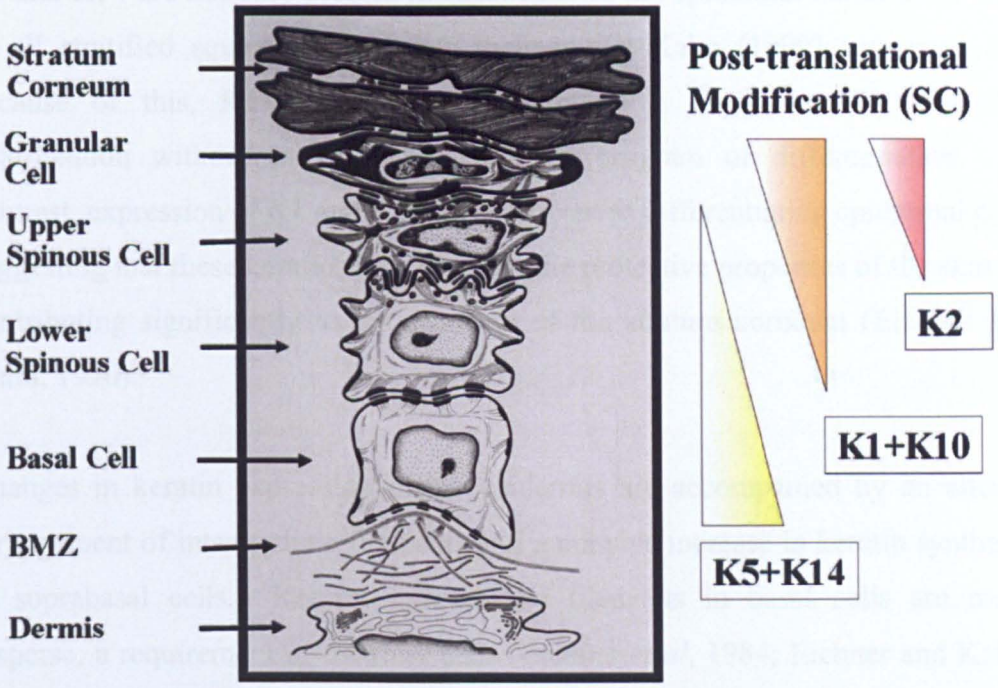

Figure 1.17: Epidermal Differentiation and Keratin

A schematic diagram of epidermal differentiation showing changes in keratinocyte morphology from the stratum basale (basal layer) to the stratum corneum and the associated changes in keratin gene expression. Basal cells mainly express K5 and K14. Cells which leave the stratum basale and commit to terminal differentiation begin expressing K1 and K10, stop expression of K5 and K14 and so levels of K5 and K14 protein progressively reduce. Cells of the stratum corneum are composed entirely of proteolytically modified keratins derived from K1 and K10 (picture courtesy of Dr P.E.Bowden, Cardiff University).

Not all keratins are expressed by individual types of epithelial cell and typically, between two to ten different keratins are expressed per cell type in various 'functional' combinations. Thus, keratins are not only epithelial specific but also show further diversity (different keratins are expressed in different epithelia), making the development regulation of these genes extremely interesting.

The process of keratin synthesis within the keratinocyte is referred to as keratinisation (Grosenbaugh and Hood, 1993). Up to 85% of the total content of a fully differentiated keratinocyte is composed of keratin intermediate filament proteins (Miller *et al*, 1999; Wattle, 2000). K5, K14 and K15 are expressed in basal cells (Woodcock-Mitchell *et al*, 1982) but become sequentially replaced by K1, K2 and K10 in suprabasal keratinocytes during terminal differentiation (Moll *et al*, 1982b; Kopan *et al*, 1987) (Figure 1.17).

K5 and K14 are not only present in basal cells of the epidermis but in basal cells of all stratified squamous epithelia. Eichner and Kahn (1990) suggested that because of this, K5 and K14 might provide a foundation for epithelial stratification without imparting a particular program of differentiation. In contrast, expression of K1 and K10 are restricted to differentiating epidermal cells suggesting that these keratins play a part in the protective properties of the skin by contributing significantly to the structure of the stratum corneum (Eichner and Kahn, 1990).

Changes in keratin expression in the epidermis are accompanied by an altered arrangement of intermediate filaments and a massive increase in keratin synthesis in suprabasal cells. Keratin intermediate filaments in basal cells are more disperse, a requirement of dividing cells (Eichner *et al*, 1984; Eichner and Kahn, 1990). Suprabasally, K1, K2 and K10 become organised into dense bundles and become orientated parallel to the cell surface (Eichner and Kahn, 1990; Reichelt *et al*, 2001). In the stratum granulosum, a protein named filaggrin is synthesised and released from keratohyalin granules as a high molecular weight precursor (Dale, 1987; Simon *et al*, 1996; Presland, 2001). Presland (2001) stated that during cornification (a process initiated in the stratum granulosum and encompassed within terminal differentiation) profilaggrin is dephosphorylated and cleaved by endoproteases to yield the mature protein, filaggrin. This stage coincides temporally with the transition of the nucleated granular cell to the anucleate cornified cell (corneocyte). Filaggrin can be considered as an IFAP and is thought to promote keratin intermediate filament aggregation and disulphide bond formation, thus forming a more compact resilient material, which contributes to the tough properties of the stratum corneum Eichner and Kahn, 1992). Keratin intermediate filaments are also referred to as tonofilaments (Matoltsy, 1976; Dale, 1987; Yoon *et al*, 2001), macrofibrils (Byrne *et al*, 1994) and keratin masses (Bragulla *et al*, 2001).

As cells migrate into the upper layers of the skin, cell membrane permeability increases allowing the passage of calcium and other ions into the cell (Kalinin *et al*, 2001). This calcium influx coincides with the expression of envoplakin,

periplakin, and involucrin which form the basis of the protective cornified envelope. Envoplakin and periplakin form stable heterotetramers, and *in vitro* data has shown that involucrin and envoplakin-periplakin heterotetramers associate with the plasma membrane in a Ca^{2+} dependent manner. The enzyme transglutaminase which is also expressed at this time, spontaneously assembles onto membranes by way of its acyl lipid adducts and as intracellular Ca^{2+} continues to rise, this enzyme joins the two plakins and involucrin together by forming stable N^{ε}-(γ-glutamyl) lysine isopeptide bonds (Kopan *et al*, 1987; Rice *et al*, 1994; Steven and Steinert, 1994; Kalinin *et al*, 2001). The enzyme also crosslinks other membrane-associated proteins such as loricrin, small proline rich (SPR) family members, repetin, trichohyalin, cystatin and desmosomal proteins. Gradually, the involucrin-envoplakin-periplakin complex and loricrin form a layer along the entire inner surface of the plasma membrane, linking the desmosomes together to form a scaffold. The resulting corneocyte lacks all organelles, microfilaments and microtubules due to degradation but maintains its shape and structure due to the cell envelope and keratin intermediate filaments network. Corneocyte filaments mainly consist of K1, K2e and K10 and these are also cross-linked to the cornified envelope, desmoplakin and envoplakin remnants, as well as involucrin, loricrin and SPR's. The final dead cornified cell thus consists mostly of bundled keratin intermediate filaments covalently attached to and enclosed within the cornified envelope.

Other keratins expressed by the epidermis include K6, K16 and K17. Although absent in normal epidermal cells, the production of these keratins are increased during disrupted epidermal homeostasis. For example, K16 is expressed in irritant contact dermatitis and K17 is expressed in delayed type hypersensitivity induced by a mumps vaccine in human skin (Jiang *et al*, 1993). Keratin 17 gene expression is also up-regulated by UVB radiation, whereas exposure to UVA radiation mainly increases K19 expression as well as K6 and both K5 and K14 (Bernerd *et al*, 2001). K6 is expressed in wound healing, as well as in hyperproliferative epidermis of psoriatic skin, as is K16 and K17 (Smack *et al*, 1994). In load bearing areas of the body, such as the soles of the feet (and foot pads in the dog), the stratum corneum is greatly thickened, giving rise to callus. The foot pad is an example of pressure keratinisation. The epidermis of human

ridged skin expresses a more complex pattern of keratins than the thinner skin at other anatomical sites, which is probably due to the greater stress that ridged skin has to withstand. In addition to K9, which is confined to regions of pressure keratinisation, palmar-plantar skin also expresses K6, K16 and K17 constitutively, which is suggestive of regional adaptations of this epidermis to a high cell turnover rate. In particular, the location of K17 positive cells within the troughs of the deep primary epidermal ridges supports the notion of functional heterogeneity of basal cells and suggests that the K17 positive sites may include stem cells. Expression of K6 and K16 in some basal and most suprabasal keratinocytes suggests a high proliferative activity of normal ridged epidermis, but may also reflect different physical properties of the suprabasal cells, in contrast with regions expressing K9 (Swensson *et al*, 1998).

The "simple keratins", K8 and K18 are expressed in simple epithelia including the kidney and liver and are the first keratin intermediate filaments to be expressed in the embryo (Waseem *et al*, 1990).

K15 has been described as a minor component of the epidermis and hair follicle but only seems to be abundant in the epithelia of the eccrine sweat gland, epiglottis and trachea. Some stratified epithelia also express K7 and K19, and these keratins have been found in both apocrine and eccrine sweat glands, mammary gland ducts and tracheal epithelium. K19 has also been identified as a minor keratin in the epidermis and hair follicle, where it localised specifically to the germinative compartments where stem cells arise. The transitional epithelia of the bladder and gallbladder express K7 and K19 in addition to the keratins characteristic of simple epithelia (K8 and K18). The simple mucosal epithelium of the small intestine and colon, and the simple epithelia of the other internal organs such as the liver and kidney have the simplest keratin expression, consisting only of K8 and K18, although some K19 expression is often observed.

1.6.4 Keratin Expression in Hair

The hair follicle consists of a complex system of multiple tissue compartments that are clearly distinguishable by their morphology, type of differentiation and

keratin expression. In the hair follicle, the patterns of keratin expression are far more complex compared to normal stratified epithelia (Lynch *et al*, 1986; Moll *et al*, 1988; Coulombe *et al*, 2003). Recently, *in situ* hybridisation and indirect immuno-fluorescence studies have identified all sixteen keratins of the human hair (Langbein *et al*, 2006 & 2007). The seventeenth member of the family, type II keratin K84 (formerly Hb4) is actually absent from the hair follicle and only exists in the filiform papillae of the human tongue (Langbein *et al*, 2001; Langbein and Schweizer, 2005).

The basal cells of the outer root sheath (ORS), which is contiguous with the epidermis of the skin, expresses the two epidermal basal cell keratins (K5 and K14) as well as small amounts of K15. Suprabasal ORS cells express K5 and K14 as well as K6a, K6b, K16 and K17 constitutively (Moll *et al*, 1982b; Lynch *et al*, 1986; Stark *et al*, 1987; Kopan and Fuchs, 1989, Langbein *et al*, 2003 & 2006).

The companion layer, which exists between the ORS and IRS and forms a functional unit with the IRS has been found to express at least four keratins which include K6, K75, K16 and K17 (Winter *et al*, 1998).

The inner root sheath (IRS), which is composed of three distinct layers (Henle, Huxley and IRS cuticle), has a more complex keratin expression. K71 is the only type II keratin to be expressed in all three layers of the IRS. Similarly, type I K25, K27 and K28 are expressed in all three layers of the IRS (Rogers *et al*, 2000; Langbein *et al*, 2006). Two type II keratins (K72 and K73) and type I (K26) are specific to the IRS cuticle (Porter *et al*, 2001; Langbein *et al*, 2003 & 2006) whereas K74 is restricted to the Huxley layer (Langbein *et al*, 2003). Interestingly, the number of type I keratins is greater in comparison to type II keratins. For example, cells of the Henle layer express three type I keratins (K25, K27 and K28) to only one type II keratin (K71).

The hair cuticle covers the surface of the entire hair once it has emerged from the epidermis and acts as a protective barrier for the hair. Studies have revealed that

the six "hard" keratins (K32, K35, K39, K40, K82 and K85) are all present within hair cuticle cells.

The matrix and the cortex, which are both encased by the hair cuticle, express different hair-specific keratins, K31-K39 (type I) and K81-K86 (type II; see Langbein *et al*, 2006 & 2007). In the centre of the hair shaft, medulla trichocytes can be identified from other cells of the hair follicle as they co-express a large number of both epithelial keratins, K6, K75, K16, K17, K26, K27, K28 and hair keratins, K81, K83, K85, K86, K31, K33a, K34, K36, K37, K39 (Stark *et al*, 1987; Bowden *et al*, 1998; McGowan and Coulombe, 2000; Langbein *et al*, 2006 & 2007).

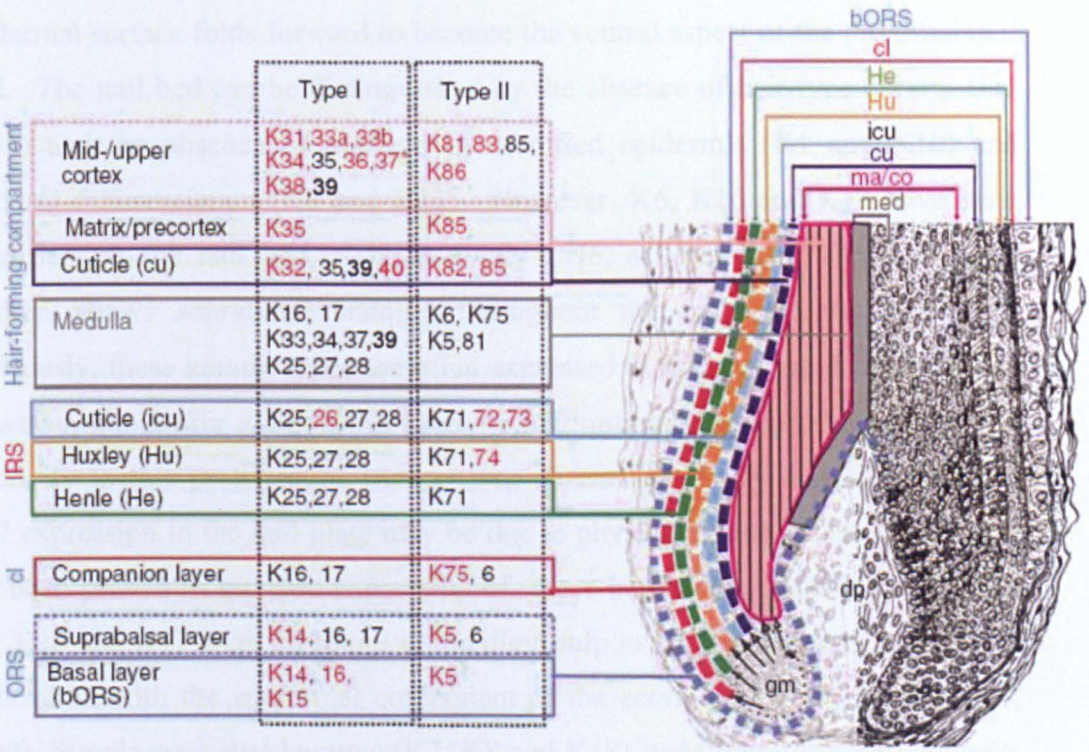

Figure 1.18: Schematic Representation of Keratin Expression within the Hair Follicle

The **ORS** is a continuing epithelium which surrounds the entire hair follicle. All other layers (**companion layer (cl)**, IRS, (**Henle (He)** & **Huxley (Hu)** layer and **IRS cuticle (icu)**, **hair cuticle (cu)**, **matrix/cortex (ma/co)**, **medulla (med)**) stem from cells in the germinative matrix (gm) which is located at the base of the hair bulb. Epithelial/hair keratins represented in red within the table to the left are solely expressed within that particular layer of the hair follicle. (adapted from (Langbein *et al*, 2006).

1.6.5 Keratin Expression in Nail

Keratins isolated from the human nail plate and hair are similar. Bowden (1993) stated that the human nail is composed of a combination of 'soft' epidermal keratins and 'hard' hair-specific keratins. In addition to this, the nail contains high sulphur matrix proteins and possibly trichohyalin. More recently, a detailed analysis of the differentiation within the nail unit has been conducted using a range of anti-keratin monoclonal antibodies (De Berker *et al*, 2000) and has demonstrated different patterns of keratin expression within the various regions of the nail unit. The nail matrix only expressed Ha1 (K31), which was also expressed in suprabasal matrix cells together with two epidermal keratins (K1 and K10; De Berker *et al*, 2000). Small amounts of K17 have also been identified towards the apex of the nail matrix and K6 and K16 were found where the epidermal surface folds forward to become the ventral aspect of the proximal nail fold. The nail bed can be distinguished by the absence of hair-type keratin Ha1 (K31) and the absence of markers of cornified epidermis (K1 and K10) and mucosal differentiation (K4 and K13). However, K6, K16 and K17 have been identified on the nail bed. The antibody LH6, a basal keratin conformation marker, shows suprabasal staining throughout the nail bed. As mentioned previously, these keratin types are often expressed in areas of rapid proliferation. However, De Berker *et al* (2000) used a Ki-67 antibody to stain the nail bed but reactivity to this proliferation marker was absent suggesting that K6, K16 and K17 expression in the nail plate may be due to physical trauma of the nail, which has been proven to increase expression of these keratin (Swensson *et al*, 1998). K6, K16 and K17 were all found in the digit pulp in limited amounts, possibly in association with the epidermal component of the eccrine duct (De Berker *et al*, 2000). Simple epithelial keratins (K7, K8 and K18) were found in small amounts in nail specimens from younger individuals.

Very little research has been conducted on the canine claw with regard to its keratin content. Butler and Wright (1989) stated that hair and nail samples from human and canine sources were analysed but no results relating to the keratin composition of canine claw appeared in this paper.

1.7 AIMS OF THESIS

The purpose of this thesis is to investigate the anatomical structure and differentiation related gene expression, principally keratin expression, within the dog claw. From a review of literature, it is apparent that detailed studies on canine claw anatomy are still lacking which is essential when planning an investigation into the molecular make-up of this structure. Therefore, the initial research has focussed on the macro- and micro-anatomy of the claw using histological techniques (Chapter 3).

Identification of keratins within the canine claw primarily focused on the extraction and analysis of these structural proteins using one-dimensional SDS-electrophoresis and western blotting techniques (Chapter 4). Other keratinised epidermal tissues such as the equine hoof and hair as well as human nail, skin and hair were used as reference materials as these structures have been studied in more detail and are comparable to the canine claw and hair.

Using the information gained from Chapters 3 and 4, a detailed microscopic analysis of keratin and keratin-associated protein expression within the dog claw was carried out (Chapter 5). Immunocytochemical studies on longitudinal histological sections of the claw with various differentiation-related protein antibodies, will define keratin expression and location within the dog claw.

These studies have provided a greater understanding of the growth and micro-anatomy of the claw and the use of immunocytochemical techniques in conjunction with one-dimensional electrophoresis and immunoblotting has helped to define the claw more accurately and provide a basis for future canine claw disease research which may lead to the development of new therapies for many canine skin and claw diseases.

CHAPTER 2

2 MATERIALS AND METHODS

2.1 TISSUE SAMPLES

Canine claw samples were obtained from the Royal Army Veterinary Corps and the dogs were put down for purposes other than for this study. There was no known history of any skin diseases. A list of all the breeds of dogs used in this study is provided below (Table 2.1). Tissues samples were obtained immediately after euthanasia. Normal human tissue sections were obtained from archival tissue specimens held in the Department of Dermatology (School of Medicine, Cardiff University).

Table 2.1: Dog Breeds Studied

(*GSD = German Shepherd, ROT = Rottweiler, SPAN = English Springer Spaniel)

Dog ID	Sex	Breed *	Neutered	Weight (Kg)
A	M	GSD	N	34.8
B	M	GSD	N	35.6
C	M	GSD	Y	36.4
D	M	GSD	N	33.7
E	M	GSD	-	-
F	M	ROT	-	-
G	M	ROT	-	-
H	M	SPAN	-	-

2.2 PREPARATION OF TISSUES FOR HISTOCHEMISTRY, IMMUNOHISTOCHEMISTRY AND IMMUNOFLUORESCENCE

2.2.1 Preparation of Canine Tissue Samples

It is important to take into account the biochemical changes that may take place over a short period of time after biopsies are taken from the parent tissue and what effect this will have on the protein epitope or enzyme activity to be examined. To ensure optimum results all tissue samples were frozen immediately after biopsy. Antibody binding to proteins such as keratins is unlikely to be affected significantly in the short term (24 hours) if biopsies were not allowed to dry out and were kept at 4°C. Ice crystal formation within the tissue samples is inevitable during the freezing process. The slower the samples are frozen the larger the ice crystals that form and consequently more tissue damage will occur as ice crystals rupture both inter- and intra-cellular membranes. To minimise this damage and to preserve tissue integrity as close to the *in vivo* state as possible, all human and canine skin samples were frozen using the protocol outlined below.

Histochemistry and immunochemistry were performed on fixed tissue that was embedded in wax blocks and sectioned by rotary or sledge microtome. The samples of whole digits were decalcified after fixation to reduce bone density.

Immunofluorescence requires frozen sections cut on a cryostat. This was difficult for skin due to the tough nature of the tissue and proved impossible for canine claws, which are large in size and very tough. In addition, the living cells are encased in a bony groove which could not be sectioned. Furthermore, the claw samples had been frozen for five days before access was possible and this led to dehydration and tissue damage making cryostat sectioning even more difficult.

Canine claw samples were obtained by cutting digits from the foot. These were rinsed in distilled water, wrapped in parafilm, labelled and stored at -20°C within a 24 hour period.

Digits were thawed and carefully cut using a band saw. A single parasaggital cut was made as close to the mid line of the claw as possible (Figure 2.1). Alternatively, the claw was cut transversely at 90° to the tubules, into five equal sections and labelled 1-5 in an ungual groove to distal direction (Figure 2.2). The claw pieces were then fixed in 50 mls of 10% neutral buffered formalin for a 48 hour period before being decalcified to soften the distal phalanx, to make cutting sections of the claw easier.

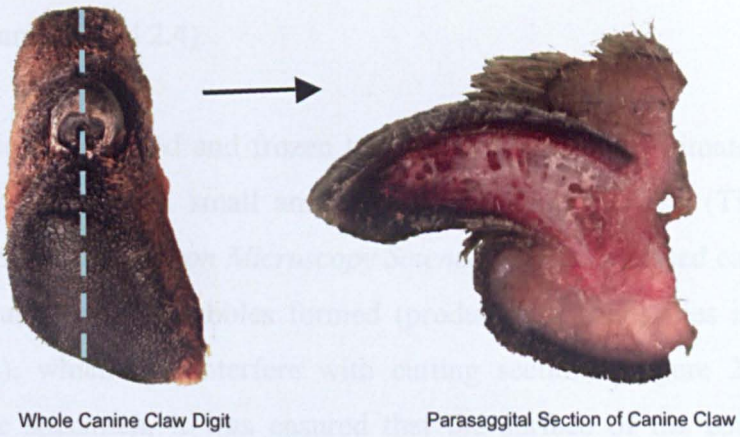

Figure 2.1: Parasaggital Sectioning of Canine Claw

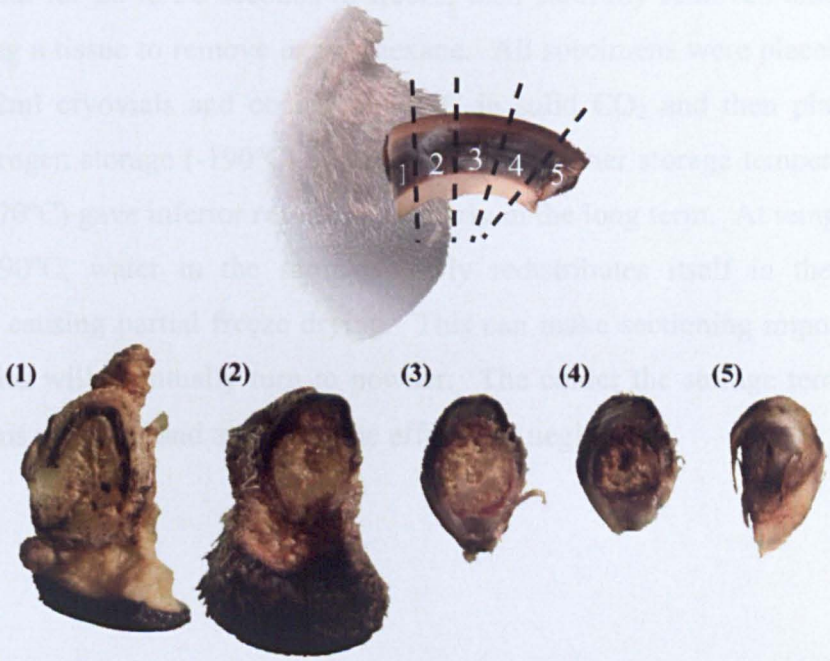

Figure 2.2: Transverse Sections of Canine Claw

Claws were divided into 5 transverse section cut perpendicular to the tubular structure in the claw.

Prior to taking any canine or human skin biopsies, long hair was carefully trimmed with a razor so that the hair did not interfere with embedding, freezing or cutting of sections. A good sized sample was found to be 3mm in diameter or half a 6mm punch biopsy. The sample should be no more than 5mm thick in its smallest dimension to allow rapid freezing throughout the tissue. Larger samples may suffer increasingly from ice crystal damage relative to the size of the sample. The majority of skin biopsies were cut so that longitudinal hair follicles were obtained as this provided more informative data than transverse or oblique sections (Figure 2.3 and 2.4).

Tissue samples were fixed and frozen to pieces of cork, approximately 10mm x 7mm x 3mm in size. A small amount of embedding medium (Tissue Tek®, O.C.T™ compound, *Electron Microscopy Sciences Ltd*) was placed carefully onto the cork ensuring no air bubbles formed (produce inconsistencies in the tissue when frozen), which can interfere with cutting sections (Figure 2.4). When mounting the specimen, it was ensured that the surface of the epidermis was perpendicular to the plane of the cork so that longitudinal hair follicle sections would be obtained. The tissue samples and cork were carefully placed into a cold hexane bath for 20 to 30 seconds to freeze, then carefully removed and quickly dried using a tissue to remove excess hexane. All specimens were placed in pre-labelled 2ml cryovials and cooled to -70°C in solid CO_2 and then placed into liquid nitrogen storage (-190°C). It was found that other storage temperatures (-20°C or -70°C) gave inferior results particularly in the long term. At temperatures above -190°C, water in the sample slowly redistributes itself in the sample container causing partial freeze drying. This can make sectioning impossible as the samples will eventually turn to powder. The colder the storage temperature the less this occurred and at -190°C the effect was negligible.

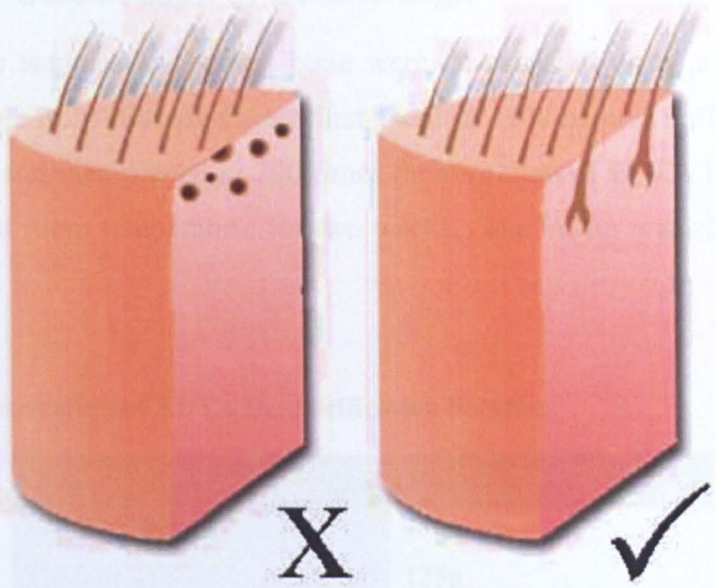

Figure 2.3: Orientation of Section for Skin Biopsy

Prior to taking any skin biopsies all long hair was trimmed or gently shaved close to the skin surface. The biopsy was mounted on the cork block in such a way that the hair follicles close to the skin surface are in the correct orientation. Thus, longitudinal hair sections (right) rather than transverse sections (left) are obtained on cutting.

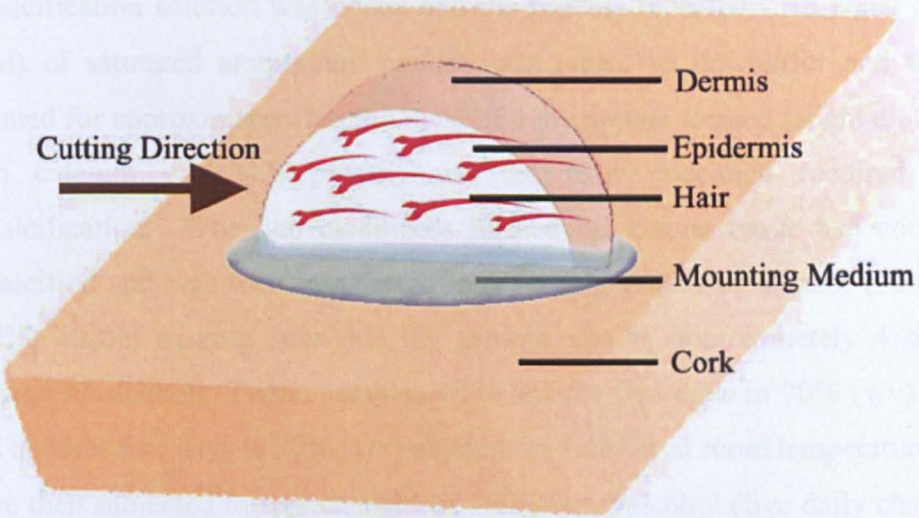

Figure 2.4: Orientation of Skin Samples for Histology

Biopsies were cut in half and mounted (cut side down) on to cork, with the hair follicles orientated along the plane of cutting. The sections that are produced were better, the more carefully this is done.

2.2.1.1 De-Calcification of Canine Digit

Canine tissue samples containing bone were de-calcified using a 0.5M EDTA solution (Table 2.2). Samples were first fixed in 10% neutral buffered formalin for 48 hours and then placed in 200 times their volume of EDTA buffer and left on a shaker at room temperature for two weeks. The buffer was changed after 7 days.

Table 2.2: Preparation of EDTA De-calcification Solution

Chemical	Quantity
0.5M EDTA	435g
1M NaOH	125g
Distilled Water	3 Litres

To test if all calcium had been completely removed from the decalcifying tissue, approximately 3ml of the 0.5M EDTA buffer was removed. This was tested with litmus paper and neutralised by adding strong ammonia solution drop by drop until the paper turned blue (pH <7). If the litmus turned dark blue more decalcification solution was added and the process repeated. An equal quantity (3ml) of saturated ammonium oxalate was added to the buffer and this was agitated for approximately ten minutes. If a precipitate formed (slight cloudiness) then calcium was still present and the claw specimen required further decalcification. When no cloudiness formed the canine tissue had completely decalcified and was then transferred into varying grades of alcohol (70%, 90%, 100%, 100%) making sure that the sample was in approximately 4 times its volume of alcohol. Tissue samples were left for five days in 70% (v/v) alcohol and another five days in 90% (v/v) alcohol on a shaker at room temperature. They were then subjected to five changes of 100% (v/v) alcohol (five daily changes on a shaker at room temperature).

2.2.1.2 Tissue Processing

Following de-calcification and treatment with graded alcohols canine tissue samples (decalcified claw and skin samples) and human skin samples were soaked in Cedar Wood Oil, which was changed daily for four days.

Samples were then placed in foil dishes containing molten paraffin wax and stored in an oven at 56°C. The paraffin wax was changed daily for five days to ensure complete removal of cedar wood oil. Tissue samples were carefully embedded in fresh paraffin wax in plastic embedding trays ensuring that the orientation of the specimen was known. The area of interest was placed face down in the bottom of the well so that it would appear on the surface of the wax block once removed from the embedding tray. The blocks were labelled and left on a cool plate to harden for 24 hours after which they were removed from the embedding tray.

Paraffin embedded claws were cut on a rotary microtome set to a depth of 5μm. Tissue sections were carefully placed in a water bath (28°C), picked up carefully onto SuperFrost® slides and allowed to dry in an incubator at 36°C overnight. Larger specimens were cut on a sledge microtome.

2.2.1.3 Haematoxylin and Eosin Staining

Haematoxylin and eosin (H&E) are most commonly used to stain connective tissue and cytoplasm. They stain tissue sections in varying intensity and shades of pink and purple providing a useful differential stain.

Volumes for the haematoxylin stain used in this study are shown in Table 2.3. The haematoxylin, potassium alum, and sodium iodate were mixed with distilled water and allowed to dissolve overnight. The chloral hydrate and citric acid were then added and the mixture boiled carefully for five minutes.

Table 2.3: Preparation of Haematoxylin Solution

Chemical	Quantity
Haematoxylin	1g
Sodium Iodate	0.2g
Potassium Alum	50g
Citric Acid	1g
Chloral Hydrate	50g
Distilled Water	100ml

Slides containing paraffin embedded claw sections were placed in a rack and heated in an oven for 20 minutes at 60°C to soften the paraffin wax. They were then de-waxed in three aliquots of xylene and varying grades of alcohol (100% twice, 90% and 70%) for five minutes each. Sections were then fully hydrated in running tap water for five minutes at room temperature and placed in distilled water until ready for use.

The surface of the haematoxylin solution was skimmed with a tissue to remove oxidized particles prior to use. The slides and holder were blotted to remove excess water before being placed in haematoxylin so the concentration of the solution was not diluted. Sections were placed in haematoxylin solution for approximately 5 minutes, thoroughly rinsed in running tap water for 5 minutes and then placed in distilled water. The sections were examined at this stage to confirm a sufficient degree of staining.

Slides were then counter-stained by placing them in a well containing 1% (v/v) aqueous eosin for 30-45 seconds depending on the age of the eosin solution. The surplus was washed off with running tap water and the slides were then placed in distilled water.

After staining, the specimens were dehydrated in ascending grades of alcohol (70%, 90%, 100% twice) and three aliquots of xylene (five minutes each). The stained sections were mouted with Ralmount media. A small amount was carefully added to the tissue section using a glass rod, taking care to leave no

bubbles. The coverslip was carefully placed over the slide allowing the Ralmount to spread beneath the coverslip ensuring complete tissue coverage. Slides were allowed to dry in a 45°C oven for 48 hours. The stained sections were then examined using a light microscope.

Microscopic examination of the tissue sections should show the cytoplasm and muscle fibres to be a deep pink, collagen a lighter pink, nuclei a deep blue and calcified bone a purplish blue.

2.3 IMMUNOHISTOCHEMISTRY

2.3.1 Avidin Biotin Complex (ABC) and Labelled Streptavidin Biotin (LSAB) Staining Method

The avidin biotin complex (ABC) method of immunohistochemical (IHC) staining is widely used to visualise antigens within animal tissues. Avidin, a large glycoprotein, can be labelled with peroxidase or fluorescein and has a very high affinity for biotin. Furthermore, biotin, a low molecular weight vitamin, can be conjugated to a variety of biological molecules such as antibodies. The ABC technique involves three reaction steps. The first is addition of unlabeled primary antibody to the tissue section. The second is addition of a biotinylated species-specific second antibody. The third is addition of a complex of avidin-biotin peroxidase. The antibody peroxidase complex is then localised by addition of diaminobenzidine tetrahydrochloride (DAB), or another substrate, to produce different colorimetric end products which can be visualised by microscopy (Figure 2.5).

The Labelled StreptAvidin Biotin (LSAB) method uses streptavidin, derived from *streptococcus avidini*, which is a recent innovation and substitutes for avidin. The streptavidin molecule is uncharged relative to animal tissue, unlike avidin (basic with an isoelectric point of 10), and therefore electrostatic binding to tissue is eliminated. In addition, streptavidin does not contain carbohydrate groups (can bind to tissue lectins) resulting in more background staining.

LSAB is technically similar to the standard ABC method (Figure 2.5). The first step requires addition of unlabeled primary antibody to the tissue section. The second is addition of a species-specific biotinylated second antibody. The third step requires an enzyme-streptavidin conjugate (HRP-Streptavidin or AP-Streptavidin). The enzyme is then visualized by application of the substrate chromogen solutions to produce different colorimetric end products. The third step can also be a fluorescent dye-streptavidin complex such as FITC-streptavidin if fluorescence labelling is required.

There are no keratin canine antibodies commercially available, so human keratin antibodies were used to identify the location of keratin antigens in canine tissues. Due to these antibodies not being species specific, the LSAB method was employed instead of the ABC method to help decrease the level of background staining which makes the results easier to interpret.

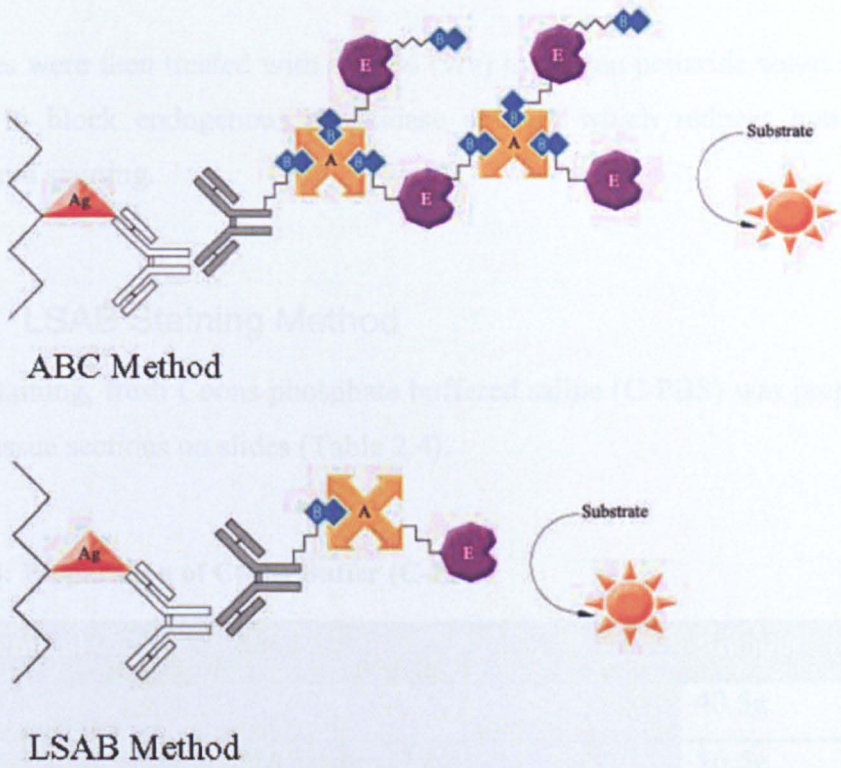

Figure 2.5: ABC and LSAB Staining Method

The antigen (Ag) binds to the primary antibody (**white**). The biotinylated second antibody (grey) binds to the primary antibody and its free biotin site (B) binds to the avidin or StreptAvidin biotin enzyme complex (ABC method) or the enzyme labelled StreptAvidin conjugate (LSAB method) (A and E). Visualisation of the antibody occurs when a **substrate** such as DAB is added to this complex and the enzyme forms a chromogenic (visible) product.

2.3.1.1 Microwave Antigen Retrieval

This method of antigen retrieval is based on microwave heating of tissue sections attached to microscope slides to temperatures of 100 °C in the presence of heavy metal salt solutions. This approach to retrieve antigens from formalin-fixed, paraffin embedded tissues and their subsequent staining by immunhistochemical techniques offers excellent immunostaining results with keratin antibodies.

Tissue sections were rinsed in tap water. They were then immersed in 0.0371% (w/v) EDTA and 1% (v/v) sodium hydroxide solution at pH8 and exposed to microwave irradiation at 450W for 12 minutes in two 5-minute irradiations with 5 minutes rest after each, and one 2-minute irradiation. The sections were then left to cool for 20 minutes before being bathed in tap water for 60 minutes and C-PBS for 5 minutes.

The slides were then treated with a 0.3% (v/v) hydrogen peroxide solution for 30 minutes to block endogenous peroxidase activity which reduces non-specific background staining.

2.3.1.2 LSAB Staining Method

Before staining, fresh Coons phosphate buffered saline (C-PBS) was prepared for rinsing tissue sections on slides (Table 2.4).

Table 2.4: Preparation of Coons Buffer (C-PBS)

Chemical	Amount
NaCl	40.5g
Di-sodium hydrogen orthophosphate dodecahydrate ($Na_2PO_4.12H_2O$)	16.5g
Distilled Water	Make up to 4L

Adjust solution to pH 7.2 with 4g Sodium dihydrogen orthophosphate dihydrate ($NaH_2PO_4.2H_2O$) in 25ml of distilled water. Leave to adjust for 10 minutes.

Paraffin embedded tissue samples on microscope slides were placed in a metal rack and heated in an oven for 20 minutes at 60°C to soften the paraffin wax. The wax was then removed by placing the rack sequentially into three aliquots of xylene and varying grades of methanol (100% twice, 90% and 70%) for five minutes each. The tissue samples were then fully reyhdrated by placing the rack carefully into a sink full of fresh water and then into distilled water until ready for use. Before use, the slides were finally bathed in C-PBS for 5 minutes. The tissue sections were then ready to undergo microwave antigen retrieval if

necessary (see section 2.3.1.1). If antigen retrieval was not needed, tissue samples on glass slides were encircled carefully with a silicon pen to prevent any solution added to the tissue from running off the slide.

If the antibody being tested was a sheep antibody then donkey serum was added to tissue sections for 30 minutes at room temperature. This was found to reduce non- specific staining. Excess serum was not rinsed from the slide but shaken carefully into a sink after 30 minutes. They were then treated with primary antibody as described.

The primary antibodies were diluted to their optimal concentrations in a phosphate buffer solution containing 0.6% (w/v) Bovine Serum Albumin (BSA). An aliquot of each antibody (200 µl) was placed on each section for one hour at room temperature. Excess primary antibody was then removed with three, 5 minute rinses of C-PBS solution at room temperature.

Secondary antibodies, which were species specific for the primary antibody used (e.g. anti-rabbit or anti-mouse biotinylated secondary antibody), were diluted to their optimal concentrations in phosphate buffer solution containing 0.6% (w/v) BSA. An aliquot of 200µl was added to each of the tissue sections, including the negative control slides and left to incubate at room temp for 1 hour. Excess secondary antibody was then removed followed by three, 5 minute rinses of C-PBS at room temperature.

Streptavidin biotinylated horseradish peroxidase complex was used as a label and was diluted with 0.6% (w/v) BSA and placed on the tissue sections. This was left to incubate for one hour at room temperature. Slides were rinsed three times in C-PBS with a change every 5 minutes.

Slides were then incubated in 0.25 mg/ml 3,3-diaminobenzidine tetrahydrochloride (DAB)/C-PBS for five minutes. The excess DAB was washed off with tap water to stop the reaction. Slides were then rinsed three times in C-PBS with a change every five minutes. Sections were then counterstained with haemotoxylin.

Finally, the sections were dehydrated through graded alcohols and then xylene, before the cover slip was placed on the section using Ralmount mounting media. The slides were dried overnight at 45°C and then stored at room temperature until examined with a conventional light microscope.

2.3.1.3 Controls

Controls must be run in order to test the methodology and assess the specificity of the antibody being used.

Positive controls were employed as well as negative controls to ensure that the antibodies tested were functioning correctly. Human skin samples were used as positive controls as well as functional comparisons to canine tissue. If the positive control tissue demonstrated negative staining, the protocol and procedure was checked and modified until a good positive staining was obtained.

Negative controls were used to test for the specificity of the antibody involved. The omission of the primary antibody from the BSA buffer or the replacement of the specific primary antibody by normal serum (must be the same species and concentration as the primary antibody) was used for control tissue samples. No staining should be observed in the resulting slides and any weak staining observed represents background.

2.3.2 The Labelled Avidin-Biotin Method for Frozen Sections

From the frozen tissue samples stored in liquid nitrogen, 10μm sections were cut using a cryostat at -20°C and then mounted using Superfrost Plus® slides. The sections were then air dried at room temperature for 10 minutes and encircled with a silicon pen. The sections were fixed using 4% (v/v) acetone at 4°C for 10 minutes, after which they were treated with donkey serum (1:10) at room temperature for 30 minutes, to limit non-specific binding. The sections were rinsed with C-PBS buffer for 15 minutes, with a change every 5 minutes prior to labelling.

All sections, except for the negative control, were incubated with a primary antibody diluted in 0.6% (w/v) BSA at room temperature for one hour. Negative control sections were incubated in BSA and C-PBS only under the same conditions. Slides were then rinsed three times in C-PBS with a change every 5 minutes. The second antibody was then applied and sections were left at room temperature for one hour. After this, the slides were again rinsed three times with C-PBS changed every 5 minutes. Streptavidin fluorescein was diluted to 1:50 in 0.6% (w/v) BSA, centrifuged for 2 minutes, applied to all slides and left to incubate at 37°C for 30 minutes.

After incubation, the slides were rinsed three times in C-PBS with a change every five minutes. Finally, an anti-fade mounting media (FluoSave™) was carefully added to each of the tissue sections and a coverslip placed over the sections.

The slides were then stored at 4°C overnight before being examined on a Nikon Optiphot binocular microscope with a fluorescent attachment, using x4, x20, x40 and x100 objectives. The light source was a mercury vapour lamp and a B-2A filter (EX- 450-490, DM 505, BA 520) was used to view the labelled sections which fluoresced green.

2.3.3 Image Capturing

The AxioCam HRc (Zeiss) camera and computer software (AxioVision 3.1) was used to capture histological, immunohistochemical and immunofluorescence images. Digitally captured images were stored on compact disc using 8 bits colour with a spatial resolution of 1300 x 1030 pixels on the computer hard drive and copies kept on CD or DVD.

2.4 PROTEIN EXTRACTION

Canine claw is an extremely tough material and requires more rigorous manipulation to extract protein even compared to human nail, hair and skin samples. Several different extraction buffers were tested however, only the

50mM Tris HCl, pH 6.8; 1% (w/v) SDS; 2% (v/v) βME buffer extracted proteins from canine skin, germinative cells of the claw and the claw plate with good yield.

2.4.1 Cytoskeletal Protein Extraction Methodology

Proteins from human skin, hair and nail were extracted using the cytoskeletal extraction method. Tissue samples were pre-washed in PBS at room temperature and then placed in a glass-glass homogeniser and a reasonable excess of Triton X-100 buffer (10 mM Tris-HCl, pH 7.5; 5 mM EDTA; 1% (v/v) Triton X-100; 0.14 M NaCl; 5 mM EGTA and 1 mM DTE). The homogenate was then transferred to a glass centrifuge tube (Corex) and spun at 12, 000 rpm for 15-20 mins at 4°C. The supernatant was discarded and the pellet was then treated with a high salt wash. An excess of high-salt KCl-buffer (10mM Tris-HCl, pH 7.5; 5 mM EDTA; 0.5% (v/v) Triton X-100; 1.5 M KCl; 2 mM EGTA; 0.5 mM DTE) was added to the Triton-buffer pellet and mixed well to disperse. The mixture was transferred to a glass-glass homogeniser and homogenised on ice for 5-10 strokes. This was left for 15-20 minutes and the process repeated. The homogenate was transferred to a centrifuge tube (15ml Corex glass) and spun at 12,000 rpm for 20 minutes at 4°C. The supernatant was discarded and the pellet was placed on ice before being treated with a low salt buffer. An excess volume of low salt buffer (5 mM Tris-HCl, pH 7.5; 2 mM EDTA; 70 mM NaCl; 0.1% (v/v) Triton X-100; 2 mM EGTA and 0.5 mM DTE) was added to the high salt pellet and thoroughly homogonised. The mixture was transferred to a centrifuge tube and spun at 15,000 rpm for 20-30 minutes at 4°C. Again, the supernatant was discarded and the pellet was drained. The cytoskeletal preparation could be stored at this stage (-20°C or -70°C) or the intermediate filament proteins (e.g. keratins) can be extracted immediately.

The dry pellets were extracted in 200 µl - 500 µl of SDS-ME buffer (50 mM Tris-HCl, pH 6.8; 1% (w/v) SDS and 2% (v/v) βME). Generally, the pellet readily dispersed and dissolved in the SDS-ME buffer but if not the mixture was agitated using a pipette. The solution was transferred to a small glass homogeniser (0.5 ml or 1 ml) and was ground well. The homogenizer was then covered with parafilm and heated at 80°C for 10-15 minutes using a water bath. The solution was further homogenised whilst it was still hot and then transferred to a 1.5 ml

eppendorf. This was spun at 15,000 rpm (max speed on the eppendorf centrifuge) for 15-20 minutes at room temperature. The supernatant was collected and stored in a clean sterile eppendorf tube.

The extract can be analysed immediately or can be stored at -20°C or -70°C until required. Prior to storage, an aliquot (50 µl) was removed and diluted for one-dimensional (1D) electrophoresis with 50µl 2D/1D dilution buffer (Table 2.5). The diluting buffer contained EDTA which is a preservative that chelates divalent cations, and reduces the activity of proteolytic enzymes that require calcium and magnesium as cofactors. The dilution buffer contains glycerol to make the sample dense so it will remain in the bottom of the well under the running buffer. Bromophenol Blue dye is added so the buffer front can be observed during electrophoresis. All samples were labelled and stored at -20°C or -70°C until ready for use. Before running any protein extract on a one-dimensional gel, samples were prepared according to section 2.5.4.

Table 2.5: Preparation of Stock Solution for Diluting Buffer (2D/1D buffer)

Stock Buffer (50ml)	Quantity
0.5 M Tris HCl, pH 6.8	5.0 ml
10 % (w/v) SDS Solution	5.0 ml
20 mM (w/v) EDTA	5.0 ml
0.5% (w/v) Bromophenol Blue	2.5 ml
99.5% (w/v) Glycerol	20.0 ml
Distilled Water	Make up to 50ml

2.4.2 Total Protein Extraction Methodology

Proteins were extracted from canine and equine claw/hoof samples using a total protein extraction protocol. Tissue samples were pre-washed in Triton X-100 (4°C, 48 hours) and rinsed with distilled water. The samples were then transferred to a 1ml glass-glass homogeniser and homogenised in 50mM Tris HCl, pH 6.8 containing 1% (w/v) SDS and 2% (v/v) βME buffer (Table 2.6). The

rotary action of the homogeniser crushed the tissue and released the proteins which then dissolve in the buffered SDS.

Table 2.6: Preparation of 50mM Tris HCl, pH 6.8; 1% SDS; 2% βME Extraction Buffer

Chemical	Quantity	Final Concentration
10% (w/v) SDS	10 ml	1% (w/v)
βME	2 ml	2% (v/v)
0.5 M Tris HCl, pH 6.8	10 ml	50 mM
Distilled Water	Make up to 100ml	

The homogenised samples were then transferred to a sterile eppendorf tube and centrifuged at room temperature for 15 minutes at 15,000 g. The resulting supernatant was transferred to a clean eppendorf tube and was labelled first extract. The resulting pellet was homogenised further by repeating the above process, centrifuged again and this supernatant was labelled the second extract.

Solutions of each extract were prepared for one dimensional electrophoresis. A 50µl aliquot of the stock extract was placed in a clean eppendorf tube, 50 µl of 2D/1D dilution buffer (Table 2.5) was added, and the mixture was stored at -20°C until required. Before running any protein extract on a one-dimensional gel, samples were prepared according to section 2.5.4.

2.4.3 Urea Protein Extraction

Keratins are soluble in 6M-10M urea in the presence of reducing agents such as β-mercaptoethanol (βME) or dithiothreitol (DTT). Thus, adequate extraction, even from tough tissues, can be achieved by homogenising in a hot (40-60°C) Tris-Urea-βME buffer. The solubilised keratins were precipitated by dialysing the urea out. The efficacies of two different dialyis solutions (Tris-SDS-DTT and Citric Acid) on canine claw samples were tested.

2.4.3.1 Tris-SDS-DTT Dialysis

Canine claw samples were finely chopped using a scalpel and heated in 10M urea, 0.1M Tris, 10% (v/v) βME extraction buffer (Table 2.7) for 24 hours at 40°C. The samples were then homogenised in 1ml of this buffer and placed in dialysis tubing sealed at one end. The other end was sealed leaving an air gap equal in volume to the liquid.

Table 2.7: Preparation of Tris-Urea-ME (pH 7.5) Extraction Buffer (100ml)

Chemical	Quantity	Final Concentration
Urea	60.06g	10M
Tris	1.211g	0.1M
βME	10ml	10% (v/v)
Distilled Water	Make up to 100ml	

The tubes were placed into a twenty fold excess of 0.1M Tris-0.1% (w/v) SDS-0.1% (w/v) DTT dialysis solution (Table 2.8) and were constantly stirred for 2 hours at room temperature. The dialysis solution was changed three times (after 1 hour, 6-12 hours and 24-48 hours). One end of the dialysis tubing was cut below the knot and the liquid squeezed out carefully into a sterile eppendorf tube and centrifuged at 13 000 rpm for 15minutes. The supernatant was discarded and the resulting pellet was dissolved in 50mM Tris HCl, pH 6.8; 1% (w/v) SDS; 2% (v/v) βME (Table 2.6). The volumes were kept to a minimum to ensure that the concentration of protein was as high as possible. A 50µl aliquot was taken and double diluted with 2D-1D dilution buffer (Table 2.5).

Table 2.8: Preparation of Tris-SDS-DTT Dialysis Solution (100ml)

Chemical	Quantity	Final Concentration
Tris	1.211g	0.1M
SDS	0.1g	0.1% (w/v)
DTT	0.1g	0.1% (v/v)
Distilled Water	Make up to 100ml	

Before running any protein extract on a one-dimensional gel, samples were prepared according to Section 2.5.4.

2.4.3.2 CASC Dialysis

Using the same methodology as above, canine claw samples were finely chopped using a scalpel extracted with Urea-Tris-ME buffer and placed in dialysis tubing as before.

Table 2.9: Preparation of CASC (pH 2.3) Dialysis Solution (100ml)

Chemical	Quantity	Final Concentration
Citric Acid	2.10g	0.1M
Trisodium Citrate	2.94g	0.1M
Distilled Water	Make up to 100ml	

The dialysis tubing containing the samples was then placed in a twenty fold excess of CASC solution (pH2.3) solution and left for 24 hours to equilibrate (Table 2.9). The contents of the dialysis tubes were centrifuged and the resulting supernatant was carefully adjusted to pH 4.5 with 0.1N NaOH, at room temperature, until a fine white precipitate appeared. If the protein concentration was too low, the precipitate may not appear immediately and samples should be left at 4°C overnight. If the pH exceeds 4.5, the precipitate will redissolve. The precipitate was then centrifuged gently at 3,000 rpm and re-dissolved in fresh CASC at pH 2.3. The precipitation step was then repeated but the precipitate was washed in a neutral Tris buffer, pH 6.8 and then dissolved in 50mM Tris HCl, pH6.8 containing 1% (w/v) SDS and 2% (v/v) βME buffer by heating at 80°C. A 50 µl aliquot from this solution was taken and double diluted with 2D-1D dilution buffer. Before running the samples on a gel, 1ml βME was added to the sample and prepared as described in Section 2.5.4.

2.5 ONE-DIMENSIONAL ELECTROPHORESIS (SDS-PAGE)

Gel electrophoresis is a powerful and convenient method of separating macromolecules according to size. Both polyacrylamide and agarose gels with pores of a specified dimension are used to separate DNA, RNA and protein mixtures. In polyacrylamide gel electrophoresis (PAGE), pore size is controlled by the percentage of acrylamide and the ratio of acrylamide to bis-acrylamide. TEMED is a polymerising agent which links the acrylamide and bis-acrylamide monomers together. This reaction also requires ammonium persulphate (APS) as an oxidising agent.

The gel can be cast as a thin rectangular slab in which several samples can be simultaneously analysed in parallel lanes. The gel is placed into a buffer which acts as an electrolyte. Platinum wires in the electrophoresis equipment conduct an electric current through the gel applying a negative charge to the top and a positive charge to the bottom of the gel.

Protein samples are denatured using sodium dodecyl sulphate (SDS) which binds to the surface of proteins and induces them to assume a rod like shape. The large negative charge that the SDS imparts masks the protein's intrinsic charge so that SDS-treated proteins have similar charge-to-mass ratios and similar shapes. When an electric current is passed through the gel, the proteins migrate towards the anode (positive electrode) at the bottom of the gel for a given time sufficient to separate the proteins into a series of discrete bands according to molecular mass. A protein's molecular mass is determined by running samples together with several "marker" proteins of known molecular mass that bracket the proteins of interest. The protein bands are visualised by an appropriate stain, such as Coomassie Blue R-250 or for more sensitive detection, silver staining.

2.5.1 Preparation

A list of the volumes and quantities of each chemical used to make up all the solutions are provided in Appendix I.

Glass plates were washed in detergent and rinsed thoroughly with tap water and then distilled water. Before use, the inner surfaces of the plates were washed with distilled water, acetone and finally diethyl-ether. The plates were assembled with the clean inner surfaces facing each other and the appropriate spacers. A line was marked at 3 cm from the top of the glass plates as an indicator for the level of gel solution to be added. The glass plate assembly was then placed in the stand and clamped to seal the bottom.

2.5.2 Resolving Gels

A 12.5% resolving gel was prepared using five stock solutions (2M Tris-HCl pH 8.8, 20mM EDTA, 1.5% (w/v) APS, 5% (w/v) SDS, 30% (v/v) Acrylamide-Bis) and distilled water according to the volumes in Tables 2.10.

Table 2.10: Preparation of Resolving Gel (12.5%)

Stock Buffer	1 Gel	2 Gels	4 Gels
2 M Tris, pH 8.8	6.40 ml	12.80 ml	25.60 ml
20 mM EDTA	1.6 ml	3.20 ml	6.40 ml
1.5% APS (Fresh)	0.74 ml	1.48 ml	2.96 ml
5% SDS	0.64 ml	1.28 ml	2.56 ml
30% Acryl-Bis	13.33 ml	26.67 ml	53.34 ml
H_2O (Distilled)	9.29 ml	18.58 ml	37.16 ml
TEMED	0.15 ml	0.3 ml	0.6 ml

N.B. Acrylamide is a potent neurotoxin and is absorbed through the skin. Appropriate safety measures should be ensured when working with this chemical.

Gel polymerisation was initiated with TEMED and the mixture carefully poured between the two glass plates ensuring that no air bubbles formed. Approximately 1 ml of organic overlay (Table 2.11) was carefully layered on top of the gel mixture to prevent oxygen entering which would affect the polymerisation of the gel.

Table 2.11: Preparation of Organic Overlay (100ml)

Chemical	Amount
Isobutanol	80.0 ml
H_2O (Distilled)	20 ml

The gel was left to set for 30-45 minutes. The organic overlay was then rinsed from the gel surface with distilled water and 1-2 ml of resolving gel overlay buffer (Table 2.12) poured onto the surface and left for 10-30 minutes. The overlay buffer can be left on the gel overnight but the plates should be sealed with cling film to prevent evaporation of the buffer.

Table 2.12: Preparation of Resolving Overlay Buffer (100ml)

Chemical	Amount
2M Tris	20.0 ml
5% (w/v) SDS	2.0 ml
20 mM EDTA	5.0 ml
Sucrose	10.0 g
H_2O (Distilled)	Make up to 100ml

Gradient gels utilise a variable acrylamide concentration (7.5-17.5%) across the gel which increases its resolving power. These are made from two different solutions (Table 2.13), 7.5% (Flask A) and 17.5% (Flask B). The gradient gel was poured between clean class plates using a gradient mixer and a peristaltic pump (approximate flow rate 6 ml per minute). A thin layer of organic overlay (1ml) was poured onto the surface of the gel and left to set for 30 minutes before being rinsed off thoroughly using distilled water. The surface of the gel was then covered with 2ml of resolving gel overlay buffer and left to equilibrate for 30 minutes. The gel was then rinsed with distilled water before the stacking gel was poured.

Table 2.13: Preparation of Gradient Gels (7.5%-17.5%)

Stock Buffer	Flask	1 Gel	2 Gels	4 Gels
2M Tris, pH8.8	A&B	3.20 ml	6.40 ml	12.80 ml
20mM EDTA	A&B	0.80 ml	1.60 ml	3.20 ml
1.5% (w/v) APS (Fresh)	A&B	0.37 ml	0.74 ml	1.48 ml
5% (w/v) SDS	A&B	0.32 ml	0.64 ml	1.28 ml
30% Acryl-Bis	A	4.00 ml	8.00 ml	16.00 ml
H_2O (Distilled)	A	7.31 ml	14.62 ml	29.24 ml
30% Acryl-Bis	B	9.33 ml	18.66 ml	37.32 ml
H_2O (Distilled)	B	1.98 ml	3.96 ml	7.92 ml
Sucrose	B	1.50 ml	3.0 ml	6.0 ml
10% TEMED (polymeriser)	A&B	0.15 ml	0.30 ml	0.60 ml

2.5.3 Stacking Gel

The stacking gel was prepared using 0.5M Tris-HCl pH6.8, 20mM EDTA, 1.5% APS, 5% SDS, 30% Acrylamide-Bis and distilled water (Table 2.14). Gel polymerisation was initiated with TEMED and the stacking gel mixture carefully poured between the glass plates onto the surface of the resolving gel (after overlay buffer had been removed). A comb was carefully inserted making sure that no air bubbles were present. Once the gels had set the combs were carefully removed and 2 ml of stacking gel overlay was added to the wells and poured off. The wells were then filled with top running buffer.

Table 2.14: Preparation of Stacking Gel

Stock Buffer	1 Gel	2 Gels	4 Gels
0.5M Tris, pH 6.8	1.00 ml	2.00 ml	4.00 ml
20 mM EDTA	0.50 ml	1.00 ml	2.00 ml
1.5% (w/v) APS (Fresh)	0.50 ml	1.00 ml	2.00 ml
5% (w/v) SDS	0.20 ml	0.40 ml	0.80 ml
30% Acryl-Bis	1.35 ml	2.70 ml	5.40 ml
H_2O (Distilled)	6.45 ml	12.90 ml	25.80 ml
TEMED	0.015 ml	0.03 ml	0.06 ml

2.5.4 Sample Preparation

Protein samples prepared for one-dimensional SDS-PAGE were heated to 60°C for 10 minutes before being centrifuged at 13,000g for 15 minutes which ensured that no sediment was loaded onto the gel. It was essential to heat all samples as many proteins have significantly hydrophobic properties and may be tightly associated with other molecules, such as lipids through hydrophobic interaction. Heating the samples to 60°C prior to loading the gel literally "shakes" up the molecules, allowing SDS to bind to the hydrophobic regions and complete the denaturation of the protein.

The objectives of sample preparation are to put the proteins into a denaturing buffer, rendering them suitable for electrophoresis, and to adjust the sample concentrations so that an appropriate amount of protein could be loaded onto a gel. Depending on the sample, between 10-20µl was loaded onto the gel. Overloading resulted in precipitation and aggregation of proteins, producing streaks and smears. Under loading resulted with very little being viewed on the gel after staining.

The apparatus was then assembled and immersed in the main tank which contained approximately 3L of bottom running buffer (Table 2.15). Approximately 500ml of top running buffer (Table 2.16) was poured carefully

into the top well ensuring that the protein samples were not disturbed and that no leaking occurred.

Table 2.15: Preparation of Bottom Running Buffer (4L)

Stock solutions can be found in Appendix I

Chemical	Store	Volume
10 X TGRB	4°C	400 ml
10% (w/v) SDS	Room Temperature	40 ml
Distilled Water	-	3560 ml

Table 2.16: Preparation of Top Running Buffer (500ml)

Stock solutions can be found in Appendix I

Chemical	Store	Volume
10 X TGRB	4°C	50 ml
10% (w/v) SDS	Room Temperature	5 ml
DTT	4°C	230 mg
Distilled Water	-	445 ml

2.5.5 Sample Preparation and Running Conditions

Gels were stacked at 200V constant (~130 mA at beginning and ~80 mA at end of stacking run). When the bromophenol blue dye reached the stacking-resolving gel interface, the gel was then run at 30 mA (constant current) per gel until the dye marker had run off the bottom of the gel. Two gels were run simultaneously in a Hoefer Gel Unit (SE 600).

2.5.6 Fixing and Staining

After electrophoresis, the gels were removed from the glass plates and fixed in 300-400 ml of SDS-Gel Fixer (Table 2.17) for one hour at room temperature or overnight. Gels were then stained in 300-400 ml of SDS-Gel Stain (0.1% (w/v) Coomassie Blue R-250, 45% (v/v) methanol and 10% (v/v) glacial acetic acid) for 1-2 hours at room temperature. The staining solution was removed and the gel

was placed in a 400-500 ml of Gel Destainer. Usually 3 changes of destainer were required to efficiently remove the blue background from the gel. The proteins on the gel could then be visualised and photographs taken by placing the gel on a lightbox. These were taken with a Nikon digital camera (D1x) with a 90mm macro lens and a green filter.

Table 2.17: Chemicals for Visualising Proteins on SDS-PAGE Gel

Chemical	Store	Quantity	Material	Amount	Notes
SDS-Gel Fixer	Room Temp	2000 ml	Methanol (Fisher) Glacial Acetic Acid (BDH) H_2O	900.0 ml 200.0 ml 900.0 ml	Did not filter. 300-500ml was used per gel and this was discarded after a single use.
SDS-Gel Stain (0.1 % (v/v) Coomassie Brilliant Blue)	Room Temp	2000 ml	Coomassie Blue R-250 Methanol Glacial Acetic Acid H_2O (Distilled)	2.0 g 900.0 ml 200.0 ml 900.0 ml	The coomassie brilliant blue R-250 dye was thoroughly dissolved in the methanol initially. The glacial acetic acid and water were mixed thoroughly together and added to the dye-methanol solution. If the dye precipitated the solution was filtered (Whatman No 1 filter paper).
SDS-Gel Destainer	Room Temp	2000 ml	Glacial Acetic Acid Methanol H_2O (Distilled)	200.0 ml 100.0 ml 1700 ml	Did not filter. 300-500 ml was used per gel.

2.6 WESTERN BLOTTING

The term "blotting" refers to the transfer of biological samples from a gel to a charged membrane and their subsequent detection on the surface of the membrane. Western blotting (also called immunoblotting because an antibody is used to detect its specific antigen) was introduced by Towbin *et al* (1979) and is a valuable technique to identify specific proteins. The specificity of the antibody-antigen interaction enables a single protein to be identified in the midst of a complex protein mixture. Western blotting can be used to obtain qualitative and semiquantitative data relating to a specific protein in a mixture.

The first step in the Western blotting procedure is to separate macromolecules

using gel electrophoresis. The separated molecules are then transferred (blotted) onto a membrane, generally nitrocellulose or polyvinylidene fluoride (PVDF). The membrane was then blocked to prevent any non-specific binding of antibodies to the surface. The transferred protein is detected with an enzyme-linked antibody as a probe. An appropriate substrate is then added and together they produce a detectable product such as a chromogenic or fluorogenic precipitate on the membrane for colorimetric or fluorimetric detection. The most sensitive detection methods use a chemiluminescent substrate that, when combined with a specific enzyme, produces light as a by-product. The light output can be captured using x-ray film, a CCD camera or a phosphor-imager that is designed for chemiluminescent detection. Whatever substrate is used, the intensity of the signal should correlate with the abundance of the antigen on the blotting membrane, and in mixtures of proteins initially separated by SDS-PAGE, should identify a single protein of a specific molecular weight.

2.6.1 Preparation

Two gels were prepared by SDS-PAGE as outlined in Section 2.5 and pre-stained molecular weight markers were used as they provide a good indication of a successful western blot transfer to the membrane. Both gels were to act as a mirror of the other so it was essential that any protein sample loaded on one gel were loaded in the same order and manner on the other gel and that an accurate record of this was made.

After electrophoresis, both gels were carefully removed from the glass plates and the stacking gel was removed using a scalpel blade and discarded. A small incision was made on the bottom right hand corner of the resolving gel so that the orientation of each gel could be identified easily. The first gel was fixed and stained as outlined in Section 2.5.6 and images were captured for comparison with western blot data. The other gel was placed in blotting buffer (0.025M Tris, 0.0182M Glycine, 20% (v/v) methanol) until ready for use (Table 2.18).

Table 2.18: Preparation of Blotting Buffer

Chemical	Amount	Final Concentration
Tris (Sigma)	3.025g	0.025M
Glycine (Sigma)	13.66g	0.0182M
Methanol (Fisher)	200ml	20%
Distilled H_2O	800ml	

Whilst the SDS-PAGE gel was running, the PVDF membrane was cut to the same size as the gel using a template. Gloves were worn at all times when handling the membrane. After the membrane was cut to size, a small incision was made on the bottom right hand corner so that the orientation of the membrane was known after immunoblotting. The membrane was placed in a tray of pre-cooled methanol (~4°C) for 1 minute ensuring no air bubbles were present. The membrane was then rinsed twice in distilled water for 5 minutes each and then transferred carefully into blotting buffer and left for 10 minutes on a shaker at room temperature.

The immunoblotting cassette was placed negative side down in a tray containing blotting buffer and a piece of the foam was placed on top of this followed by a piece of filter paper cut to the same size as the foam. The SDS-PAGE gel was carefully placed on top of the filter paper positioned near the bottom of the cassette. Great care was taken to ensure that no air bubbles were trapped underneath the gel as this could interfere with protein transfer. The membrane was then placed on top of the gel carefully lining up both edges so that an exact copy of the gel would be obtained. Again, it was essential to ensured that no air bubbles were trapped between the membrane and the gel. The second piece of filter paper was then placed carefully on top of the membrane followed by the remaining piece of foam. The cassette was then clasped shut making sure that none of the contents slipped. This was transferred to the immunoblotting tank (Figure 2.6) which contained blotting buffer. A magnetic stirrer was placed in the bottom of the tank so that an even electrolyte mix and temperature was maintained during the transfer. A cooling system was also used to ensure that the apparatus did not overheat. Immunoblots were run overnight at 30V (0.1A).

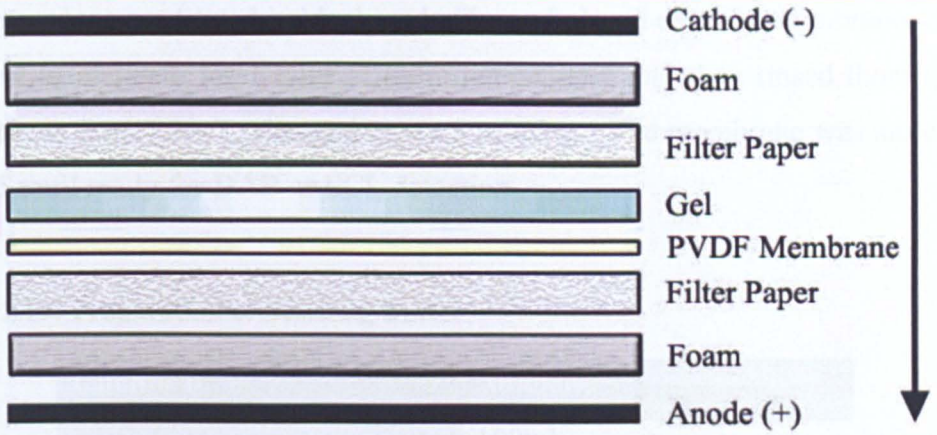

Figure 2.6: Schematic of Western Blot Transfer Method

Following electrophoresis, proteins in a polyacrylamide gel can be transferred to a positively charged membrane using Western Blot apparatus. The gel and membrane are sandwiched between two stacks of filter paper that have been pre-soaked in blotting buffer and submerged in the same buffer. The membrane is placed near the anode (positively charged), and the gel is placed near the cathode (negatively charged). SDS-coated negatively charged proteins are transferred to the membrane when an electric current is applied.

Once the transfer was complete, the SDS-PAGE gel was placed in fixative (Section 2.5.6) and then stained with coomassie blue to visualise any remaining protein on the gel. The membrane was carefully rinsed in TBS-T for 2 minutes and then placed in blocking buffer (5% (w/v) non-fat milk in TBS-T; see Table 2.19) to incubate for 1 hour at room temperature on an orbital shaker or overnight at 4°C. Stock solutions for western blot buffers are provided in Appendix I.

The membrane was rinsed three times (5 minutes each) in TBS-T before being placed in a solution containing the primary antibody which had been diluted using blocking buffer. The membrane was incubated in the primary antibody solution for 1 hour at room temperature on an orbital shaker so that an even spread of the solution was obtained over the entire membrane. Following incubation, the membrane was rinsed briefly in two changes of TBS-T and then thoroughly rinsed by subjecting the membrane to three, 5 minute rinses to ensure that all primary antibody solution was removed. Whilst the membrane was being rinsed, the biotinylated secondary antibody was diluted in Blocking Buffer. The membrane was again incubated in the secondary antibody for 1 hour at room temperature on an orbital shaker. After this, the membrane was rinsed twice briefly and then three times with TBS-T changed every 5 minutes. The streptavidin biotinylated

HRP complex was diluted in blocking buffer and placed over the membrane. This was left to incubate for 1 hour at room temperature and then rinsed thoroughly three times with TBS-T, changed every 5 minutes. The membrane was stored in TBS-T until ready for DAB or ECL detection.

Table 2.19: Preparation of Blocking Buffer

Chemical	Amount
TBS-T	100ml
Non-fat Milk (Marvel)	5g

2.6.2 Diaminobenzidine (DAB) Detection

A diaminobenzidine solution was used as one of the methods to detect the presence of keratin antigens on the immunoblot membrane. Aliquots of 0.6 mg/ml 3,3-diaminobenzidine tetrahydrochloride (DAB)/TBS-T solution were prepared and stored at 4°C. Using forceps, the membrane was placed carefully on SaranWrap™ and when ready, 2µl of 30% (v/v) H_2O_2 was added to the DAB solution and the mixture carefully poured over the membrane and left to develop for 2-3 minutes. To end the reaction, the membrane was placed in distilled water and finally rinsed in TBS-T. The membrane was wrapped in SaranWrap™ and covered in tin foil to ensure no light could enter and placed in a fridge. Images of the blots were captured using a Nikon Digital Camera (See section 2.5.6).

2.6.3 ECL Detection

An equal volume of detection solution 1 was mixed with solution 2 allowing sufficient total volume to cover the membranes. The final volume required was 0.125 ml/cm^3 membrane. Excess TBS-T was removed and the membrane was placed protein side up, on a sheet of SaranWrap™. The ECL detection reagent was pipetted on to the membrane and incubated for 1 minute at room temperature. The excess was then drained off by holding the membrane gently with forceps and touching the edge against a tissue. The blot was then placed protein side down onto a fresh piece of SaranWrap and this was wrapped around the membrane to

form an envelope. Avoiding too much pressure on the membrane, the SaranWrap was smoothed out to ensure no air bubbles were trapped. In a dark room using film safe red lighting, the wrapped blot was then placed protein side up in an X-Ray cassette and a sheet of Hyperfilm ECL was carefully placed over the membrane. The cassette was then closed and left to expose for 15 seconds. The film was then carefully removed using forceps and placed in a tray containing developer until the bands appeared. The film was then placed in water for a few seconds to remove any excess developer before being transferred into fixer for approximately one minute. Finally, the film was placed in a tray under running water for about 15 minutes and then allowed to air dry.

ECL immunoblot images were captured using a Nikon Digital Camera (See Section 2.5.6).

CHAPTER 3

3 ANATOMICAL STRUCTURE OF THE DOG CLAW

3.1 INTRODUCTION

Budras and Seidel (1992) attempted to eliminate confusion in the literature on the segmental anatomy of the canine claw. They suggested a logical classification based on topographical examination and tried to introduce terminology that would adequately describe both the equine hoof and the claws of domestic animals. This work was based on an anatomical study of 20 dog claws and five different regions were defined in the proximal to distal direction: periople, crown horn, wall horn, sole horn and pad. They also studied the detailed structure of the adjacent tissue and examined the structure of the epidermal and dermal components by SEM. They concluded that the structure of the adjacent tissue differed in these defined regions. For example, the crown horn was characterised by dermal papillae and epidermal tubule formation while the wall horn had more of a dermal/epidermal plate structure and no tubules. Furthermore, they described the sole as producing a soft and crumbly horn material and they found large tubules in the region between the tip of the bone and the tip of the claw (identified as terminal horn). Many, but not all of these observations have been confirmed, and in some instances extended, by the present study.

However, a detailed account of the micro-anatomy of the canine claw is lacking from the literature and no work has been done to relate the molecular analysis of claw structural proteins to the micro-anatomy. Thus, the aim of this work was to define the macro- and micro-anatomy of the canine claw to provide a robust framework for understanding structural protein expression within this complex tissue.

The macro-anatomy of the claw was investigated to provide a background framework and this included removing the claw from the phalanx and examining each component carefully using a dissecting microscope. In addition, both longitudinal and transverse sections of the canine digit were cut and stained to investigate the micro-anatomy (tissue histology) of the claw in microscopic detail.

3.2 METHODS

3.2.1 Macro-Anatomy

The foot pad was carefully removed from digit III of the left hind paw of dogs D and F using a scalpel and examined under a dissecting microscope. The claw fold was examined *in situ* prior to removal, after which the claw and underlying phalanx were subjected to collagenase (48 hours at room temperature) to allow separation. The whole claw was removed carefully removed from the underlying distal phalanx and each of the components examined under a dissecting microscope. Representative specimens were photographed (Nikon D1x Digital SLR Camera) and then stored in distilled water to prevent drying out.

Parasaggital views of whole canine claw were obtained digits I and II from the left hind limb of dogs A and D and cutting them in half using a band saw along the midline of the claw. Transverse sections of digits I and IV from the left hind limb of dogs B, F and H were obtained by cutting the claw into five equal sections at 90° to the tubular structures. They were labelled 1-5 in an ungual groove to distal direction and sections were stored in formalin for histological examination after macroscopic studies had been performed. Comprehensive notes and sketches of the macroscopic anatomy of the claw were made and photographs of various claw components were taken (Nikon D1x Digital SLR Camera).

3.2.2 Micro-Anatomy

Histological techniques were employed to examine the microscopic architecture and relationship of the different types of tissue in the canine claw, and secondly provide a detailed investigation of the structure of the individual cells (cytology) to learn more about the physiological function of these tissues.

After examining and recording the macroscopic details of the parasaggital and transverse views of the dog claw gross sections, these were fixed in formalin for 48 hours. Claw sections were then de-calcified in EDTA for three weeks, processed in cedar wood oil and embedded in paraffin wax. Histological sections

(5µm) obtained with a sledge microtome, were mounted on APES coated slides and left to dry in an oven (37°C) for 24 hours.

The slides were then de-waxed and re-hydrated in three aliquots of xylene and varying grades of alcohol (100% (v/v) twice, 90% and 70%), rinsed in distilled water and stained with haematoxylin solution for approximately 5 minutes. Finally, sections were then counter-stained with 1% (w/v) aqueous eosin for 30-45 seconds.

After staining, the specimens were dehydrated in ascending grades of alcohol (70%, 90%, 100% twice) and three aliquots of xylene. The stained sections were covered with Ralmount media and a coverslip was carefully placed over each slide. Slides were allowed to dry in a 45°C oven for 48 hours and the stained sections could then examined using a light microscope.

3.3 Results

3.3.1 Macroscopic Anatomy of the Dog Claw

Macroscopically, the canine digit can be divided into six regions: bony phalanx, hairy skin, claw fold, keratinised claw (horn) plate, sole and pad (Figure 3.1).

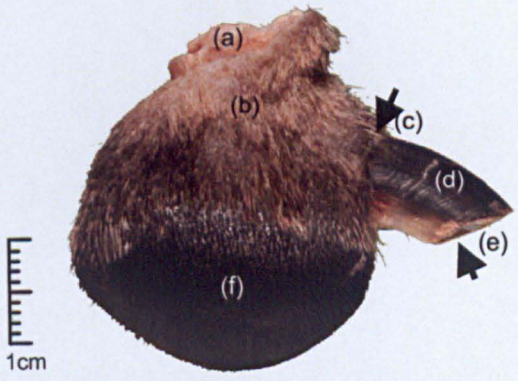

Figure 3.1: Side view of Canine Digit

The six major regions of the canine digit are shown: (a) second phalanx, (b) hairy skin, (c) claw fold, (d) claw (horn) plate, (e) sole and (f) digital foot pad.

The canine claw (horn) plate was a hard keratinised covering of the distal phalanx. The beak like shape was characteristic and the proximal end of the claw slotted into the bony ungual groove. The hair-bearing skin covering the upper part of the digit becomes specialised as it meets the claw, forming the claw fold, an area of hairless skin that was fixed to the claw plate surface.

The claw plate was not solid but a tubular structure and formed an incomplete tube, which did not meet on the underside (Figure 3.2). A softer epithelium, known as the sole, filled in the gap on the underside (ventral surface) of the claw. The sole was firmly connected to the claw plate on the dorsal aspect but was more loosely connected ventrally.

The digital pad varied in appearance when comparing the edges to the centre (Figure 3.2). Ridge-like structures were extremely prominent in the region adjacent to the claw but these coalesced towards the centre of the pad. The ventral surface of the claw tip was separated from its corresponding digital foot pad by a groove. At this point, the tubular structures were more undulating and 'finger' like in appearance.

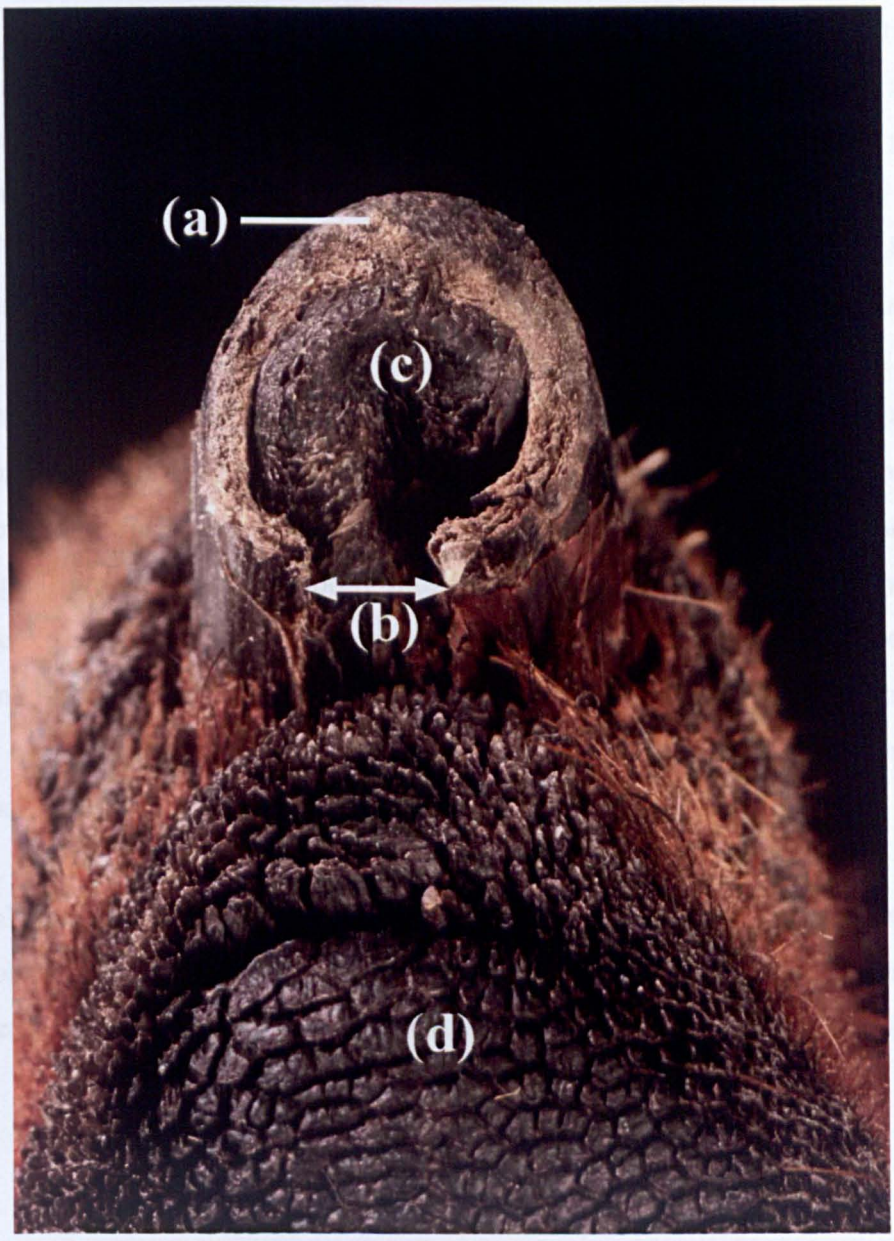

Figure 3.2: Underside View of Canine Digit

Underside view of a canine digit showing the tubular nature of the claw plate (a), the gap on the underside of the claw forming an incomplete tube (b), sole material inside the terminal portion of the claw (c) and the papillated pad (d).

After collagenase digestion, the claw plate was removed and the main structures of the distal phalanx were identified (Figures 3.3, 3.4, 3.5 & 3.6). The ungual process was a smooth beak like structure, which projected from the ungual crest (Figure 3.3). Surrounding the proximal end of the ungual process and housed within the ungual crest was the ungual groove, which appeared as a horseshoe with a bony interruption on the ventral side of the phalanx, stopping the groove being a complete circle (Figures 3.4 & 3.6). It is this shape of the ungual groove that causes the claw plate to form an incomplete tubular structure. On the dorsal side of the ungual process, a major prominence of the longitudinal ridge (LR) was observed (Figures 3.5 & 3.6). This structure was widest in the proximal claw and narrowed continually along the phalanx and disappeared at the tip. The longitudinal ridge leaves a clear indentation in the claw plate, which locks around this bony structure (Figure 3.5). When the distal phalanx was removed from the claw and examined, it showed that the longitudinal ridge extended right back into the ungual groove creating a bony interruption on the dorsal aspect of the claw (Figure 3.6). Although this bony interruption was found in nearly all of the claws examined, there were instances where the longitudinal ridge was not observed to totally block the ungual groove. This finding did not appear to be claw or breed specific.

Dermal laminae were more apparent on non-pigmented claw (horn) plates and were observed to run parallel to the longitudinal ridge. However, it was difficult to ascertain macroscopically if they also existed on the longitudinal ridge (Figure 3.5).

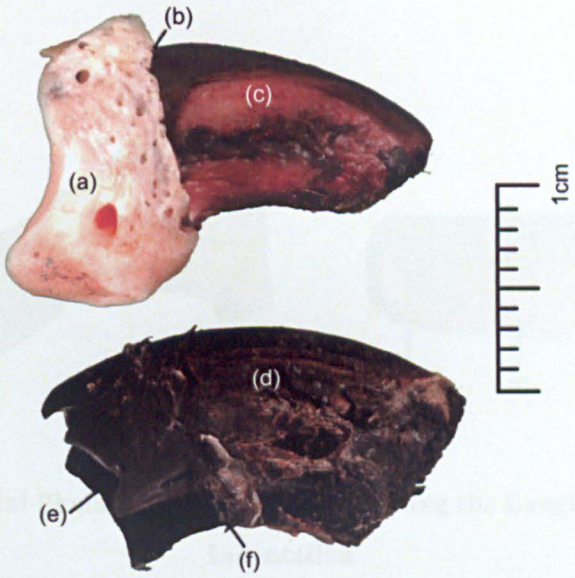

Figure 3.3: Distal Phalanx (above) after removal of Claw Plate (below)

The major regions of the bony distal phalanx (a-c) and the separated claw (horn) plate (d-f) are labelled: (a) ungual crest, (b) ungual groove, (c) ungual process covered in periosteum and dermal tissue, (d) claw (horn) plate, (e) inner claw sheath still attached to the claw (this region of claw was located within the ungual groove) and (f) sole.

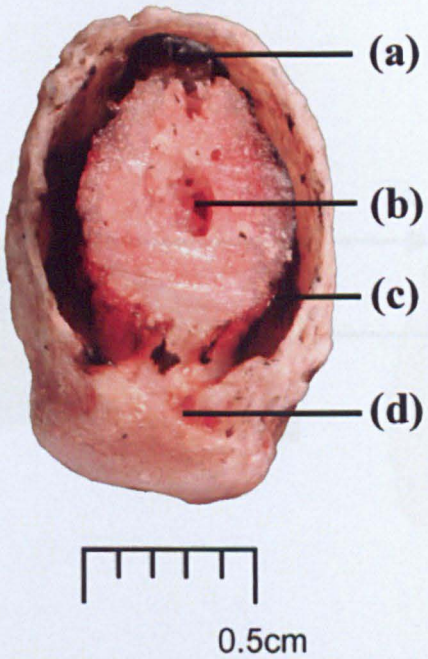

Figure 3.4: Distal Phalanx showing Bony Region on Ventral Side of Ungual Groove

The ungual process that projects beyond the ungual groove was removed and the remaining distal phalanx photographed end on. This highlights the ungual groove and both the dorsal and ventral bony projections. The four major regions are marked: (a) longitudinal ridge (b) remaining portion of the ungual process (c) ungual groove and (d) bony region on ventral side of distal phalanx

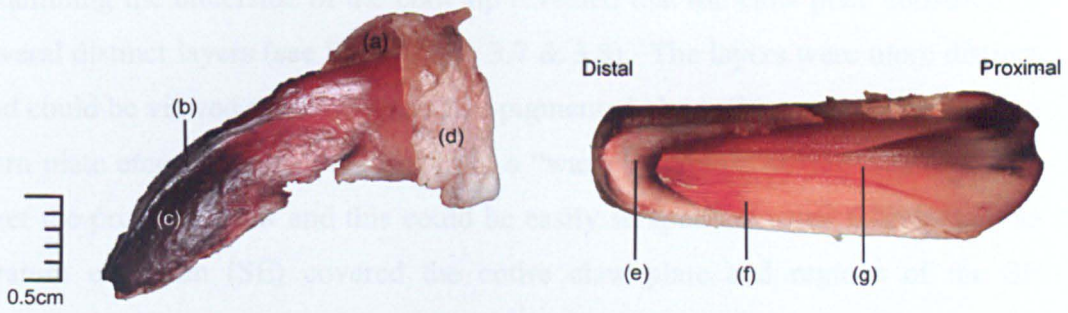

Figure 3.5: Distal Phalanx and Claw Plate showing the Longitudinal Ridge Indentation

The major structures of the distal phalanx are shown: (a) ungual groove, (b) longitudinal ridge, (c) ungual process and (d) ungual crest. Note that the distal phalanx has been damaged and is not complete. The inner aspect of the horn plate shows three main regions: (e) sole, (f) epidermal laminae and (g) longitudinal ridge indentation on the claw, which provides a "lock and key" mechanism with the distal phalanx, preventing rotation of the horn around the bone.

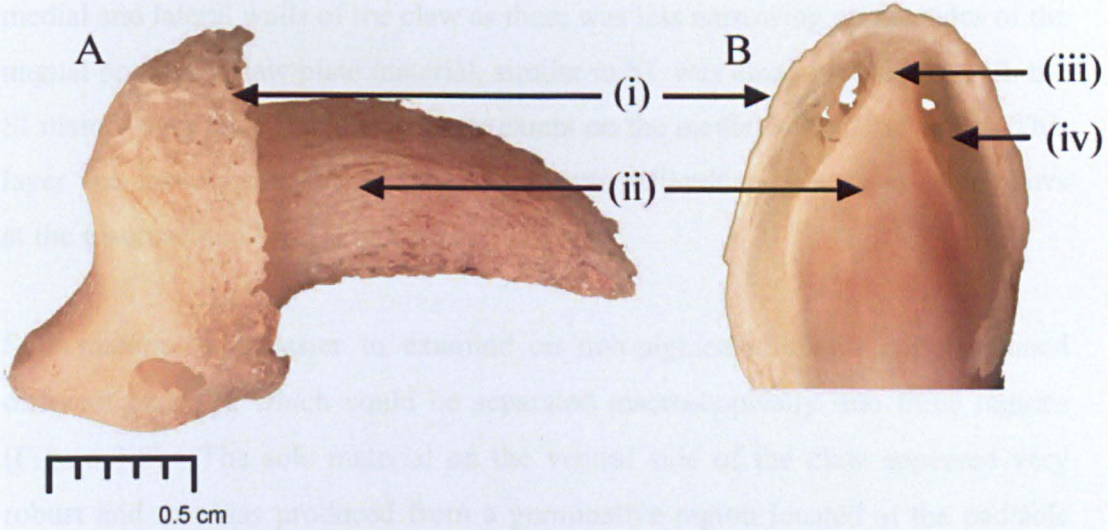

Figure 3.6: Distal Phalanx of the Canine Claw

Side view **(A)** and head on view **(B)** of distal phalanx showing the major structures: (i) ungual crest, (ii) ungual process, (iii) longitudinal ridge and (iv) ungual groove.

Examining the underside of the claw tip revealed that the claw plate consisted of several distinct layers (see Figures 3.2, 3.7 & 3.8). The layers were more distinct and could be viewed more easily in non-pigmented claws (Figure 3.7). Where the horn plate emerged from the claw fold, a "waxy" visible covering was observed over the proximal claw and this could be easily scraped off using a scalpel. The stratum externum (SE) covered the entire claw plate and regions of the SE towards the claw tip were often damaged.

At the claw tip, the stratum medium (SM) was observed lying immediately beneath the SE. It appeared thickest on the dorsal surface and thinned out towards the lower medial and lateral walls (Figure 3.7). The stratum internum (SI) was located on the innermost portion of the claw plate and this formed another compact layer that was thicker on the dorsal aspect of the claw when viewed at the claw tip. The outline of the SI at the claw tip adopted the shape of the longitudinal ridge (LR) due to SI material filling the emerging gap between the claw plate and the bony phalanx. From this point, the LR continually became less pronounced distally along the ungual process. Thus, the SI was thinner on the medial and lateral walls of the claw as there was less narrowing on the sides of the ungual process. Claw plate material, similar to SI, was also observed beneath the SI mainly over the LR and to a lesser extent on the medial and lateral walls. This layer was loosely connected to the SI and was difficult to identify in some claws at the macroscopic level (Figure 3.7).

Sole material was easier to examine on non-pigmented claws and contained different textures, which could be separated macroscopically into three regions (Figure 3.8). The sole material on the ventral side of the claw appeared very robust and this was produced from a germinative region located at the pad/sole joint and extended over the underside of the claw, filling in the gap between the lower lateral and medial walls of the claw plate. For the purpose of this thesis, this region has been termed sole 1 (S1). S1 material contained a fissure, which was visible in the centre of the cleft on the ventral claw and extended from the foot pad/sole joint to the claw tip. After carefully removing the horn plate from

the distal phalanx, S1 was noted to connect to the bony prominence on the ventral part of the phalanx as well as connecting to the epithelium of the digital foot pad. Another type of sole material, termed sole 2 (S2), was present on the inside of the claw plate that covered the medial and lateral walls and S2 increased in thickness distally (Figures 3.8 & 3.9). S2 was smooth and spongy compared to the other sole types and acted as a "cushion" between the hard, keratinised claw plate and the underlying distal phalanx. Towards the apex of the digit, a different texture of sole material was present, termed sole 3 (S3), which was tough and more rubbery compared to S1 and S2. S3 covered the entire tip of the ungual process and a depression was observed in the centre, which looked like an upside down 'V' that was connected to the fissure in S1 along the underside of the claw.

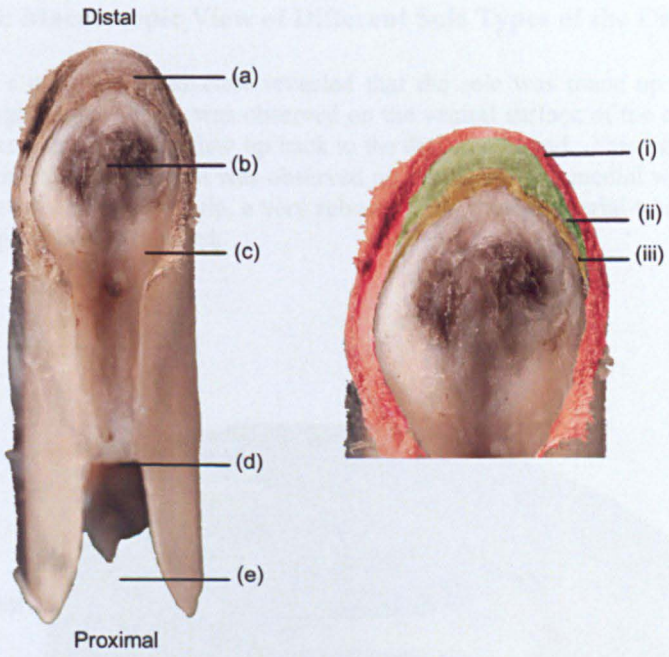

Figure 3.7: Underside View of Canine Claw Horn.

The major structures on the underside of the canine plate are shown: (a) claw plate, (b) sole, (c) fissure in sole material, (d) start of sole production where bony region of ungual groove ends and (e) location of bony region in ungual groove inhibiting claw production all the way around the distal phalanx. A section has been enlarged and coloured to show the different regions of horn in the claw. (i) The **stratum medium** ***(red)*** appeared more compact in the dorsal region becoming less dense in the lower lateral and medial walls. (ii) The **stratum internum** ***(green)*** appeared to consist of more than one layer but this was difficult to ascertain in such a macroscopic view. (iii) Thickening also occurred below the SI layer ***(yellow)*** mainly over the longitudinal ridge (LR) and to a lesser extent on the medial and lateral walls. An approximate outline of the LR can be traced within the SI where new horn was generated to replace the LR which decreased in size in a distal direction.

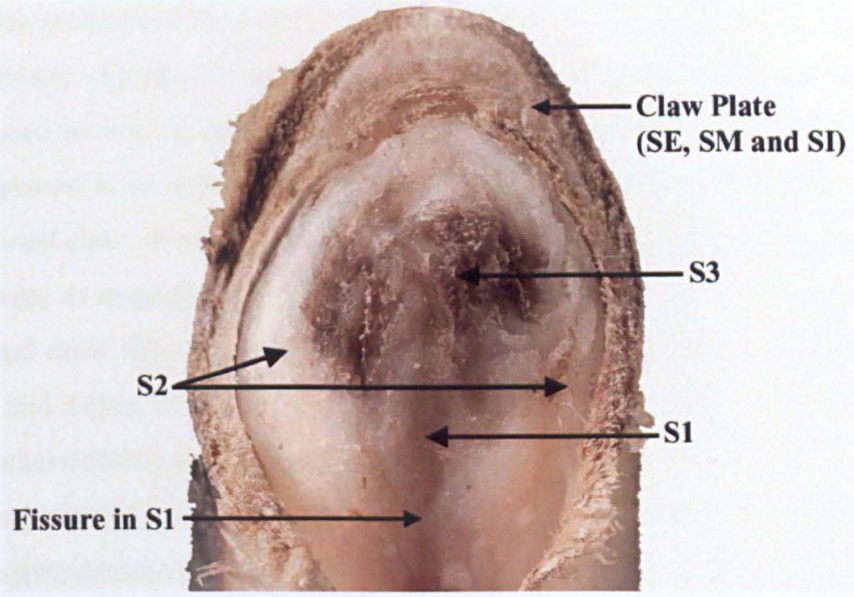

Figure 3.8: Macroscopic View of Different Sole Types of the Canine Digit

The underside of a non-pigmented claw revealed that the sole was made up of more than one epithelium. A tough, compact sole was observed on the ventral surface of the claw and contained a fissure, which extended from the claw tip back to the digital foot pad. This has been termed sole 1 (S1). A pale, smooth sole material was observed on the lateral and medial walls, termed sole 2 (S2). Covering the apex of the claw tip, a very robust, rubbery sole material was seen, termed sole 3 (S3). The claw plate is also labelled.

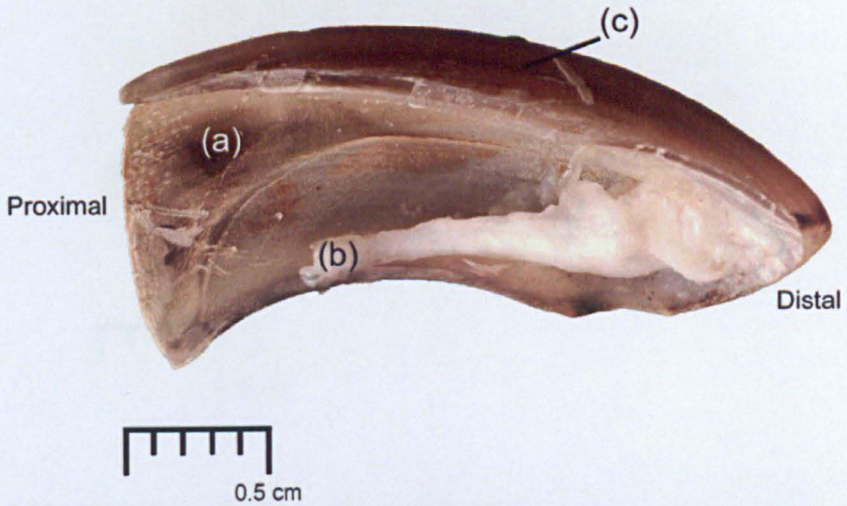

Figure 3.9: Inside View of Canine Claw Plate Showing Location of Sole 2 (S2)

The claw plate is shown with the proximal portion on the left and three prominent regions are labelled: (a) The area where the longitudinal ridge leaves a clear indentation on the inside of the horn plate, (b) S2, which originated as the claw plate emerged from the claw fold approximately one third the way along the distal phalanx and only existed on the lower parts of the lateral and medial walls and (c) external surface of horn plate.

Transverse sections of the proximal claw provided further information about claw plate anatomy. Firstly, it was established that the SM was the only horn section to be produced within the ungual groove of the distal phalanx and production of this layer appeared to be asymmetric. After several transverse sections were cut from the proximal claw, it was noted that the horn plate did not appear as a solid "horse shoe" shape as expected but was broken by bony interruptions. Several holes in the ungual crest that accommodate arteries and veins were also observed. The arteries and veins travel through the ungual crest into the underlying ungual groove where claw germinative cells are located. These small pores in the ungual crest can be used as a basic guide to demonstrate the shape of the ungual groove and an approximate outline of this structure can be obtained (Figure 3.10). This demonstrated that the groove was deepest in the dorsal region and narrowest towards the lateral and medial walls.

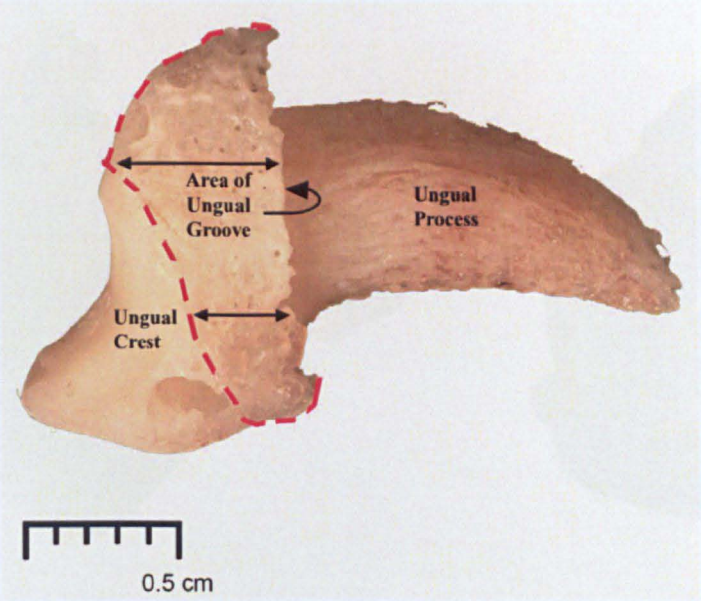

Figure 3.10: Side View of Canine Claw Showing the Shape of the Ungual Groove.

Macroscopic examination of the ungual crest of the distal phalanx revealed a thin porous bony region, which defined the shape of the ungual groove located beneath the ungual crest. As the diagram demonstrates, the ungual groove was not of uniform depth all the way around and was deepest on the dorsal region of the digit.

The shape of the groove suggested that SM horn production was initiated on the dorsal surface of the ungual groove where the groove was deepest. In claws where the longitudinal ridge completely blocked the groove, SM horn was produced either side of this bony ridge, which created a notch in the resulting claw plate. In more dorsal transverse sections, SM horn increased over the lateral and medial walls until it reached a point where it traversed most of the ungual groove creating a "horse shoe" structure (Figure 3.11). Inspection of some collagenase treated claw capsules revealed that the ventral portion of the proximal edges of the horn plate extended deeper into the ungual groove. As the proximal edge of the claw horn plate mirrors the shape of the groove, this projection would suggest that the ungual groove was not smooth in circumference and that indentations exist in the lower parts. This may be another anchoring mechanism in addition to the LR, which would help to prevent sideways rotation of the horn plate over the distal phalanx. The indentations on the lower lateral and medial walls were only observed in some of the claws tested and were not breed or digit specific.

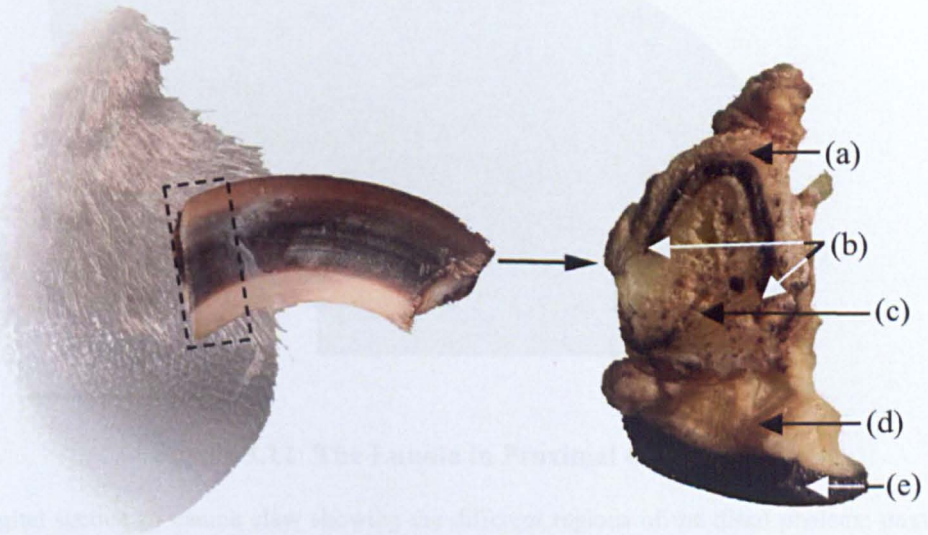

Figure 3.11: Transverse Section 1 (TS1) Showing Claw Plate Development in the Proximal Claw

Due to the slight angle this TS1 was cut, the SM was observed to extend further down one side of the ungual groove (b), suggesting that SM production is not uniform around the whole claw. The ungual crest (a), ungual process of distal phalanx (c), subcutaneous fat of the digital pad (d) and epidermis of the digital foot pad (e) are labelled.

In TS1 and parasaggital sections, the dermis thickened considerably immediately beneath the stratum medium of the claw plate. It reduced slightly in thickness towards the medial and lateral walls and in transverse sections taken further down the claw, it also thinned out and formed a small groove where stratum medium horn production ceased (Figure 3.12). The dermal mesenchyme thickness at this point changed considerably to a thin, uniform translucent layer, which covered the rest of the ungual process. Where the alteration in dermal thickness occurred, a groove formed that marked the point at which stratum internum (SI) horn production began. A similar thick dermal structure occurred in both human fingernails and in the equine hoof, known as the lunula and the coronary cushion respectively. For the purpose of this thesis, this thickened dermal structure will be referred to as the lunula, as the claw bares more resemblance to the human nail in both structure and function.

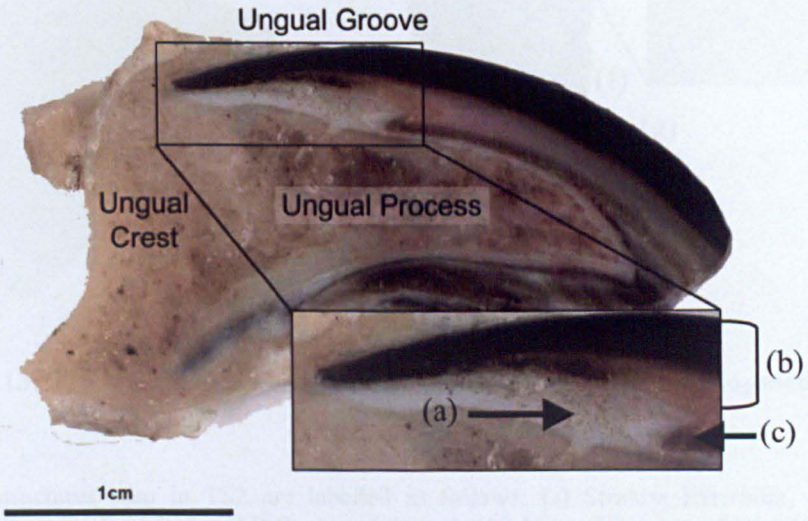

Figure 3.12: The Lunula in Proximal Claw

A parasaggital section of canine claw showing the different regions of the distal phalanx: ungual process, ungual crest and ungual groove. The lunula appeared as a pale material (a) in the proximal claw lying over the longitudinal ridge and beneath stratum medium horn (b). Where the lunula terminates, a groove is formed (c) within which stratum internum horn production begins. At this point, the dermis thins dramatically and forms a thin pale layer covering the rest of the ungual process.

Moving distally, TS2 and TS3 samples were very similar and both demonstrated a slight thickening of the SM (Figure 3.13). At this level, the SM was present on both the dorsal aspect and lateral walls of the claw and was uniform in thickness. The longitudinal ridge (LR) was extremely prominent at this position creating a

large bony projection on the dorsal side of the ungual process. This formed what appeared to be a rounded 'key hole' structure in transverse section and the area that the notches created in the LR, was filled by expansion in the SI layer. The SI was a lot thicker on the dorsal ridge of the claw and thinned out along the medial and lateral walls. In some claws, this region was pigmented while in other claws it was non-pigmented and this did not appear to be claw or breed specific.

At this location along the claw, the ungual process projected from the ungual crest. On the underside, where no horn plate production occurred, a soft pale epithelium (termed S1) was observed.

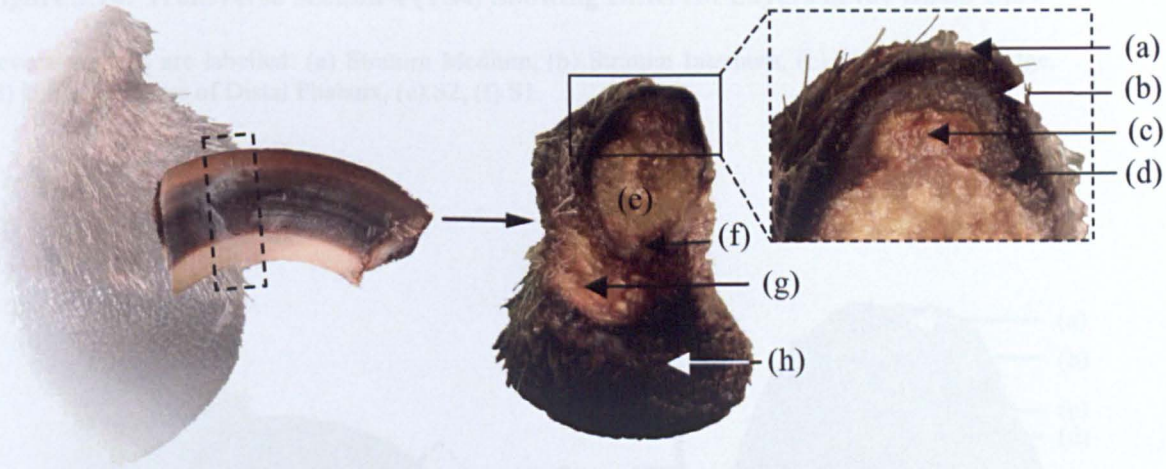

Figure 3.13: Transverse Section 2 (TS2) Showing Claw Plate Development at the Claw Fold

The major structures seen in TS2 are labelled as follows: (a) Stratum Externum, (b) Stratum Medium, (c) Longitudinal Ridge, (d) Stratum Internum, (e) Ungual Process of Distal Phalanx, (f) S1, (g) Subcutaneous Fat of Digital Foot Pad and (h) Epidermis of Digital Foot Pad.

In TS4 sections, both horn plate and sole had increased in thickness to compensate for the decrease in ungual process volume (Figure 3.14). The signature 'keyhole' appearance of the longitudinal ridge had now become less apparent due to a constant reduction in size and this was eventually replaced by lighter horn material (SI), which adopted the shape of the 'keyhole'. Moving distally, TS5a revealed a new, thin, translucent layer located over the dorsal surface of the ungual process, which connected the claw plate to the underlying phalanx (Figure 3.15).

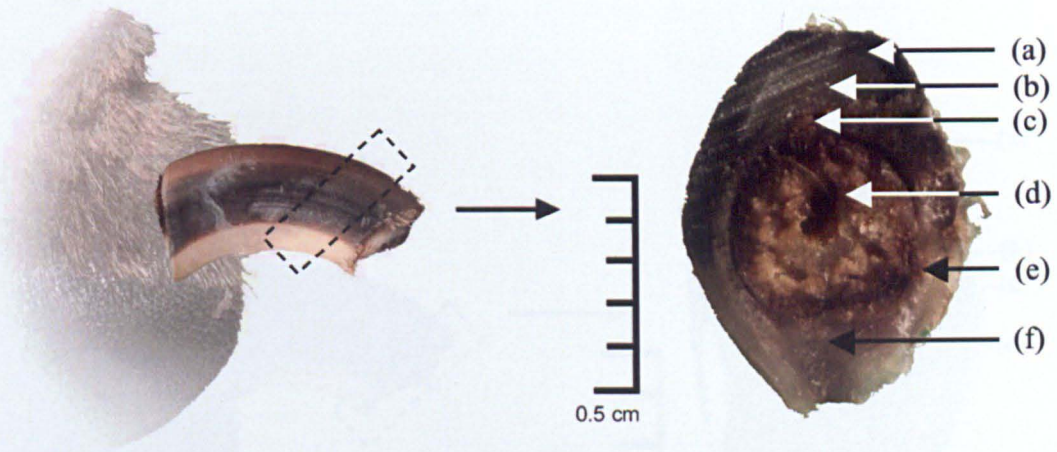

Figure 3.14: Transverse Section 4 (TS4) Showing Different Layers in the Distal Claw

Several regions are labelled: (a) Stratum Medium, (b) Stratum Internum, (c) Longitudinal Ridge, (d) Ungual Process of Distal Phalanx, (e) S2, (f) S1.

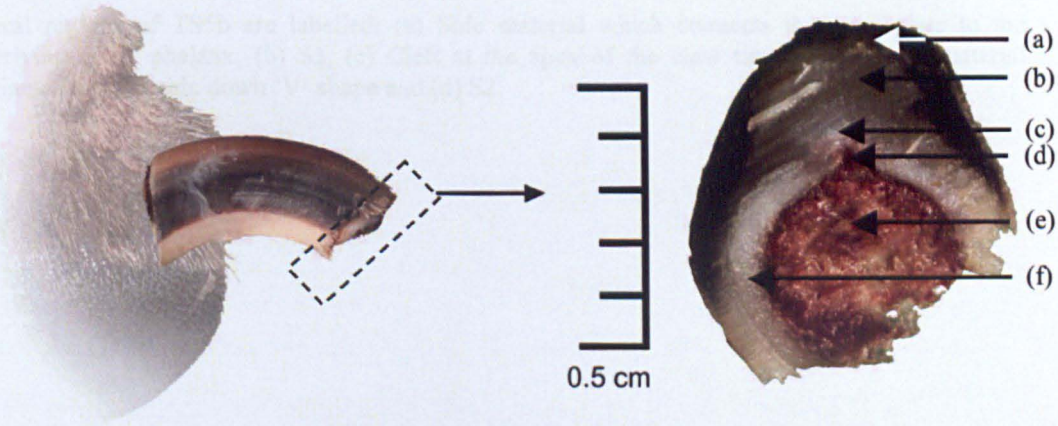

Figure 3.15: Transverse Section 5a (TS5a) showing Different Layers at the Claw Tip

Several regions of TS5a are labelled: (a) Stratum medium, which had slightly thinned on the dorsal surface probably due to wear and tear, (b) Stratum Internum, (c) Thin layer which connects claw plate to underlying distal phalanx (d) Longitudinal Ridge, (e) Ungual Process of Distal Phalanx and (f) S2.

At the very tip, only sole material was found in TS5b sections (Figure 3.17), as the surrounding horn plate had fallen away leaving only the soft, rubbery sole which 'plugs' the distal tip of the ungual process. Although hard to visualise, as all sole material was pale in colour, a rough outline of each region could be seen.

A distinctive cleft appeared at the apex of the tip outlining a region where the sole material culminates in an upside down 'V' shape.

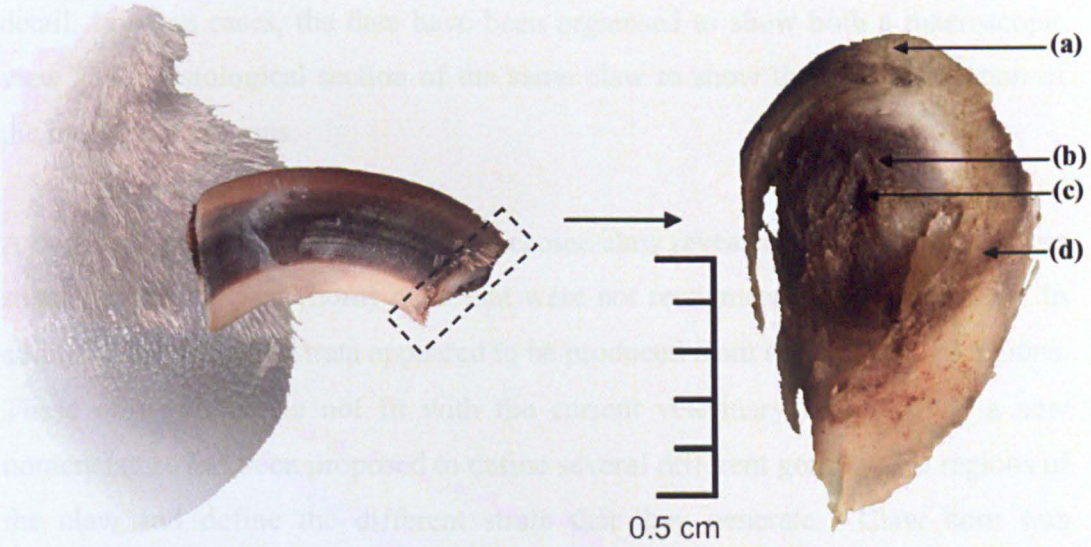

Figure 3.16: Transverse Section 5b (TS5b) Showing Different Sole Types

Several regions of TS5b are labelled: (a) Sole material which connects the claw plate to the underlying distal phalanx, (b) S3, (c) Cleft at the apex of the claw tip where the S1 material terminates in an upside down 'V' shape and (d) S2.

3.3.2 Microscopic Anatomy of the Canine Claw

Parasaggital and transverse sections of the canine digit were stained with haematoxylin and eosin to reveal the claw and its components in microscopic detail. In some cases, the data have been organised to show both a macroscopic view and a histological section of the same claw to show the precise location of the individual sections.

A detailed microscopic analysis of the canine claw revealed a number of different strata within the claw (horn) plate that were not recognised macroscopically. In addition, the different strata appeared to be produced from several distinct regions. These observations do not fit with the current veterinary literature, so a new nomenclature has been proposed to define several different germinative regions of the claw and define the different strata that they generate. Claw horn was produced from at least seven distinct germinative regions (GR 1-7) and sole horn was produced from a further three regions (GR 8-10).

Table 3.1: Germinative Regions of the Canine Claw.

Ten germinative regions (GR1-10) have been defined and these produced distinct structures in the claw: ICS, SE, SM1, SM2, SM3, SM4, SI1, SI2, S1, S2, S3 and S4.

Germinative Region (GR)	Old Literature	Claw Structure Produced	Dermal Configuration
GR1	Basal Matrix	ICS, SE and SM1	Micro-Papillated
GR2	Basal Matrix	SM2 (contains tubules)	Papillated
GR3	Not defined	SM3	Micro-Papillated
GR4	Not defined	SM4	Micro-Papillated
GR5	Terminal	SI1 (contains tubules)	Micro-Papillated
GR6	Sterile Matrix	SI2	Micro-Papillated
GR7	Not defined	Sole 4 (S4)	Papillated
GR8	Not defined	Sole 1 (S1)	Papillated
GR9	Not defined	Sole 2 (S2)	Laminar
GR10	Not defined	Sole 3 (S3)	Papillated

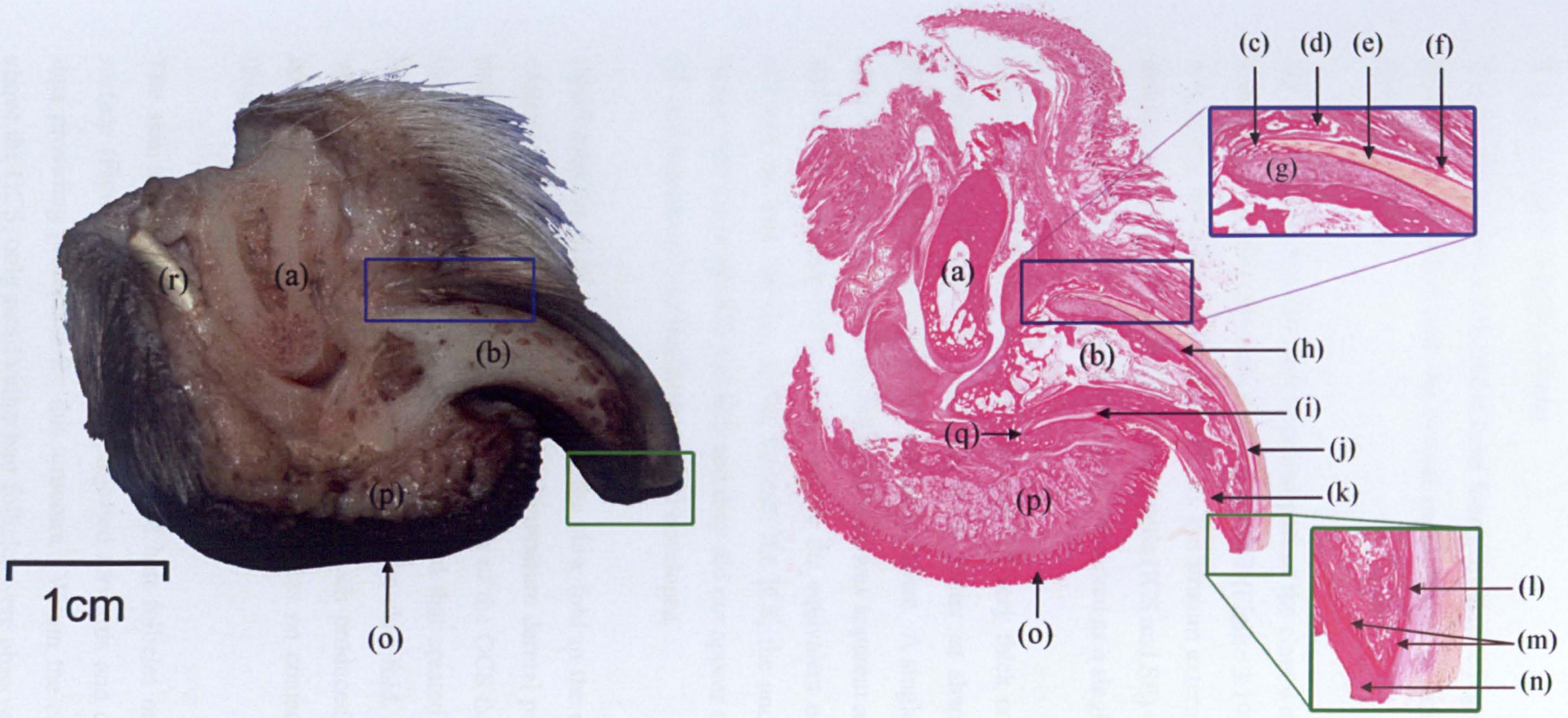

Figure 3.17: Parasaggital Macroscopic View and corresponding Histology from the same Canine Digit.

Macroscopic view (left) and histological section (right) of the same canine digit showing: (a) second phalanx, (b) ungual process (distal phalanx) (h) GR5 (produces SI1), (i) region where S1 on ventral claw surface joins to digital foot pad, (j) GR6 (micro-papillated germinative region producing SI2), (k) S1 material produced by papillated GR8 located on the ventral surface of the claw, (o) digital foot pad epidermis, (p) subcutaneous fat of digital foot pad, (q) claw horn produced in the lower region of the ungual groove and (r) deep digital flexor tendon. **Blue box**, higher power view of the claw fold: (c) GR1 and GR2, (d) ungual groove, (e) SM1-4, (f) claw fold (OCS, ICS, SE and SM1-4) and (g) lunula. **Green box** shows higher power view of claw tip: (l) GR7 (produces S4), (m) GR10, (papillated germinative region producing S3) and (n) S3.

3.3.2.1 Claw (Horn) Plate

The proximal claw contained at least four germinative regions (GR1-4) where the epithelium interacted with the dermal mesenchyme in different ways to produce distinct epithelia.

GR 1 was located at the most proximal part of the claw within the ungual groove. These germinative cells were adjacent to GR2 (Figure 3.19) and gave rise to three cell layers: the inner claw sheath (ICS), the stratum externum (SE) and the outer stratum medium (SM1). Some of these cells (ICS and SE) were initially quiescent as they moved distally and were initially observed as a single cell layer.

Cells of the OCS were compressed and had very thick cornified envelopes. In comparison, cells of the ICS were a lot flatter in shape and this layer was distinguished from the OCS as it was more dense. A single cell layer of cuboidal cells which stained darker on H&E sections was apparent and connected the OCS and the ICS (Figure 3.21). This may be the equivalent of the companion layer (CL) of the hair follicle. Lying beneath the ICS, the underlying SE cells were larger than those of OCS and ICS and they did not appear as dense. Nonetheless, SE still possessed very distinct cornified envelopes.

Small papillae were observed inside the claw fold in the region where the OCS expanded. These structures resembled immature dermal papillae but were not as pronounced those seen in GR2. The region of the OCS thickening that occurred inside the claw fold produced dense material that created a plug to fill the gap between the claw plate and the OCS within the claw fold. This specialised layer was continuous with the skin epidermis, which produced a specialised stratum corneum within the claw fold where there was no contact with the claw plate (Figure 3.19).

The skin of the claw fold only contained hair follicles on its most distal inner surface (Figure 3.19). The hairs projected forwards and covered the claw fold, thus providing protection for this structure. Within the claw fold, immediately above the OCS, only small vellus hair follicles were observed (Figure 3.19).

Just prior to the claw fold, the OCS and ICS cells began to differentiate in a dorsal direction while the SE cells differentiated in a ventral direction. Active proliferation and differentiation thickened this region on either side of the ICS. Where the cornified layers of the ICS and OCS met, a fracture plane was created, which could be seen clearly as the claw horn emerged from the claw fold (Figures 3.20 & 3.21). In addition to this, the cornified single cell layer of the ICS cuticle (ICScu) was more compressed and stained darker on H&E claw sections than the rest of the ICS and was anchored in a 'ratchet' like manner to the cornified cells of the SE (Figure 3.21). The ICScu was distinct from both the ICS and SE by having smaller cells, which stained a darker orange/pink layer on H&E claw sections. It was not clear from the histology what was happening to the ICS but this layer appeared to regress as the claw moved distally and remnants were visible between the OCS and SE as the claw horn emerged from the claw fold (Figures 3.20 & 3.21).

Once the SE had left the claw fold, a distinct cornified layer was seen on the outer surface and these differentiated cells had very distinct cornified envelopes (Figure 3.20). The SE covered the entire claw surface but some loss of the outer cornified layer of the SE was observed distally. In parasaggital sections, a thin but distinct layer running immediately beneath the SE had a low cell density and no tubules (Figures 3.19, 3.20 and 3.21) making the outer region of the stratum medium (SM1) quite distinct.

The stratum medium was composed of a further three layers. GR2 was a papillated germinative region located within the ungual groove, which produced a layer of higher cell density lying beneath SM1 (Figures 3.19, 3.20 and 3.21). This layer, termed SM2, contained tubules which arose from specialised epithelia directly above the dermal papilla (Figures 3.20, 3.20 and 3,22). Similar to human hair follicle, tubules contained a central medulla surrounded by a cortex and were observed to run entire length of the claw.

Adjacent to GR2, the smaller papillae of germinative region (GR3) gave rise to another high cell density layer (SM3), which unlike SM2 was free of tubules.

The fourth layer (SM4) lay below SM3 and was less dense than both SM2 and SM3. This layer was produced from another group of germinative cells (GR4) located adjacent to but distal from GR3 (Figures 3.18 and 3.19). This layer was also differentially stained with eosin, so the upper portion had only a few eosin positive cells while the lower portion appeared pink as the entire cell absorbed the eosin. Thus, SM4 cells contain an eosinophilic protein that occurred at higher levels in the lower portion of the layer.

The activity at GR3 and GR4 thickened the claw plate from the inside as the claw moved distally over the phalanx up to the point where GR5 was located.

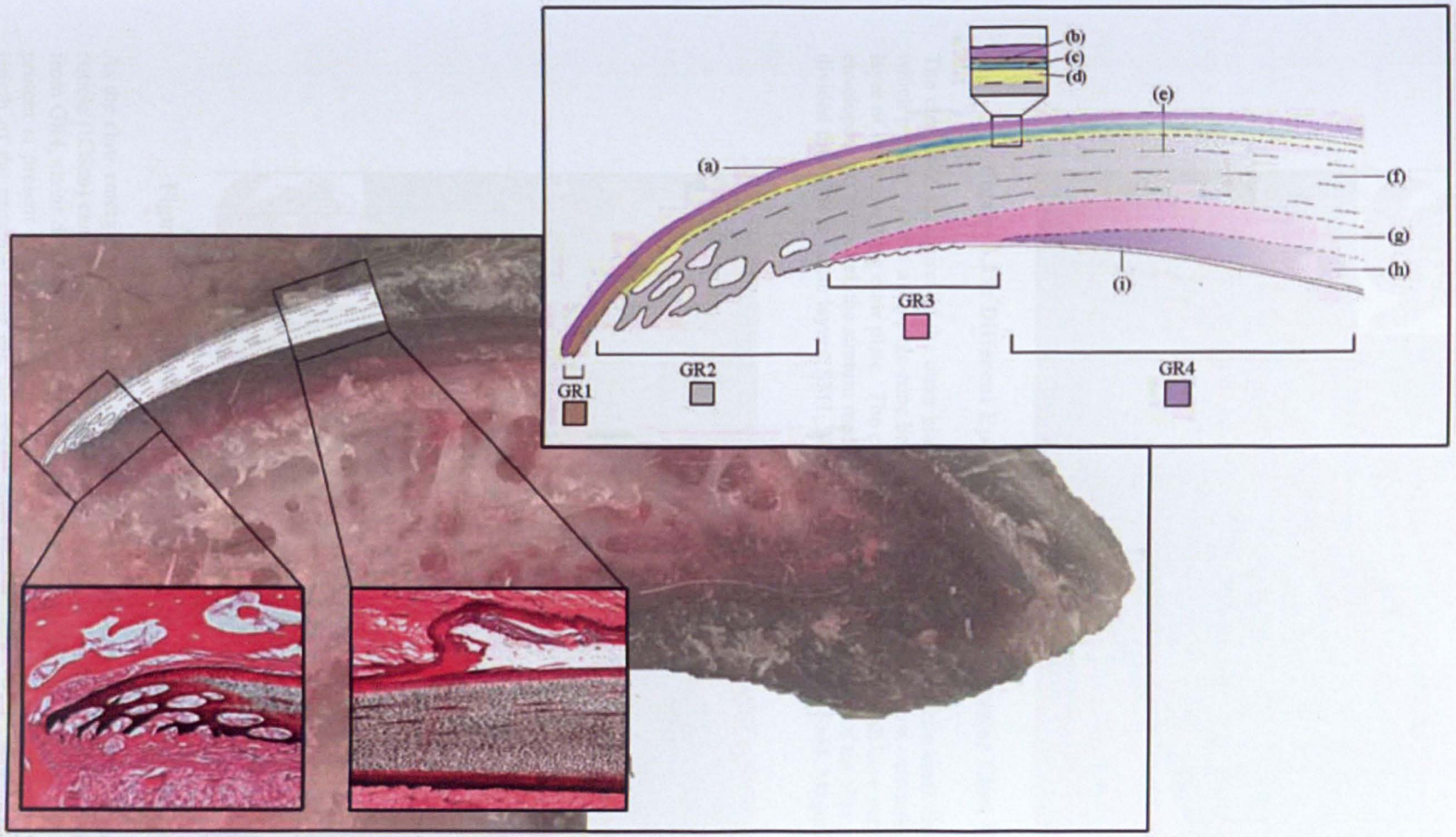

Figure 3.18: Location of Germinative Regions (GR1-GR4) in Proximal Claw

The proximal claw contained at least four germinative regions (GR1-4) where the epithelium interacted with the dermal mesenchyme in different ways to produce distinct epithelia. Several structures are labelled: (a) Outer Claw Sheath (OCS) (b) Inner Claw Sheath (ICS) (c) Stratum Externum (SE) (d) Stratum Medium (SM) 1 (e) Tubules (f) SM2 (g) SM3 (h) SM4 (i) Proliferating cells. Magnification of histological sections: x40.

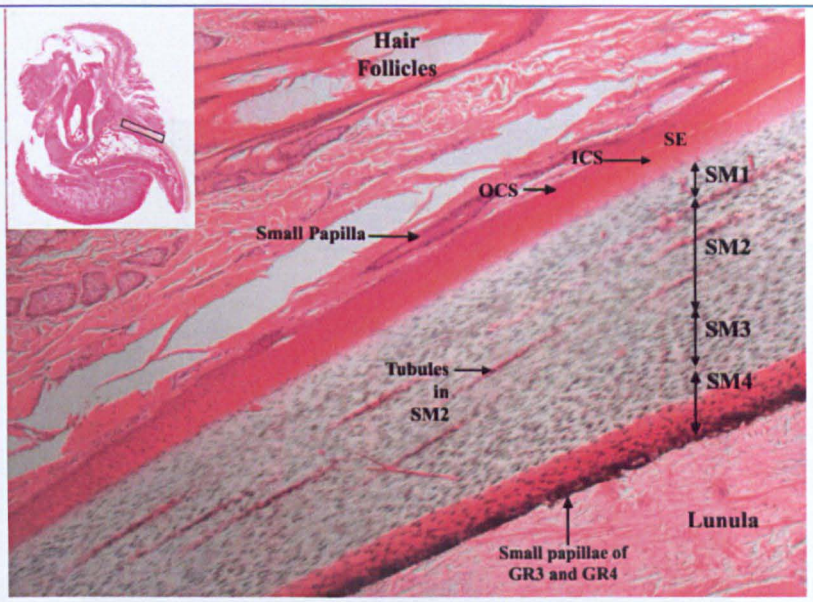

Figure 3.19: Different Epithelial Layers in the Canine Claw Fold

The claw fold comprises of the outer claw sheath (OCS) adjacent to the inner claw sheath (ICS), which probably forms a slippage zone between the OCS and the stratum externum (SE), the outer layer of the underlying claw plate. The cells within these three layers all have very thick cornified envelopes. At this level, the stratum medium (SM) makes up the bulk of the claw plate and can be divided into four separate layers: SM1, SM2 (contains tubules), SM3, SM4. Magnification x40.

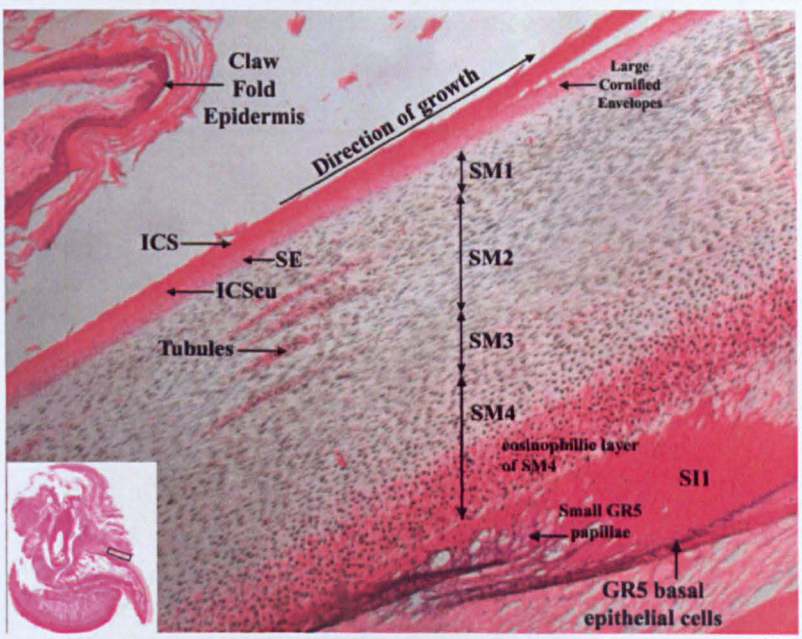

Figure 3.20: ICS, ICScu and SE in the Proximal Canine Claw

As the claw emerges from the claw fold, the ICS separates from the SE and the inner claw sheath cuticle (ICScu) can be seen as a thin layer between the ICS and the SE. SM4, which is generated from GR4, stains differentially with eosin, so the bottom half is pink, inferring that an eosinophilic protein is present in this material. The lower pink portion of SM4 continues down the entire length of the proximal claw but the colour does fade distally. As SM4 production ceases, the lunula, which lies beneath SM4 thinned out and formed the lunula groove in which a new germinative region (GR5) produced SI1 from this point forward. Magnification x40.

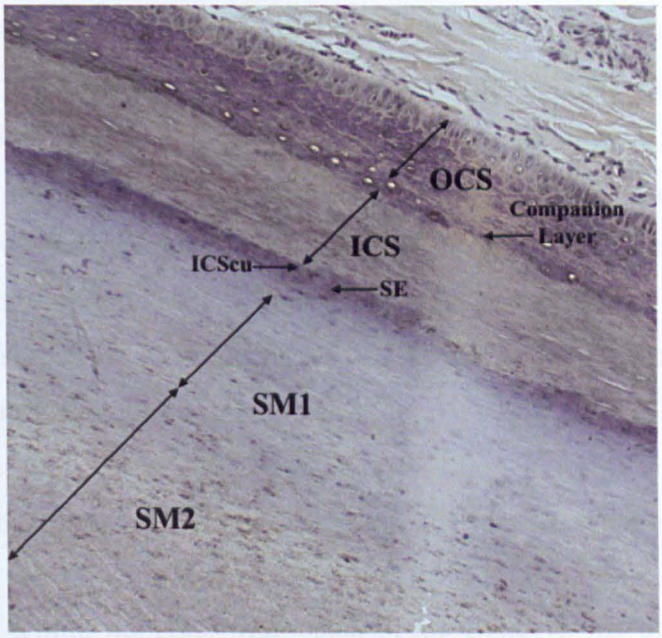

Figure 3.21: Companion Layer in the Proximal Canine Claw

Detailed inspection of the many different strata in the region of the claw fold revealed a single cell layer located between the OCS and ICS, which may be the equivalent of the companion layer (CL) identified as a slippage zone in the hair follicle. Magnification x40.

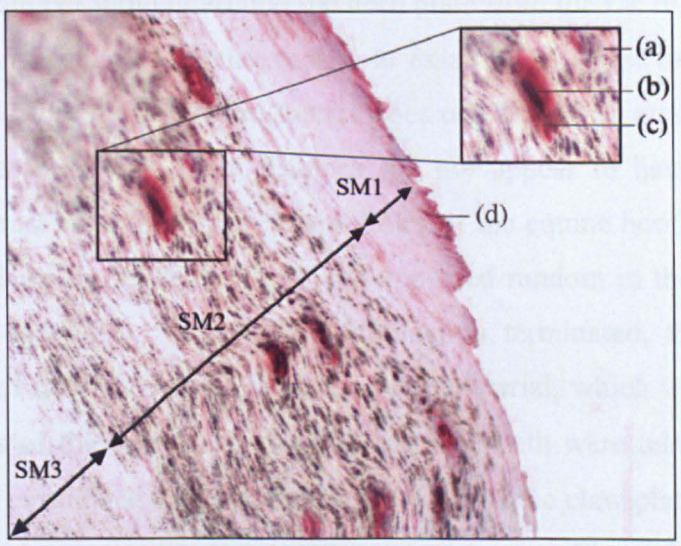

Figure 3.22: Section of Claw Plate showing Tubules within SM2

A section of claw plate showing SM1 (no tubules), SM2 (contains tubules) and SM3 (no tubules); magnification x20. The inset details the region around a single tubule, which in veterinary literature is termed inter-tubular horn (a), dark central medulla (b) and a reddish cortex (c). The stratum externum (SE) is also labelled (d); magnification x40.

Histological transverse sections obtained from within the ungual groove demonstrated how claw plate growth initially starts on the dorsal surface. In many samples, the SM did not initially form a complete "horse-shoe" shape and was interrupted where the LR created a blockage in the ungual groove (Figure 3.23). Moving distally, but still within the groove, claw plate production spread round into the ventral portion of the lateral and medial walls eventually forming the distinct "horse-shoe" shape. This occurrence supported the theory that the ungual groove sloped, and was deepest at the dorsal side and gradually narrowed ventrally, as demonstrated in Figure 3.25.

In transverse histological sections, SM2 production occurred initially on the dorsal surface, shortly followed by SM3 and SM4 horn production moving in a distal direction within the claw fold. Due to the shape of the ungual groove as discussed earlier, the papillated germinative region generating SM2 was only observed on the top half of the ungual groove. This idea was supported further by a lack of tubular structure within the lower half of the medial and lateral horn plate walls. Tubules in the dorsal part of SM2 began to decrease considerably in both size and number moving around the horn plate from the LR to the lateral and medial walls. Eventually, tubules ceased to exist in the lower half of the claw plate suggesting that the papillated matrix does not extend all around the ungual groove (Figures 3.23 and 3.24). Tubules did not appear to have any specific pattern in contrast to the well patterned tubules of the equine hoof, quantified by Reilly and colleagues (1996 & 1998), and appeared random in their distribution (Figures 3.23 and 3.24). Where SM2 production terminated, the germinative region produced only SM3 and SM4 claw plate material, which was observed in the lower parts of the lateral and medial walls and both were tubule free. Both SM3 and SM4 terminated sequentially on the walls of the claw plate and SM3 did not extend into the most ventral part of the ungual groove (Figure 3.24). The final contribution to the overall 'horse-shoe' shape of the horn plate was made by SM4, which extended past SM3 in transverse sections and made up the most ventral part of the lateral and medial walls. A histological transverse section was provided in Figure 3.23 and a cartoon demonstrating proximal claw growth is shown in Figure 3.24.

SM1-4 horn production occurred over a highly thickened dermis, which was similar in anatomy to the lunula of the human nail. Transverse sections revealed that it was thicker in the dorsal claw and narrowed slightly moving around into the lower lateral and medial walls. Prior to GR4 ending, the lunula thinned out and only appeared over the longitudinal ridge.

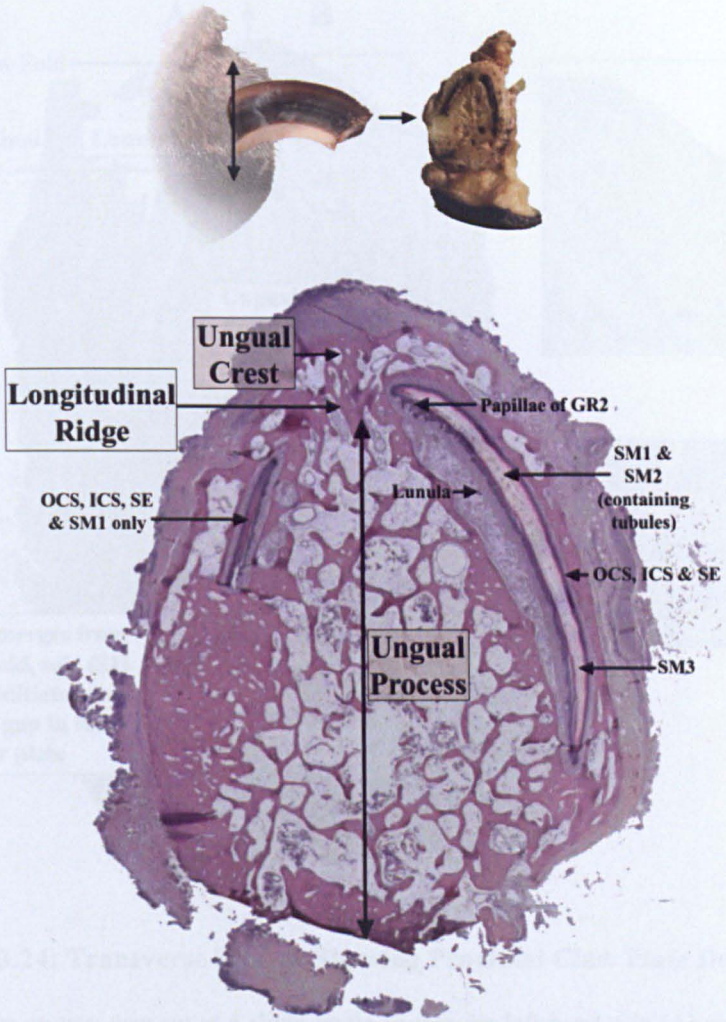

Figure 3.23: Transverse Section showing Claw Plate Development in the Ungual Groove

As the ungual groove is not uniform in depth, horn production initiates near the dorsal surface of the digit where the groove is at its deepest. Firstly, GR1 produces the ICS, SE and SM1, which can be seen on the left hand side of the H&E section. As this section was cut at an angle, horn growth to the right of the section was more advanced (right side not cut as deep as left side) and shows the papillated GR2 that generates SM2. GR2 overlies the thickened dermis of the lunula, which narrows in a ventral direction. In the lower medial and lateral walls, GR2 gradually regressed and this was accompanied by a reduction in tubule size and number in the walls of the claw plate. GR3, which had very small papillae extended further round the lateral and medial walls and produced SM3. In some claws examined, the LR interrupted horn production by creating a bony point on the dorsal surface of the claw plate. Magnification x20.

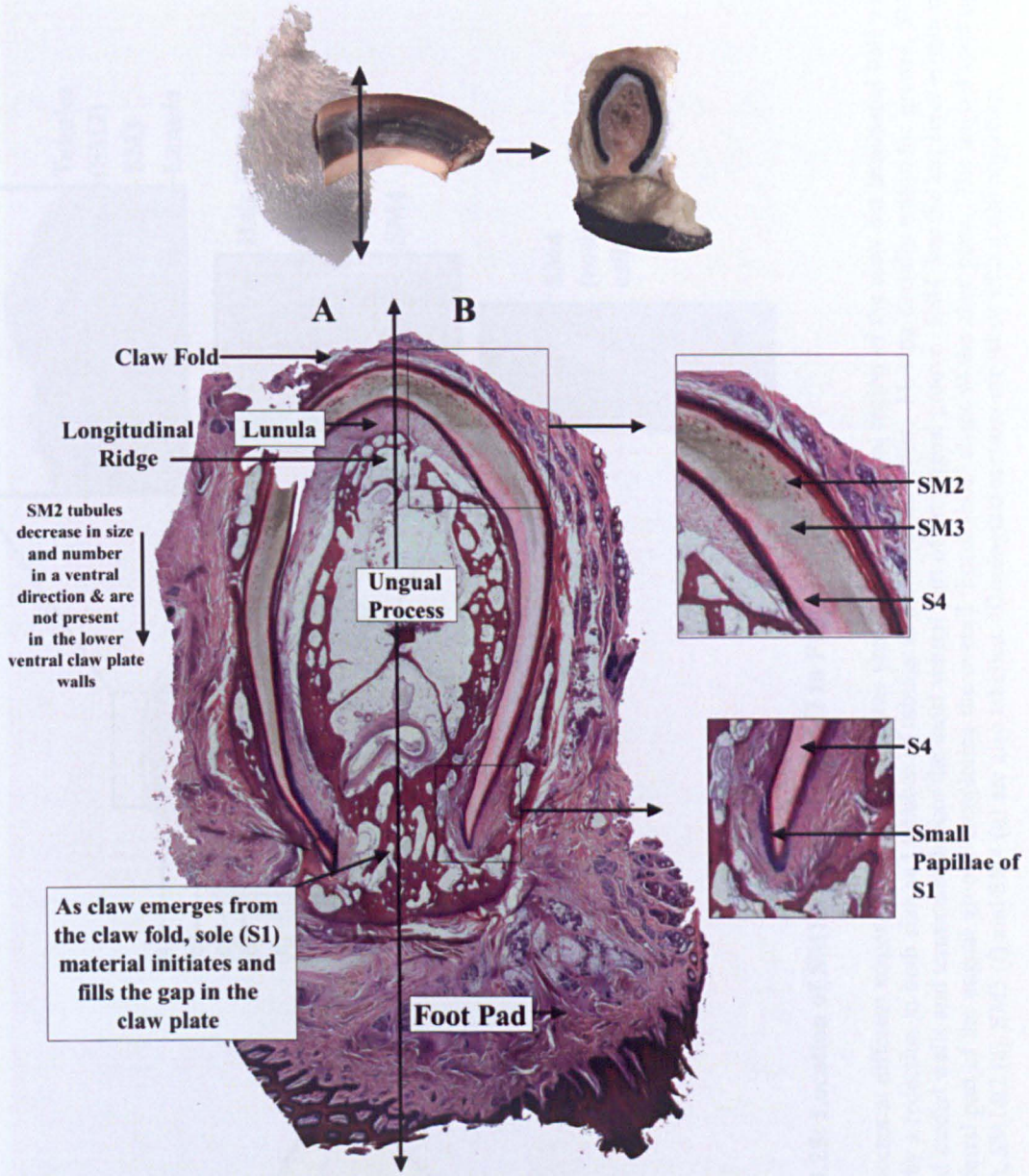

Figure 3.24: Transverse Section Showing Proximal Claw Plate Development

This transverse section was cut at a slight angle so that the left hand side (A) was more proximal than the right hand side (B). On side A, the lunula was prominent and lay beneath SM1-4. As the claw grew distally (B), the lunula thinned and SM4 horn material production increased where the eosinophilic cells extended around the ungual groove in the lower walls of the claw. The section also revealed that SM2 horn only covered the dorsal and part of the lateral and medial walls, seen by a reduction in both tubule size and number in a ventral direction. In the lower parts of the walls, SM3 and SM4 terminated sequentially and completed the overall "horse-shoe" shape of the claw plate. In the most ventral part of the claw plate, small papillae were observed, which were thought to be the beginning of sole horn production. See Figure 3.25 for a cartoon of the different layers from this. Whole transverse image was taken with a x2 objective while the insets are high power images (original magnification: x20) of the key areas.

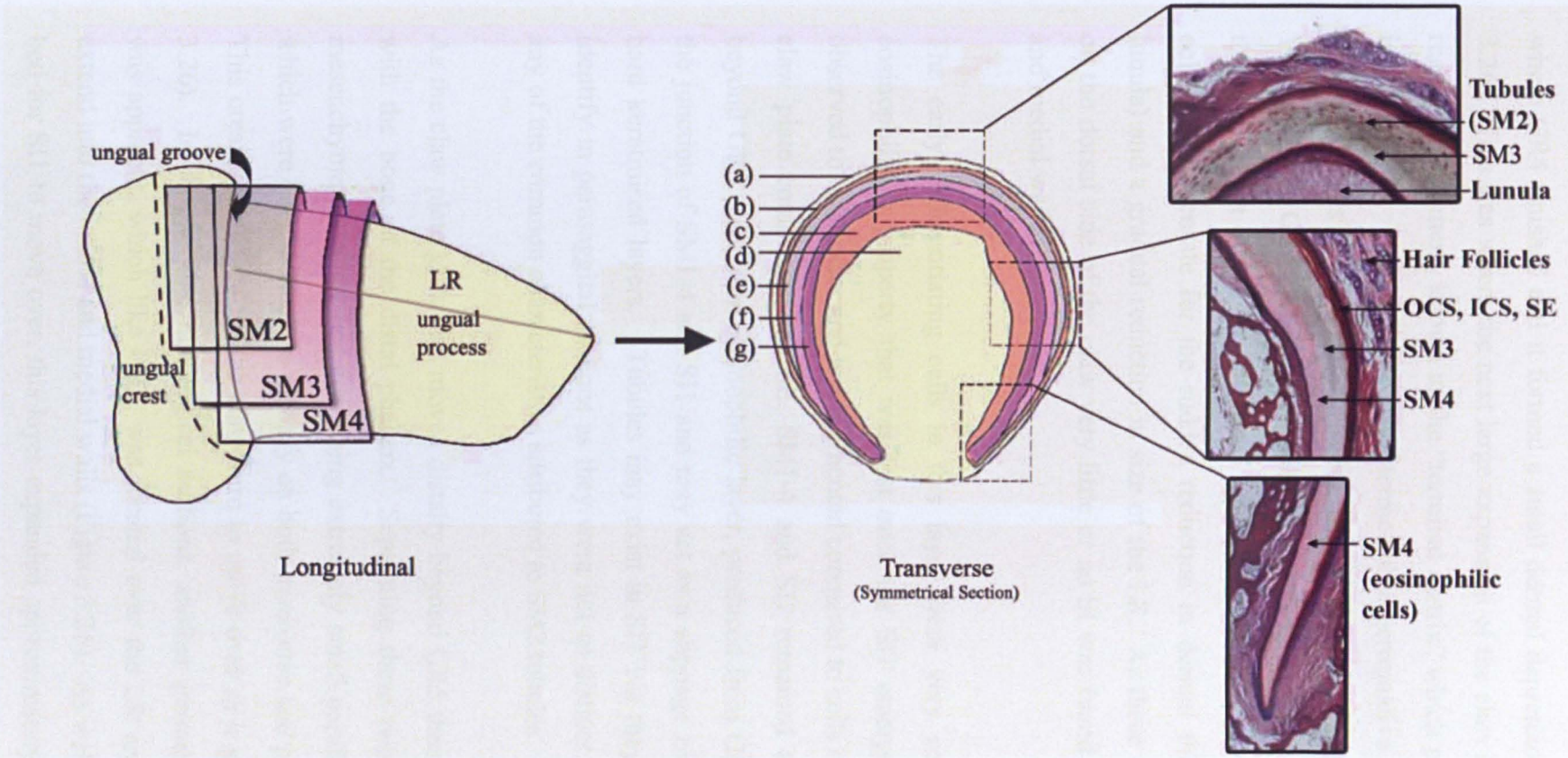

Figure 3.25: Location of SM1-4 and SI1and SI2 in Proximal Claw

Due to the slope within the ungual groove, SM growth occurs at different stages. Initially, SM1-2 was produced in the dorsal region of the claw but terminated half way down the lateral and medial walls of the claw, identified by a reduction in both size and number of tubules in a ventral direction. Moving dorsally within the groove, SM3 was produced which extended further round the lateral and medial walls and terminated before the most ventral part of the ungual groove. SM4 was the last layer within the groove to be produced and this extended into the most ventral part of the ungual groove completing the overall 'horse-shoe' shape of the claw plate. The ungual crest (a), OCS, ICS & SE (b), lunula (c), longitudinal ridge (LR) (d), SM1&2 (e), SM3 (f) and SM4 (g) are also labelled. Histological sections are taken with a x20 objective.

Parasaggital sections revealed that the lunula of the claw terminated abruptly where GR4 finished and it formed a small dermal depression (Figures 3.20 and 3.26). This was where the next large expansion of the claw horn occurred. This region was formerly known as the "terminal matrix" which produced the stratum internum (SI). However, we have termed this germinative region 5 (GR5, see Figure 3.26) as it was not the last horn producing structure in the canine digit. The papillated GR5 was located within the lunula depression, which only covered the bony notch of the LR. It was a small germinative region that produced SI1 cells to compensate for the sudden reduction in dermal thickness (loss of the lunula) and a gradual reduction in size of the LR. As these structures only exist on the dorsal side of the claw very little or no SI was found on the lower lateral and medial walls.

The early differentiating cells in this layer were very compact and heavily eosinophilic, a property that was lost once the SI1 emerged. SI1 cells were observed to be smaller and less pigmented compared to cells of the SM cells. The claw plate comprising the SE, SM1-4 and SI1 remained a constant thickness beyond GR5. The thin eosinophilic layer, produced from GR4, was observed at the junction of SM1-4 and SI1 and may act as a slippage zone between the two hard keratinised layers. Tubules may exist in SI1 but they proved difficult to identify in parasaggital sections as they were not as distinct and did not possess any of the common characteristics attributed to SM2 tubules.

As the claw plate grew and moved distally beyond GR5 there was closer contact with the bone of the distal phalanx. Separating these two tissues was a thin mesenchyme and claw bed containing extremely small papillae (micro-papillae), which were very difficult to identify on both transverse and parasaggital sections. This created a surface for the claw horn to move over as it grew distally (Figure 3.26). In longitudinal histological sections, another germinative region (GR6) was apparent, which like GR5, was located over the LR and did not appear to extend into the lateral and medial walls (Figure 3.26). As well as acting as a claw bed for SI1 to move over, this layer expanded approximately half way down the ungual process and contributed further to the SI1 by producing SI2. Cells in this

layer are very similar to SI1 cells and the two layers are very difficult to identify in histological sections (Figure 3.26).

The curvature of the distal phalanx and the reduction in size of the LR in the distal claw created an increasing gap which was filled by SI2 (Figure 3.30). In the veterinary literature, GR6 was referred to as the "sterile matrix" but this now seems inappropriate to an area of cell growth.

3.3.2.2 Sole

The sole was another modified type of skin differentiation, and this material appeared to be extremely compact. The cells of the sole had very distinct cornified envelopes and this structure probably plays a role in protection of the underlying distal phalanx.

Microscopic analysis confirmed that there were four main types of sole in the canine claw, three of which (S1-S3) were identified in the macroscopic study. An additional type of sole (S4) was identified as a thin cellular strip between SI2 and S3 at the claw tip. Four different germinative regions (GR7-GR10) generated the sole material. GR7 was located near the tip of the claw between S3 and the lower portion of the claw horn (SI2) and filled the gap created by the final curvature, and eventual lack, of the distal phalanx. This region was generated from small micro-papillae that extended from GR9 laminae at the claw tip. These cells were comparable in structure to cells belonging to the other sole types in possessing numerous cornified envelopes and having a distinct physical appearance, so we have termed this layer S4. Similar to SI1 and SI2, S4 material only existed over the dorsal side of the claw and appeared to fuse the dorsal claw plate (SM1-4 and SI1-2) to S3 (Figures 3.26, 3.27 and 3.30).

At the bony notch on the ventral side of the ungual crest (Figure 3.4), two different epithelia were identified which were connected together initially and produced sole 1 (S1) and digital foot pad (Figures 3.27 and 3.31). On the ventral surface of the claw adjacent to the distal phalanx, S1 was produced from the heavily papillated GR8. This was a highly dense epithelium containing small

oblong cells with distinct cornified envelopes. The digital foot pad epithelium lay adjacent to this material and the component cells were highly compact and flattened producing a thick dense stratum corneum. The two epithelia had very different histological appearance and grew away from each other further down the claw. S1 covered the entire ventral surface of the ungual process and filled the gap between the lateral and medial walls. It initially remained at a constant depth but thickened moving in a distal direction where it was eventually attached to S2 on its lateral and medial sides (Figure 3.29) while at the claw tip, fused firmly to S3 to create a solid plug, which covered the entire tip of the ungual process (Figure 3.27).

At the point where GR5 expanded and generated SI2 over the LR, the laminar cells over the lateral and medial walls were also expanding. Germinative cells in this region appear to be programmed to produce a different epithelium that was very compact and dense. In addition, the component cells were extremely flattened and had very large distinct CE. We have termed this region of claw GR9 and expansion occurred here to produce sole 2 (S2). S2 extended from the left and right of the crevices created by the LR, thickened in a ventral and distal direction over the lateral and medial walls, and filled in the gap created between the regressing bony phalanx and the claw plate. It formed another type of claw bed by maintaining a strong but flexible bond between the claw plate and phalanx as well as acting as a slippage zone to allow the claw plate to grow over the phalanx (Figure 3.28). Both S1 and S2 epithelium had a very distinct stratum granulosum and stratum lucidum (Figure 3.29).

Towards the tip, the dermal configuration altered from laminar to papillated, and the germinative cells in this region (GR10) produced S3, an extremely dense material whose cells were more flattened and contained thicker, visible cornified envelopes compared to the other types of sole. S3 was connected firmly to S1 on its ventral side as well as to S4 and S2 over the dorsal ridge and the medial and lateral walls of the claw digit (Figure 3.27).

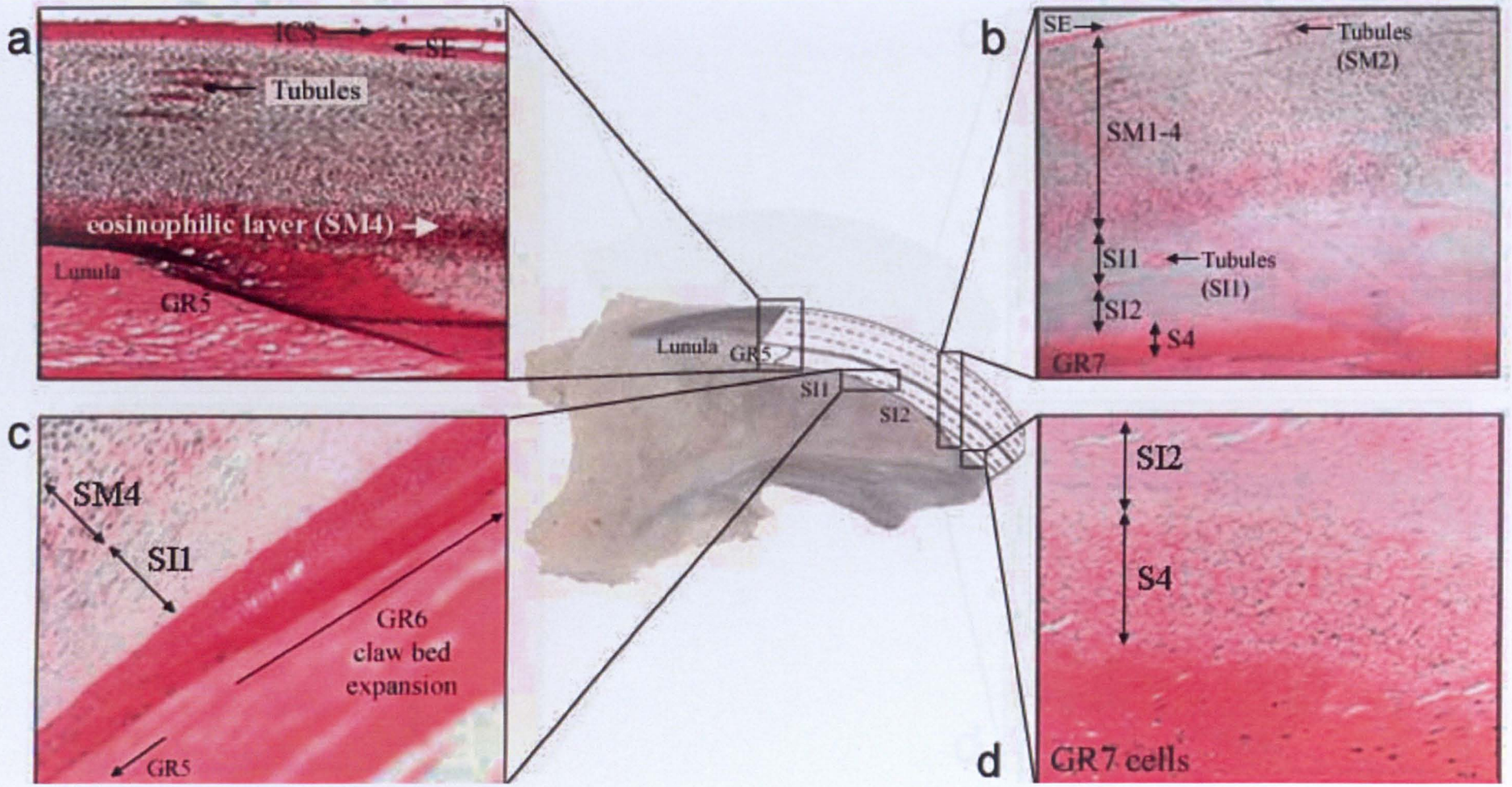

Figure 3.26: GR5-GR7 Location in the Canine Claw

Several layers of different horn material buffer the zone between the distal phalanx and the claw plate. The SM makes up a small portion of the claw plate material and connects to SI1 on the dorsal side of the claw. Beneath, SI1 was generated from the papillated GR5 located in a dermal groove created post lunula (a). Small tubules were observed in SI1 horn (b). SI2 material was added distally from the micro-papillated GR6 (c). Here, the laminae expand and a large volume of cells were generated in a short time. At the claw tip, the dermis changed and a papillated GR7 produced a material equivalent to the other sole types (S1-S3) that we have termed S4 (d). Magnification x40.

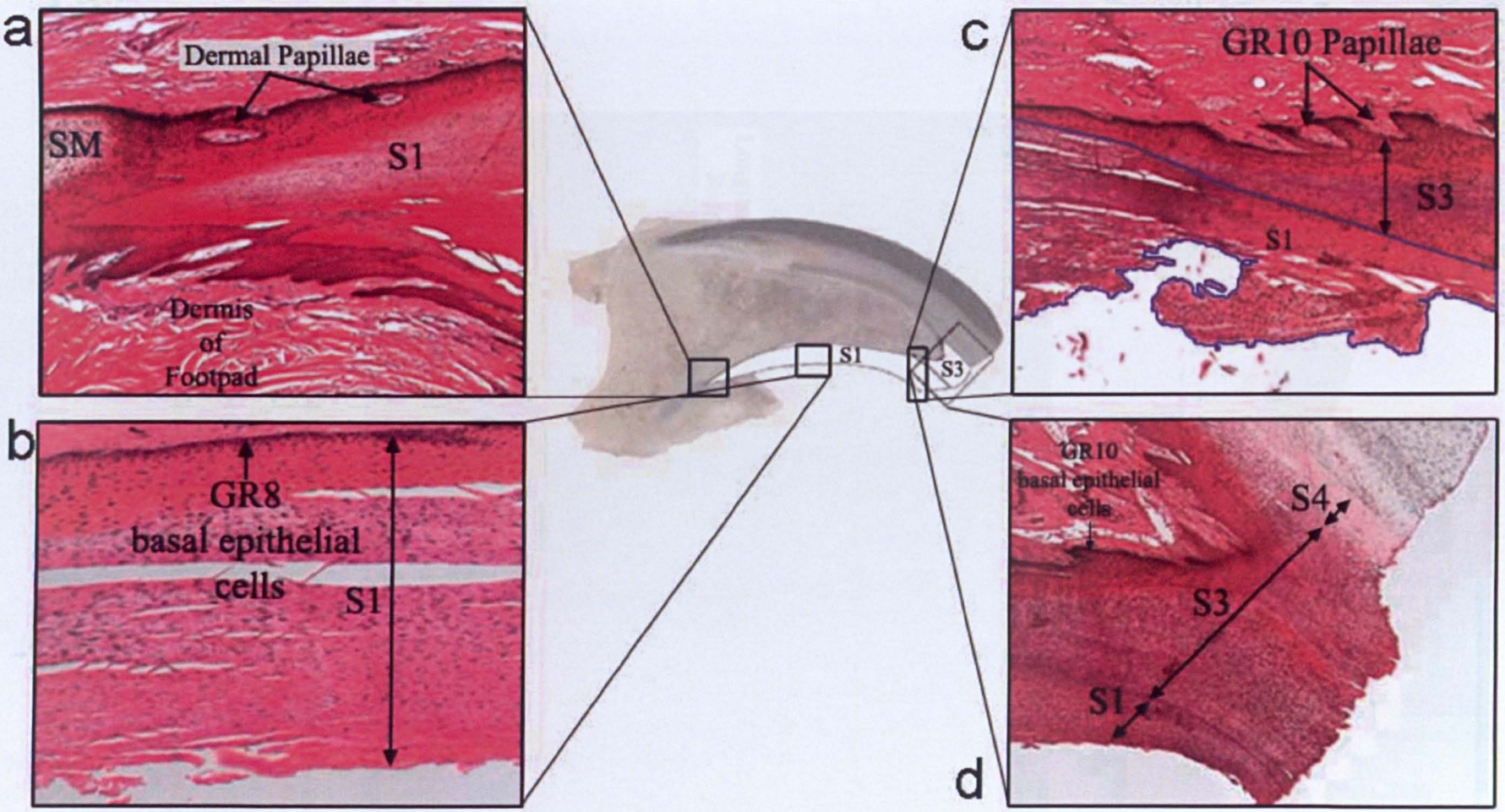

Figure 3.27: GR8 and GR10 Location in the Canine Claw

S1 was generated from papillated matrix, GR8 that extended back into the region of the digital pad on the ventral surface (a). Like all sole types, S1 had very distinct cornified envelopes and created a dense epithelia which covered the ventral surface of the claw (b). At the claw tip, S3 was generated from the papillated GR10 and connected to S1 on the ventral side (c) and S4 on the dorsal side (d). All histological sections have been taken with a x40 objective.

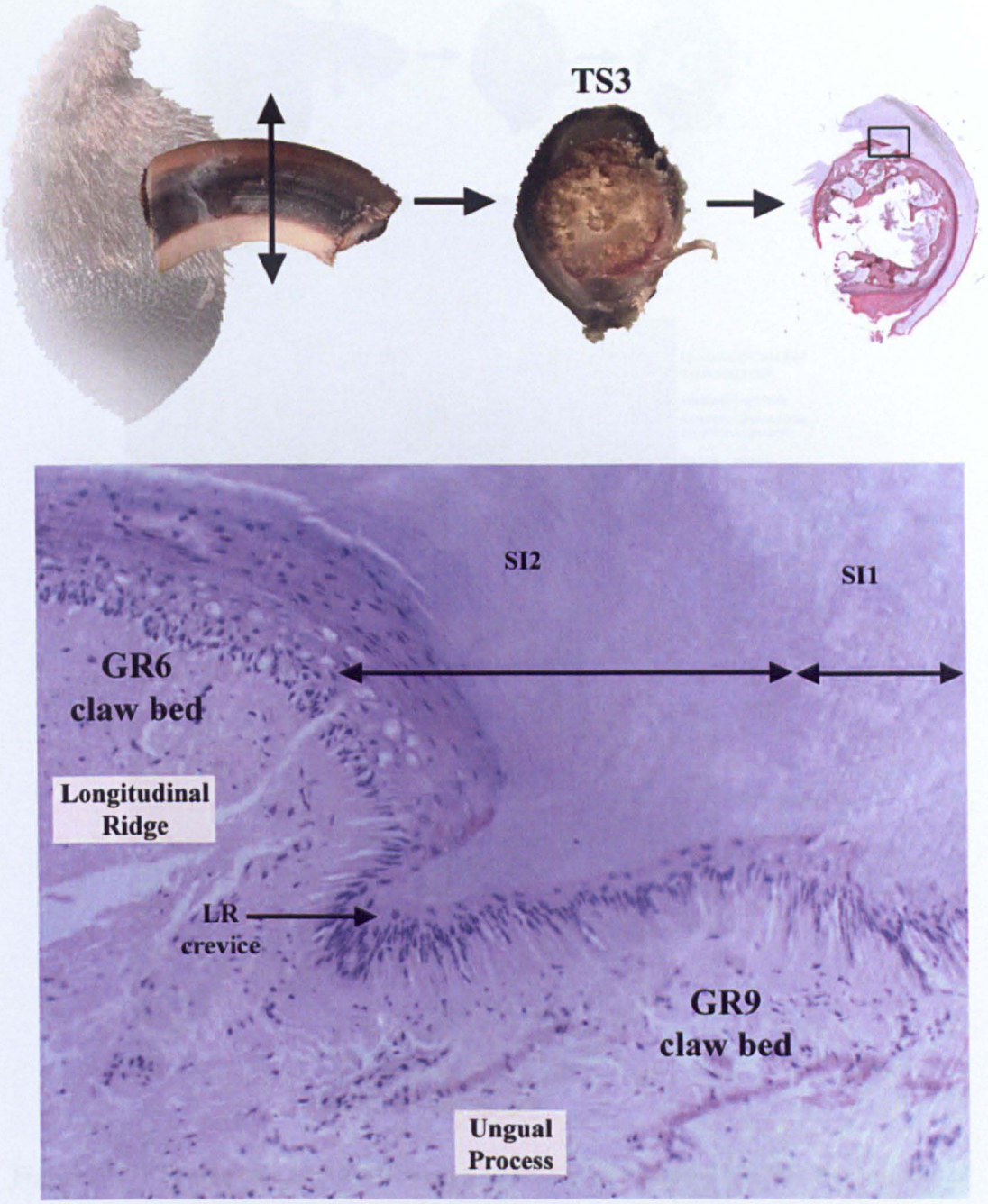

Figure 3.28: Transverse Section Showing Location of GR6 (SI2) and GR9 (S2)

GR6 covered the LR and generated SI2 horn material. In the LR crevice, the laminar GR9 (S2) was observed and created a claw bed for the claw plate to grow over. As the ungual process reduced in size in a distal direction, GR9 thickened and created soft S2 which not only provides the claw with more flexibility but also sealed the gap between claw plate and bone. Magnification x40.

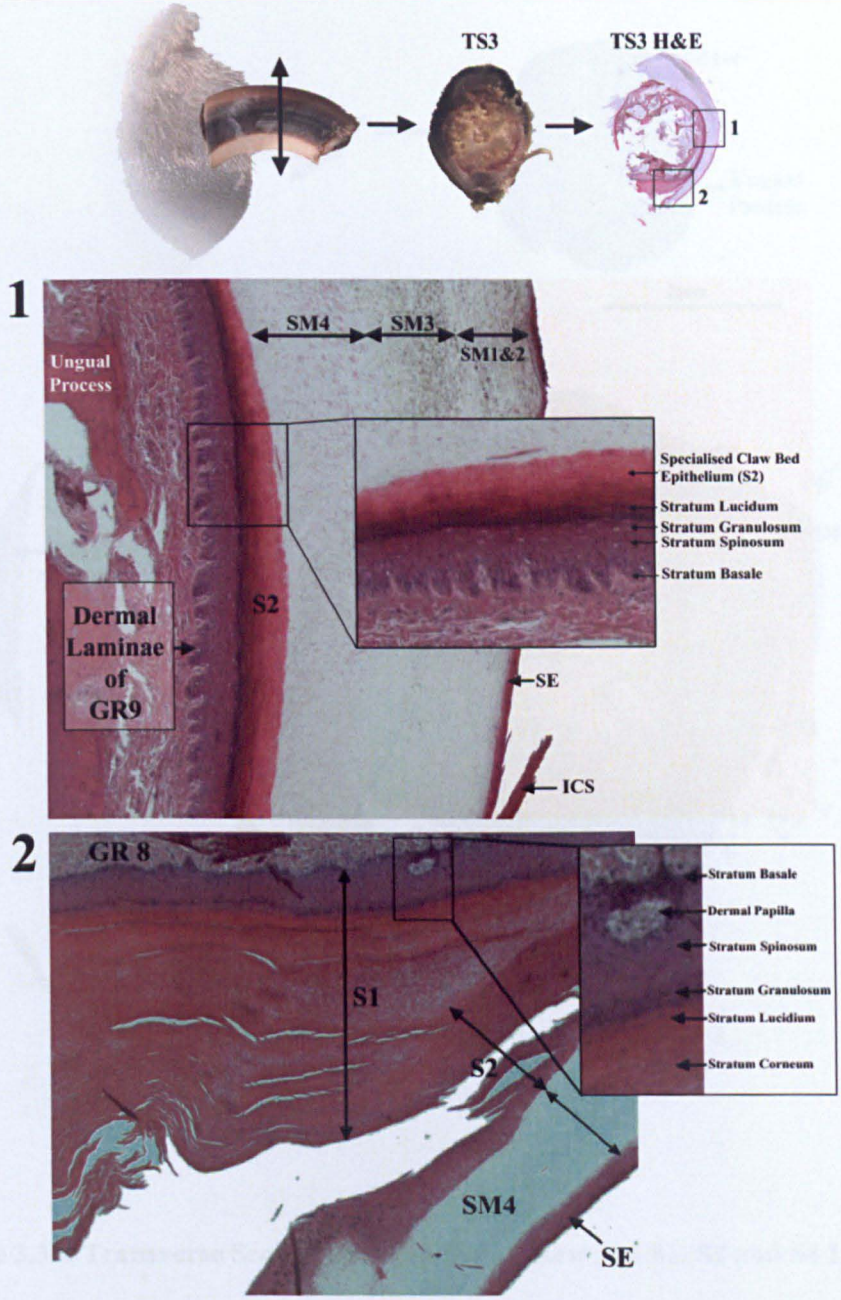

Figure 3.29: Transverse Section Showing Location of S1 and S2 (Claw Bed) in the Claw

S1 was generated from the papillated GR8 and was a highly dense epithelium containing small oblong cells with distinct cornified envelopes. S2 was produced from the laminar GR9 and ran adjacent to S1. This layer was more dense than S1 and thickened in a ventral and distal direction. All types of sole (S1-S4) had a very prominent stratum granulosum, which appeared as a dark strip in all differentiating sole epithelia. Magnification x20 while insets are high-power images (magnification: x100) of the key areas.

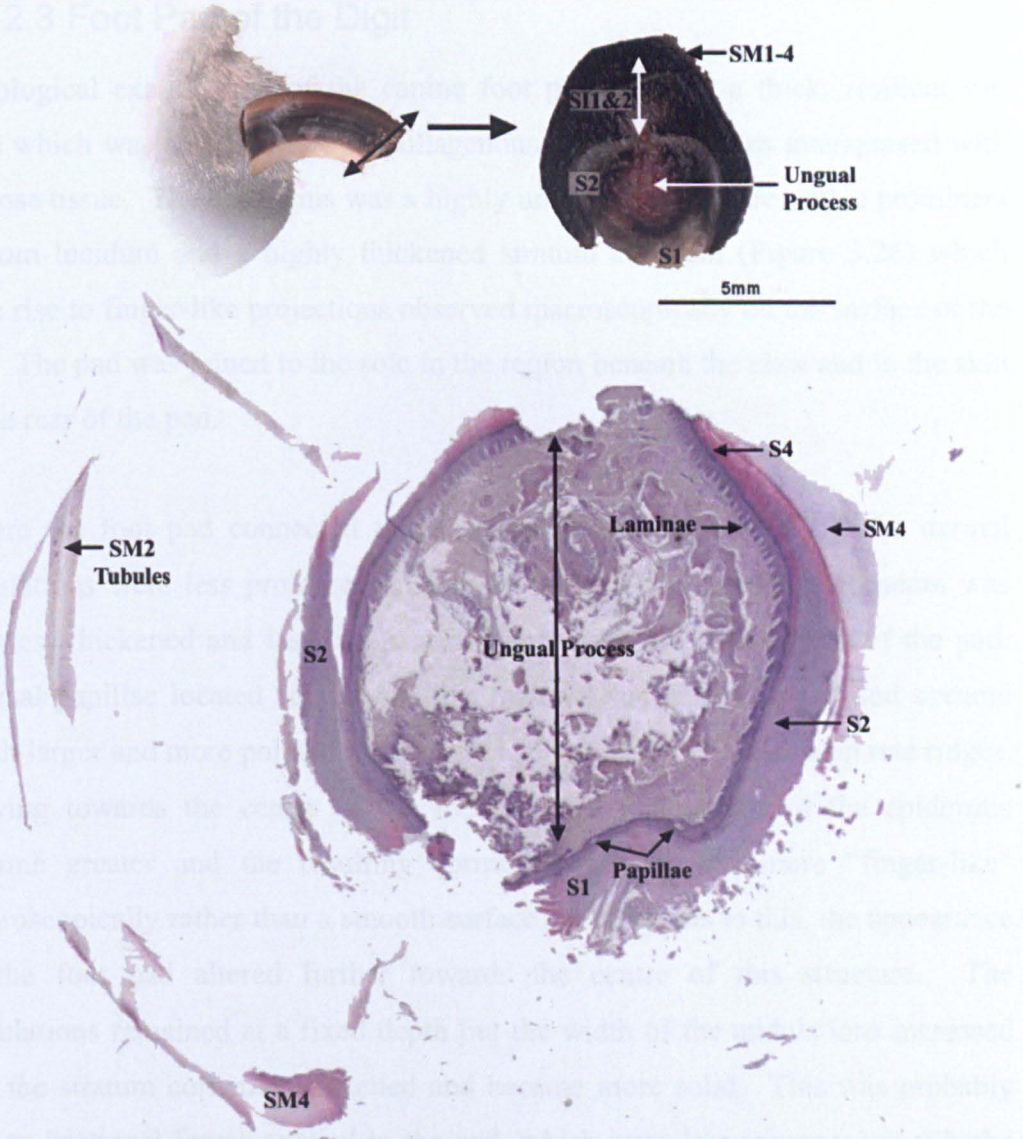

Figure 3.30: Transverse Section showing Distal Claw and S1, S2 and S4 Location

At the distal end of the claw, S2 (claw bed) material had thickened considerably to compensate for the size reduction of the ungual process. Due to the fragile nature of this sample, the majority of the horn plate was torn away during sectioning and processing. However, the distance between the outer part of the horn plate and the ungual process is now considerable and the gap that is missing would have been filled with SI2 material had the section not been damaged. The LR is not present and GR 7 epidermal laminae begin to produce S4 material in the dorsal region of the claw. S4 was easily viewed in H&E sections as the cells have very distinct cornified envelopes compared to S3. Magnification x4

3.3.2.3 Foot Pad of the Digit

Histological examination of the canine foot pad revealed a thick, resilient sub cutis which was an admixture of collagenous and elastic fibres interspersed with adipose tissue. The epidermis was a highly undulating structure with a prominent stratum lucidum and a highly thickened stratum corneum (Figure 3.26) which gave rise to finger-like projections observed macroscopically on the surface of the pad. The pad was joined to the sole in the region beneath the claw and to the skin at the rear of the pad.

Where the foot pad connected to the sole (Figure 3.27 and 3.31), the dermal undulations were less prominent and more flattened. The stratum corneum was also less thickened and less compact in comparison to other regions of the pad. Dermal papillae located adjacent to this material suddenly changed and became much larger and more pointed in structure and the epithelium had deep rete ridges. Moving towards the centre of the foot pad the undulations of the epidermis became greater and the resulting cornified material was more "finger-like" macroscopically rather than a smooth surface. Contiguous to this, the appearance of the foot pad altered further towards the centre of this structure. The undulations remained at a fixed depth but the width of the undulations increased and the stratum corneum thickened and became more solid. This was probably due to frictional forces applied to the pad, which were less apparent towards the periphery. Primary epidermal ridges of the foot pad were longer and more slender in comparison to the broader and shallower secondary ridges which were located either side of the primary ridge. The secondary ridges were located beneath the grooves that limit the papillary ridge.

The foot pad had abundant eccrine sweat glands but these decreased in number towards the edge of the pad. Although the pad was a hair free structure, hair follicles were observed towards the edge of the foot pad where it comes into contact with the skin. Skin surrounding the foot pad-skin junction was a lot smoother and the undulations were less prominent and smaller in diameter.

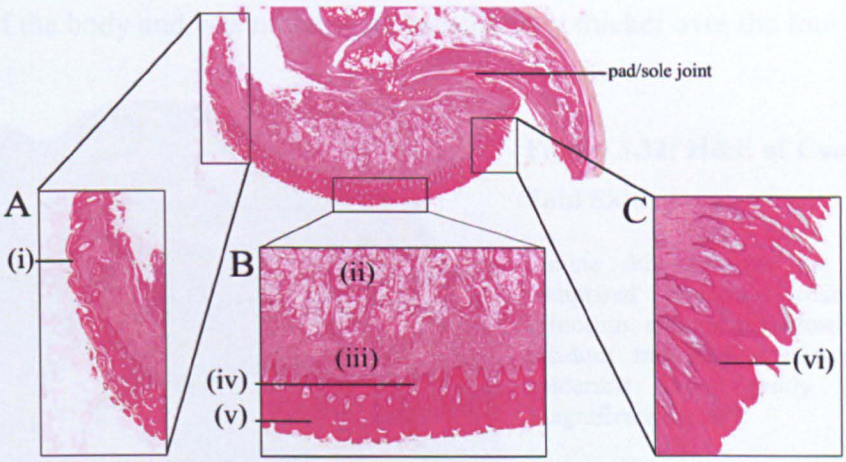

Figure 3.31: Canine Digital Foot Pad

(A) As the digital pad approached the skin, the dermal papillae were less pronounced compared to the other regions of the foot pad; magnification x20. The stratum corneum also thinned where it joined to the skin of the leg (i). (B) Towards the centre of the digital pad, the papillae are slightly larger and more compact; magnificaion x20. This is the region that receives the most surface contact and the flattened epithelial ridges appeared worn down. (C) Towards the pad/sole joint, the dermal papillae became very pronounced and more pointed, and the stratum corneum was very undulated with a prominent stratum lucidum; magnification x20. Several other structures have been labelled: (ii) subcutaneous fat and eccrine sweat glands, (iii) dermis, (iv) dermal papillae, (v) stratum corneum and (vi) stratum lucidum.

3.3.2.4 Canine Skin and Hair

Histological sections of canine skin taken from around the claw fold showed a moderately undulating epidermis. The epidermis at the claw fold is significantly thinner and less undulating compared to the epithelium of the digital foot pad. The skin epithelium, termed epidermis, consisted of five layers: stratum basale, stratum spinosum, stratum granulosum, stratum lucidum and the stratum corneum (Figure 3.33). The stratum basale was formed from a single layer of cells attached to a basement membrane. The cells were large and columnar in appearance. The stratum spinosum was between two and three cells in thickness and these spinous cells were more flattened and polyhedral. The stratum granulosum appeared as a region of flattened cells with shrunken flattened nuclei. The stratum lucidum formed a thin, bright pink stained region that separated the stratum corneum from the stratum granulosum. The stratum corneum was approximately 6 cells thick and was well developed. The underlying dermis was largely composed of a connective tissue network (collagen and elastin) dotted with fibroblasts. The

dermis sat on a layer of adipose tissue that varied in thickness depending on the region of the body and was noted to be considerably thicker over the foot pad.

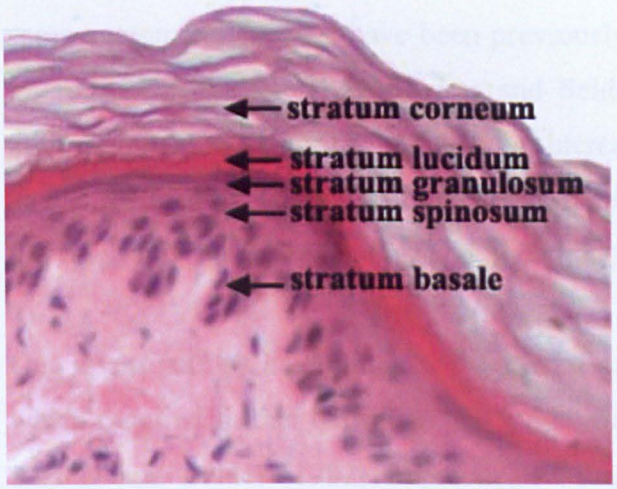

Figure 3.32: H&E of Canine Claw Fold Skin

Canine skin covering the claw fold comprised stratum basale, stratum spinosum, stratum granulosum, stratum lucidum and stratum corneum. The epidermis was gently undulated. Magnification x100

The majority of the skin around the claw fold had abundant hair follicles. The primary hair follicle was the largest, most anterior hair in a compound hair follicle compared to the surrounding smaller secondary hair follicles. The hair roots were separate but just below the sebaceous glands, the hairs entered a common follicle and emerged in a cluster. It was noted that the secondary hairs closest to the primary hairs were larger and became progressively smaller the further away they were positioned. The proximal end of the follicle was joined by a tiny arrector pilli muscle, the other end of which was connected to an attachment plaque near the dermal papillae. The smallest of the secondary hair follicles produced hair that did not appear to contain a medulla (Figure 3.33).

Figure 3.33: H&E Transverse Section of Canine Compound Hair Follicles

A transverse section of canine skin obtained from the claw fold region was stained with H&E to highlight the compound hair follicles (primary and secondary) and some sebaceous glands. The IRS of the hair follicle is shown as a bright pink ring surrounding the hair shaft on these H&E sections. The ORS encircles the IRS and was an epithelium that was continuous with the epidermis. Magnification x40.

3.4 DISCUSSION

Although detailed studies on the micro-anatomy of the canine claw are lacking, some anatomical features have been previously described at the level of the light microscope (Mueller, 1999; Budras and Seidel, 1992). However, this detailed microscopic analysis of the dog claw has increased our knowledge of the anatomy and introduced definitions that have deviated from the more common terms used the veterinary literature (Budras and Seidel, 1992).

Our investigations have elucidated an even more complex structure to the claw which required further definition and made adapting the terminology proposed by Budras and Seidel (1992) impractical. Previous studies have already noted similarities between human nail and human hair follicles, (Hallman *et al*, 2002; Dawber *et al*, 1994; Hashimoto, 1971) and our studies have also highlighted similarities between the canine claw and mammalian hair follicles in general. In view of this, terms used in the hair literature have been adopted as well as incorporating some of the old claw terminology, where necessary, new terms have been introduced and adapted to describe comparable structures within the canine claw.

Germinative cells located at the most proximal part of the claw (GR1) produce three single cell layers which initially lie dormant and then give rise to the outermost part of the claw horn (ICS, SE, and SM1). The ICS appears to be comparable to the inner root sheath (IRS) of the hair follicle and this structure is believed to originate from germinative cells of the epithelium near the base of the dermal papilla (Rogers *et al*, 1998). These cell lineages appeared dormant until they reach a specified region of the claw fold where they expanded from a single cell layer to produce the ICS and SE. These findings agree with Mueller (1999) who stated that the basal layer of the epithelium was most active in the area of the claw fold and this caused claw growth in a circular fashion. Nonetheless, Mueller (1999) did not state which structures were produced within the claw fold. The ICS, which lies between the OCS and the SE, was thought to permit the passage of the continually moving claw and allow it to glide distally past the overlying static epithelium of the OCS. The ICS thus functions as part of a slippage zone in

much the same way as the IRS in the hair follicle.

At the point where the claw emerged from the claw fold, the ICS separated from the underlying SE. It was at this point that differentiation of the SE produced a cornified layer that ran over the proximal surface of the claw and eventually peeled away approximately one third of the way along the total claw length. This suggested that within the region of the claw fold, the cells of the SE became activated by an unknown mechanism and began to differentiate and produce a cornified layer. In the hair follicle, the IRS cuticle is attached to the hair fibre cuticle (SE in the claw), which makes a complementary engagement and forms ratchet type inter-digitations that pull the IRS and hair fibre through the hair follicle together. A similar mechanism may also be operative in the claw, where the ICS is bound to the SE until the claw emerges from the claw fold. However, detailed TEM studies would be required to provide sufficient detail to confirm these initial suggestions.

The outer claw sheath (OCS) appeared comparable to the outer root sheath (ORS) of the hair follicle. Both structures are a continuation of the epidermis and produced in the embryo by an invagination of the epithelium into the underlying mesenchyme. The distal OCS cells produced material that sealed the claw fold to the claw plate surface and so prevent foreign material entering the claw fold. This protects the underlying germinative cells (GR1 and GR2) from subsequent infection and damage.

The small immature papillae observed above the OCS may be the "wart like mounds" observed in the periople region of the claw recorded by Budras and Seidel (1992). These small papillae appeared where the OCS expanded and may be the equivalent of the ORS bulge in the human hair follicle. Hair follicle bulge stem cells are potentially bipotent because they can give rise not only to cells of the hair follicle but also to epidermal cells (Taylor *et al*, 2000). This was clearly evident in the canine claw fold as the OCS papillae brought about an increase in ICS and SE thickness as well as generating a thick epithelial OCS plug which sealed the claw fold to the claw plate preventing any bacterial assault to the stem cells of the claw.

A thin single cell layer was observed between the ICS and the OCS and this layer may be equivalent to the companion layer of the hair follicle. Rogers (1964) suggested that the border between the companion layer and the ORS in the hair follicle acts as the slippage plane that allows the growing hair fibre to move past the surrounding tissue and it did appear from our studies that a similar layer was acting as a slippage zone between OCS and ICS. It has also been speculated that the companion layer plays a nutritive role as it accompanies the IRS in its vertical ascent through the hair follicle (Rothnagal and Roop, 1995). The companion layer in the canine claw fold was most apparent in histological sections of the region where the ICS expanded, so its role here might be to provide the ICS with the nutrients required to expand and function.

The SE covered the entire surface of the claw and probably has a similar function to the hair cuticle, providing the claw plate with a protective coating. However, unlike hair cuticle cells, which appear like "fish scales" on the external surface of the hair shaft, the cells of the SE are much smaller and more similar to epidermal stratum corneum in structure. This produces a tough but soft material rather than the hard cuticle of the hair fibre.

Given that nails evolved from claws (Hamrick, 1999), it is possible that the eponychium and dorsal layer of the human nail contains an OCS, ICS and SE equivalent. Farren et al (2004) reported that the dorsal layer was composed of flat, overlapping slate like sheets, which were orientated in the plane of the nail. This may be the equivalent of the SE of the claw but further investigation would be required to prove more evidence that this suggestion is correct.

The bulk of the proximal claw was produced from three adjacent groups of germinative cells (GR2, GR3 and GR4). Each of these germinative regions produces different cell lineages, which collectively comprise what is known as the stratum medium (SM). The SM of the claw was thought to be the equivalent of the hair cortex. The papillated GR2, which produces SM2, has been likened to the germinative region of the hair follicle bulb. The non-papillated GR3 and GR4, which give rise to SM3 and SM4 respectively, have been previously described in

the literature as "terminal matrix" and noted to be the germinative region that produced the deep stratum medium. However, SM3 and SM4 cells were not recognised in these earlier studies (Clark, 1971).

The tubules within SM2 are produced as a result of the papillated GR2. Tubules were identified as small streaks in longitudinal sections and circular in transverse sections. Tubules stained positive for eosin suggesting that these are cellular in nature and therefore, less rigid in comparison to the surrounding claw horn material of the SM. Thus, it was thought that tubules may provide the hard keratinised claw with some flexibility. Similarly, the central medulla of the hair follicle which is comparable to SM2 tubules, consists of a column of cells centrally placed within the cortex (SM2 inter-tubular horn equivalent) of the hair fibre. After keratinisation, or degeneration of the hair shaft, a central air canal is left in the absence of the medulla (Hashimoto, 1988). It was not confirmed whether or not SM2 tubules at the claw tip were hollow tubes. Budras and Seidel (1992) stated that transverse sections through claw plate revealed tubules to be circular in shape at the proximal end becoming triangular and then oval distally before becoming completely indistinct in the distal claw. Contrary to this, our findings indicated that the tubular structures remained constant throughout the length of the SM2 and tubules were still recognisable at the claw tip. However, tubule shape did differ between the dorsal ridge and medial and lateral walls. Tubules in the dorsal region were numerous and were large and round but became smaller and more flattened in structure as well as gradually decreasing in number in SM2 located in the lateral and medial walls. In the bottom half of the horn plate walls, no tubules were present suggesting that the dermal component within the lower part of the ungual groove was not papillated. It was thought that horn tubules are larger in the dorsal horn plate as this region receives the most contact with the ground and thus requires a greater capacity for shock absorption.

The lower part of SM4 contained cells, which were highly eosinophilic when stained with haemotoxylin and eosin, creating a visible pink strip along the parasaggital section of the claw plate. This layer was connected to the underlying SI1 allowing a slippage zone for SM to grow as well as providing a flexible region between SM and SI to prevent shearing forces between these two claw

plate components.

It was thought that the thickened dermal region observed in the proximal claw was comparable to the lunula of the human nail and the perioplic and coronary cushion of the equine hoof. All are thickened dermal components located in the proximal digit but only the most proximal part of the human fingernail is papillated (De Berker *et al*, 2000). In the canine claw, the entire surface of the thickened dermis (GR1-4) was papillated but the papillae in GR2 were much larger than those in GR3 and GR4 and smaller tubules would be more difficult to identify even in histological sections. Similarly, in the equine hoof, the whole surface of this thickened dermal region (perioplic and coronary cushion) contains small papillae that are responsible for tubular structures that are present in all SM regions of equine hoof horn, differing from the canine claw where only SM2 is tubular. Due to the canine claw and human fingernail sharing many anatomical similarities, including a similar design in the shape of the proximal dermis, this structure in the claw has been termed the lunula. In the claw, GR1-4 were located over the lunula and generated SM1-4 of the horn plate respectively. Similarly, germinative cells in the region over the lunula of the human nail produce the "intermediate layer" which makes up the bulk of the human nail plate (Farren *et al.* 2004). Therefore, it would be reasonable to suggest that the bulk of the human nail plate is equivalent to the canine SM and a lack of SI within the human nail is a result of a flattened nail bed where no extra horn material is required to fill in a region between nail plate and distal phalanx. A lack of tubules within human nail plate may be a result of the "germinative matrix", located within the proximal nail bed, being thinner and more flattened compared to the equivalent regions in the claw or hoof, which are papillated structures that may have been lost through evolution. On the other hand, perhaps the tubules are so small and indistinct in the human fingernail that they have never been identified. Dermal papillae have been identified in the proximal human fingernail germinative matrix so it would be expected that the nail plate should contain tubules (De Berker *et al*, 2000).

As the claw plate emerged from the claw fold, the lunula reduced in size so that it only covered the LR of the dorsal claw. It also thinned considerably and created a dermal groove where the small GR5 was located. The SI1 and SI2 resulted from a

mass production of small compact, non-pigmented cells from GR5 and GR6 respectively. In parasaggital sections, it was difficult to identify the small papillae of GR5 but small tubular structures were apparent in the dorsal part of SI1 providing the hard claw plate with further flexibility.

After GR5 had produced the thin horn layer of SI1, the LR was noted to narrow in a dorsal direction. It was thought that the LR was probably a mechanism to prevent side-ways rotation of the horn plate over the bone. Transverse sections of the dog claw demonstrated the 'lock and key' effect that this structure imposed on the horn plate, securely anchoring it to the distal phalanx (Budras and Seidel, 1992). Indeed, when the horn plate was removed from the distal phalanx, the resulting indentation from the LR was clearly seen on the inside of the claw plate. In some specimens, the LR was more prominent and formed a blockage within the ungual groove forcing the SM to form around the bony notch and creating a groove in the proximal horn plate. It was thought that this further decreased any risk of sideward rotation of claw horn within the groove. On close examination of the whole horn plate and various histological claw sections, no laminae were observed in the region of the LR though SEM studies would be required to provide further evidence. Nonetheless, SEM work on the dermal papillary body of the feline claw revealed that the proximal LR had a smooth surface with longitudinal, parallel orientated indentations (GR6 equivalent) which changed distally in the lateral parts into small dermal micro-ridges (GR7 equivalent) supporting our theory that there are no laminae within the longitudinal ridge of the dog claw (Bragulla *et al*, 2001).

GR6 contained extremely small papillae, which covered the LR of the dorsal claw. This germinative region has been previously reported and is known as the "sterile matrix" in the older claw literature (Le Gros Clark, 1936). Le Gros Clark (1936) observed that the sterile matrix was a thin epithelium no more than two cells thick. Although Le Gros Clark (1936) did not clearly define where these observations were made within the canine claw, our studies revealed the main cellular contribution from GR6 was over the LR of the dorsal claw and to a lesser extent over the lateral and medial walls. This layer was termed this layer SI2 as its cells were very similar to SI1 and it was often difficult to identify each layer

histologically. The papillated GR6 was initially two cells thick and acted as a claw bed for the overlying claw plate. As the LR began to reduce in size, approximately one third down the ungual process, GR6 basal cells expanded considerably and produced an epithelium that filled in the gap created between the claw plate and the decreasing LR. The underside of the macroscopic claw clearly showed how SI2 adopted the shape of the LR and the dorsal claw tip resembled the human nail pathology observed in pachyonychia congenita.

There is a conflicting argument in equine and bovine hoof literature as to whether or not epidermal laminae contribute to the thickness of the horn plate. Leach and Oliphant (1983) stated that the morphologic features of cells of the secondary epidermal laminae of the equine hoof indicated that the laminae were composed of immobile populations of cells and the primary epidermal laminae moved past the secondary laminae by breaking desmosomes connecting these two cell populations thus allowing movement of the hoof over the underlying distal phalanx. Contrary to this, Budras et al, (1998) challenged Leach and Oliphant (1998) and reported that a small, but important, amount of horn production results from the activity of the laminar portion of the epidermis. However, their findings were taken from bovine hoof wall and not equine hoof wall. In addition, Budras and Seidel (1992) noted a large increase in horn plate depth in the dog claw due to a cellular contribution from epidermal laminae and stated that the 'sterile bed theory' proposed by Leach and Oliphant (1983) was totally unjustified.

All theories disputing the case for the sterile bed theory cannot be compared as the morphology of the distal phalanx in the bovine, equine and canine digit are very different. The findings within the canine claw suggest that thickening from the epidermal laminae only occurs in regions where the bone moves away from the horn plate, thus, the resulting cells act to fill the gap. Studies on human nail and equine hoof support this hypothesis. De Berker and Angus (1996) noted that there was no, or very little, cellular contribution from the nail bed in human nail. Due to the nail bed being relatively flat, the bone does not curve away from the nail and thus, there is no requirement for further nail production from the nail bed to fill in a gap. Similarly, the distal phalanx of the equine hoof does not curve away from the hoof wall resulting in very little cellular contribution from the laminae in

the hoof wall. However, in horses suffering from chronic laminitis, the distal phalanx of the hoof rotates away from the hoof wall creating a gap (Hendry *et al*, 1997; Pollitt, 1998). In severe cases, a "laminar wedge" forms which is where the epidermal laminae of the hoof wall proliferate rapidly to compensate for the newly formed gap caused by the rotation of the bone (Kuwano et al, 2002). This supports our theory that this is not a "sterile bed" as the laminae will generate new horn material if it is required. There now appears to be sufficient evidence to suggest that the whole concept of the sterile bed theory should be rejected.

It is also known that small micro-ridges cover the dermal nail bed of the human nail and these ridges may be rudimentary dermal laminae that have survived the evolution from claw to human nail. A lack of dermal papillae in the proximal human nail however, may be due to the flatness of the digit. For example, the equine hoof is an upright structure and this has allowed a greater area for dermal papillae within the proximal hoof. On the other hand, the canine claw is a more flattened structure than the hoof and papillae are less prominent and more smoothed out. Similarly, the human nail has completely flattened to the point that there is no room for any visible dermal papillae in the proximal nail, therefore the human nail relies on laminae for greater surface contact. Comparable to the human nail, dermal laminae exist post lunula within the canine claw.

There is debate over the presence of a sole in the canine claw. Fowler (1980) states that the claw has no sole but this paper discusses the carnivore claw and does not differentiate between species. Nevertheless, this thesis identifies the sole as a soft, rubbery and sometimes crumbly material encompassed by the claw horn plate. There are four main regions within the sole (S): S1, S2, S3 and S4.

On the ventral claw, GR8 generated S1, which was a dense material that thickened distally generating the sole as observed macroscopically in the horn plate cleft on the ventral claw. While S1 emanated from a papillated germinative region located along the ventral claw, unlike SM2, no tubules were observed. This agrees with previous work that described this structure as tubule free (Budras and Seidel, 1992). Using scanning electron microscopy images of the claw tip, Budras and Seidel (1992) revealed that there was a greater abundance of papillae at the tip of

the digit and that they were thinner in comparison to the papillae that produced S1 material located on the ventral claw. On the lateral and medial walls of the claw, S2 material was generated from the laminar GR9, which existed over the lateral and medial walls. Previous studies on the canine claw have concluded that the corium within the region of the sole is papillated and not laminar (Dobler, 1969; Clark 1971; Schummer *et al*, 1981; Budras and Seidel, 1992) suggesting that GR9 and S2 have not been identified as a separate sole within the claw. Contrary to this, Bragulla *et al* (2001) did acknowledge that the sole was produced from a laminar claw bed but did not identify different sole types within this structure. Where the ungual process reduced in size half way down the claw, GR9 expansions occurred over the walls creating a dense epithelium (S2) which buffered an increasing gap created between the claw plate and bony phalanx in the distal claw. This not only fused the lateral and medial wall claw plate to the underlying distal phalanx but also created a slippage zone for the claw plate to move over. S2 also attached to S1 on the ventral surface of the claw and sealed the gap between sole and claw plate on the ventral aspect. On the underside of the claw, S2 was observed macroscopically at the claw tip and encompassed the lower half of S3 material.

S3 was generated from GR10, a papillated matrix that covered the tip of the ungual process. This was an extremely dense sole material probably required to reduce bacterial invasion at the claw tip. This was attached on its dorsal side to S4, which was thought to be equivalent to the white line of the equine and bovine hoof. Budras and Seidel (1992) acknowledge the white line in the dog claw and stated that it was easily recognised in longitudinal sections, especially in darkly pigmented claws. However, in their transverse claw diagram, they labelled the border between the SM and SI as the white line. Due to the prominence of the LR in this diagram, the transverse section appeared to have been taken from half way down the claw. At this point SI1 and SI2 material is generated to buffer the gap created by the reduction in the LR size. Our studies found that S4 (white line equivalent) was only generated towards the tip after the LR had nearly disappeared. Histological sections showing S4 suggested that this thin cellular layer that contained very distinct cornified envelopes, fused S3 and the claw plate.

The material that exists between claw plate and ungual process, which we have termed S2, was by definition claw bed, comparable to the human nail bed. Cells in this region have very distinct cornified envelopes, typical of cells belonging to the nail bed. If we were to imagine the claw plate flattened out, S2 would provide a soft, spongy layer that would prevent shearing forces between claw plate and mesenchyme as well as provide a slippage zone for the claw plate to slide over during outward growth. De Berker (2000) demonstrated that suprabasal human nail bed cells were K6, K16 and K17 positive so it would be interesting to see if S2 cells had a similar keratin expression.

As the ungual process reduced greatly in size towards the claw tip, S2 (claw bed) expanded to fill in any gap created and provided a protective, cushioning layer for the claw plate. At the apex of the ungual process, the overall resulting gap was filled by a specialised and expanded claw bed, which we have termed S3. All of the sole material, including S1, which covered the ventral surface of the ungual process, and S4, which sealed the claw plate and S3, are a form of specialised "skin" differentiation, similar in many respects to the canine foot pad.

Canine foot pads provide both traction and shock absorption. The histology of longitudinal foot pad sections demonstrated a highly undulating epidermis that is commonly seen in areas of pressure keratinisation. The dog's weight is spread over these foot pads, which have a thickened hypodermis full of adipose tissue to act as a shock absorber. The stratum corneum was highly thickened and compressed towards the centre of the foot pad and serves to protect the surface of the pad from wear. Due to the large frictional forces exerted on this structure, the cell turnover rate is thought to be more rapid in these regions. Primary epidermal ridges contain the intra-epidermal portion of the eccrine duct. They are the site of eccrine bud formation and are therefore known as 'glandular ridges' (Swensson, *et al*, 1998). The formation of primary ridges and eccrine glands precedes the development of secondary epidermal ridges, producing a characteristic pattern of alternating primary and secondary ridges, which is also seen in human palmar plantar skin (Swensson, *et al*, 1998). The abundance of eccrine glands in the digital foot pad aids in scent marker production in dogs. As only male dogs were used in this study, it would be interesting to note if less eccrine glands are present

in digital foot pads of female dogs, as they are not as territorial as the male.

There are several anatomical areas within the claw that are still difficult to define and further work needs to be done in order to answer many of the questions raised by the current histology study. However, these investigations have provided a preliminary working model for growth and differentiation of the canine claw, which will aid interpretation of the immunocytochemical and other molecular data presented in the following chapters.

CHAPTER 4

4 EXTRACTION AND ANALYSIS OF PROTEINS FROM CANINE, EQUINE AND HUMAN TISSUES

4.1 INTRODUCTION

No records of protein extraction and analysis were found in the canine claw literature but comparable structures (human nail, equine hoof and bovine hoof) have received more attention in this respect (Baden, 1984; Kitahara and Ogawa, 1991; Grosenbaugh and Hood, 1992; Wattle 2000; De Berker *et al*, 1996). Previous work extracting proteins from human nail, hair and equine hoof detailed buffers containing urea, dithiothreitol (DTT) and iodoacetamide in alkaline conditions (Marshall and Gillespie, 1982; Wattle 2000). Goddard and Schubert (1935) reported that reducing agents such as β-mercaptoethanol or dithiothreitol dissolve keratin only in alkaline conditions and that they act very quickly without bringing about any chemical alteration other than reduction of disulphide bonds. Herbert and Matoltsy (1956) tested different concentrations of urea, different pH, and different reducing agents to extract keratins for analysis. As hard keratins are more insoluble than soft keratins due to a greater number of disulphide bonds, Ross and Schatz (1973) stated that carboxymethylation with excess of iodacetate eliminated interference by sulphydryl compounds. Treatment with iodacetate permanently blocks sulphydryl groups and prevents further disulphide bridging. However, this action dramatically affects the molecular weight and charge of the molecule, so protein analysis does not provide accurate information on the size and charge of the native protein. In addition, these methodologies were not required to extract soft keratins and as a result, such covalent modifications in hard keratin extraction methods made it difficult to compare the biochemical properties of hard and soft keratins. This was a major factor that had to be considered when comparing keratins from both soft (canine skin) and hard epithelia (canine claw) in this study.

The original aim was to examine what, if any, differences in keratin expression occurred within the different regions of the canine claw employing methodologies

reported in both the human nail and equine hoof literature. However, initial protein extraction experiments with canine claw highlighted the difficulty of extracting keratins from such a robust hardened epithelium. Thus, several experiments were designed to modify established extraction techniques to remove keratins from human hair, nail and skin and apply these to canine hair, skin and the stratum externum, stratum medium and stratum internum of the claw. This would then provide a methodology that would allow a fair comparison between the different types of epithelia examined.

4.2 METHODS

4.2.1 Tissue Sample Preparation

Canine claws were obtained from the left hind limb of dogs E, F, G and H (Table 2.1) and were all washed in PBS prior to separation. Owing to the complexity of the claw, it was not possible to separate this structure into its germinative regions or all the different strata identified in Chapter 3. Instead, the claw was divided into its main macroscopic layers. From the anatomy study, it was established that the proximal claw contained only OCS, ICS, SE and SM1-4 material. This was labelled sample site 1 and was carefully removed from the claw using a scalpel. The soft layers of the OCS, ICS and SE were carefully scraped from the underlying SM1-4 using a scalpel blade so these could be extracted separately. The mid claw section contained all the main strata of the horn plate (SE, SM1-4 and SI1 and SI2) and was labelled sample site 2. Whole horn plate samples from this region were used when optimising the conditions for total protein extraction. Once this had been achieved, separation of the horn plate into the different strata was performed based on previous knowledge of the anatomy and the macroscopic differences such as colour variations and visible fracture lines between layers. However, further separation of the SM layer into its four regions (SM1-4) or the SI layer into SI1 and SI2 was not achieved, as differences between these layers could only be observed at the microscope level. SE samples taken from site 2 should not contain any OCS or ICS material, so a comparison with OCS, ICS and SE from site 1 should highlight differences between the SE and the other two regions (OCS and ICS). Sole material was carefully obtained from the claw

(sample site 3) and was not sub-divided as it was difficult to discern the individual sole components (S1-S4) at the macroscopic level (Figure 4.1). All horn plate samples were chopped carefully into fine pieces using a scalpel blade to make homogenisation easier. No differences were noted between the individual dog claws tested in this study.

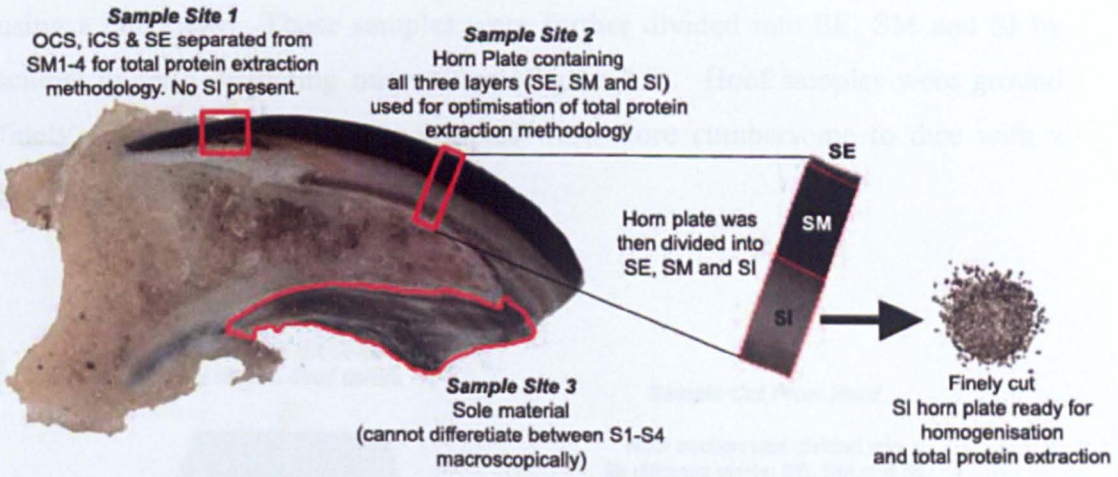

Figure 4.1: Canine Claw Sampling Sites

Using a band saw, a single parasaggital cut was made close to the midline of the claw. Samples from various sites of the claw were obtained. Sample site 1 included OCS, ICS, SE and SM1-4, which was located in the ungual groove. Once removed from the claw, the surface layers (OCS, ICS and SE) were scraped off the remaining claw plate (SM1-4) with a scalpel. Sample site 2 included all three layers of the horn plate (SE, SM1-4, and SI1-2) and was used to optimise the total protein extraction method. To analyse the different keratins within the different strata, sample site 2 was divided macroscopically into SE (obtained by scraping the surface of the horn plate using a scalpel), SM and SI. On the dorsal side of the claw, sample site 3 included all layers of the sole (S1-4), which could not be further divided macroscopically.

Canine hair samples were plucked from around the claw digit using tweezers to ensure follicular material was included. The lower portion of the hair follicles (containing hair fibre, IRS and ORS) were snipped off and rinsed in PBS before being placed in a sterile glass-glass homogeniser for protein extraction.

Skin samples were obtained carefully from around the digit area using a scalpel. The hair was plucked to remove as much follicular material as possible. The epidermis was separated from the dermis after heating the skin in PBS to 65°C for thirty seconds. The epidermis was peeled cleanly off the dermis using a pair of tweezers and placed in a sterile eppendorf on ice until ready for protein extraction. Alternatively, samples were frozen at -20°C for future use. Canine digital pad

epidermis was obtained by cutting a section of skin from the centre of the pad using a scalpel. The bulk of the dermal material (white) was easily removed from the epidermis (pigmented) but as this was a heavily papillated epithelium, some remnants of dermal mesenchyme may have been included.

Midline dead centre (MDC) hoof samples from both horse and donkey were cut using a band saw. These samples were further divided into SE, SM and SI by scalpel under a dissecting microscope (Figure 4.2). Hoof samples were ground finely using a pepper mill, as samples were more cumbersome to dice with a scalpel compared to dog claw plate.

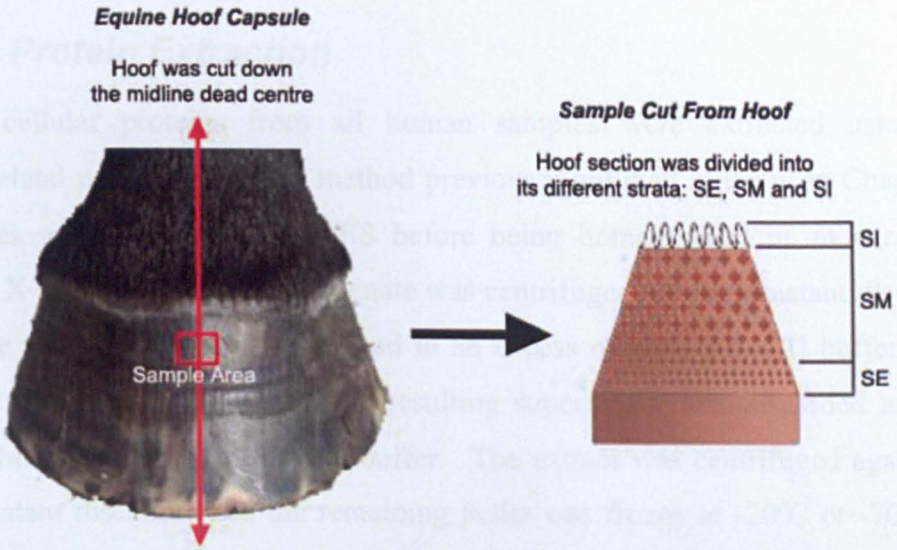

Figure 4.2: Equine Hoof Sample Region

A section of hoof was carefully removed from the midline dead centre (MDC) region of a hoof capsule using a band saw. The removed section was further divided using a scalpel into the stratum externum (SE), stratum medium (SM) and stratum internum (SI) and each of the samples were individually ground up into small pieces ready for homogenisation.

Human nail samples were obtained by clipping finger nails from healthy individuals. No proximal nail samples were collected. Nail clippings were cut finely, rinsed in PBS and a 1mg sample was placed in a 1ml glass-glass homogeniser ready for protein extraction.

Human hair samples were obtained by plucking hairs from healthy individuals and cut near the base so that the lower hair shaft, surrounded by follicular material

(IRS and ORS), was extracted. Hair samples were washed in PBS and a 5mg sample was placed in a 1ml glass-glass homogeniser ready for protein extraction.

Archival normal human tissue specimens were obtained from the Department of Dermatology (School of Medicine, Cardiff University). The epidermis was removed from the dermis by heat separation as previously described and stored on ice until ready for use. Palmar-plantar stratum corneum material was carefully removed from healthy individuals using a scalpel and washed in PBS. A 5mg sample was placed in a 1ml glass-glass homogeniser until ready for protein extraction.

4.2.2 Protein Extraction

Total cellular proteins from all human samples were extracted using the cytoskeletal protein extraction method previously outlined in detail in Chapter 2. Samples were pre-washed in PBS before being homogenised in an excess of Triton X-100 buffer. The homogenate was centrifuged, the supernatant discarded and the resulting pellet homogenised in an excess of high-salt KCl buffer. The extract was centrifuged again, the resulting supernatant was discarded and the pellet homogenised in a low salt buffer. The extract was centrifuged again, the supernatant discarded and the remaining pellet was frozen at -20°C or -70°C for future use or extracted immediately. Keratin intermediate filament (IF) proteins were extracted by homogenising the pellets in a 0.05M Tris HCl buffer at pH 6.8 containing 1% (w/v) SDS and 2% (v/v) βME.

When the cytoskeletal extraction process was tested on canine claw and hair tissue, very little keratin was removed due to the resilient nature of this epithelium. Thus, modifications to the extraction method were made so that more cellular material would be broken down and more protein extracted from the claw. The following sections outline modifications made to the total protein extraction methods described in Chapter 2, (section 2.4.2.) that were required to extract proteins from tissue as tough and resilient as the canine claw and hair.

4.2.3 Pre-soaking of Canine Claw and Equine Hoof Samples

Due to the robust nature of the canine claw, complete homogenisation of this material was often extremely difficult to achieve resulting in samples with low protein yield. To overcome this, claw samples were pre-soaked to soften the hard horn plate sufficiently to allow easier homogenisation, ultimately breaking down more cellular material and releasing more protein into the homogenate. Two different agents were tested: Phosphate buffered saline (PBS) which was already used to clean all samples before homogenisation, and the detergent, Triton X-100.

5mg samples of claw plate samples from digit 4 of dogs E, F, G and H were soaked in one of the following solutions as stated:

- PBS for 24 hrs at 4°C
- PBS for 48 hrs at 4°C
- Triton X-100 for 24hrs at 4°C
- Triton X-100 for 48 hrs at 4°C
- Triton X-100 for 4 hrs at 65°C
- PBS for 4 hrs at 65°C

Samples were then homogenised thoroughly in 500µl Tris-HCl buffer (0.05M, pH 6.8) containing 5% (w/v) SDS and 5% (v/v) βME buffer, prepared for one-dimensional SDS gel analysis on a 12.5% gel slab and visualised with CBB R250 after electrophoresis.

4.2.4 Reducing Agent Concentration

The total protein extraction methodology employed in the Dermatology Department, Cardiff University used a 0.05M Tris HCl, pH 6.8 buffer containing 1% (w/v) SDS and 2% (v/v) βME, which worked efficiently to extract protein from human tissue but was not effective on canine horn plate samples. Furthermore, the resulting SDS gels often displayed smeared lanes with poor separation of proteins. The concentration of the detergent (SDS) was increased to

combat the more resilient nature of the canine horn plate and βME was replaced with DTT to investigate if this improved protein resolution on the gel. To test the different reducing agents, 5mg of finely chopped canine horn plate was homogenised in 500µl of 0.05M Tris HCl, pH 6.8 under different extraction conditions. 5mg of horn plate samples from digit 4 of dogs E, G, F and H were homogenised in Tris-HCl buffer containing different levels of SDS and reducing agent (βME or DTT).

- 5% (w/v) SDS and 5% (v/v) βME
- 10% (w/v) SDS and 10% (v/v) βME
- 5% (w/v) SDS and 5% (w/v) DTT
- 10% (w/v) SDS and 10% (w/v) DTT

Each homogenate was placed in a sterile eppendorf and centrifuged at room temperature for 15 minutes at 15,000 rpm. The resulting supernatant was transferred to a sterile eppendorf and labelled "first extract". It was thought that due to the degenerative nature of the extraction process on the horn plate that the resulting pellet may be easier to homogenise and further protein could be extracted. Thus, the remaining pellet was further homogenised by repeating the above process, centrifuged and the supernatant obtained was labelled "second extract". Both extracts were prepared for one-dimensional electrophoresis as described in Chapter 2.

Urea protein extractions of horn plate samples were also performed. Canine claw plate (5mg) was finely chopped and heated in 0.1M Tris buffer containing 10M urea and 10% (v/v) βME for 24 hours at 40°C. Samples were then homogenised in 1ml of this urea buffer and dialysed in either 0.1M Tris, 0.1% (w/v) SDS and 0.1% (w/v) DTT solution or CASC (0.1M Citric Acid, 0.1M Trisodium Citrate) solution (See Section 2.4.3). All samples were prepared for analysis by one-dimensional gel electrophoresis as described in Chapter 2.

4.2.5 SDS-PAGE and Western Blotting

All protein extracts were loaded on either a 12.5% gel or a 7.5-17.5% gradient gel and visualised with CBB R250 according to the methodology outlined in Chapter 2. During the development of the protein extraction methodology for canine tissue, 12.5% gels were used as they were easier to produce but they did not provide the best protein resolution. After creating a protein extraction method suitable for canine tissue, all tissue samples (human, canine and equine skin, hair and nail/claw/hoof) were subsequently run on 7.5-17.5% gradient gels. These gels are more time consuming to make but allow better separation of a mixture of proteins with a greater molecular weight range than a gel with a fixed acrlyamide concentration (see methods for details).

The monoclonal antibodies listed in Table 4.1 were the only ones identified to work correctly on both human and canine tissue. The optimal antibody and label dilutions used for western blotting are provided for each antibody and label. Optimisation of primary antibody concentration was carried out to ensure the best results. In general, lower concentrations of both primary and secondary antibodies are required with ECL compared to colorimetric detection. Western blots were prepared using normal human skin or hair follicle material total protein extracts as they expressed the keratin antigens required. The resulting membrane was then cut into several strips. One blot was prepared for each primary antibody dilution to be tested. The immunoblots were incubated in TBS-T for 1 hour at room temperature with constant agitation before being rinsed briefly in three changes of fresh TBS-T buffer every five minutes. Several dilutions of primary antibody were then prepared (e.g. 1/100, 1/500, 1/1000, 1/2500, 1/5000) and one blot strip was incubated in each dilution for 1 hour at room temperature with agitation. Following this, the strips were rinsed three times in fresh TBS-T buffer every five minutes. The secondary antibody was diluted initially using only one concentration, and the membranes were incubated for 1 hour at room temperature with agitation. Each membrane was rinsed as before in TBS-T buffer. The streptavidin biotinylated HRP complex was diluted initially using only one concentration and placed on the membranes. This was left to incubate for 1 hour at room temperature and then strips were rinsed thoroughly three times with TBS-

T, changed every 5 minutes. The membranes were stored in TBS-T until ready for DAB or ECL detection. The antibody dilution that produced the best signal with the minimum background was selected. After determining the correct primary antibody concentration, the secondary antibody and label concentrations were modified to produce the best results.

Other keratin antibodies tested included K9, which only worked on human tissue and did not cross react with canine tissue. Hair-specific keratin antibodies, (Ha1, Ha2, Hb1 and Hb2) and epithelial keratin antibodies (K1, K2 and K6) did not react with either human or canine tissue in the western blots.

Table 4.1: Primary Antibody Dilutions for Western Blotting

Primary Antibody	Product Name	Source	Primary Antibody Dilution	Secondary Antibody Dilution	Streptavidin Biotinylated HRP Complex
K5	-	Binding Site	1/1000	1/100	1/100
K9 Human tissue only	Ks9.70/Ks9.216	Abcam	1/1000	1/400	1/1000
K10	LH2	Biogenesis	1/1000	1/400	1/1000
K14	-	Binding Site	1/500	1/400	1/1000
K16	LHK6B	Donated by Prof Mike Philpott (Queen Mary College, London)	1/400	1/100	1/100
K17	RPmK17	Donated by Dr Rebecca Porter (Cardiff University)	1/5000	1/1000	1/1000

* The dilutions above provided optimal results for both human and canine tissue except the K9 antibody, which does not cross-react with canine tissue.

4.3 Results

Tissue samples from human, canine and equine skin, hair and nail/claw/hoof were analysed by one-dimensional electrophoresis (SDS-PAGE) using either 12.5% gels or 7.5-17.5% gradient gels (see methods for details). No differences were noted between the individual dog claws tested in this study.

4.3.1 Analysis of Protein Standards

Aliquots of seven proteins of known molecular mass (phosphorylase b, bovine albumin, pyruvate kinase, glutamate dehydrogenase, actin, carbonic anhydrase and lysozyme) were dissolved in Tris-SDS-βME buffer as described in section 2.4.2. The proteins were run individually on a 12.5% polyacrylamide gel, adjusted for protein concentration and a mixture made that represented equal amounts of each standard. This mixture was then run on another 12.5% gel together with the individual standards and visualised with Coomassie Brilliant Blue (CBB) R250 (Figure 4.3). The proteins covered a molecular weight range from 94kDa to 14kDa and the mixture was used to calibrate subsequent gels.

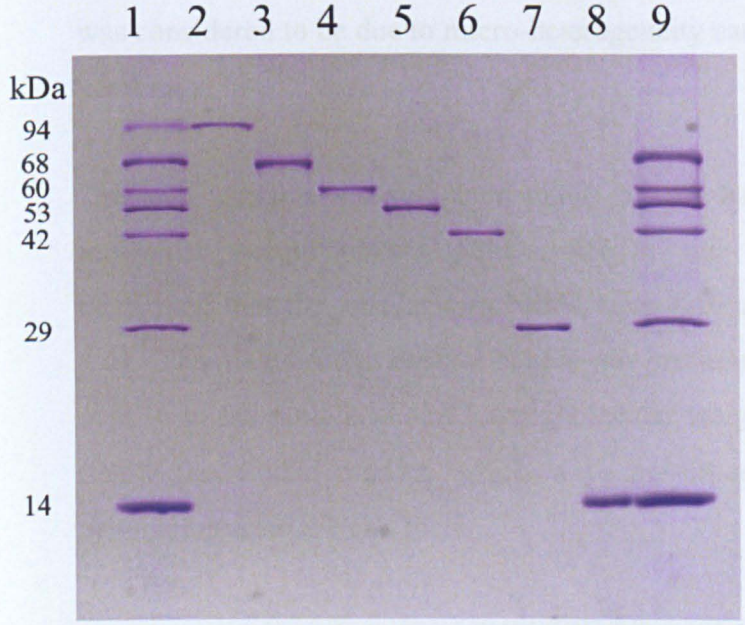

Figure 4.3: SDS-PAGE of Protein Standards

Individual protein standards (**lanes 2-8**) and a standard mixture (**lanes 1 & 9**) were analysed on a 12.5% slab gel (SDS-PAGE). The standards were: Phosphorylase b (PHOS, **lane 2**), Bovine Serum Albumin (BSA, **lane 3**), Pyruvate Kinase (PK, **lane 4**), Glutamate Dehydrogenase (GLDH, **lane 5**), Actin (ACT, **lane 6**), Carbonic Anhydrase (CA, **lane 7**) and Lysozyme (LYS, **lane 8**). All individual standards were loaded at 10µl and the mixture at 15µl.

4.3.2 Analysis of Human Nail, Hair and Skin

Proteins were extracted from samples of human skin (dermis, epidermis, and stratum corneum), hair and nail tissues following cytoskeletal extraction as described in Chapter 2. These protein extracts were analysed on 7.5-17.5% gradient gels and visualised with CBB R250 (Figure 4.4).

Human epidermal extracts (lane 1) contained four major proteins (68kDa, 60kDa, 58kDa and 50kDa), representing the four major epidermal keratins (K1, K5, K10 and K14 respectively), and western blot analysis confirmed the presence of K5, K10 and K14 (Figures 4.4 and 4.5). Human dermal extracts demonstrated a much more complex protein profile (lane 2) containing high molecular weight collagens and some smaller keratins (K5 and K14) probably of epithelial appendage origin. Extracts of palmar-plantar stratum corneum from heel skin (lanes 3) demonstrated the presence of several proteins in the keratin molecular weight range (40-70kDa) with bands at 65kDa, 60kDa, 56kDa, 48kDa, 46kDa and ≤42kDa. Western blotting confirmed some of these proteins to represent K9, K10 and K17 (Figure 4.5). In addition, a faint band visible at 48kDa was shown to be K16 although the western blot band was extremely faint. The smearing observed between bands was considered to be due to micro-heterogeneity caused by mild proteolysis of the keratins.

The nail extracts showed four main protein bands (Figure 4.4, lane 5) of molecular weight 65kDa, 58kDa, 48kDa and 46kDa and western blotting confirmed that the smaller two bands were K16 and K17 respectively (Figures 4.6). The main protein band at 58kDa was presumed to be K6 given the presence of K16 in the sample. Faint lower molecular weight bands appeared around and below the 42kDa marker, which were presumed to be hair-specific keratins originating from the nail plate.

Finally, the human hair extract (lane 6) contained four main protein bands. These were of 65kDa, 60kDa, 48kDa and 42kDa (Figure 4.4). Western blot analysis using human epithelial keratin antibodies identified K5, K16 and K17, although the K17 band was extremely faint (Figure 4.6). The human hair-specific keratin

antibodies used in this study did not work when used in western blot analysis so the identity of some of the protein bands could not be established. Nonetheless, given that these proteins have been extracted from human hair samples, and are located within the hair-specific keratin molecular weight range, it can probably be assumed that these are canine hair-specific keratins.

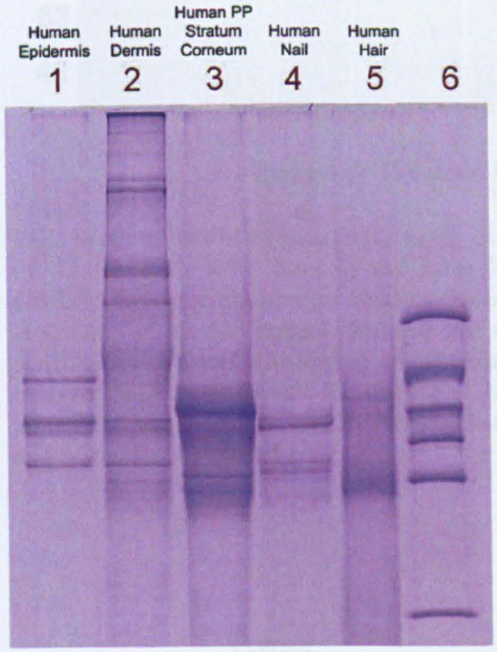

Figure 4.4: SDS-PAGE of Human Skin, Nail and Hair Extracts

Cytoskeletal protein extracts of human epidermis (**lane 1**, 8µl), human dermis (**lane 2**, 10µl), human palmar plantar stratum corneum (**lane 3**, 4µl), human nail (**lane 4**, 10µl) and human hair (**lane 5**, 20µl). Protein standard (**lane 6**) defined the molecular weight range (29-94kDa). SDS-PAGE gradient gel (7.5-17.5%).

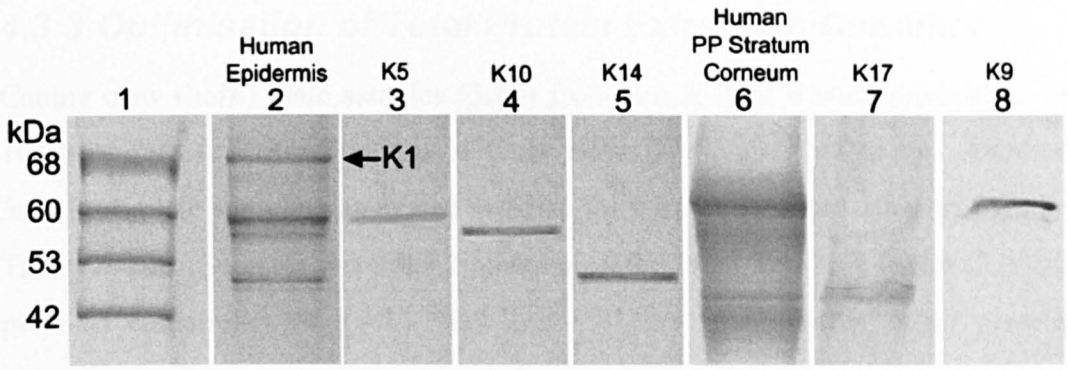

Figure 4.5: Western Blot of Human Skin Samples

ECL Western blot of cytoskeletal protein extracts of human epidermis demonstrated the presence of K5 (**lane 3**), K10 (**lane 4**) and K14 (**lane 5**). The total cytoskeletal extract stained with CBB250 shows all four major keratins (**lane 2**, 8µl) and the band at 68kDa was thought to be K1. However, as the K1 human antibody did not work in western blot analysis this could not be confirmed. Western blotting of cytoskeletal extracts of human palmar-plantar stratum corneum revealed K17 (**lane 7**) and K9 (**lane 8**). Again, a total protein extract stained with CBB R250 shows the whole keratin profile (**lane 6**, 4µl) and protein standards stained with CBB R250 are shown on the left (**lane 1**).

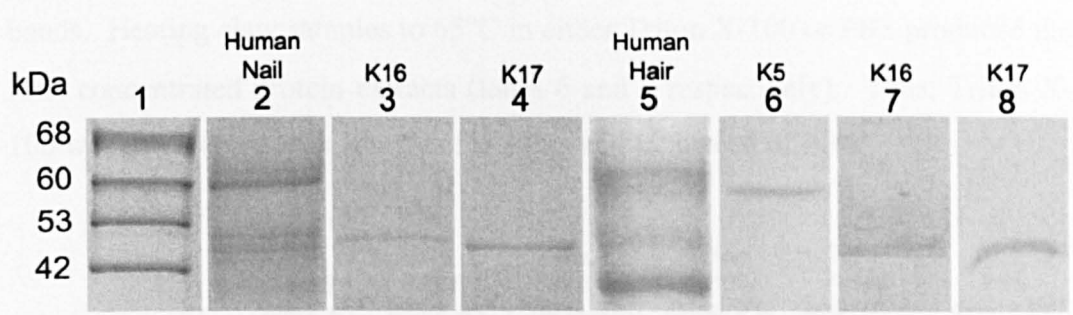

Figure 4.6: Western Blot of Human Nail and Hair

ECL Western blot analysis on total protein extracts from human nail tip clippings confirmed that two epithelial keratins, K16 (**lane 3**) and K17 (**lane 4**), were present within these samples. Two protein bands were observed level with 60kDa marker and these may represent K5 and K6. However, this could not be confirmed, as the K6 antibody was not suitable for Western Blot studies. Human hair (hair shaft plus follicular material) samples revealed that K5 (**lane 6**), K16 (**lane 7**) and K17 (**lane 8**) were all present within these samples. Lanes **1, 2** and **5** were stained with CBB R250 and show the protein standard mix (**lane 1**) that was used to calibrate the gel and a total human nail (**lane 2**) and human hair (**lane 5**) extract. Both human nail and hair samples also demonstrated multiple protein banding between 40kDa and 42kDa which was within the molecular weight range for hair-specific keratins. Unfortunately, it could not be confirmed that these bands were hair-specific keratins, as human hair-specific keratin antibodies used in this study did not work in western blots.

4.3.3 Optimisation of Total Protein Extraction Conditions

Canine claw (horn) plate samples (5mg) from site 2, digit 4 were pre-soaked in 10mls of PBS or Triton X-100 at 4°C for either 24 hours or 48 hours. Another 5mg horn plate sample was heated at 65°C for 4 hours in either 10ml of PBS or Triton X-100. Samples were then homogenised in 500µl Tris-HCl buffer (0.05M, pH 6.8) containing 5% (w/v) SDS and 5% (v/v) βME buffer (total protein extraction). These extracts were loaded on a 12.5% gel and visualised with CBB R250 (Fig. 4.7).

Canine claw extracts pre-soaked in PBS for 24 hours (lane 2) or 48 hours (lane 3) did not soften claw material sufficiently and homogenisation was extremely difficult. Subsequently, claw samples pre-soaked in PBS produced faint protein bands. In comparison, claw samples pre-soaked in Triton X-100 for 24 hours (lane 4) or 48 hours (lane 5) softened claw material adequately and almost total homogenisation of the claw sample was achieved, resulting in stronger protein bands. Heating claw samples to 65°C in either Triton X-100 or PBS produced the least concentrated protein extracts (lanes 6 and 7 respectively). Thus, Triton X-100 was used to pre-soak samples for 24hrs at 4°C instead of PBS.

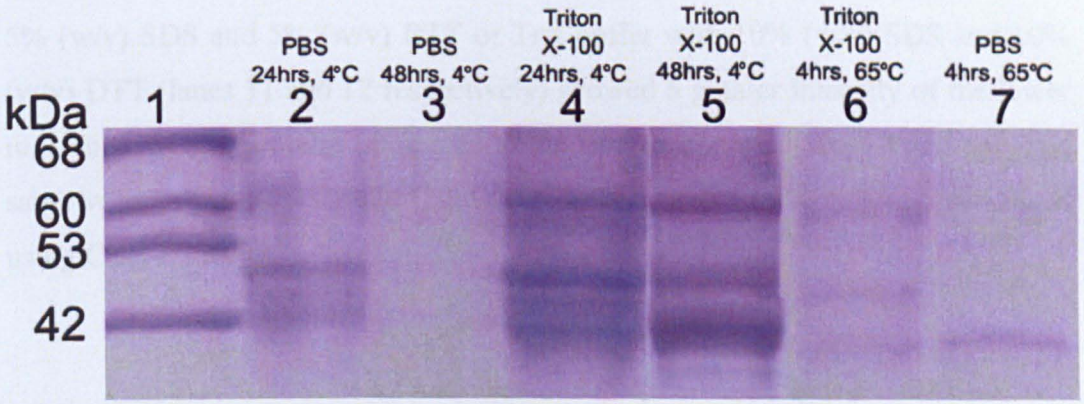

Figure 4.7: Optimisation of Total Protein Extraction Conditions: Pre-soaking Tissue

Different buffers were used to pre-treat the samples prior to total protein extraction. 5mg samples of canine claw (horn) plate from site 2 on the 4th digit were soaked in PBS for 24 hours at 4°C (**lane 2**), PBS for 48 hours at 4°C (**lane 3**), Triton X-100 for 24 hours at 4°C, (**lane 4**) and for 48 hours at 4°C, (**lane 5**), Triton X-100 for 4 hours at 65°C (**lane 6**), PBS for 4 hours at 65°C (**lane 7**). Protein standards are shown on the left (**lane 1**). All lanes were loaded at 10µl and proteins were visualised using CBB-R250 (SDS-PAGE, 12.5% gel).

Optimisation of the detergent and reducing agent concentrations (Figure 4.8) established that 5mg samples of canine (horn) plate pre-soaked in Triton X-100 (24hrs, 4°C) and homogenised in 500µl of Tris buffer containing 10% (w/v) SDS and 10% (v/v) βME (lane 3) produced bands of much greater intensity compared to a Tris buffer containing 5% (w/v) SDS and 5% (v/v) βME (lane 2). Proteins extracted from claw plate samples using 500µl of Tris buffer with 5% (w/v) SDS and 5% (w/v) DTT or Tris buffer with 10% (w/v) SDS and 10% (w/v) DTT (lanes 4 and 5 respectively) produced protein profiles of similar intensity to Tris buffer with 5% (w/v) SDS and 5% (v/v) βME. No protein bands were observed with urea extracted horn plate samples that were dialysed in Tris-SDS-DTT (lane 6) but faint protein bands were observed in CASC dialysed samples (lane 7). However, the results with the urea extraction were generally poor and more often than not, no protein was found in either of the dialysed extracts. Re-extraction of the pellets (second extracts) with Tris buffer plus 5% (w/v) SDS and 5% (v/v) βME (lane 9) again produced weak bands, which were similar in intensity to the first extraction. However, second extracts of the pellets extracted with Tris buffer plus 10% (w/v) SDS and 10% (v/v) βME pellets (lane 10), displayed an extremely faint protein outline suggesting that nearly all keratin material was removed during the first extraction. Re-extraction of pellets using either Tris buffer with 5% (w/v) SDS and 5% (w/v) DTT or Tris buffer with 10% (w/v) SDS and 10% (w/v) DTT (lanes 11 and 12 respectively) showed a greater intensity of the lower molecular weight proteins compared to the first extractions (lanes 4 and 5). The same volume for each sample (20µl) was loaded onto 12.5% gels and visualised using CBB R250.

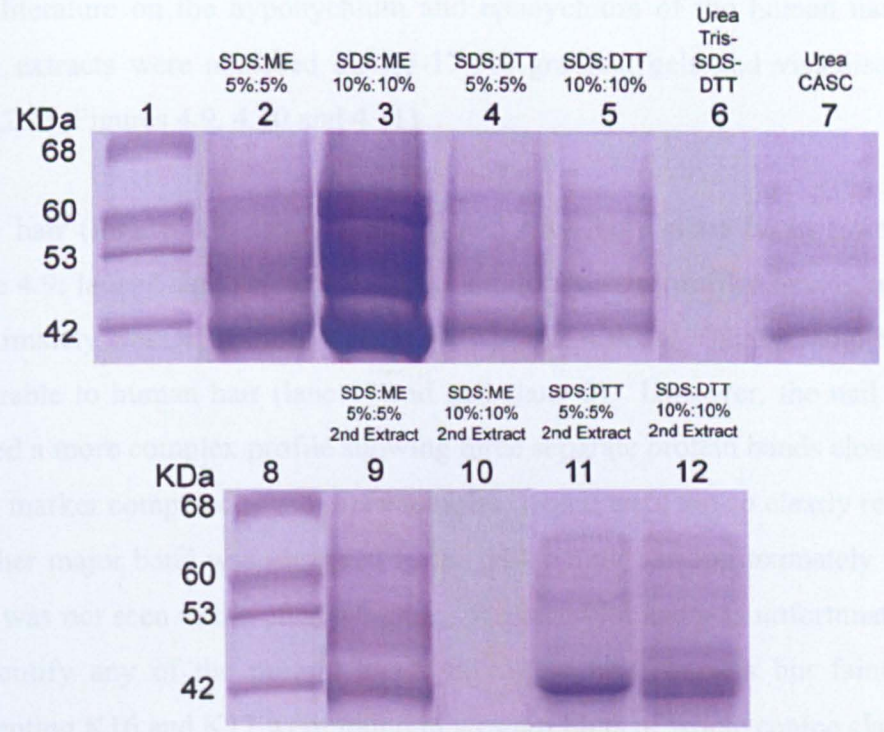

Figure 4.8: Optimisation of Total Protein Extraction Conditions: Detergent and Reducing Agent Concentrations

5mg samples of canine claw plate from site 2 on the 4th digit were soaked in Triton X-100 (48 hours, 4°C) and extracted with Tris-HCl containing either SDS: βME (5%:5%, **lane 2**, or 10%:10%, **lane 3**) or SDS:DTT (5%:5%, **lane 4** or 10%:10%, **lane 5**). 5mg canine claw plate samples treated with a urea extraction buffer and dialysed in Tris-SDS-DTT (**lane 6**) or CASC dialysis solution (**lane 7**). Pellets from the Tris-SDS-βME extractions were re-extracted in the same buffers (**lanes 9** and **10**) as were those in Tris-SDS-DTT (**lanes 11** and **12**). All samples were loaded at 20µl and the protein standard mixture (**lanes 1** and **8**) was used to calibrate the gel (SDS-PAGE, 12.5%).

In conclusion, from this optimisation study, to obtain reasonable levels of a representative mixture of protein from 5mg of claw plate, samples were homogenised in 500µl of extraction buffer containing 0.5M Tris HCl (pH 6.8), 10% (w/v) SDS and 10% (v/v) βME. The volume loaded onto each gel had to be determined for each individual sample so that overloading or under loading did not occur. Generally, 10µl of 10mg/ml claw extract produced clear protein profiles with good resolution.

Using the optimised total protein extraction, canine hair, claw plate, digital foot pad and skin samples were compared to human hair, nail, palmar-plantar skin and interfollicular skin respectively. Additionally, canine sole (sample site 3) and OCS, ICS and SE (sample site 1) were extracted and the results compared to data

in the literature on the hyponychium and eponychium of the human nail. All protein extracts were analysed on 7.5-17.5% gradient gels and visualised with CBB R250 (Figures 4.9, 4.10 and 4.11).

Canine hair (Figure 4.9: lanes 3 and 4) and claw horn plate taken from site 2 (Figure 4.9: lanes 5 and 6), demonstrated similar protein profiles having bands at approximately 65kDa, 58kDa, 48kDa and below 42kDa. These samples were comparable to human hair (lane 1) and nail (lane 2). However, the nail extract revealed a more complex profile showing three separate protein bands close to the 53kDa marker compared to the other samples, which were not so clearly resolved. A further major band was observed in the nail samples at approximately 56kDa, which was not seen in the other samples. Western blot analysis unfortunately did not identify any of the protein bands in canine hair samples but faint bands representing K16 and K17 were found in western blots of whole canine claw plate extracts.

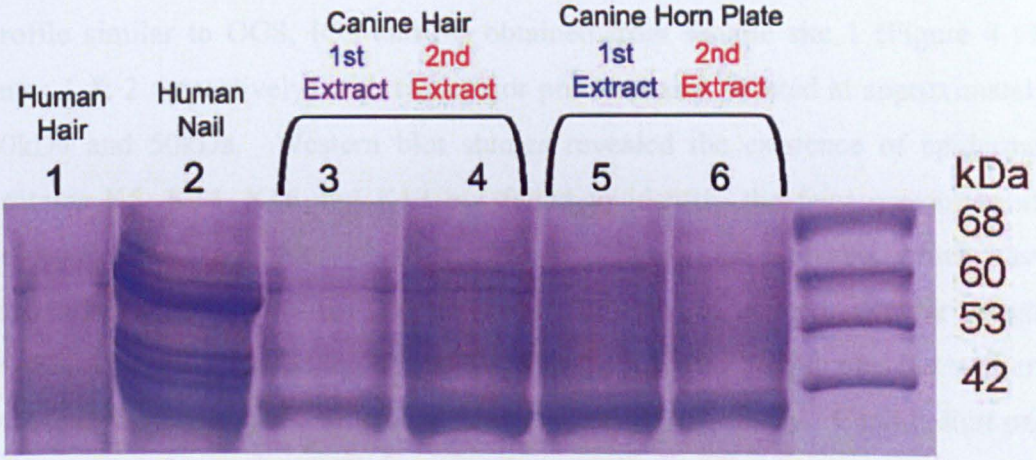

Figure 4.9: SDS-PAGE of Human Hair, Nail, and Canine Hair and Horn Plate Extracts

Total protein extracts of human hair (**lane 1**, 15µl), human nail (**lane 2**, 15µl), canine hair (first extract, **lane 3**, 4µl. Second extract, **lane 4**, 7µl), canine claw plate (first extract, **lane 5**, 10µl; second extract, **lane 6**, 10µl). A protein standard mix (**lane 7**) was used to calibrate the gel (SDS PAGE, 7.5-17.5%).

Canine skin samples displayed a similar protein profile to human skin with four major proteins (68kDa, 60kDa, 58kDa and 50kDa) making up the majority of the extract (Figure 4.10). These probably represent the four major epidermal keratins, K1, K5, K10 and K14 respectively. Western blot analysis confirmed the presence of K5, K10 and K14 (Figure 4.13) but as the human K1 antibody did not cross-react with canine tissue, the 68kDa protein band was not confirmed to be K1.

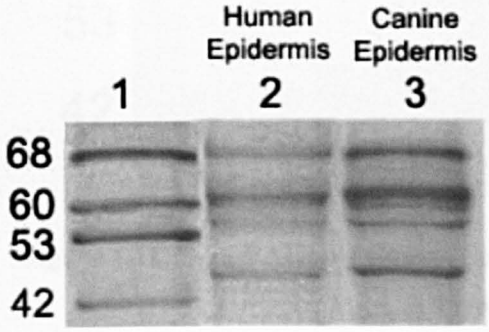

Figure 4.10: SDS-PAGE of Human Skin and Canine Skin

Cytoskeletal protein extracts of normal human skin (**lane 2**) and normal canine skin (**lane 3**). Protein standards (**lanes 1**) were used to calibrate the gel (SDS PAGE, 7.5-17.5% gradient gel) and all proteins were visualised with CBB R250.

Canine sole taken from sample site 3 (see Figure 4.1) demonstrated a protein profile similar to OCS, ICS and SE obtained from sample site 1 (Figure 4.11: lanes 1 & 2 respectively) with two major protein bands located at approximately 60kDa and 50kDa. Western blot studies revealed the existence of epidermal proteins K5, K14, K16 and K17 but failed to identify the faint protein bands below the 60kDa marker which may be one of the K6 isoforms which have molecular weight of 58kDa (Figure 4.15). Proteins of lower molecular weight (<42kDa) were observed in both sole and OCS, ICS and SE samples but western blot analysis could not confirm the identities of these proteins. Canine digit pad (lane 4) demonstrated a different but still complex protein profile when compared to human palmar-plantar stratum corneum (lane 5). Both extracts confirmed the presence of several proteins in the keratin molecular weight range (40-70kDa) with proteins bands at 60kDa, 58kDa, 56kDa, 53kDa, 48kDa, 45kDa, and ≤42kDa. Western blotting confirmed some of these proteins to represent K10 and K16 in canine digital foot pad extracts. Unfortunately, the human K9 antibody did not cross-react with canine tissue so the presence of K9 in canine digital foot pad could not be confirmed.

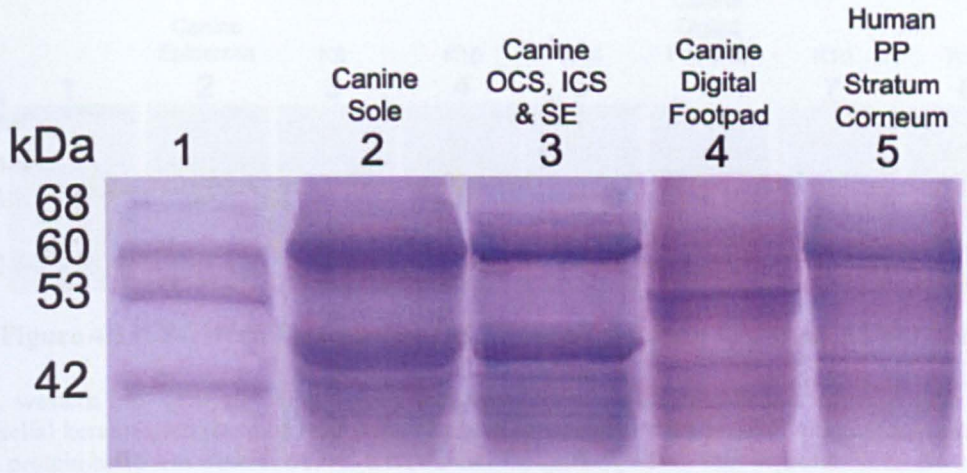

Figure 4.11: SDS-PAGE of Canine Sole, OCS, ICS & SE, Digital Foot pad and Human Palmar Plantar Skin

Total protein extracts of canine sole (**lane 2,** 15µl), canine OCS, ICS & SE (**lane 3,** 15µl), canine digital foot pad (**lane 4,** 15µl) and human palmar-plantar stratum corneum (**lane 5,** 10µl). Canine sole protein profiles strongly resembled OCS, ICS and SE horn plate samples with two main protein bands at 60kDa and 50kDa. Low molecular weight proteins were observed at 48kDa, 46kDa and ≤42kDa in both samples. Protein standards (**lane 1**) were used to calibrate the gel (SDS PAGE 7.5-17.5% gradient).

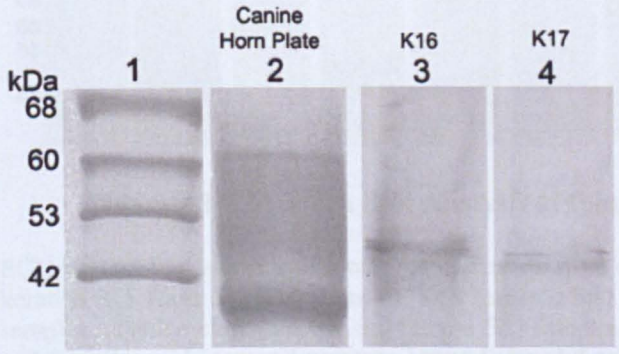

Figure 4.12: Western Blot Analysis of Canine Horn Plate

ECL western blot analysis of total protein extracts from canine claw plate confirmed that two epithelial keratins, K16 (**lane 3**) and K17 (**lane 4**), were present within these samples. Lane 1 and 2 were stained with CBB R250 and show the protein standard mix (**lane 1**) that was used to calibrate the gel and a total canine claw plate extract (**lane 2**). Canine claw plate demonstrated a major protein band between 40kDa and 42kDa, which is within the molecular weight range for hair-specific keratins. It could not be confirmed that this band was a hair-specific keratin as the human hair-specific keratin antibodies used in this study did not work in western blots.

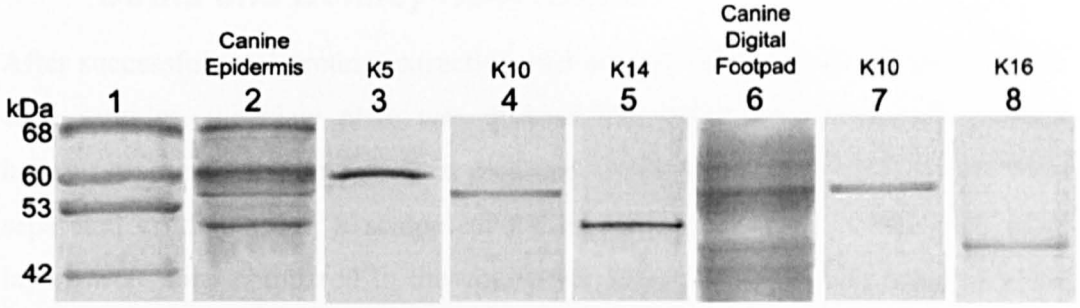

Figure 4.13: Western Blot Analysis of Canine Epidermis and Digital Foot pad

ECL western blot analysis of total protein extracts from canine epidermis confirmed that three epithelial keratins, K5 (**lane 3**) K10 (**lane 4**) and K14 (**lane 5**), were present within these samples. One protein band was observed level with the 68kDa marker, which may represent K1. However, this could not be confirmed, as the K1 human antibody was not suitable for western blotting. Canine digital foot pad samples revealed that K10 (**lane 7**) and K16 (**lane 8**) were present within these samples. Lanes **1, 2** and **6** were stained with CBB R250 and show the protein standard mix (**lane 1**) that was used to calibrate the gel and total canine epidermis (**lane 2**) and digital foot pad (**lane 6**) extracts.

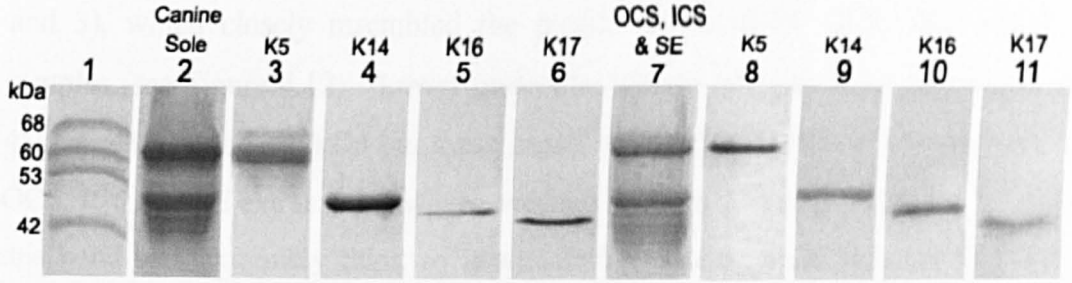

Figure 4.14: Western Blot Analysis of Canine Sole and OCS, ICS & SE

ECL western blot analysis of total protein extracts from canine sole confirmed that four epithelial keratins, K5 (**lane 3**), K14 (**lane 4**), K16 (**lane 5**) and K17 (**lane 6**) were present within these samples. Canine claw fold (OCS, ICS and SE) samples revealed that K5 (**lane 8**), K14 (**lane 9**) and K17 (**lane 11**) were all present. Lanes **1, 2** and **7** were stained with CBB R250 and show the protein standard mix (**lane 1**) that was used to calibrate the gel and total canine sole (**lane 2**) and claw fold epithelium (OCS, ICS and SE) (**lane 7**). Canine claw fold epithelium (OCS, ICS and SE) samples also demonstrated multiple protein banding between 40kDa and 45kDa which was within the molecular weight range for hair-specific keratins. It could not be confirmed that these bands were hair-specific keratins as human hair-specific keratin antibodies used in this study did not work in western blotting.

4.3.4 Protein Analysis of the Canine Claw Plate, Horse Hoof Strata and Donkey Hoof Strata.

After successful total protein extraction and western blot analysis of whole canine claw samples, the claw plate was divided into three morphologically defined layers (stratum externum, stratum medium and stratum internum), which were separated crudely using a scalpel and dissecting microscope. The claw plate layers were then compared to the equivalent layers of the equine hoof. Canine claw samples (4^{th} digit) were cut into sections, separated into the different strata and soaked in Triton X-100 buffer (48 hours, 4°C). 5mg samples were homogenised in 500µl of Tris buffer containing 10% (w/v) SDS and 10% (v/v) βME. The protein extracts were analysed on 7.5-17.5% gradient gels (SDS-PAGE) and visualised with CBB R250 (Figure 4.12).

Canine claw stratum externum (SE) extracts obtained from sample site 1 demonstrated two major protein bands at 60kDa and 50kDa (Figures 4.15: lanes 2 and 3), which closely resembled the profile produced by OCS, ICS and SE samples (see Figure 4.12). Lower molecular weight proteins were also found at 48kDa, 46kDa and ≤42kDa but these bands were a lot weaker in comparison to OCS, ICS and SE extracts. However, western blot analysis only identified K5 and this band was extremely faint, so it was difficult to ascertain whether this was specific staining or background.

Stratum medium (SM) extracts demonstrated a different protein profile to the SE extracts with a series of bands grouped closely together in the 40kDa to 60kDa range (Figures 4.15: lanes 4 and 5). The majority of the protein bands were narrow and not very concentrated but two major bands were found at 40kDa and 45kDa. Stratum medium extracts taken from different claws and different dogs demonstrated uniform protein profiles and the only differences that occurred were due to protein concentration. Western blotting confirmed that K16 and K17 were present in these extracts.

Stratum internum (SI) samples demonstrated a similar protein profile to the SM samples (Figures 4.15: lanes 6 and 7). Four protein bands were identified at

62kDa, 61kDa, 45kDa and 40kDa. Western blotting identified K5 and K14 as well as K16 and K17 in these extracts.

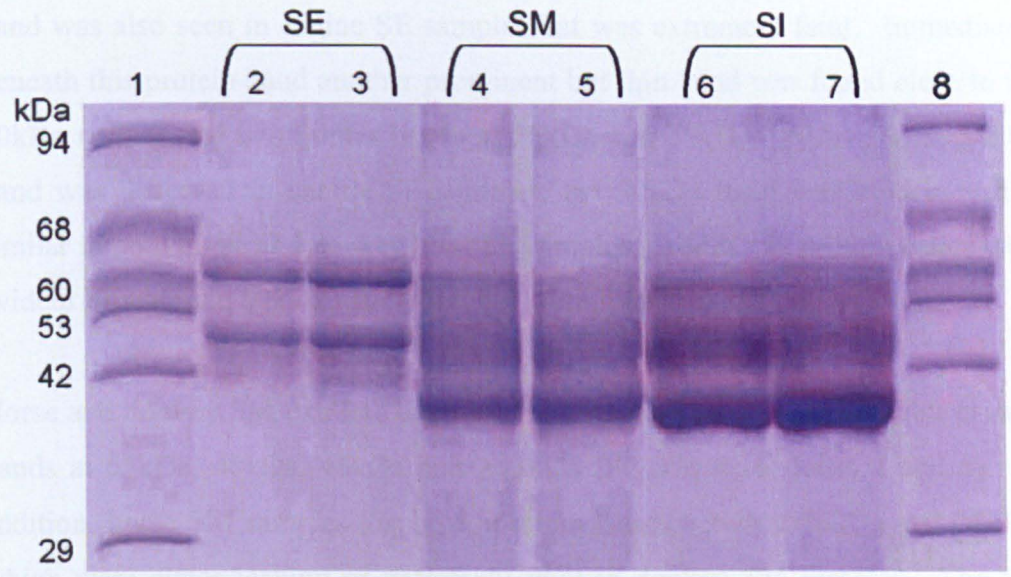

Figure 4.15: SDS-PAGE Analysis of Total Protein Extracts of Canine Claw (Stratum Externum, Stratum Medium and Stratum Internum)

Canine claw plate from samples from site 2 of the 4th digit were divided macroscopically into stratum externum (SE), stratum medium (SM) and stratum internum (SI). Total proteins were extracted from 5mg samples as described and all samples were loaded at 10µl. SE (**lane 2**), SE (**lane 3**), SM (**lane 4**), SM (**lane 5**), SI (**lane 6**) and SI (**lane 7**). Protein standards (**lanes 1** and **8**) were used to calibrate the gel (SDS-PAGE, 7.5-17.5% gradient).

Similarly, equine hoof samples were separated into SE, SM and SI (Figure 4.16). Horse and donkey hair were obtained from above the coronary band, mid-line dead centre (MDC). 5mg samples were treated with Triton X-100 for 48 hours before being homogenised in 1ml of 0.05M Tris HCl, pH6.8 buffer containing 10% (w/v) SDS and 10% (v/v) βME. The protein extracts were analysed on 12.5% gels, which did not provide a good protein resolution when compared to the canine tissue extracts which were analysed on gradient gels. Reasons for not running horse and donkey samples on a gradient gel were due to time restrictions and limited sample size.

A similar protein profile was identified when comparing protein bands from the different strata of horse and donkey hoof to canine claw. Akin to SE samples of the canine claw, horse and donkey hoof samples revealed a series of protein bands grouped closely between 40kDa and 65kDa although several protein bands could

be seen at about 40kDa rather than the large solid band observed in the canine claw extracts (Figure 4.16: lanes 2 and 3). One major difference observed in equine SE samples was a major band located at about the 65kDa region. This band was also seen in canine SE samples but was extremely faint. Immediately beneath this protein band another prominent but thin band was found close to the 60kDa marker and two fainter bands at 56kDa and 50kDa. Although no 56kDa band was observed in canine SE samples, the 50kDa band was evident and is similar in both horse and donkey hoof SE samples. Additional protein bands were evident beneath the 50kDa band but these were faint and difficult to interpret.

Horse and donkey SM extracts demonstrated similar protein profiles with protein bands at 65kDa, 48kDa, 46kDa and ≥42kDa (Figures 4.16: lanes 4 and 5). In addition, horse SM samples displayed protein bands between 56kDa and 60kDa, which were either lacking or extremely faint in donkey SM samples. The SM protein profiles generated from both equine and canine samples loosely resembled each other as both contained three definite groups of proteins bands with the first group located around the 60kDa marker, the second around the 50kDa region and the third below the 42kDa marker. However, equine protein bands were sharper and more defined compared to canine and donkey SM protein bands.

Horse and donkey hoof SI samples were less concentrated compared to SM samples but essentially included the same protein bands (Figures 4.16: lanes 6 and 7). Horse SM and SI protein profiles were also very similar with one major protein band located at about 40kDa that was lacking in both donkey SM and SI samples.

The varying intensities of the protein bands in all samples is a reflection of the difficulty experienced extracting protein from such hard and robust material as the hoof, claw and hair. Furthermore, most of this material is predicted to be made up of hair-specific keratins, which could not be confirmed by blotting as the available human antibodies did not cross-react so western blot analysis was not done.

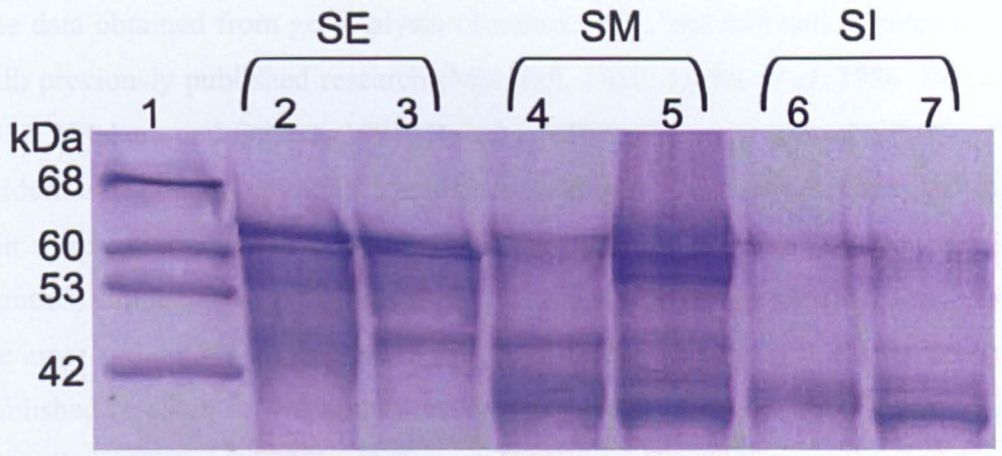

Figure 4.16: SDS-PAGE Analysis of Total Protein Extracts of Horse and Donkey Hoof

Horse and donkey hoof were separated into stratum externum (SE), stratum medium (SM) and stratum internum (SI). Each 10mg sample was pre-soaked in PBS (4°C, 48hrs) and was homogenised in Tris buffer containing 10% (w/v) SDS and10% (v/v) βME. Donkey SE (**lane 2**), horse SE (**lane 3**), donkey SM (**lane 4**), horse SM (**lane 5**), donkey SI (**lane 6**) and horse SI (**lane 7**). All extracts loaded at 10µl and protein standards (**lanes 1** and **10**) were used to calibrate the gel(SDS-PAGE 12.5%).

4.4 DISCUSSION

The data obtained from gel analysis of human skin, hair and nail extracts agreed with previously published research (Marshall, 1983; Lynch *et al*, 1986; Bowden, 1987; Kitahara and Ogawa, 1991, Bowden, 1993; Shimomura *et al*, 2002). The epidermis expressed epithelial keratins in a defined and sequential manner while hair differentiation was more complex involving a separate group of hair-specific keratins, which make up the hair fibre, and several epithelial keratins, which form the inner and outer-root sheaths. Analysis of human nail extracts also agreed with published research in that protein bands were present between 44kDa and 46kDa as well as 48kDa, 50kDa, 56kDa and 58kDa, demonstrating a mixture of both "hard" and "soft" keratins. Lynch *et al* (1986) stated that the presence of both types of keratin within the nail plate suggested that precursor cells of the hair cortex and nail plate share a major pathway of epithelial differentiation. Preliminary data obtained on the canine claw samples was somewhat similar to the situation with human nail and indicated that the keratins present were a mixture of epithelial keratins from the skin epidermis and hair-specific keratins from the hair-fibre.

Protein extracts taken from the claw fold (**OCS, ICS** and **SE**) contained proteins of 46kDa, 48kDa, 50kDa, 56kDa, 58kDa, 60kDa and 68kDa. Further investigation using western blotting revealed that K5, K14, K16 and K17 were all expressed within the different layers of the claw fold but K10 was absent. It was thought that the small faint band observed beneath the 60kDa standard would probably be K6 and the larger protein band located near the 68kDa region would be K1. Unfortunately, K1 and K6 antibodies did not work in western blot analysis so this could not be confirmed. Comparable studies investigating keratin expression within the human nail agree with the present findings. De Berker *et al* (2000) stated that the eponychium (nail fold) of the human nail expresses K1, K16, K6 as well as K10 and furthermore, Perrin *et al* (2004) reported that K5 and K17 were also expressed within the human nail fold. Akin to this, the different layers of the hair follicle have been shown to express the keratins that have been identified within the canine claw fold including a lack of K10, which supports our hypothesis that the canine claw fold is similar to the hair follicle as well as to

human nail fold (eponychium). Other keratins identified within the ORS and IRS of the hair follicle include K6 (58kDa), K15 (50kDa), K25-K28 and K71-K74 (Langbein *et al*, 2003 & 2006) could not be identified in canine claw fold as the human keratin antibodies did not cross-react with canine tissues. Lynch *et al* (1986) suggested that the nail and hair share a common pathway of terminal differentiation and the present data would support this notion.

The lower molecular weight proteins (45kDa and ≥42kDa) observed in the claw fold samples were considered to be a contribution from the **stratum externum** (**SE**), which was included in claw fold samples. Previous research on human nail fold as well as hair ORS and IRS layers has revealed that these structures do not contain any "hard" keratins of lower molecular weight (42-45kDa). Proteins isolated from the stratum externum of both canine claw and equine hoof were similar in size to human K5 (60kDa) and K14 (50kDa) but western blot analysis of these samples did not confirm that these two protein bands were the epidermal keratins, K5 and K14. This was not due to a lack of human-canine cross-reactivity as we had already demonstrated that K5 and K14 were expressed in the canine claw fold (skin epidermis) indicating that the human antibodies did cross-react with canine proteins. If the claw is likened to the hair follicle, the SE is probably the equivalent of the IRS cuticle (ICU) or hair shaft cuticle (CU). Human hair studies on the ICU have confirmed that K71-K74 are expressed within this region and these proteins have a molecular weight of approximately 58 kDa (Porter *et al*, 2001), close to that of K5, which may explain the protein band observed near the 60kDa marker. Hair-specific type I keratins (K35 and K32), are also expressed in the hair shaft cuticle and these have molecular weights of approximately 47.5kDa and 50kDa respectively, similar to K14, which again may explain the bands observed in SE samples in the 50kDa region. However, human hair-specific keratin antibodies did not cross-react with canine tissue and the K6irs (K71-K74) antibody could not be used for western blotting, so further studies are required to confirm the identity of these two proteins.

Differential protein expression was observed when examining extracts of canine claw and equine hoof epithelia. In particular, the protein profile of the SE differed from that of the **stratum medium** (SM) and **stratum internum** (SI). Both

species demonstrated a similar change in profile. Bands of lower molecular weight (≤42kDa) were present in the SM and SI but were missing from the SE extracts. Western blot analysis did not reveal which keratins these were but it is probable that they are hair-specific-keratins, as these are known to make up the bulk of the nail plate in humans (Lynch *et al*, 1986; Bowden *et al*, 1987; Perrin *et al*, 2004). Very faint bands representing K16 and K17 were also observed in some SM and SI western blots (data not shown) as well as sole (S1-4) western blots. Although immunocytochemical analysis would be required to establish the exact location of these keratins, their existence within canine SM, SI and sole was not entirely unexpected. Bowden (1987), De Berker *et al* (2000) and Perrin *et al* (2004) reported that K16 and K17 as well as K6 were expressed in the suprabasal cells of the nail bed (S2 equivalent in canine claw) and are present within the nail plate (SM1-4 and SI1 & SI2 equivalent). Additionally, the human nail disease, pachyonychia congenita (PC), characterised by hypertrophic nail dystrophy, is caused by missense mutations within the coding sequence of K6 isoforms, K16 and K17 (Bowden *et al*, 1995; McLean *et al*, 1995) suggesting the existence of the keratins within the human nail plate. Furthermore, these mutations cause hypertrophy of the nail bed that takes on the appearance of a rubbery, crumbly material, similar to canine sole. The keratin profile of this region would have to be assessed using immunocytochemical techniques, which would provide a better understanding of the different germinative regions within the proximal claw, and the different SM layers as these could not be accurately divided macroscopically for electrophoretic analysis.

In both canine claw and equine hoof, SI samples again demonstrated similar protein profiles with the majority of protein bands being in the 42-45kDa region with faint bands at 60kDa. Western blot analysis did not reveal which keratins were present so it can only be assumed that the majority of the proteins of the SI are related to hair-specific keratins. With no anatomical comparative equivalent in the human nail, which is a flattened structure, the "buffering/filling" nature of SI horn is not required. Thus, comparative protein studies were made with SI material from equine hoof. Wattle (2000) conducted a study on keratin expression within the SM and SI of hoof samples from horses suffering from acute laminitis mainly using antibodies that were not specific to one keratin

protein. For example, one of the antibodies used, CK8.12, is specific to keratins with molecular weights of 59.5kDa, 56.5kDa, 55.3kDa, 52kDa, 49.6kDa and 47.2kDa, whereas another antibody used (AE13), showed specificity towards acidic hair-specific keratins. From this study, it can be seen that the protein profile of equine hoof SI samples is very similar to that obtained in this study with the majority of keratins being of low molecular weight. According to Wattle (1998), these are probably the "so-called hard keratins" suggesting that the bulk of the SI is comprised of hair-specific keratins. Keratins of higher molecular weight were also found in these extracts and they were identified as K10 and K14.

Canine sole material was difficult to extract due to its small size and awkward location within the claw capsule. Thus, separation of the sole into its different components (S1-4) was physically impossible. Extracts of total protein from canine sole protein produced a profile somewhat similar to that from canine claw fold (OCS, ICS and SE) and western blot analysis confirmed that these were K5, K14, K16 and K17. Human nail studies agree with this, where the hyponychium, the sole equivalent of the nail, is thought to express K5 and K17 (Perrin *et al*, 2004). However, further immunocytochemical analysis is now required to obtain a better understanding of protein expression in this complex region of the claw.

Total protein extractions of canine foot pad revealed a similar but still more complex protein profile compared to human palmar-plantar extracts. Many protein bands were observed and western blot analysis confirmed that some of these were K5, K10, K14, K16 and K17. This agrees with previous protein studies carried out on human palmar plantar skin. De Berker (2000) stated that K6, K16 and K17 were present in the digit pulp of the human finger and their expression was restricted to the ridges of the undulating palmar epidermis. This could not be confirmed without further immunocytochemical analysis, but as both human nail and canine claw share many similarities, it would probably be the case.

As both canine foot pad and human palmar-plantar samples were obtained in a similar manner, this suggests that the morphology of the canine foot pad is different from human palmar-plantar skin. In addition, canine foot pad extracts

contained collagen while the human samples did not. Previous research has shown that the morphology of the dermal-epidermal junction of the canine pad to be extremely undulating (Meyer and Tsukise, 1995) and this was confirmed by our observations. Thus, when cutting canine pad parallel to the surface, collagen containing dermis and some living keratinocytes are removed with the stratum corneum. As human palmar-plantar epidermis is less undulating, so an incision would not reach the dermis, hence no collagen would be extracted. The more complex protein profile of canine foot pad can also be attributed to the fact that living epidermal cells were included in the canine foot pad extract unlike the human palmar-plantar extract, which only included stratum corneum. The protein profile of human palmar-plantar epidermis was known to become more complex from the stratum spinosum to stratum corneum (Dr P.E. Bowden, Cardiff University: *personal communication*), and this was also true of the hair follicle in that the protein profile of the hair bulb region was more complex than that of the hair fibre (Bowden *et al*, 1987; 1993; Rogers *et al*, 1998).

Due to the highly insoluble nature of keratins and the general robustness of the canine claw, a great deal of time and effort was devoted to optimising protein extraction methods so that a reasonable amount of protein could be extracted. It has been demonstrated that human hair, skin and nail can be extracted with a 5% (w/v) SDS and 5% (v/v) βME in a Tris buffer, and in the case of skin, only 1% (w/v) SDS and 2% (v/v) βME is required. However, a higher concentration of detergent and reducing agent was required to release proteins from dog claw samples (Tris buffer with 10% (w/v) SDS and 10% (v/v) βME). Unfortunately, no two-dimensional electrophoretic analysis of canine claw canine claw analysis was possible due to the low protein concentration of the extracts. Furthermore, it was also difficult to quantify keratin proteins within these samples as analysis of re-extracted pellets showed that not all of the proteins had the same extractability. Some keratins are released from the structure more easily than others, so obtaining reproducible representative fractions of the keratin content is difficult (Zahn, 2002; own personal observations).

These methods are only semi-quantitative and can only reveal significant changes in keratin expression or differences between the expression in different tissues.

This method alone would therefore be unsuitable for assessing small changes in protein synthesis in such a complex structure. As a result, the decision was made that sufficient information had been obtained from the one-dimensional electrophoresis and western blot analysis so instead of delaying the study further by optimising the conditions for two-dimensional electrophoresis, time would be better spent on immunohistochemical analysis with the human antibodies that would cross-react with the canine proteins.

CHAPTER 5

5 IMMUNOHISTOLOGICAL ANALYSIS OF GENE EXPRESSION IN CANINE CLAW

5.1 INTRODUCTION

It is already evident from these studies that the canine claw is a far more complex structure than previously reported in the veterinary literature and comprises several different tissues that are undergoing different and distinct types of differentiation. For this reason, accurate identification of keratin and keratin-associated proteins within the claw is difficult and extremely challenging. The initial attempt to identify keratins within specific macroscopic regions of the canine claw using one-dimensional SDS-PAGE and western blotting was a partial success. Our findings revealed that several proteins within the keratin molecular weight range (40-70 kDa) were present in extracts of dog claw and the existence of K5, K14, K16 and 17 within the epidermis of the claw fold was confirmed. However, from this anatomical study, we know that the proximal claw is very complex and consists of several different layers and distinct germinative regions so the exact location of keratins within the claw using these methods could not be achieved, as accurate separation of the claw into its many layers proved too difficult.

In order to provide more information on the detailed keratin expression within the claw, the use of immunohistochemical techniques proved to be the best approach. Keratin monoclonal antibodies have been shown to be useful markers for identification of epithelial cells and neoplasms of epithelial origin when used in immunohistological studies (Vos *et al*, 1989; Desnoyers *et al*, 1990; Sandusky *et al*, 1991). Using the information gained from the anatomy study, commercially available and donated monoclonal antibodies were used to examine the expression of keratins and other differentiation-related proteins (involucrin and filaggrin) within the canine claw by immunohistochemistry.

Several antibodies to individual human epidermal keratins (K1, K5, K6, K9, K10, K14, K16 or K17), human hair-specific keratins (Ha1 [K31], Ha2 [K32], Ha3-1 [K33a], Hb1 [K81] and Hb2 [K82]) and one mouse hair follicle keratin (K6irs1 [K71]) on canine skin and claw. However, only K5, K14, K6, K16 and K17 cross-reacted with paraffin embedded canine tissue and mouse K6irs1 worked in frozen sections. We also tested involucrin, filaggrin, transglutaminase and Ki67 antibodies but these did not cross-react with canine tissue.

5.2 METHODS

Parasaggital sections of claws from dogs F, G and H were fixed in neutral buffered 10% (v/v) formalin for 48 hours, and then embedded in paraffin. Transverse sections were obtained from digit 2 (Figure 2.2) as previously described (see Chapter 2).

It was important to ensure that the distal phalanx remained in place as this would aid in keeping the claw structure together as well as provide more histological information. However, all claw samples containing bone material had to be decalcified and softened before being sectioned on the microtome (see Chapter 2 for detailed methods) and parts of some sections were inevitably lost.

Paraffin embedded claw sections were cut at 5µm and applied to APES coated glass slides. The sections were re-hydrated by sequential immersion in xylene, graded concentrations of alcohol, and tap water. The tissue sections were immunohistochemically stained using the labelled streptavidin biotin (LSAB) method. All specimens were incubated with primary and secondary antibodies at room temperature for one hour, followed by three 5 minute rinses in C-PBS. The antibodies were detected using 3,3-diaminobenzidine tetrahydrochloride (DAB) and 0.1% (v/v) hydrogen peroxide in 0.6% (w/v) BSA/PBS for 5 minutes. The sections were then lightly counterstained with haematoxylin.

Immunofluorescence staining was carried out using the same methodology but Streptavidin Fluoroscein Label was used instead of Streptavidin Biotinylated Horseradish Peroxidase Complex. Sections were mounted using FluoSave™

Reagent and left to dry overnight at 4°C before being viewed on a Nikon microscope with fluorescence optics.

The optimal staining procedure for each protein antigen was determined by staining normal canine tissues either untreated or following microwave irradiation (antigen retrieval technique). Optimal staining periods and temperatures were chosen following trials in which normal tissue sections were incubated with monoclonal antibodies either for 1 hour at room temperature or for 16 hours at 4°C. The optimal dilution for each of the monoclonal antibodies was determined by testing antibodies at serial double dilutions from 1/25 to 1/800 and then modified to give the optimal staining. A list of the keratin antibodies used, together with the optimal dilutions, is shown in Table 5.1.

Table 5.1: List of Keratin Antibodies used in the Study

Protein Type	Product Name	Source	Optimal Dilution (Canine Tissue)	Optimal Incubation Period and Temperature
K5	-	Binding Site	1/500	1 hour/ RT
K6	-	Donated by Prof Mike Philpott (Queen Mary College, London)	1/50	1 hour/ RT
mK6irs*	-	Donated by Dr Rebecca Porter (Dundee University)	1/100	Overnight/ 4°C
K10	LH2	Biogenesis	1/5000	1 hour/ RT
K14	-	Binding Site	1/100	1 hour/ RT
K16	LHK6B	Donated by Prof Mike Philpott (Queen Mary College, London)	1/100	1 hour/ RT
K17		Donated by Dr Rebecca Porter (Dundee University)	1/400	Overnight/ 4°C

*This antibody would only work on frozen canine skin that had been cut with a cryostat and stained using immunofluorescence techniques. As canine claw was too hard to section using the cryostat, these antibodies could not be used on claw sections.

All tissues were stained with each antibody in duplicate and human tissue sections were used as positive controls. Claw sections were also treated with 0.6% (w/v) PBS/BSA alone, omitting the primary antibody to provide a negative control.

5.3 RESULTS

Five monoclonal antibodies to different human keratin proteins (K5, K6, K14, K16 or K17) cross-reacted with canine tissues. No major differences in staining pattern were observed between the individual dogs claws tested. Incubation of corresponding tissue specimens of each of the dog claws with the antibodies resulted in a similar staining pattern within each specimens. However, minor differences in staining intensity were noticed in similar tissue specimens from different animals. In general, the staining obtained in canine tissues was felt to be appropriate where comparisons could be made to the equivalent human tissue.

5.3.1 Human Epidermis and Appendages (Hair Follicles, Sebaceous Glands and Sweat Glands)

Antibodies to individual human keratins (K5, K14, K16 or K17) were initially tested on human epithelia to ensure that they stained appropriate structures and were subsequently used as controls for canine comparisons. K5 and K14 was expressed in basal epidermal cells whereas K16 was expressed restricted to the ORS of hair follicles was not expressed in sebaceous glands. K17 expression was also observed in ORS but stained the sebaceous gland duct and epithelial cells surrounding the acini.

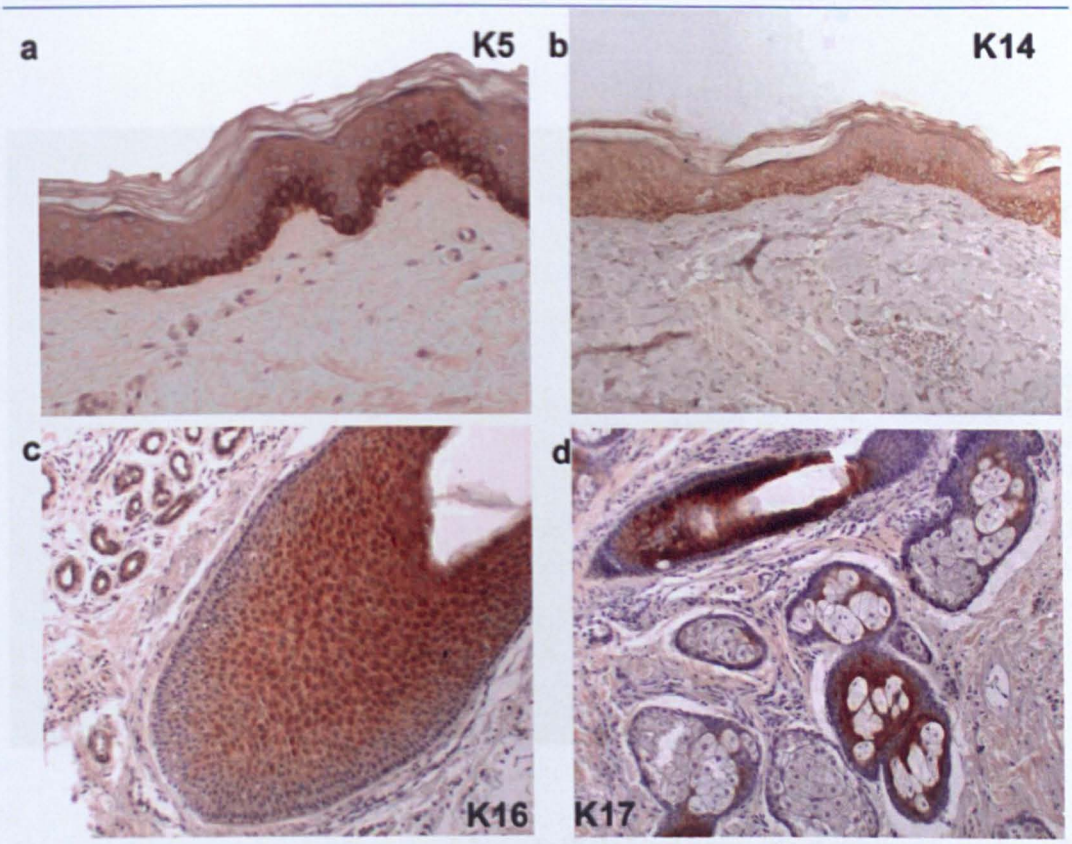

Figure 5.1: Keratin Expression in Human Epidermis and its Appendages

Immunoperoxidase staining of human skin sections with antibodies to K5, K14, K16 or K17 showed that these keratins stained specific epithelial structures: (a) K5 expression in epidermal basal cells; magnification x40, (b) K14 in epidermal basal cells; magnification x40 (c) K16 expression in hair follicle ORS; magnification x100 and (d) K17 expression in sebaceous gland duct and epithelial cells surrounding the acini, magnification x40.

5.3.2 Canine Epidermis and Appendages (Hair Follicles, Sebaceous Glands and Sweat Glands)

Hair-specific keratin antibodies (Ha1, Ha2, Hb1) were found to non-specifically stain paraffin embedded canine epidermis and its appendages. Preliminary work on frozen sections of canine epidermis showed that human Ha1 antibodies did cross-react when using immunofluorescence techniques and stained the cortex of canine hair follicles as expected (data not shown). Similarly, an antibody to mouse K6irs1 (K71) worked effectively on frozen canine skin (cryostat sections) and staining of IRS cells could be clearly seen in the hair follicle (Figure 5.2).

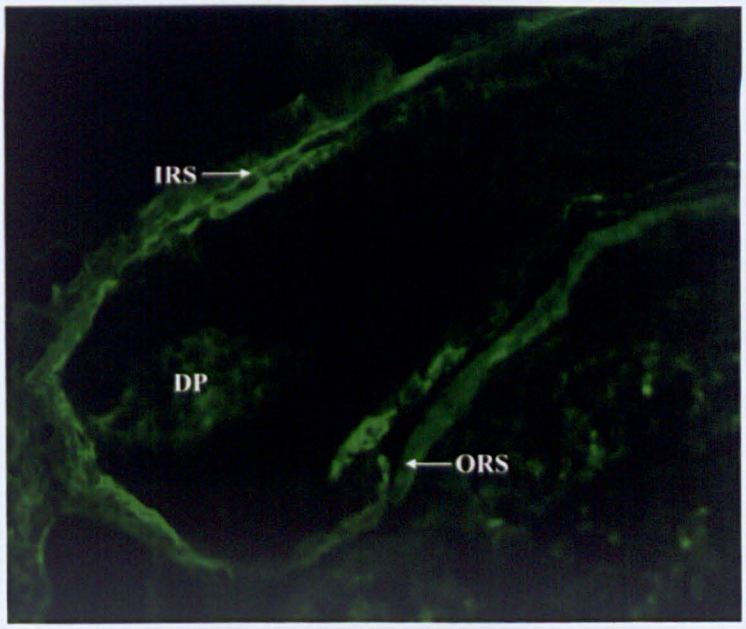

Figure 5.2: *Immunofluorescence* of Canine Hair Follicle using mK6irs Antibody

Canine hair follicle showing expression of mK6irs1 in the IRS. Some non-specific (background) staining was observed in cells of the ORS and dermal papilla (DP). Magnification x100.

Canine skin contained compound hair follicles as seen in sections stained with H&E (Figure 5.3a). K5 and K14 expression was found in basal cells of the epidermis, sebaceous gland, sweat gland and outer root sheath (ORS) of the hair follicle (Figure 5.3b, d). This was especially prominent in the hair follicle ORS. Canine epidermis did not express K6, K16 and K17 (data not shown) but these keratins were expressed by the hair follicle ORS, the epithelium surrounding sebaceous acini, the sebaceous gland duct and the sweat gland (Figure 5.3c, e, f). In sweat glands, K6 and K16 expression was restricted to the duct, while K17 was expressed in myoepithelial cells. K17, but not K16, was expressed in sebaceous gland ducts while K6 was expressed in all the appendages and was especially abundant in the hair follicle ORS and sebaceous gland.

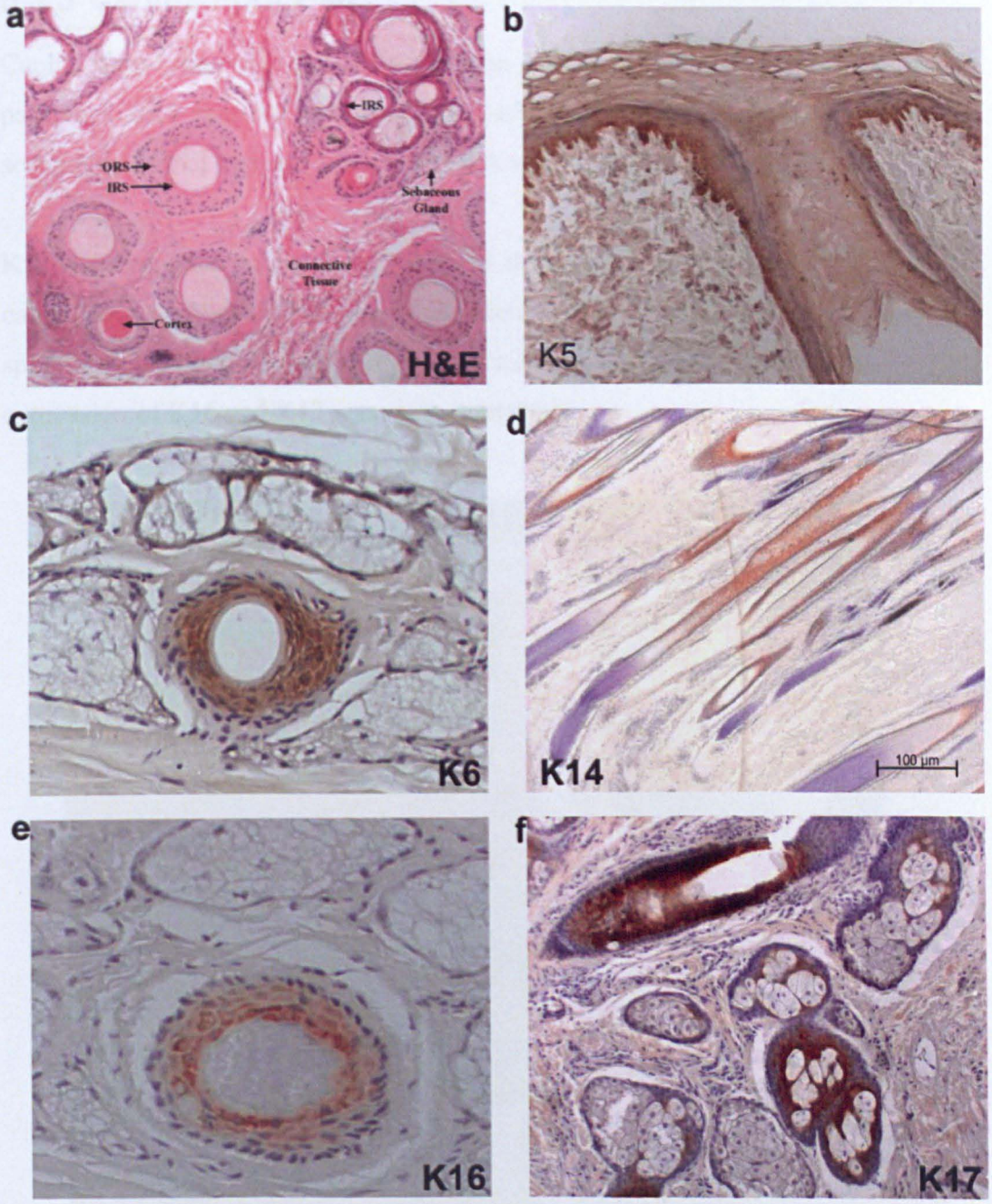

Figure 5.3: Keratin Expression in Canine Epidermis and its Appendages

Canine skin sections were stained with H&E (a) to show the abundant hair follicles and sebaceous glands. Other sections were treated with antibodies to K5, K14, K16 or K17 and visualised by immunoperoxidase (brown) staining (b-f). These keratin antibodies stained specific epithelial structures in canine skin sections: (a) K5 expression in epidermal basal cells (b) K14 expression in epidermal basal cells (c) K16 expression in hair follicle ORS and (d) K17 expression in sebaceous gland duct and epithelial cells surrounding the acini. Panels a, c, d and e are x40 magnification and panels b and f are x100.

5.3.3 Canine Foot Pad

Canine foot pad was similar to human palmar-plantar skin but was more papillated such that the epidermis had very deep rete ridges, with primary and secondary dermal papillae and a very thick undulating stratum corneum.

K5 was expressed in basal cells and in the immediate suprabasal cells of the canine foot pad but only background staining was observed in more superficial spinous cells (Figure 5.4a). K14 had a similar distribution (data not shown). The expression of K16 and K17 was more interesting.

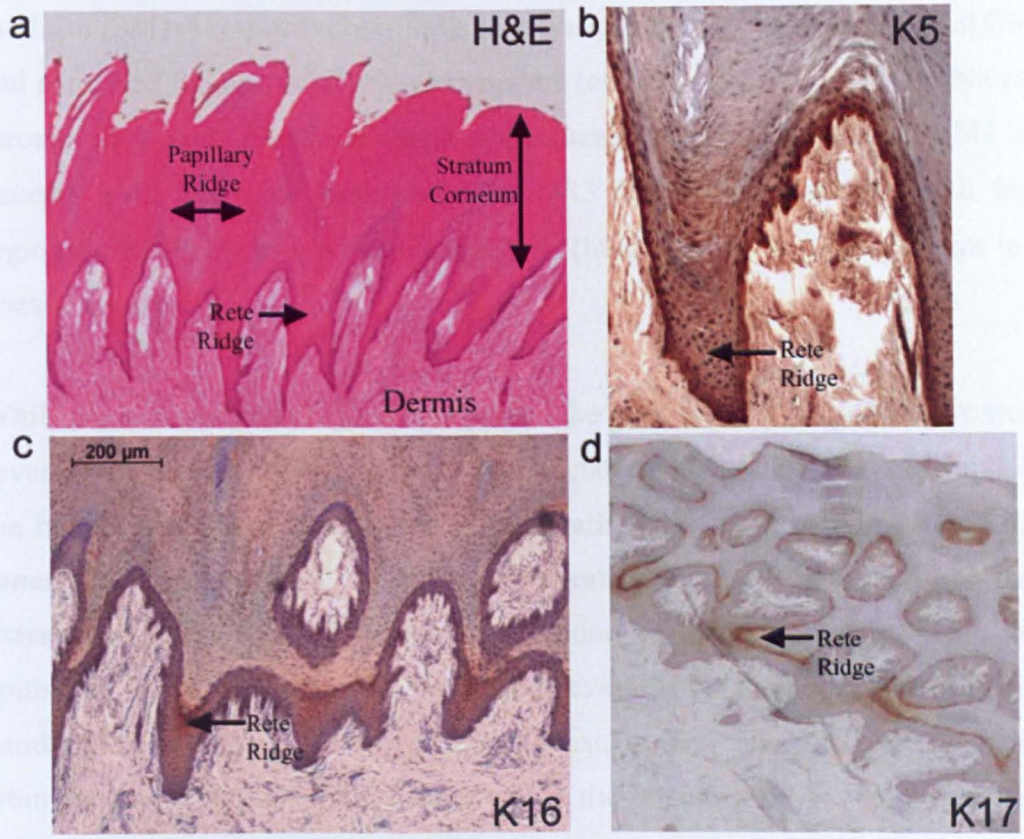

Figure 5.4: K5, K16 and K17 Expression in Canine Digital Foot pad

Canine foot pad was stained with H&E (a) to show the abundant stratum corneum, deep rete ridges and large dermal papillae. Other sections were treated with antibodies to K5, K16 or K17 and visualised by immunoperoxidase (brown) staining (b-d). These human keratin antibodies stained specific epithelial structures in canine foot pad: (b) K5 expression in basal cells; magnification x40 (c) K16 expression suprabasal cells located in the centre of the rete ridge; magnificaton x20 and (d) K17 expression in a similar location in the rete ridge; magnification x4.

Both were found to be expressed in suprabasal cells of the rete ridge and were not expressed in the epithelial cells that were located over the top of the dermal papillae (Figure 5.4b, c). However, while the immunostaining patterns for these two keratins were similar, there were not identical. K16 stained more suprabasal cells in the centre of the rete ridges whereas, K17 was only expressed in a narrow region of suprabasal cells.

5.3.4 Germinative Regions 1-4, OCS, ICS, SE & SM1-4

Four main germinative regions (GR1-4) were identified in the proximal claw from examining the microanatomy and each produced a different layer of the **stratum medium** (SM1-4 respectively). SM2 horn was generated from the papillated GR2 and contained tubules, which were cylinders (or rods) of soft epithelium that ran through SM2 along the whole length of the claw (Figure 5.5a). SM3 and SM4 lay beneath SM2 and were generated from GR3 and GR4 respectively. All four regions (GR1-4) lay over a thickened dermis (lunula) which decreased in size in a distal direction.

While the stratum medium (SM1-4) formed the bulk of the claw plate, there were several other layers which made the whole claw structure appear comparable to the human hair follicle: the **outer claw sheath** (OCS), **companion layer** (CL), **inner claw sheath** (ICS), **inner claw sheath cuticle** (ICScu) and **stratum externum** (SE). The OCS was a continuation of the skin epidermis and this epithelium grew from a basal layer inwards towards the claw plate. On the other hand, both the ICS and SE could be traced back to a single cell layer, generated from the micro-papillated GR1 deep within the ungual groove. Approximately half way down the claw fold, the OCS expanded and the epithelial cells sealed the skin of the claw fold to the claw plate. The ICS also expanded and created a slippage zone for the claw plate (SE, SM and SI) to move out of the claw fold as growth occurred distally.

K5 was expressed in basal cells and possibly immediate suprabasal cells of the papillated GR2 (Figure 5.5b). This was also true of K14 but the data was not so

clear (Figure 5.5d). Both K5 and K14 were expressed in the OCS in all layers (both basal and suprasbasal).

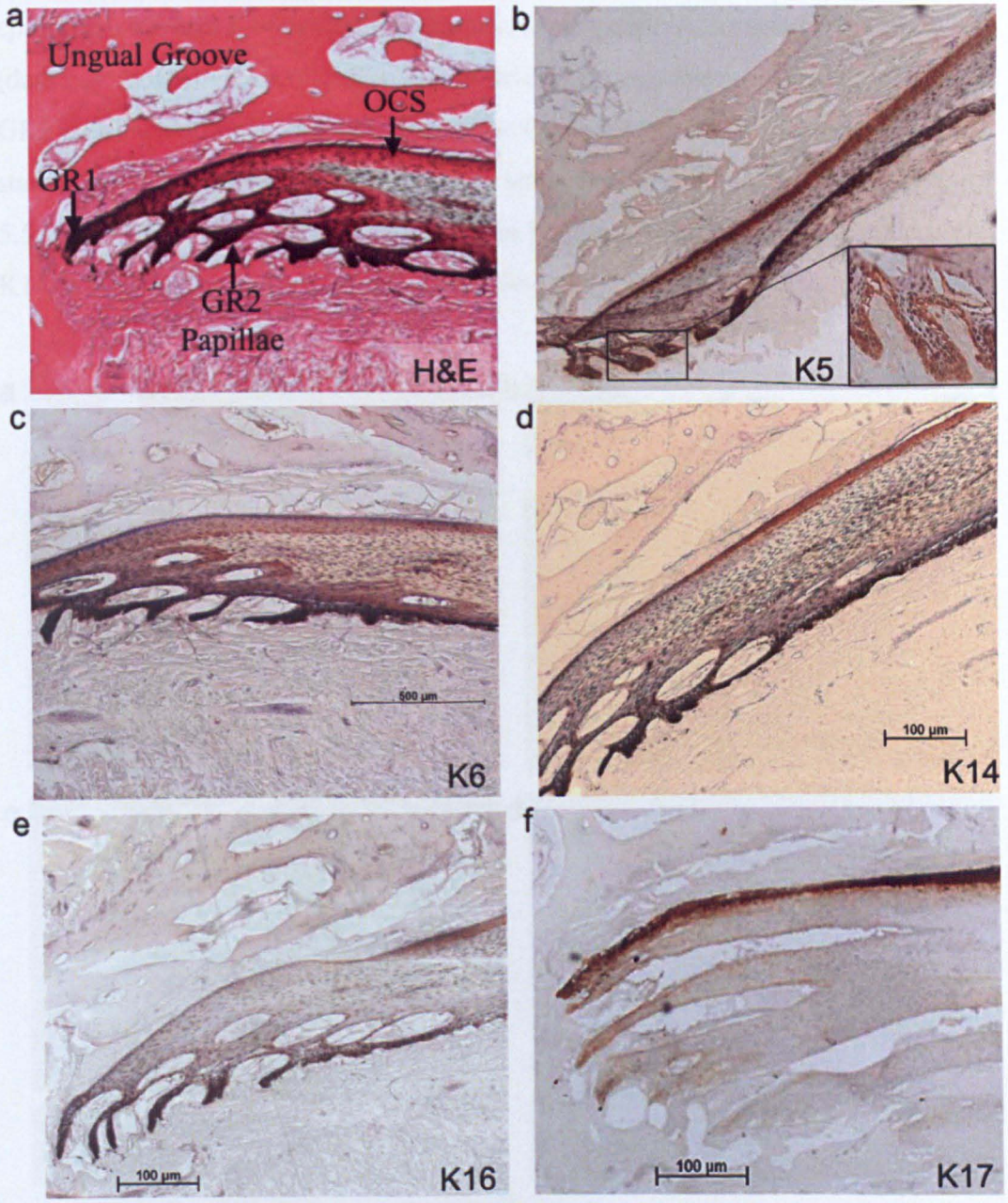

Figure 5.5: Parasaggital Sections of Proximal Canine Claw within the Ungual Groove showing Keratin Expression in Germinative Regions (GR1 and GR2)

Parasaggital section of the proximal canine claw showing the region within the ungual groove stained with H&E, magnification x40 (a). The small GR1 and much larger papillated GR2 are clearly shown. The other sections were treated with antibodies to K5, K6, K14, K16 or K17 and visualised by immunoperoxidase (brown) staining (b-f). These human keratin antibodies stained specific epithelial structures in the proximal canine claw: (b) K5 stained in basal cells of GR2 and the OCS above the claw plate, magnification x40, (c) K6 staining restricted to suprabasal cells at apex of GR2 papillae and the tubules within SM2, magnification x40, (d) K14 staining was similar to K5 but also stained the tubules, magnification x40 (e) K16 lightly stained the OCS, tubules and cells at the apex of GR2, magnification x40 and (f) K17 expression was heavy in the OCS, not apparent in tubules and light in the papillated GR2, magnification x100.

However, once the OCS emerged from the claw fold at the junction with the skin epidermis, K5 and K14 reverted to basal cell only expression typical of this tissue (data not shown). K6 expression was restricted to suprabasal cells at the apex of GR2 papillae and only light staining of the OCS was observed (Figure 5.5c). K16 staining in the OCS was weak while K17 stained this region very strongly (Figure 5.5e, f). K6 and K16 stained the tubules in SM2 and these appeared to stain with K14 as well but not with K17 (Figures 5.5c-f and 5.6b-d).

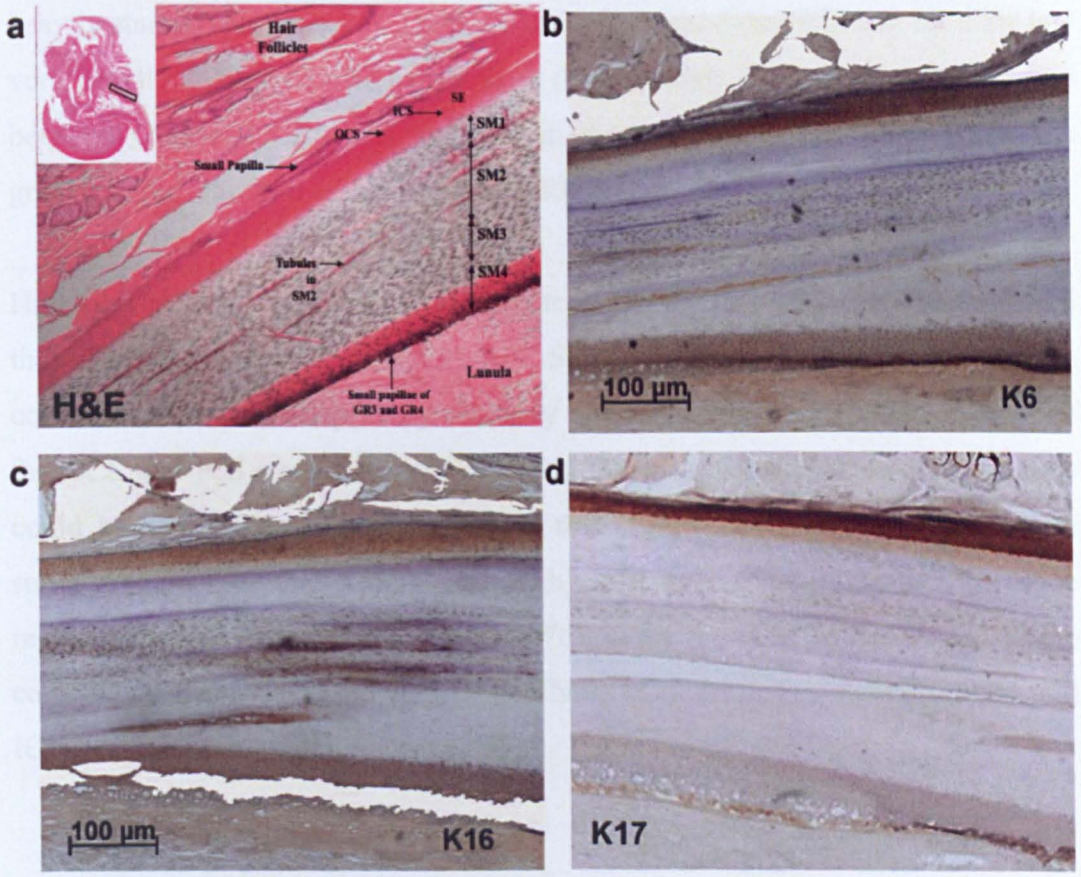

Figure 5.6: Parasaggital Sections of Proximal Canine Claw within the Claw Fold showing Keratin Expression in Germinative Regions (GR3 and GR4)

Parasaggital section of the proximal canine claw showing the region within the claw fold stained with H&E, magnification x40 (a). This region shows the claw plate, the expanding OCS, ICS and SE above, the central SM containing tubules in SM2 and the micro-papillated germinative regions (GR3 and GR4) underneath the claw plate. The other sections were treated with antibodies to K6, K16 or K17 and visualised by immunoperoxidase (brown) staining (b-d). These human keratin antibodies stained specific epithelial structures in the canine claw: (b) K6 stained the tubules in SM2, the expanding OCS region above the claw plate and the claw bed below; magnification x40, (c) K16 was similar to K6 but the OCS and claw bed were stained less and the tubules more; magnification x40 and (d) K17 staining was very prominent in the OCS and appeared to stain the claw bed more heavily in the region of GR4 than GR3, with a visible boundary a little over halfway along the section; magnification x40.

Moving distally along the claw plate but still within the claw fold, the papillated GR2 gave rise to two micro-papillated germinative regions (GR3 and GR4). Over this region, horn material was added to the underside of the claw to thicken the plate from beneath. These regions produced SM3 and SM4 which thicken in a distal direction (Figure 5.6a). In this region of the canine claw, K6 antibodies stained the OCS above the claw very heavily, the tubules in SM2 moderately and the claw bed heavily (Figure 5.6b). The K16 antibody stained the same structures but OCS and claw bed were more lightly stained while the tubules were more heavily stained (Figure 5.6c). The K17 antibody stained the OCS and the claw bed very heavily and the tubules hardly at all (Figure 5.6d). Furthermore, the junction between GR3 and GR4 was apparent in this section, as K17 expression was greater in the claw bed associated with GR4 than that associated with GR3.

High power views of the upper claw plate in the region of the claw fold showed the detailed structure of the OCS, ICS, SE, SM1 and SM2 (Figure 5.7). In the control section with no primary antibody (Figure 5.7a), the cellular structure of the OCS and ICS were clearly visible and the companion layer and ICS cuticle could be seen. K6 antibody staining in this region was most prominent in the suprabasal cells of the OCS (Figure 5.7b). The K17 antibody stained the same region but more prominently (Figure 5.7d), while the K16 antibody stained the cells between the OCS and ICS, which have been termed companion layer and ICS cuticle (Figure 5.7c).

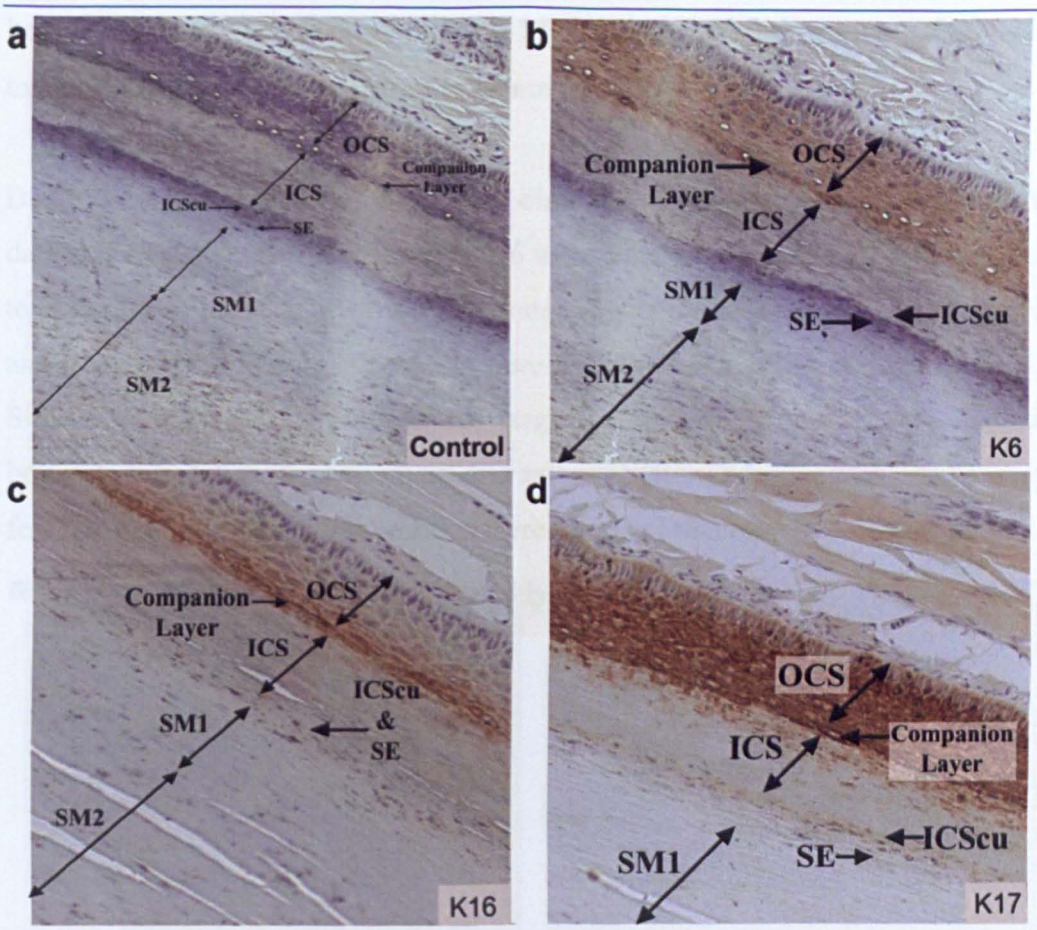

Figure 5.7: High Power Images of the Upper Claw Plate in the region of the Claw Fold showing Keratin Expression in the Different Layers (Immunohistochemistry)

High power images of parasaggital sections of the proximal canine claw showing the region within the claw fold. This region shows the OCS, ICS, SE, SM1 and SM2 in detail. One section was a control with no primary antibody; magnification x100 (a) and the other sections were treated with antibodies to K6, K16 or K17 and visualised by immunoperoxidase (brown) staining (b-d). These human keratin antibodies stained specific epithelial structures in the canine claw: (b) K6 stained suprabasal cells of the OCS and was also prominent in the companion layer; magnification x100 (c) K16 was similar to K6 but stained the outer regions of the OCS to a greater extent; magnification x100 and (d) K17 stained all cells of the OCS heavily and some lighter staining was also apparent in both inner and outer margins of the ICS; magnification x100.

5.3.5 Germinative Regions 5 and 6 (SI1 and SI2)

The small micro-papillated region located within a dermal groove where the lunula terminated has been termed GR5. This was more prominent over the longitudinal ridge (LR) and produced a large amount of **stratum internum 1** (SI1) which filled the gap created by reduction of the lunula and LR. The micro-papillated germinative region more distal has been termed GR6 and this created a

bed for the claw plate to grow over the LR and when the LR reduced in size, GR6 expanded and generated **stratum internum 2** (SI2).

Due to the crude manner of cutting the claw for histological analysis, some of the data was misleading. As GR5 and GR6 were located over the LR, it was difficult to ensure that these regions were included when obtaining parasaggital sections and it was found that most sections were cut either to the left or right of the LR. Similarly, with transverse sections, large amounts of anatomy were excluded between cuts and it was extremely difficult to locate GR5. For this reason, only a few reasonable parasaggital sections were obtained that show GR5 (Figure 5.8).

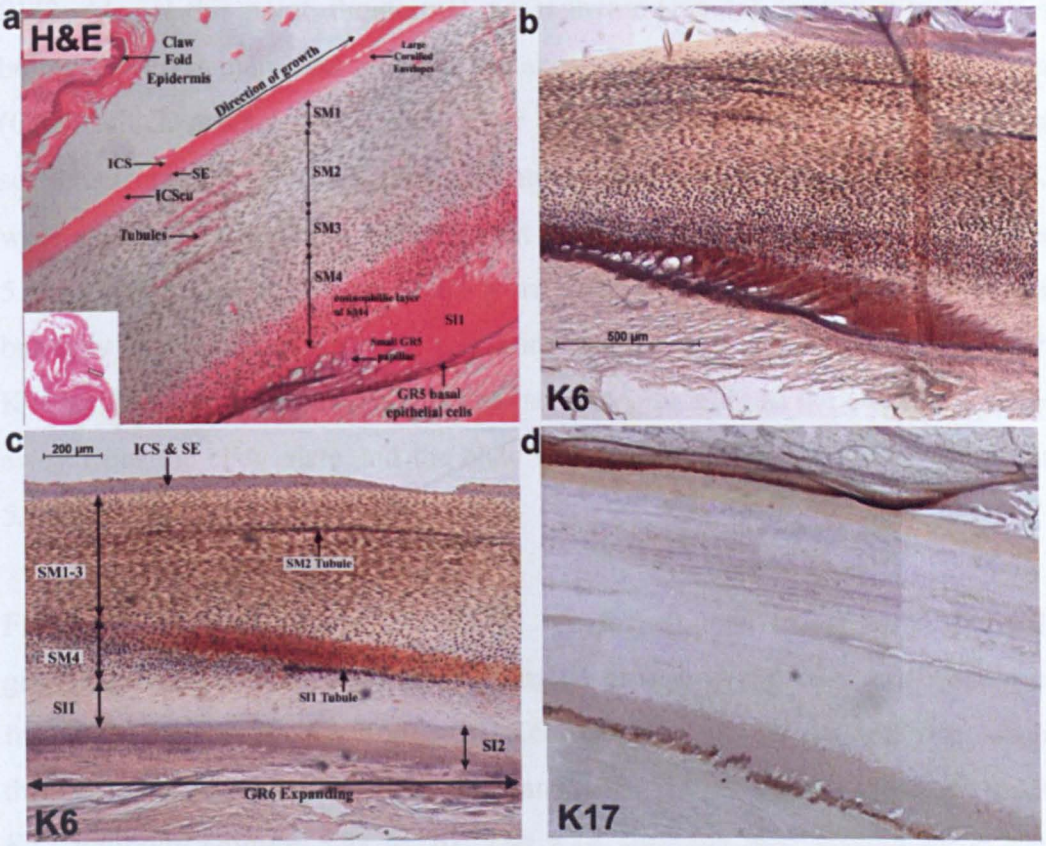

Figure 5.8: Parasaggital Sections of Canine Claw emerging from the Claw Fold showing Keratin Expression in Claw Plate and Claw Bed

Parasaggital section of the proximal canine claw showing the region emerging from the claw fold stained with H&E; magnification x40 (a). This region shows the distinct layers of the claw plate (ICS, SE, SM1-4), the claw fold epidermis above and the expanding GR5 region that generates SI horn below. The other sections were treated with antibodies to K6 and K17 and visualised by immunoperoxidase (brown) staining (b-d). These human keratin antibodies stained specific epithelial structures in the canine claw: (b) K6 stained the expanding claw bed below the claw plate and the tubules in SM2; magnification x40, (c) K6 also stained the very eosinophilic portion of SM4 further down the claw plate in the region where SI2 is added under the claw plate; magnification x40 and d) K17 stained the OCS (observed bending away from the claw as it emerged from the claw fold) and the claw bed in the region of GR4; magnification x40.

In the region where the claw plate emerged from the claw fold, the OCS was observed to bend away from the claw and join with the skin covering the upper digit. The slippage plane between the OCS and the ICS then split apart and the ICS formed a coating on the surface of the claw plate. Eventually, the ICS split off more distally land left only the stratum externum (SE) covering the claw plate from this point onwards (Figure 5.8a).

The claw plate was considerably thicker in this region and consisted of SE and SM1-4. The lower portion of SM4 stained brightly with eosin as did the tubules in SM2. Also at this point, the dermal mesenchyme (lunula) decreased in thickness below the claw plate and allowed for expansion of another germinative region (GR5) which produced the upper layer of the stratum internum (SI1). Staining sections from this region with keratin antibodies showed that large amounts of K6 were expressed in the claw bed where it expanded to accommodate GR5 (Figure 5.8b). In addition, high levels of K6 were found in the eosinophilic layer in SM4 but only low levels of K6 were found in the claw bed (Figure 5.8c). Again, the K17 antibody did not stain the tubules but heavy staining of the OCS as it peeled away from the claw plate and the claw bed of this region was observed (Figure 5.8d).

Figure 5.9 shows an overview of the whole proximal claw region from the germinative regions deep within the ungual groove to the claw plate emerging from the claw fold. Antibodies to K6 and K16 clearly stained the tubules throughout SM2 and stained the GR1 and GR2 epithelia more heavily than the K17 antibody (Figure 5.9a, c, d). The K14 antibody also stained these same regions (Figure 5.9b). K6 expression appeared to be greatest in the claw bed distal from the ungual groove (Figure 5.9a, lower right side of section) while K16 and K17 expression were more prominent in the OCS. Finally, the K17 antibody had a specific affinity for the claw bed in the region of GR4 (Figure 5.9d, lower right side of section).

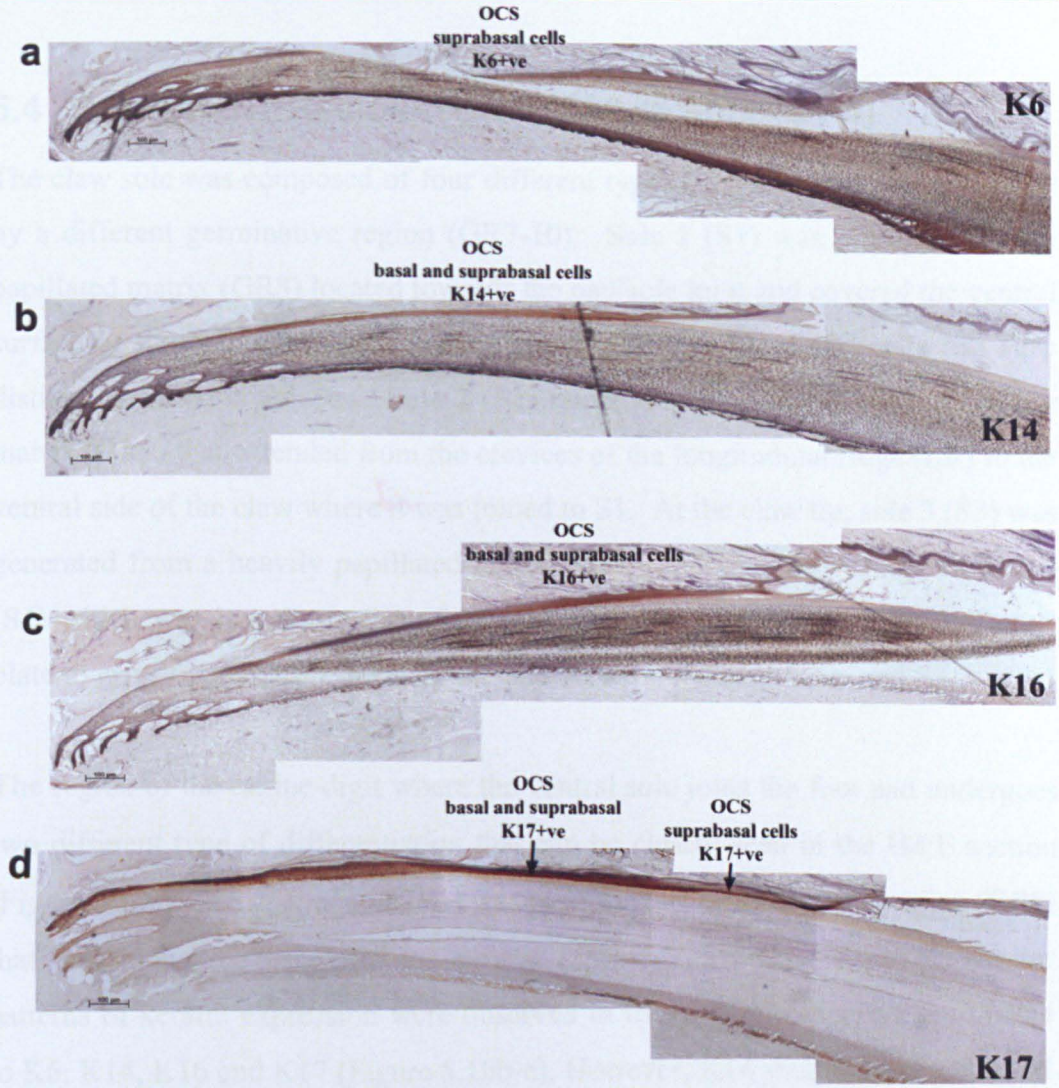

Figure 5.9: Parasaggital Section Composites of the Proximal Canine Claw showing Keratin Expression (Immunohistochemistry).

Parasaggital section composite giving an overview of the whole proximal canine claw from the ungual groove to the region where the claw plate emerges from the claw fold. The sections were treated with antibodies to K6, K14, K16 or K17 and expression of these keratins visualised by immunoperoxidase (brown) staining (a-d). These human keratin antibodies stained specific epithelial structures in the canine claw: (a) K6 stained the tubules in SM2, the OCS region above the claw plate and the claw bed below; magnification x40. (b) K14 also stained the tubules in SM2, the OCS above the claw plate and basal cells of the claw bed; magnification x40. (c) K16 stained tubules in SM2, OCS cells and epithelial cells in GR1 and GR2; magnification x40 and (d) K17 staining was very prominent in the OCS and stained the claw bed more heavily in the region of GR4 than GR3; magnification x40.

5.4 Germinative Regions (GR7-10) and Sole (S1-4)

The claw sole was composed of four different types each of which was produced by a different germinative region (GR7-10). **Sole 1** (S1) was produced from a papillated matrix (GR8) located towards the pad/sole joint and covered the ventral surface of the ungual process. This layer was a very dense and cells had very distinct cornified envelopes. **Sole 2** (S2) material was produced from a laminar matrix (GR9) that extended from the crevices of the longitudinal ridge (LR) to the ventral side of the claw where it was joined to S1. At the claw tip, **sole 3** (S3) was generated from a heavily papillated region (GR10). Lying above S3 was **sole 4** (S4) which was less dense than S1-3 and created a slippage zone for the claw plate to grow over as well as filling the gap between the claw plate and S3.

The region of the canine digit where the ventral sole joins the foot pad undergoes two different type of differentiation that can be clearly seen in the H&E section (Figure 5.10a). The ventral sole (S1) was produced by a germinative region (GR8) that runs along the length of the ventral aspect of the distal phalanx. Similar patterns of keratin expression were observed in these structures using antibodies to K6, K14, K16 and K17 (Figure 5.10b-e). However, K14 stained basal cells and some areas at the junction between these two structures (Figure 5.10c) while K6, K16 and K17 stained suprabasal cells to differing extents (Figure 5.10b, d, e).

The distal claw was much more complex in terms of sole composition and the germinative regions producing these structures (Figure 5.11). The claw plate extended beyond the point where the bony distal phalanx terminated, which generated a cavity. This cavity was filled by S3, a compact rubbery sole material that was produced by a papillated germinative epithelium (GR10), which covered the very end of the distal phalanx. Finally, S4 was another type of sole that was produced from a micro-papillated germinative region (GR7) on the dorsal side of the distal phalanx. Antibodies to K6 and K16 stained supra basal cells of the epithelium in the region of GR7 and GR10 (Figure 5.11a, b) but much more staining of these cells was apparent with antibodies to K17 (Figure 5.11c).

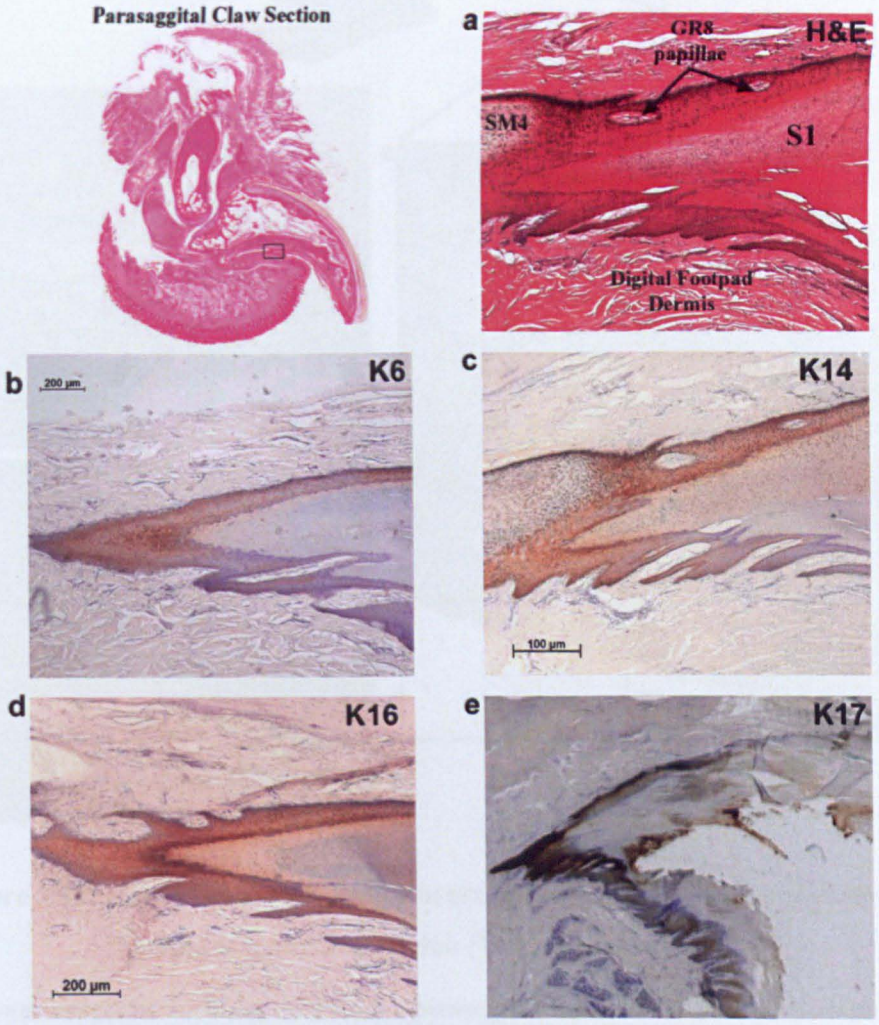

Figure 5.10: Parasaggital Section of Canine Digit showing Keratin Expression (Immunoperoxidase) in the Region where the Foot pad and Sole (S1) meet.

High power images of a parasaggital section of the canine digit in the region marked showing where the sole (S1) joins the foot pad on the underside of the claw. One section shows H&E staining of this region (a) while the other sections (b-e) were treated with antibodies to K6, K14, K16 or K17 and expression was visualised by immunoperoxidase (brown) staining: (b) K6 stained the sole epithelium and parts of the foot pad epidermis; magnification x40. (c) K14 also stained the sole epithelium and basal cells of the foot pad epidermis; magnification x40. (d) K16 stained the sole epithelium and the foot pad epidermis; magnification x40 and (e) the K17 section was photographed at a lower power but also showed expression in sole epithelium and the foot pad epidermis, magnification x40. Image (a) was obtained by using a Nikon D1x Digital SLR Camera.

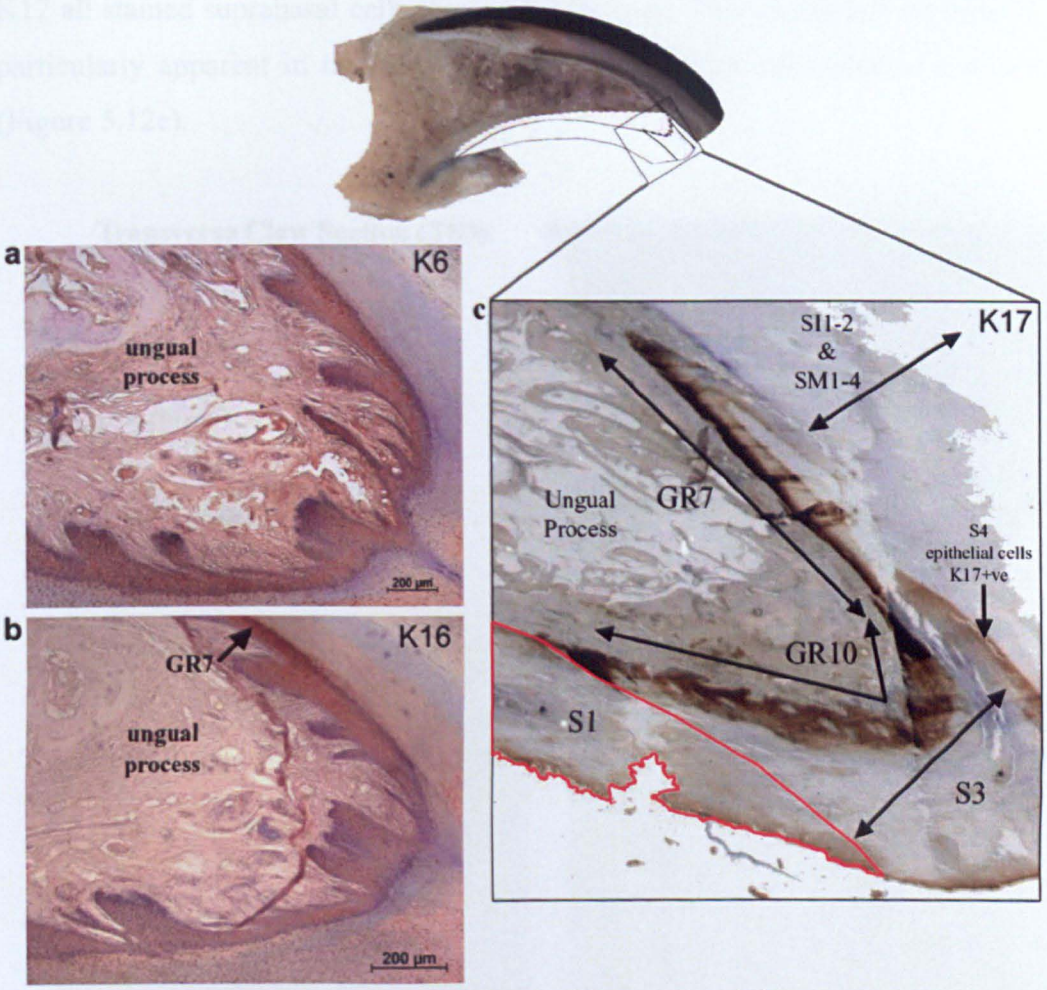

Figure 5.11: High Power Views of a Parasaggital Section of Distal Canine Claw showing Keratin Expression (Immunohistochemistry)

High power images of the distal claw from a parasaggital section through a canine digit showing GR7 and GR10 that produce sole horn. Sections (a-c) were treated with antibodies to K6, K16 or K17 and expression was visualised by immunoperoxidase (brown) staining: (a) K6 lightly stained suprabasal cells of claw bed epithelia (GR7 and GR10); magnification x40 (b) K16 was similar; magnification 40 and (c) K17 stained the same epithelia but more prominently; magnification x40.

Transverse sections (TS3 and TS5) were also stained with various keratin antibodies to reveal keratin expression in different regions around the claw: ventral sole, medial and lateral walls and longitudinal ridge (Figures 5.12-5.15). TS3 sections in the ventral claw region showed S1 (produced by GR8) and the lower part of S2 which feeds down the lateral and medial walls of the claw plate, composed of SM4 and SE (Figure 5.12a). S1 and S2 have different properties in terms of their appearance and texture but the epithelium that generates both of them has similar keratin expression. Basal cells of the epithelium associated with GR8 and GR9 stained with an antibody to K5 (Figure 5.12d) while K6, K16 and

K17 all stained suprabasal cells (Figure 5.12b, c, e). This suprabasal staining was particularly apparent in the higher power view of K16 immuunohistochemistry (Figure 5.12e).

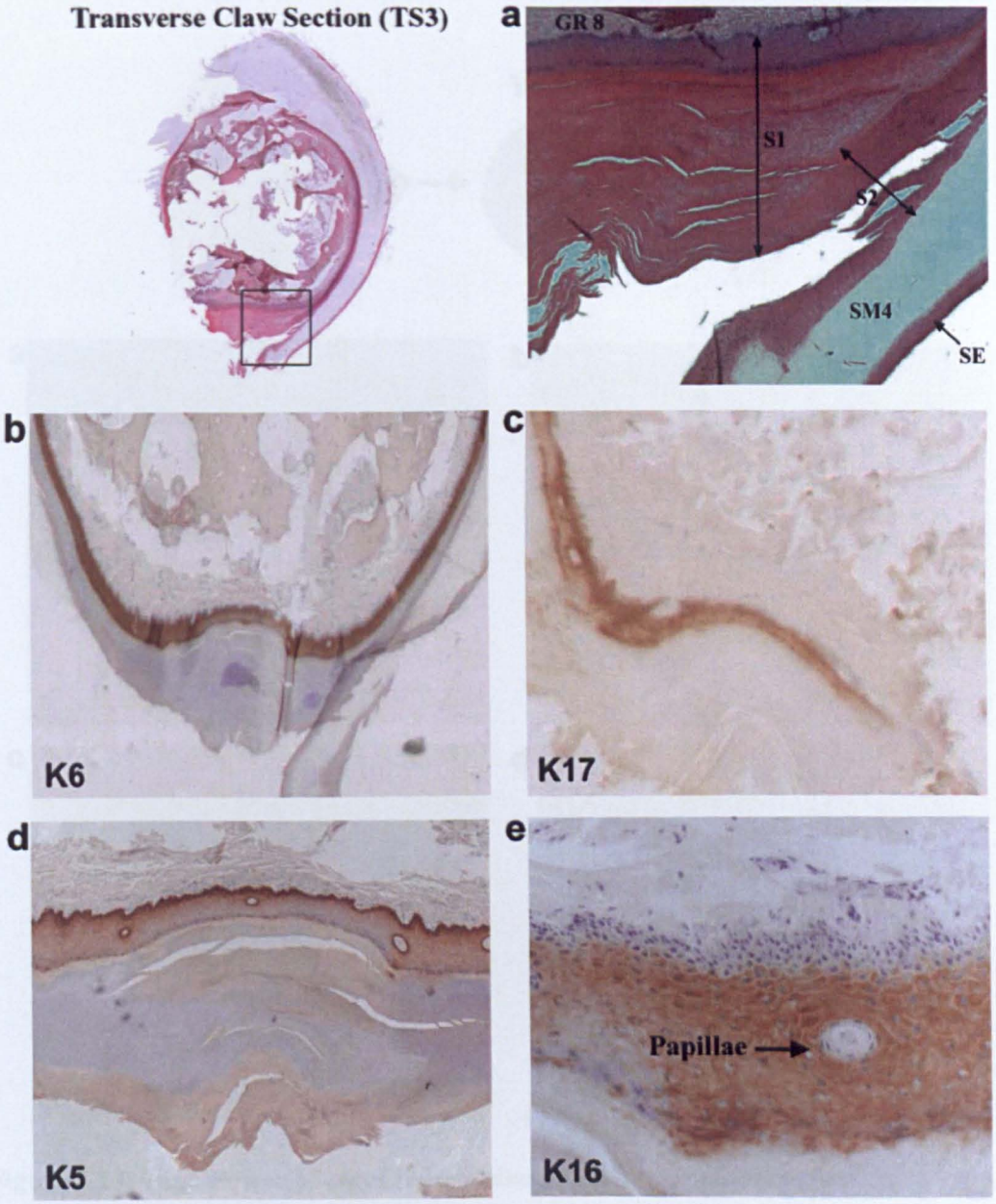

Figure 5.12: High Power Views of the Lower portion of a Transverse Section (TS3) of a Canine Digit showing Keratin Expression (Immunoperoxidase)

High power images of a transverse section (TS3) of a canine digit in the region where the sole meets the medial and lateral walls of the claw plate. The H&E section (a) shows two different type of sole (S1 and S2) and the germinative epithelium (GR8) that produces S1; magnification x40. The epithelial cells of GR8 stain with K6; magnification x20 (b), K16 (not shown at this magnification) and K17; original image magnification x40 (c). K5 staining was basal magnification x20 (d) and viewed at an even higher power, K16 staining was suprabasal; magnification x100 (e).

High power views (Figure 5.13a) of a TS3 section across the middle of the claw in the region of the longitudinal ridge (LR) clearly showed a difference between the germinative region covering the thickened dorsal aspects if the claw (GR6) and that running down the lateral and medial walls (GR9).

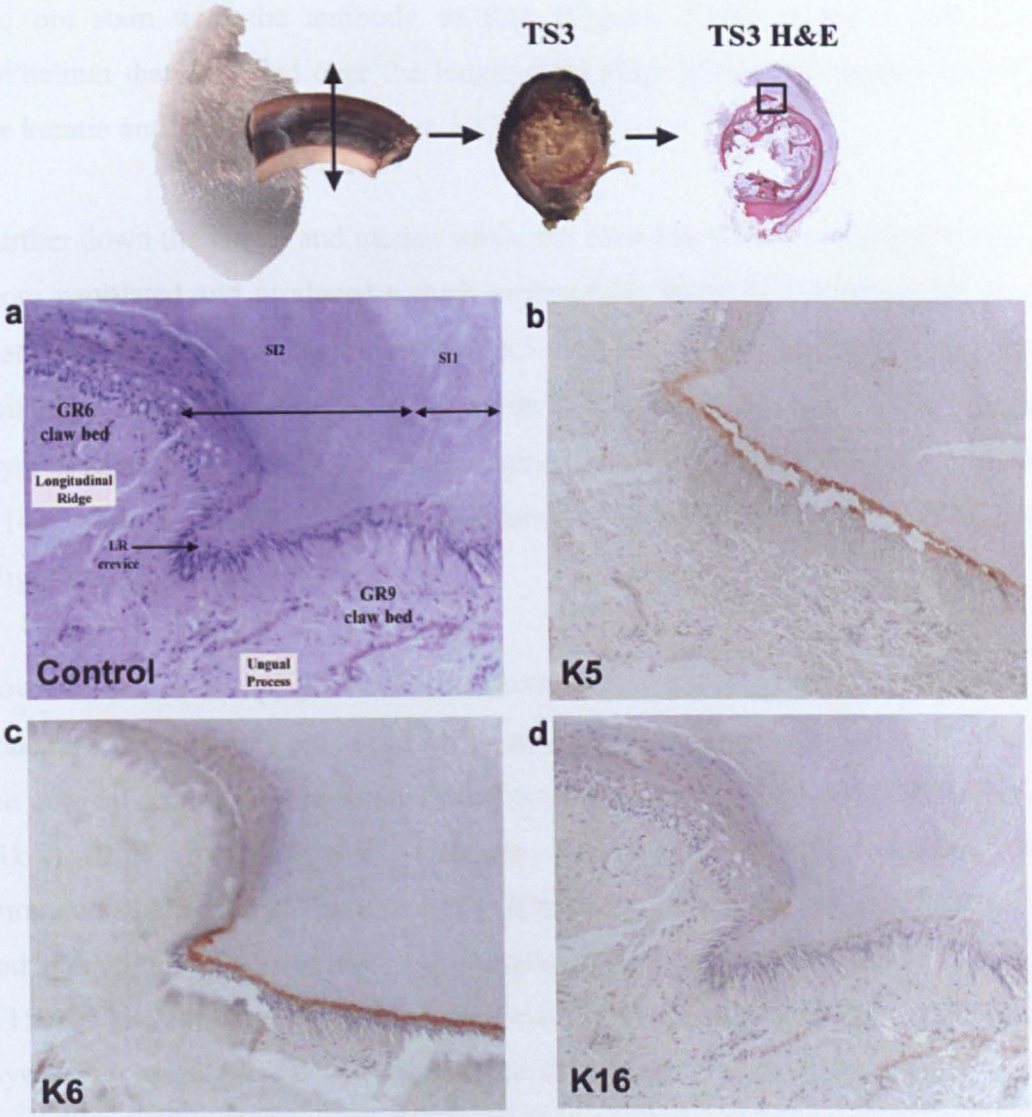

Figure 5.13: High Power View of Longitudinal Ridge in Transverse Section (TS3) of Canine Digit showing Keratin Expression (Immunohistochemistry)

High power views of the LR in a transverse section (TS3) through the canine digit (as shown above). One section (a) is a control counterstained with haematoxylin containing no primary antibody; magnification x40 and the other sections (b-d) were treated with antibodies to K5, K6 or K16 and keratin expression was visualised by immunoperoxidase (brown) staining: (b) K5 stained the claw bed epithelium of GR9 but no staining was seen over the LR (GR6); magnification x40 (c) K6 stained suprabasal cells in the same region; magnification x40 and (d) K16 did not stain this region at all; magnification x40.

The claw bed in the region of GR9 was composed of large columnar basal cells located over the medial and lateral walls and extending inside of the LR crevice. These cells were initially negative with all the keratin antibodies tested but as the claw bed expanded, further along the claw distally, the basal cells were positive for K5 (Figure 5.15b, c). Suprabasal cells were positive for K5, K6 and K17 but did not stain with the antibody to K16 (Figures 5.13c, d and 5.15d). The epithelium that extended over the longitudinal ridge (GR6) was negative for all the keratin antibodies tested (Figure 5.13b-d).

Further down the lateral and medial walls, the claw bed (GR9) expanded, became more papillated and produced a thick eosinophilic layer (S2) between the claw plate and the claw bed (Figure 5.14). A K5 antibody stained the basal cells of this epithelium but also a few cells higher up which could represent another basal layer (Figure 5.14b). K14 antibodies stained basal and suprabasal cells (Figure 5.14c) while K6 and K16 antibodies stained only suprabasal cells of this layer (Figure 5.14d, e).

Towards the claw tip, TS5 sections showed the ungual process of the distal phalanx surrounded by sole horn (S2) generated from GR9 (Figure 5.15). While the original sections did have the dorsal portion of the claw attached (SM1-4 and SI1-2), this material was lost on processing of the sections for immunohistochemistry. These sections clearly showed that the basal cells of claw bed epithelium (GR9) in this region stained with an antibody to K5 (Figure 5.15b), while antibodies to K6 and K17 stained suprabasal cells across the whole layer (Figure 5.15c, d). In addition, another layer that stained with K5 was apparent between GR9 and S2 (Figure 5.15b and inset).

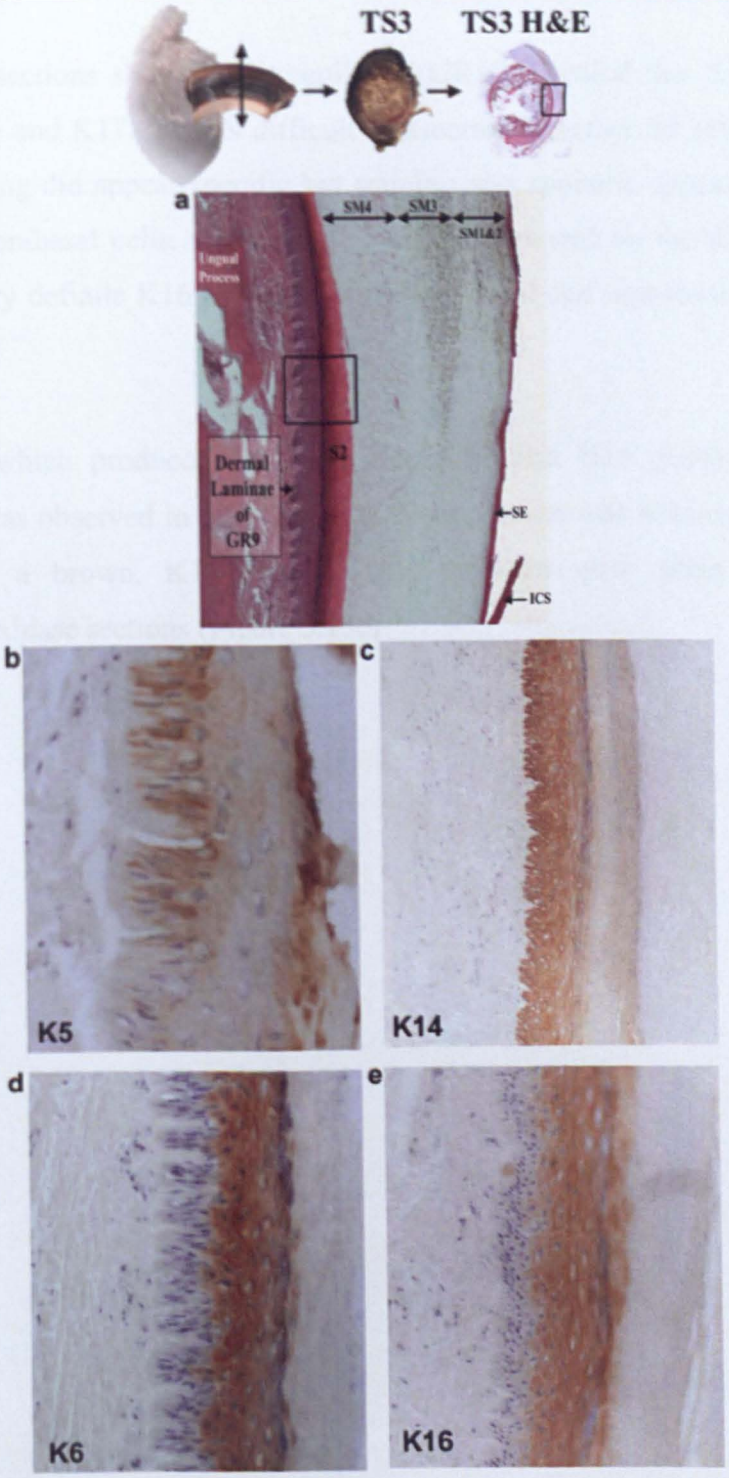

Figure 5.14: High Power Views of Lateral Wall Claw Bed in Transverse Section (TS3) of Canine Digit showing Keratin Expression (Immunohistochemistry)

High power images of the claw plate lateral wall from a transverse section (TS3) through a canine digit. (a) H&E showing bone (left), mesenchyme, claw bed epithelium and claw plate (right); magnification x20. The other sections (b-e) were treated with antibodies to K5, K6, K14 or K16 and expression was visualised by immunoperoxidase (brown) staining: (b) K5 stained basal cells of claw bed epithelium (GR9) and small cells at junction with S2; magnification x40 (c) K14 stained all cells (basal and suprabasal) of epithelium; magnification x20 (d) K6 stained only suprabasal cells in same region and (e) K16 was same as K6; magnification x40.

Parasaggital sections showing the papillated GR10 revealed that S3 basal cells expressed K6 and K17. It was difficult to ascertain whether S3 cells expressed K16 as staining did appear specific but staining was sporadic appearing in some basal and suprabasal cells. However, S3 material located on the dorsal surface showed a very definite K16 positivity with both basal and suprabasal cells being K16 positive.

GR7 cells, which produced S4, were K6, K17 and K16 positive and K14 expression was observed in basal cells. K17 expression was retained in S4 cells and formed a brown, K17 positive strip between claw plate and S3 in immunoperoxidase sections (Figure 5.15c)

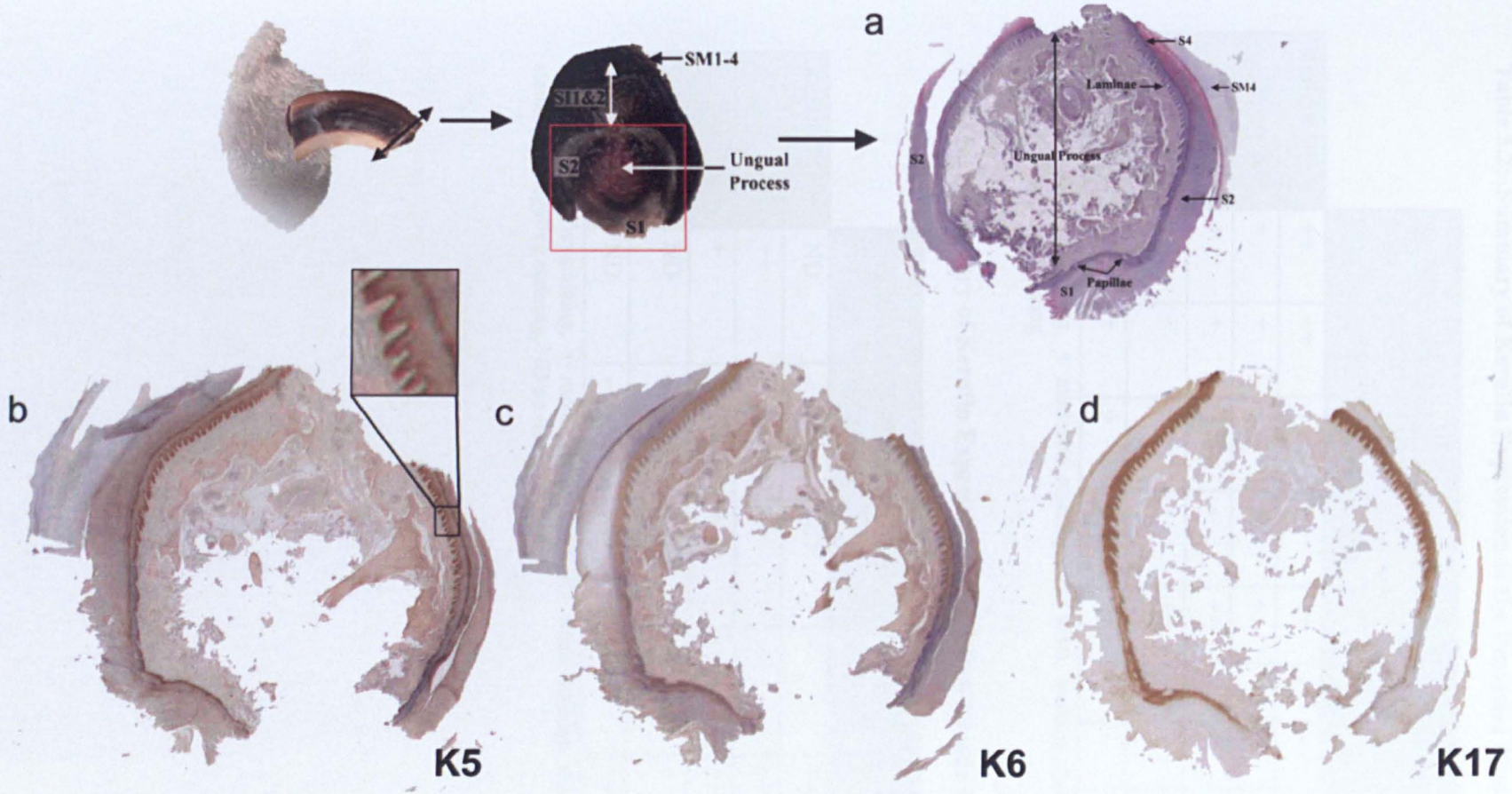

Figure 5.15: Transverse Sections (TS5) of the Canine Digit at the Claw Tip showing Keratin Expression (Immunohistochemistry)

Transverse Section (TS5) of the Canine Digit at the Claw Tip showing claw bed epithelium running from the dorsal ridge round to the ungual process to the ventral aspect. The upper regions containing SM1-4 and SI1-2 have been lost in processing so the sections represent the area in the red box. One section (a) is a control counterstained with haematoxylin containing no primary antibody; magnification x4 and the other sections (b-d) were treated with antibodies to K5, K6 or K17 and expression was visualised by immunoperoxidase (brown) staining: (b) K5 stained basal cells of claw bed epithelium and a layer of cells running between the claw bed and epithelium (GR9) and S2; magnification x4 [inset shows higher power of original image], (b) K6 stained suprabasal cells in the same epithelium but not the other layer; magnification x4 and (c) K17 stained the same epithelium but more prominently; magnification x4.

Table 5.2: Summary of Keratin Expression in the Proximal Canine Claw

		Location in Proximal Canine Claw									
		GR1 (SM1)	GR2 (SM2)	GR3 (SM3)	GR4 (SM4)	OCS	CL	ICS	SE	SM1-4	Tubules
Keratin	K5	++	++	+	+	++	-	-	-	-	-
	K6	+	+	+	++	+	++	-	-	-	++
	K14	+	+	+	+	++	-	-	-	-	-
	K16	+	+	+	+	++	++	-	-	-	++
	K17	++	+	+	++	++	++	-	-	-	+/-

++ clear, specific staining, + moderate staining, +/- weak staining (not necessarily specific staining), - negative staining

Table 5.3: Summary of Keratin Expression in the Distal Canine Claw (GR5-GR10)

		Location in Canine Claw					
		GR5 (SI1)	GR6 (SI2)	GR7 (S4)	GR8 (S1)	GR9 (S2)	GR10 (S3)
Keratin	K5	ND	-	ND	+	++	ND
	K6	++	-	++	++	++	+
	K14	+	-	+	++	++	+
	K16	ND	-	+	++	+	++
	K17	ND	-	++	++	++	++

++ clear, specific staining, + moderate staining, +/- weak staining (not necessarily specific staining), - negative staining, ND no data obtained

5.5 Discussion

Human hair follicles and nails both express epithelial (soft) keratins and hair-specific (hard) keratins (De Berker *et al*, 2000; Langbein, *et al*, 2006). So far we have tested a number of human monoclonal antibodies to differentiation related epithelial proteins on parasaggital and transverse sections of canine claw and have identified regions within this structure which are comparable to both human hair follicles and nails.

The results of this study revealed that five specific antibodies against individual human keratins (K5, K6, K14, K16 or K17) could detect equivalent proteins in canine epithelia using LSAB immunohistochemical methods. The reactions of these antibodies to canine epithelia were similar to the human equivalent and uncovered some interesting structures within the canine claw revealing that the canine claw fold bares a close resemblance to the human hair follicle.

GR1-4 was located within the ungual groove of the proximal claw and keratin expression within these regions resembled both the human hair follicle and the nail. Basal cells in the papillated GR2 were K5 and K14 positive. Epithelial cells at the apex of each papillae were K6 and K16 positive inferring that GR2 at this location was programmed to produce a soft epithelium which formed the tubular structures embedded in SM2. Parasaggital claw sections showed that tubules were K6 and K16 positive along the whole length of the claw plate. GR4, which produced SM4, contained a strip of 'soft' epithelial cells which were found to be K6 positive and K6 expression remained in the lower eosinophilic half of SM4. Close inspection of high power views also revealed that some individual cells were K6 positive in the upper half of SM4. The expression of K6, K16 and K17 in a complementary pattern in the intervening papillae regions of GR2 and along the claw bed may also be explicable in physical terms. It is known from studies of skin fragility disorders that the primary role of keratins in epidermal cells is to reinforce them so that they do not lyse upon physical pressure. It seems very likely that different keratins provide cells with different properties of resistance and plasticity to equip the epithelial cells for the physical stresses of each particular body site. Although K6, K16 and K17 were originally thought to be

primarily associated with hyperproliferation, and are over expressed in conditions such as psoriasis (Weiss *et al,* 1984; Leigh *et al,* 1995; Paramio *et al,* 1999), similar specific staining of these keratins has been observed around the perimeter of scabs in wound healing (Takahashi *et al,* 1994; Wawersik *et al,* 2001; Patel *et al,* 2006). Our data supports the idea that K6, K16 and K17 may provide elasticity to hard keratinised structures and this is achieved by embedding soft epithelia such as tubules which express these keratins in the hard claw plate to provide periodic regions of flexibility in a stiff structure. Thus, tubules might act as "shock absorbers" within hard claw/hoof structures. Similarly, the K6 positive strip observed in SM4 would also provide the hard claw plate with flexibility as well as strength to prevent it from being torn apart during locomotion and prevent shearing forces between SM1-4 and the underlying SI.

K6, K16 and K17 were also constitutively expressed in the canine foot pad in an intermittent pattern along the epidermal ridges (rete ridges) between the dermal papillae. This also supports the idea that K6, K16 and K17 are not only associated with a hyperproliferative epithelia but can impart flexibility to epithelia and make them less prone to shearing forces. K16 and K17 were expressed in suprabasal cells in the primary epidermal ridges but as sequential sections were not used and double immunofluorescence was not an option, the precise location of these two keratins could not be ascertained. However, comparable studies on human palmar-plantar skin demonstrated that K16 and K17 were expressed in different regions relative to the primary epidermal ridges and K9 expression was particularly high in the primary ridges and lower in the secondary ridges (Swensson, 1998). As the human K9 antibody did not work on canine sections we were unable to examine K9 expression in the canine foot pad but the observed keratin staining was generally comparable to the human palmar-plantar studies (Swensson *et al,* 1998; De Berker *et al,* 2000). Reasons for this unusual keratin expression are thought to be due to the physical constraints acting on palmar-plantar skin. Of all the epidermal tissue covering the body, palmar-plantar epidermis is subjected to the most extreme and extensive physical stress. In the canine foot pad, the raised papillary ridges take most of the compression stress on the pad during locomotion. This is also the region where the human palmar-plantar specific keratin (K9) has been reported to be most highly expressed

(Swensson, 1998), suggesting that the function of K9 is to provide additional reinforcement in this stress-bearing epidermis. The observation that the basal keratins (K5 and K14) had different immunostaining patterns in the foot pad has also been documented by Swensson and colleagues (1998) who suggested that a different regulation mechanism for K5 and K14 exists in human palmar-plantar epidermis.

SM2 tubules were K6 and K16 positive but did not appear to show K17 expression. In comparison, human hair follicle studies have shown that the central medulla is K6, K16 and K17 positive as well as expressing a number of hair-specific keratins. Similar to the tubules, the hair medulla is known to provide flexibility to the hair shaft by producing an epithelial tube through the centre.

Aside from SM2 tubules and the epithelial strip located in SM4, cornified SM1-4 and SI1 and SI2 cells did not demonstrate any epithelial keratin staining and they were thought to contain only hair-specific keratins. In our SDS-PAGE analysis of the canine claw plate (Chapter 4), total protein extracts taken from isolated SM1-4 tissue of canine claws revealed proteins in the hair-specific keratin molecular weight range, which supports the idea that these hard keratinised layers are composed mainly of hair-specific keratin. Unfortunately, human hair-specific keratin antibodies did not cross-react with paraffin embedded canine skin samples. However, Ha1 antibody did stain cryostat sections of canine skin and demonstrated positive staining of the hair cortex using immunofluorescence techniques. This positive reaction on frozen sections might be the result of different fixation methods used. Keratin detection in canine tissues is considerably influenced by the fixation method and formalin fixation has been reported to result in reduced keratin staining, an occurrence which has also been observed for human tissues (Battifora and Kopinski, 1986; Vos *et al*, 1989). In addition to this, Vos and colleagues (1989) noted that PAP methods appear to be less sensitive on paraffin sections than on cryostat sections.

Bowden (1993) stated that the human nail is composed of a combination of 'soft' epidermal keratins and 'hard' hair-specific keratins but the exact location of the 'soft' keratins within the nail plate was never achieved. Further to these studies,

De Berker and colleagues (2000) demonstrated that as well as hair-specific keratins, small amounts of K17 were identified towards the apex of the nail matrix. Images from this paper showed parasaggital sections of human nail and the GR2 equivalent structure appeared to have small micro-papillae, comparable to the GR2 in canine claw. Since the human nail has evolved from a claw structure (Hamrick, 2002), it can be assumed that similar keratin expression exists in the human nail matrix and K6, K16 and K17 may exist in small tubules running through the hard nail plate providing the nail with some degree of plasticity and flexibility.

K6, K16 and K17 expression in GR2-GR4 cells and tubules within the claw plate may also provide an explanation for similar keratin expression observed in the human nail disease, Pachyonychia Congenita (PC). PC is a group of largely autosomal dominant genodermatoses characterised by hypertrophic nail dystrophy accompanied by varying features of ectodermal dysplasia. There are two main clinical subtypes, PC-1 has been shown to be caused by mutations in the genes encoding keratins K16 (McLean *et al*, 1995) and K6a (Bowden *et al*, 1995). These keratins are co-expressed in the epithelial tissues affected in PC-1 (Weiss *et al*, 1984). In contrast, PC-2 has been shown to result from mutations in the K17 gene (McLean *et al*, 1995), and its Type II partner, K6b (Smith *et al*, 1998). It was already acknowledged anatomically that the dorsal side of the macroscopic claw resembled the nail pathology observed in pachyonychia congenita. With the many anatomical similarities identified between canine claw and human nail, it is possible that although the physical structure of the tubules and the K6 positive layer of the SM4 may be lacking in human nails, K6, K16 and K17 expression exists within the human nail plate as well as the nail bed, and may contribute to the phenotype observed in PC.

It was established from the claw anatomy study that the *ungual groove* was deeper on its dorsal side and narrowed in a ventral direction but the exact contours of the groove were not identified. Given that the claw plate was curved and mirrored the shape of the ungual process, it was thought that GR2-GR4 may be set at an angle facing upwards within the ungual groove. This region rapidly produced claw plate where GR1-4 cells were K6, K16 and K17 positive. These keratins are

markers for hyperproliferative epithelia and suggested that cells within the groove were generated very quickly and if set at an angle would create a curve in the claw plate. However, further SEM/TEM studies would have to be carried out to confirm this suggestion.

The outer claw sheath (OCS) is continuous with the epidermis, therefore it was expected that this layer would express epidermal keratins and not hair-specific keratins. K14 was expressed in this layer and it was noted that expression in the OCS was greater in the inner, suprabasal cells. However, the OCS differed from the epidermis in that it expressed K6, K16 and K17. This was comparable to ORS of the human hair follicle where numerous investigations on keratin composition have revealed that K5, K6, K14, K16 and K17 represent the main keratins of the ORS (Lynch *et al*, 1986; Coulombe *et al*, 1989; Stark *et al*, 1987; Winter *et al*, 1998; Langbein *et al*, 1999). In the human nail, the proximal nail fold contains cells that are also K6 and K16 positive and provides further evidence that the canine claw and human nail share many similarities.

The companion layer of the claw fold, which exists between OCS and ICS formed a functional unit with the ICS and was found to express K6, K16 and K17 which conforms to previous research on the human hair follicle (Winter *et al*, 1998). However, ICS cells did not react with any of the human keratin antibodies tested and this agrees with comparable studies on human hair follicles where expression of specific keratins (K25-K28 and K75-K74) has been demonstrated in the various layers of the IRS (Rogers *et al*, 2000; Porter, *et al*, 2001; Langbein *et al*, 2003 & 2006). A mouse K6irs1 (K71) antibody was tested on cryostat sections of canine skin and positive immunofluorescence staining of the IRS of canine hair follicles was found. However, this antibody failed to work on paraffin embedded canine claw sections so the presence of these keratins within the ICS could not be confirmed. Similarly, SE cells did not stain with any of the antibodies tested and conformed to comparable hair follicle research where hair cuticle cells are known to express another set of specific keratins (K32, K35, K39, K40, K82 and K85).

GR5 and GR6 were located over the LR only on the dorsal aspect of the claw. It was difficult to ensure that the claw digit was cut exactly down the centre and the

LR was often excluded from parasaggital sections. Thus, care had to be taken when interpreting keratin expression data from parasaggital claw sections as what we thought was GR6 was actually GR9 (located to the left and the right of the ridge). Similarly, the manner in which transverse sections were obtained meant that a large amount of anatomy was being excluded from the area between sections. As GR5 was a small region, it was difficult to locate in transverse sections. The keratin data obtained from this region revealed that GR5 was K6 and K14 positive. SI1 cells were negative for both keratins. Unfortunately, no other keratin data was obtained for this region due to the section being damaged during cutting. GR6 was an extension from GR5 and initially provided a claw bed for SI1 horn before it expanded and produced large amounts of SI2 horn to fill the gap created between the reduced LR and claw plate. Transverse claw sections did not demonstrate K6, K14, K16 or K17 in GR6 or SI1 cells. Keratins K6, K16 and K17 are known to be markers of a hyperproliferative epidermis and comparable studies in the human nail have shown that the nail bed is K6, K16 and K17 positive and cells from this region contribute to nail plate thickness (De Berker, 2000). Conversely, the same transverse sections showed GR9 cells, located within the LR crevices, to be K5, K6, K14 and K17 positive but these were K16 negative. Moving in a ventral direction K16 expression increased where the GR9 expanded and produced S2, which was a soft sole epithelium. This region was more comparable to the human nail bed described by De Berker *et al* (2000) suggesting that perhaps the cellular contribution from the nail bed is a *soft sole type comparable* to canine S2.

From the anatomical studies, it has now been established that sole material actually comprises four different epithelia (S1-4) produced from different germinative regions (GR7-10). All types of sole showed K5, K6, K14, K16 and K17 expression. GR7 was K6, K16 and K17 positive and similar to GR4, generated a K6 positive epithelial strip (S4) which created a slippage zone for the claw plate as well as attaching it to the underlying S3. This supported our previous idea that cells expressing K6, K16 and K17 had different properties providing resistance and plasticity, and that in the case of S4, equipped the epithelial cells for the physical stresses formed between the claw plate and the sole (S3).

Although, some human keratin antibodies (K5, K14, K6, K16 and K17) appeared to cross-react with canine tissue and stained the appropriate layers when compared to human skin, differences in keratin gene protein sequences between species does exist and as a result, we cannot be certain that the human keratin antibodies are staining the canine tissue correctly. However, keratin genes have been shown to be highly conserved between humans and dogs (Lauchaume *et al*, 1998; Credille *et al*, 2001; Schleifer *et al*, 2003; Minor *et al*, 2005). Credille and co-workers (2005) identified that canine KRT1 and KRT2 shared a greater homology with humans than with mice based on both genomic and amino acid sequences. Also, sequence comparison and structural analysis of the KRT9 gene has shown marked similarity with the human gene and alignment of human and dog predicted amino acid sequences confirmed the high similarity, reaching 75% identity and 95% similarity in the rod domain (Lachaume *et al*, 1998).

In conclusion, some monoclonal antibodies raised against human keratins can be used to study keratin expression in canine epithelial tissues. These preliminary studies on keratin expression within the canine claw have demonstrated that OCS, ICS and SE are comparable to the ORS, IRS and hair fibre cuticle of the human hair follicle respectively, and that GR2-4 are comparable to the ventral proximal nail matrix of the human nail. K6, K16 or K17 expression in specific patterns and areas of the claw have demonstrated that these 'soft' keratins aid in providing the 'hard' claw plate with plasticity by preventing shearing forces and allowing independent movement in and between claw plate layers.

CHAPTER 6

6 CONCLUSIONS AND FUTURE WORK

6.1 CONCLUSIONS

The canine claw is an extremely complex structure consisting of several cell types that undergo tissue specific differentiation and is the product of several specific germinative regions (GR). These GR are located along the length of the claw bed and contribute to the thickness, strength and resilience of the overall structure. Our investigations have elucidated that the structure of the claw is more complex than previously appreciated, and we have proposed new terminology as adapting the terminology proposed by Budras and Seidel (1992) was impractical. Previous studies have already noted similarities between human hair follicles and nail (Dawber *et al*, 1994; Hashimoto, 1971) and our studies have also highlighted similarities between the canine claw and mammalian hair follicles in general. In view of this, terms used in hair literature have been adapted to the canine claw, ~~but~~ as well as incorporating some of the old claw terminology, where necessary. The new terms introduced describe comparable structures within the canine claw in terms of mammalian embryology and cell biology (Tables 6.1, 6.2 and 6.3).

Table 6.1: Comparable Structures in Human Hair Follicle and Canine Claw

Hair Follicle Structure	Canine Claw Equivalent
ORS	OCS
Companion Layer	Companion Layer
IRS	ICS
IRScu	ICScu
Hair Cuticle	SE
Dermal Papilla	Lunula
Cortex	SM1-3
Medulla	SM2 tubules and SM4

Table 6.2: Comparable Structures in Human Nail and Canine Claw

Human Nail Structure	Canine Claw Equivalent
Eponychium	OCS, ICS, SM1
Cuticle	SE
Matrix	GR1 and GR2
Nail Plate	Claw Plate (SM1-4)
Lunula	Lunula
Nail Bed	Claw Bed (GR9)
Hyponychium	Sole (S1-4)
Digit Pulp	Digital Foot Pad

Table 6.3: Comparable Structures in Equine Hoof and Canine Claw

Equine Hoof Structure	Canine Claw Equivalent
Periople	OCS, ICS, SE, SM1
Stratum Medium (SM)	SM1-4
Perioplic Cushion	Lunula
Stratum Internum (SI)	SI1
Tubules	Tubules (in SM2 and SI1)
White Line	Sole (S4)
Sole	Sole (S1-S4)
Frog	Digital Foot Pad

In many ways, the proximal canine claw closely resembled the proximal human nail and hair follicle. The outer claw sheath (OCS) appeared to be comparable to the outer root sheath (ORS) of the hair follicle and both structures are a continuation and a modification of the epidermis. Small papillae were located along the inside of the claw fold adjacent to the OCS, which might be related to the hair follicle bulge.

Germinative region 1 (GR1) was located deep within the ungual groove and produced three single cells layers which initially remained as single cell layers along the outer aspect of the claw plate. These cell layers expanded distally to

produce the outermost part of the claw horn (ICS, SE and SM1). Small papillae located along the claw fold may be regions of stem cell activity somewhat equivalent to the hair follicle bulge. These appeared in the region where the ICS, SE and SM1 structures expanded but this could not be proved as the proliferative marker we tested (Ki67) did not cross-react with canine tissue. Immunohistological analysis of this region showed that antibodies to K6, K14, K16 or K17 stained the OCS and all except K14 stained the companion layer. The ICS and SE did not stain with any of the keratin antibodies tested which was anticipated as these are IRS and hair cuticle equivalents, which are known to express IRS specific (K25-K28 and K71-K74) and hair cuticle specific (K32, K35, K39, K40, K82 and K85) keratins (Langbein *et al*, 2006). If the ICS is comparable to the hair follicle then it too should contain the Henle and Huxley layers but these were not identified in this study. Staining with a K74 antibody, which is a specific marker for the Huxley layer, as well as with K6, K16 or K17 antibodies would be required to determine if these layers exist within the ICS. Furthermore, the use of an antibody to K75 might be able to define the companion layer, adjacent to the Henle layer.

The papillated GR2 could be viewed as a modified hair follicle where each GR2 papillae resembled the dermal papillae. Like the hair follicle dermal papillae, germinative cells located at the apex of each GR2 papillae generated a 'soft' epithelial tube (tubule) which ran the entire length of the hard claw plate and was comparable to the medulla of the hair follicle. Tubules were found to be K6 and K16 positive and these may provide the hard claw plate with flexibility. These two keratins have also been found in the human nail plate but their exact location has never been identified. Since the human nail has evolved from the claw, it is possible that the nail plate contains thin microscopic strips which are K6, K16 and K17 positive but further studies would have to be done to confirm this.

GR3 and GR4 lie over a thickened dermal mesenchyme (lunula), which is comparable to the dermal papillae of the hair follicle and the lunula of the human nail. This may be a region of specialised mesenchyme that can induce specific programmes of differentiation in the overlying epithelial cells as happens in the hair follicle. These germinative regions produce SM3 and SM4 respectively

which differ in structure and we have also shown that K17 expression in these two germinative regions differs.

SM3 and SM4 are equivalent to the cortex of the human hair and the human nail plate. None of the keratin antibodies tested reacted with any of the cells in SM1-4 other than the tubules and part of SM4. As these appear to be the equivalent of the hair cortex and human nail plate, these structures will express hair-specific keratins, providing the claw plate with toughness and resilience.

Another interesting structure within the canine claw was the soft epithelial strip, which was formed by an expansion in SM4. This strip was eosinophilic and reacted with K6 antibodies. It ran the entire length of the claw plate but did fade distally. High power microscopic views did show that the eosinophilic content was present throughout SM4 but much more prominent in the lower part. If we consider that this K6 positive region of SM4 is a type of large tubule within the claw plate somewhat similar to the hair follicle medulla, then a common biological design can be seen in all these structures. As discussed earlier, K6, K16 or K17 expression within these structures may not only represent the hyperproliferative nature of this epithelium but may also provide the tissue with elasticity to prevent shearing forces between the hard epithelia and the underlying claw bed.

GR5 was comparatively small, densely eosinophilic and highly K6 positive and this gave rise to the large dense tubular upper stratum internum (SI1), inferring that it may be a region of rapid cell production. However, as the proliferative marker did not work on canine tissue we could not provide evidence for this observation. In addition, GR5 was only found on the dorsal aspect of the claw and was not present on the medial and lateral walls, which have no stratum internum. Thus, when cutting and sectioning claws, GR5 was not always visible and varied in structure on the sections depending on the original position of the cut made through the claw with a band saw. Parasaggital sections were often cut to the left or right of this structure or at an angle across the dermal groove where GR5 is located, making histological sections difficult to interpret. It was also difficult to locate when cutting transverse sections and transverse cuts were often not

perpendicular to claw growth resulting in one side of the claw section being more advanced in growth than the other, which again led to confusing results. Only K6 and K14 data were obtained on sections showing this structure and many of the paraffin embedded section were damaged in this region. For these reasons, we do not have a clear view of the structure and function of this region.

Nonetheless, it is known that SI1 is produced to fill in the gap created between the reduction in size of the longitudinal ridge (LR) that occurs distally along the length of the claw. GR5 is micro-papillated and forms very small and quite often indistinct tubules within SI1. This situation is comparable to the equine and bovine hoof, which also contain tubules within the equivalent SI.

Where the ungual process curves and comes to a tip, the small micro-papillae of GR6 expand along the dorsal ridge and produce SI2, which fills the gap between SI1 and the mesenchyme covering the bony ungual process. Interestingly, GR6 did not appear to react with any of the keratin antibodies tested which was unexpected since the other regions of claw bed were either K6, K16 or K17 positive and all showed basal cell staining for K5 and K14. Initially, it was thought that the reason for these perplexing results was due to experimental error but transverse sections, which contained GR6, as well as laminar GR9, located immediately to the left and right of the LR, showed clear K5, K14 and K17 staining of GR9 epithelial cells but the adjacent GR6 epithelium on the same section was negative. This infers the presence of specialised keratins, or even claw-specific keratins and this warrants further investigation into GR6 gene expression. Comparable studies on the feline and canine claw have discussed the LR and noted that no laminae exist within this region, which conforms to our findings. However, these studies have not examined cells within this region thoroughly and more remains to be discovered in this region, which is still not well understood.

On the medial and lateral walls, the dermal configuration of GR9 is different, and large columnar cells, which are keratin negative, cover this region. GR9 generates a soft horn (S2) on the lateral and medial walls, which thickens in a ventral and distal direction. It was thought that S2 was comparable to the small expansion of

cells observed from the human nail bed (De Berker *et al*, 2000), and that S2 and the other sole types (S1, S3 and S4), were the equivalent of the hyponychium of the human nail. Keratin analysis of S2 horn cells revealed that a single cell layer between the expanding S2 and the claw plate remained K5, K14, K6 and K17 positive but K16 negative. This layer was also observed in transverse sections taken at the claw tip. We were only able to do limited analysis on this single cell layer that connects the large 'soft' epithelia of S2 to the 'hard' claw plate and further investigation is required.

The papillated GR10 was an extension of, and adjacent to, GR8 and covered the entire tip of the unugal process. This region produced S3 horn which sealed the distal end of the claw and provided a rubbery buffer between the claw horn tip and the tip of the bony ungual process. Suprabasal S3 cells expressed K6, K16 and K17 which was a common theme amongst the sole epithelia. On the dorsal side of the claw, S3 connected to S4, which was produced from GR7 and contained smaller papillae. GR7 cells were also K6, K16 and K17 positive and the resulting thin epithelial strip that was generated, remained K17 positive. It was thought that S4 was the equivalent of the white line observed in the equine hoof (Reilly *et al*,1997; Bragulla *et al*, 1998) and this region acts to provide some independent movement between claw plate and S3 sole horn. In the equine hoof, the white line is of great clinical significance as a barrier against ascending bacterial invasion of the hoof, as observed in white line diseases. Budras and Seidel (1992) also referred to the '*zona alba*' (white line) in their canine claw studies and Sonnex *et al*, (1991) discussed the 'onycho-corneal band' of the human nail which connects the most proximal part of the fingertip stratum corneum to the nail plate. Further investigation into this structure would be required to see if S4 is the canine claw equivalent.

6.2 Future Work

The micro-anatomy study has contributed greatly to the current veterinary literature but further work still needs to be performed to answer many of the questions raised in this study. Additionally, different breeds of dog as well as dogs from different geographical locations should be studied, as variations

between breeds may exist. Gunaratnam and Wilkinson (1983) noted that the rate of hair growth varied between individual dogs and in some Nordic breeds, the hair appears to be held in a telogen state for years, probably a method of keeping the dog warm. Similarly, it would be interesting to see if claws obtained from dogs in hot or dry regions were different to those of dogs living in wet or cold regions, as modifications to the claw may occur to suit the surroundings. Although no anatomical differences were identified between breeds or between digits from the same foot, no comparisons were made with the dew claw. This digit is equivalent to the human thumb fingernail but its purpose has been lost through evolution and is located higher up the leg away from the foot (see Figure 1.8). Macroscopically, the dew claw is smaller, more curved and as the tip does not reach the ground, the claw plate is much longer and sharper as no surface frictional wear occurs.

Due to the tough nature of the canine claw, a great deal of time and effort was dedicated to optimising protein extraction methods so that a reasonable amount of protein could be extracted for SDS-PAGE analysis. Although, SDS-PAGE and western blotting did identify several epithelial keratins within different regions of the claw, the exact locations of these keratins could not be determined and separation of the claw into its different strata was inaccurate. In addition, these methods are only semi-quantitative and can only reveal significant changes in keratin expression or differences between the expression in different tissues. This method alone was therefore unsuitable for assessing small changes in protein synthesis in such a complex structure. As a result, the decision was made that sufficient information had been obtained from the one-dimensional electrophoresis and western blot analysis so instead of delaying the study further by optimising the conditions for two-dimensional electrophoresis, time would be better spent on immunohistochemical analysis with the human antibodies that would cross-react with the canine proteins.

Further problems were encountered during processing claw material for immunohistological examination. Firstly, cutting the claw into either parasaggital or transverse sections using a band-saw was not accurate. Parasaggital sections required halving the claw exactly down the midline so to include the LR but this was difficult and cuts were often made at an angle across the LR. This resulted in

histological sections that did not show GR6 along its entire length and care had to be taken when studying histological slides that GR9, located to the left and right of the ridge, was not being viewed instead. Additionally, the five transverse sections that were cut along the length of the claw were too far apart and resulted in a lot of important anatomical information being excluded between sections. A better approach would have been to make more transverse cuts along the claw, creating a better image of the anatomy and subsequently, keratin expression within different regions of the canine claw. However, due to limited samples and time this was not achieved.

The rotary microtome used in this study was not large enough and it often damaged paraffin embedded claw sections. For example, transverse section 2 (TS2) was damaged during cutting and could not be used in the microscopic study. Total decalcification of the bone was time consuming but had to be done as this interfered greatly with cutting and could potentially damage the microtome blade and the paraffin embedded claw sections. Unfortunately, the hard claw plate could not be softened sufficiently to guarantee that the blade would not "shatter" the surface the of the paraffin embedded block when being cut on the microtome.

Nonetheless, histological slides were obtained showing the various germinative regions of the canine claw and many were used for immunohistological studies. Several human keratin antibodies were tested as well as several other antibodies. Only a few human keratin antibodies were found to cross-react with canine tissue and due to slight differences in the sequence of human and canine keratin genes, it could not be certain that these antibodies reacted correctly on dog epithelia (Lauchaume *et al*, 1998; Credille *et al*, 2001; Schleifer *et al*, 2003; Minor *et al*, 2005). Therefore, the next step would be to produce antibodies to canine keratins (epithelial, IRS and hair-specific), which would stain the tissue correctly. Furthermore, micro-dissection of the canine claw followed by the preparation of frozen sections would allow double-labelled immunofluorescence studies. This would highlight any areas of the claw where cells were expressing both 'hard' and 'soft' keratins in the same section at the same time and would be useful to examine keratin expression in regions that form boundaries between the different

tissues of the claw. Additionally, a canine antibody specific to Ki67 would be extremely informative to identify the proliferative activity of the several different germinative regions within the claw plate. The information gained from these studies would provide a solid framework for comparable studies on human nail and equine and bovine hoof.

The application of molecular biology techniques to study canine claw gene expression was initially envisaged as the final part of this study. However, difficulties experienced with the micro-anatomy, protein extraction and immunohistochemistry prevented this work form going ahead. Some canine gene sequences were available when this work was being done and others have been published since (Lauchaume *et al*, 1998; Credille *et al*, 2001; Schleifer *et al*, 2003; Minor *et al*, 2005). Thus, it is now possible not only to conduct *in silico* bioinformatics to compare the canine keratin genes to those in man and rodents (rats and mice), but examining keratin expression in the canine claw at the level of mRNA by tissue *in situ* hybridization or RT-PCR would greatly increase our knowledge of the gene expression in this complex tissue aspect. The recent advances in laser capture microscopy would also be a useful application and some regions of the canine claw sections could be removed and studied in more detail in terms of gene expression. Finally, the application of recent advances in the understanding of stem cell biology and the developmental patterning of complex tissues to the canine claw might be quite illuminating.

Overall, this project has provided a strong foundation for further claw anatomy research and many avenues of further study have been opened. While much has been contributed to the understanding of the complex canine claw, as always there is still much to be done.

APPENDIX

7 Reagents and Stock Solutions

7.1 Reagents Used for Histology

Table 7.1: Reagents Used for Histology

Chemical Name	Company	Formula Weight	Catalogue Reference
EDTA (Ethylenediaminetetraacetic acid disodium salt dihydrate for Electrophoresis >99%)	Sigma-Aldrich	372.24	E5513
Ethanol (99.7-100% (absolute) AnalaR)	VWR International Limited	-	101074F
Xylene (Histological)	Fisher Scientific	106.16	*X3P-1GAL*
Cedar Wood Oil	VWR International Limited	-	23686.232
Pelleted Paraffin Wax	R.A. Lamb	-	W1
Haematoxylin	Fisher Scientific	-	H/0010/46
Eosin	Fisher Scientific	-	15288-1000
Sodium Iodate ($NaIO_3$)	Sigma-Aldrich	197.89	S4007
Potassium Alum (Aluminium potassium sulfate 99+% SpeciFied	Fisher Scientific	474.38	A/2400/53
Citric Acid ≥99%	Sigma-Aldrich	192.12	240621
Chloral Hydrate	Sigma-Aldrich	165.40	C8383
Trisodium Citrate	Sigma-Alrich	294.10	S1084
Mounting Medium	Invitrogen	-	VX088010

REAGENTS AND STOCK SOLUTIONS FOR SDS-PAGE ELECTROPHORESIS

Table 7.2: Stock Solutions for Gel Electrophoresis

All solutions were filtered (Millipore 0.45µm) unless stated otherwise, and stored at 4°C (or room temperature as stated) and used within a month, unless otherwise stated.

Buffer	Store	Quantity	Material	Amount	Notes
2.0 M Tris HCl, pH 8.8	4°C	250 ml	Trizma (Sigma) HCl (2 N Stock) H_2O (Distilled)	60.57 g 40.0 ml 100.0 ml	Adjust to pH 8.8 (± 0.05) with 2N HCl and add distilled H_2O to 250 ml
0.5 M Tris HCl, pH 6.8	4°C	100 ml	Trizma (Sigma) HCl (2N Stock)(Fisher) H_2O (Distilled)	6.06 g 15.0 ml 50.0 ml	Adjust to pH 6.8 (± 0.05) with 2 N HCl and add distilled H_2O to 100 ml
20 mM EDTA, pH 7.5	4°C	100 ml	EDTA (Sigma)	0.745 g	-
5 % (w/v) SDS	Room Temp	100 ml	SDS (Sigma)	5.00 g	-
10 % (w/v) SDS	Room Temp	100 ml	SDS (Sigma)	10.00 g	-
30% (w/v) Acrylamide/Bis	4°C	250 ml	Acrylamide (IBI) Bis Acrylamide (IBI)	73.00 g 2.00 g	Acrylamide solutions should be stored in a dark bottle
1.5% (w/v) Ammonium Persulphate	-	10 ml	Ammonium Persulphate (Sigma)	0.15 g	Make solution fresh immediately before use. Do not filter and do not store
10 % (v/v) TEMED	4°C	5 ml	TEMED (Sigma) H_2O (Distilled)	0.5 ml 4.5 ml	Do not filter
Organic Overlay Buffer	Room Temp	100 ml	Isobutanol (BDH) H_2O (Distilled)	80.0 ml 20.0 ml	Do not filter
Resolving Overlay Buffer	Room Temp	100 ml	2 M Tris 5 % (w/v) SDS 20 mM EDTA H2O (Distilled)	20.0 ml 2.0 ml 5.0 ml 73.0 ml	Do not filter
Sucrose Buffer	Room Temp	100ml	2M Tris 5% (w/v) SDS 20mM EDTA H_2O (Distilled)	20 ml 2.0 ml 5.0 ml 73.0 ml	Do not filter

Table 7.3: Stock Solutions for Gel Electrophoresis Continued

Buffer	Store	Quantity	Material	Amount	Notes
Stacker Overlay	Room Temp	100 ml	0.5 Tris 20 mM EDTA 5 % (w/v) SDS H_2O (Distilled)	10.0 ml 5.0 ml 2.0 ml 83.0 ml	Do not filter
SDS-PAGE Running Buffer (10x TGRB)	4°C	1000 ml	Trizma (Sigma) Glycine (Sigma) H_2O (Distilled)	30.30 g 144.10 g 900.0 ml	Make up to 1000 ml Do not filter
0.5% (w/v) Bromophenol Blue	Room Temp	20 ml	Bromophenol Blue H2O (Dilstilled)	0.1g 20.0 ml	Do not filter

7.2 Reagents Used for Western Blotting

Table 7.4: Reagents used for Western Blotting

Chemical Name	Company	Molecular Weight	Catalogue Reference
Trizma® Base (Primary Standard and Buffer, ≥99.9% (titration), crystalline)	Sigma-Aldrich	121.14	T0153
Marvel Milk	Marvel	-	-
Sodium Chloride SigmaUltra, ≥99.5%	Sigma-Aldrich	58.44	S7653
Tween 20	Dakocytomation	-	S1966
Kaleidoscope Prestained Standards (10-250 KDa)	Biorad	-	161-0234
ECL Detection Kit	Amersham Biosciences	-	RPN2109

7.3 Stock Solutions For Western Blotting

Table 7.5: TBS (10X)

Chemical	Amount
Tris	24.2g
NaCl	80g

Bring up to 1L with distilled water
Adjust to pH 7.6 with HCl

Table 7.6: TBS-T

Chemical	Amount
TBS (X10)	*100ml*
Distilled Water	900ml
Tween 20	1ml

REFERENCES

ACHTEN, M.G. (1968) On the embryology and histochemistry of the normal nail and ungual pathology, *Journal of Medicine Lyon*, **49**, (141), 705-726.

ADAM, W.S., CALHOUN, M.L., SMITH, E.M. and STINSTON, A.W. (1970) *Microscopic anatomy of the dog: a photographic atlas*, Springfield, III., C.C. Thomas.

AL-BAGDADI, F.K.A., TITKEYMER, C.W. and LOVELL, J.E. (1979) Histology of the hair cycle in male beagle dogs, *American Journal of Veterinary Research*, **40**, (12), 1734-1741.

ALBERTS, B., JOHNSON, A., LEWIS, J., RAFF, M., ROBERTS, K. and WALTER, P. (2002) *Molecular biology of the cell*, 4th edition, New York, Garland P

AOKI, N., SAWADA, S., ROGERS, M.A., SCHWEIZER, J., SHIMOMURA, Y., TSUJIMOTO, T., ITO, K. and ITO, M. (2001) A novel type II cytokeratin, mK6irs, is expressed in the huxley and henle layers of the mouse inner root sheath, *Journal of Investigative Dermatology*, **116**, 359-365.

ARNOLD, I. and WATT, F. (2001) C-Myc activation in transgenic mouse epidermis results in mobilisation of stem cells and differentiation of their progeny, *Current Biology*, **11**, (8), 558-568.

ASTBURY, W.T. and MARWICK, T.C. (1932) X-ray interpretation of the molecular structure of feather keratin, *Nature*, **130**, (3278), 309-310.

AUGHEY, E. and FRYE, F. (2001) *Comparative veterinary histology with clinical correlates*, London, London Mason Publishing.

AUXILIA, S.T. and HILL, P.B. (2000) Mast cell distribution, epidermal thickness and hair follicle density in normal canine skin: possible explanations for the predilection sites of atopic dermatisis, *Veterinary Dermatology,* **11,** 247-254.

BADEN, H.P. and KUBILUS, J. (1984) A comparative study of the immunologic properties of hoof and nail fibrous proteins, *Journal of Investigative Dermatology*, **83**, 327-311.

BAKER, K.P. (1974) Hair growth and replacement in the cat, *British Veterinary Journal,* **130,** 327-335.

BATTIFORA, H. and KOPINSKI, M. (1986) The influence of protease digestion and duration of fixation on the immunostaining of keratins, *The Journal of Histochemistry and Cytochemistry,* **34,** (8), 1095-1100.

BAWDEN, S.C., MCLAUGHLAN, C., NESCI, A. and ROGERS, G. (2001) A unique type I keratin intermediate filament gene family is abundantly expressed in the inner root sheaths of sheep and human hair follicles, *Journal of Investigative Dermatology,* **116,** 157-166.

BERGVALL, K. (1998) Treatment of symmetrical onychomadesis and onychodystrophy in five dogs with omega-3 and omega-6 fatty acids, *Veterinary Dermatology,* **9,** 263-268.

BERNERD, F., DEL BINO, S. and ASSELINEAU, D. (2001) Regulation of keratin expression by ultraviolet radiation: differential and specific effects of ultraviolet B and ultraviolet A exposure, *Journal of Investigative Dermatology,* **117,** 1421.

BIKLE, D.D. and PILLAI, S. (1993) Vitamin D, calcium and epidermal differentiation, *Endocrine Reviews*, **14,** 3-19.

BOLLIGER, C.H. (1991) The equine hoof: morphological and histological findings, Dissertation, Veterinariae Medicinae, Zurich

BOORD, M.J., GRIFFIN, C.E. and ROSENKRANTZ, W.S. (1997) Onychectomy as a therapy for symmetric claw and claw fold disease in the dog, *Journal of the American Animal Hospital Association*, **33**, 131-138.

BOWDEN, P.E., QUINLAN, R.A., BREITKREUTZ, D. and FUSENIG, N.E. (1984) Proteolytic modification of acidic and basic keratins during terminal differentiation of mouse and human epidermis, *European Journal of Biochemistry*, **142**, 29-36.

BOWDEN, P.E., STARK, H.-J., BREITKREUTZ, D. and FUSENIG, N.E. (1987) Expression and modification of keratins during terminal differentiation of mammalian epidermis, *Current Topics in Developmental Biology: The Molecular and Developmental Biology of Keratins*, **Chapter 22**, 35-68. Academic Press, Orlando, Florida, USA.

BOWDEN, P.E. (1993) Keratins and Other Epidermal Proteins, in *Molecular Aspects of Dermatology*, Editor G.C. Priestly, **Chapter 2**, 19-54. John Wiley & Sons Ltd.

BOWDEN, P.E., HAINEY, S., PARKER, G. AND HODGINS, M.B. (1994) Sequence and expression of human hair keratin genes, *Journal of Dermatological Science*, 7, S152-S163.

BOWDEN, P.E., HALEY, J.L., KANSKY, A., ROTHNAGEL, J.A., JONES, D.O. AND TURNER, R. (1995) Mutation of a type II keratin gene (K6a) in Pachyonychia congenital, *Nature Genetics*, **10**, 363-365.

BOWDEN, P.E., HAINEY, S.D., PARKER, G., JONES, D.O., ZIMONJIC, D., POPESCU, N. and HODGINS, M.B. (1998) Characterisation and chromosomal localisation of human hair-specific keratin genes and comparative expression during the hair growth cycle, *Journal of Investigative Dermatology*, **110**, 158-164.

BRAGULLA, H. and HIRSCHBERG, R.M. (1998) Horse hooves and bird feathers: two model systems for studying the structure and development of highly adapted integumentary accessory organs – the role of the dermo-epidermal interface for the micro-architecture of complex epidermal structures, *Journal of Experimental Zoology Part B: Molecular and Developmental Evolution*, **298B**, (1), 140-151.

BRAGULLA, H., ERNSBERGER, S. and BUDRAS, K.-D. (2001) On the development of the papillary body in the feline claw, *Anatomica Histologica Embryologica*, **30**, 211-217.

BRAGULLA, H. (2003) Fetal development of the segment-specific papillary body in the equine hoof, *Journal of Morphology*, **258**, 207-224.

BRAGULLA, H. and HURSCHBERG, R.M. (2003) Horse hooves and bird feathers: two model systems for studying the structure and development of highly adapted integumentary accessory organs - the role of the dermo-epidermal interface for the micro-architecture of complex epidermal structures, *Journal of Experimental Zoology (Molecular Development Evolution)*, **298B**, 140-151.

BREEN, M., LANGFORD, C., CARTER, N., HOLMES, N., DICKENS, H., THOMAS, R., SUTER, N., RYDER, E., POPE, M. and BINNS, M. (1999) FISH mapping and identification of canine chromosomes, *Journal of Heredity*, **90**, (1), 27-30.

BUDRAS, K.D., SCHIEL, C. and MULLING, C. (1998) Horn tubule of the white line: an insufficient barrier against ascending bacterial invasion, *Equine Veterinary Education*, **10**, (2), 81-85.

BUDRAS, K.D. and SEIDEL, M. (1992) Die segmentale gliederung und hornstruktur an der kralle des hundes, *Anatomia Histologica Embryologica*, **21**, (4) 348-363.

BURCH, R.E., WILLIAMS, R.V., HAHN, H.K.J., JETTON, M.M. and SULLIVAN, J.F. (1975) Serum and tissue enzyme activity and trace-element content in response to zinc deficiency in the pig, *Clinical Chemistry,* **21,** 568-577.

BURGESON, R.E. and CHRISTIANO, A.M. (1997) The dermal-epidermal junction, *Current Opinion in Cell Biology,* **9,** 651-658.

BUTCHER, E.O. (1951) Development of the piliary system and the replacement of hair in mammals, *Annals of the New York Academy of Sciences*, **53**, (3), 508-516.

BUTLER, W.F. and WRIGHT, A.I. (1989) Hair growth in the greyhound, *Journal of Small Animal Practice,* **22,** (10), 655-661.

BYRNE, C., TAINSKY, M. and FUCHS, E. (1994) Programming gene expression in developing epidermis, *Development,* **120,** 2369-2383.

CLARK, W.E.L.G. (1971) *The tissues of the body*, Oxford, Clarendon Press.

COLLIN, C., OUHAYOUN, J.P., GRUND, C. and FRANKE, W.W. (1992) Suprabasal marker proteins distinguishing keratinizing squamous epithelia: cytokeratin 2 polypeptides of oral masticatory epithelium and epidermis are different. *Differentiation.* 51:137–148.

COULOMBE, P.A. (2003) Wound epithelialization: accelerating the pace of discovery, *Journal of Investigative Dermatology*, **121**, (2), 327-337.

CHU, P.G. and WEISS, L.M. (2002) Keratin expression in human tissues and neoplasms, *Histopathology,* **40,** 403-439.

CREDILLE, K.M., LUPTON, C.J., KENNIS, R.A., MAIER, R.L., DZIEZYC, J., CASTLE, S., REINHART, G.A., DAVENPORT, G.M. and DUNSTAN, D.W. (2000) The role of nutrition on the canine hair follicle: a preliminary report, *Current Research in Canine Dermatology*, 10-15.

CREDILLE, K.M., VENTA, P.J., BREEN, M., LOWE, J.K., MURPHY, K.E., OSTRANDER, E.A., GALIBERT, F. and DUNSTAN, R.W. (2001) DNA sequence and physical mapping of the canine transglutaminase 1 gene. *Cytogenetics and Cell Genetics*, **93**, 73-76.

CREDILLE, K.M., GUYON, R., ANDRE, C., MURPHY, K. TUCKER, K., BARNHART, K.F. and DUNSTAN, R.W. (2005) Comparative sequence analysis and radiation hybrid mapping of two epidermal type II keratin genes in the dog: keratin 1 and keratin 2e, *Cytogenetic Genome Research*, **108**, 328-332.

COSTARELIS, G. (2006) Epithelial stem cells: a folliculocentric view, *Journal of Investigative Dermatology*, **126**, 1459-1468.

COULOMBE, P.A., KOPAN, R. and FUCHS, E. (1989) Expression of keratin 14 in the epidermis and hair follicle: insights into complex programs of differentiation, *The Journal of Cell Biology*, **109**, 2295-2312.

DALE, B.A. (1987) Developmental expression of human epidermal keratins and filaggrin, *Current Topics in Developmental Biology*, **22**, 127-150.

DAVENPORT, G.M. and REINHART. G.A. (2000) The impact of nutrition on skin and hair coat, *Current Research in Canine Dermatology*, 4-9.

DAWBER, R.P.R., DE BERKER, D.A.R. and BARAN, R. (1994) Science of the nail apparatus, *Diseases of the nail and their management*, Blackwell Publishing, 1-31.

DE BERKER, D.A. (2000) Management of nail psoriasis, *Clinical Dermatology*, **25**, 357-362.

DE BERKER, D.A. and ANGUS, B. (1996) Proliferative compartments in the normal nail unit, *British Journal of Dermatology*, **135**, 555-559.

DE BERKER, D., WOJNAROWSKA, F., SVILAND, L., WESTGATE, G.E., DAWBER, R.P.R. and LEIGH, I.M. (2000) Keratin expression in the normal nail unit: markers for regional differentiation, *British Journal of Dermatology,* **142,** 89-96.

DESNOYERS, M.M., HAINES, D.H. and SEARCY, G.P. (1990) Immunohistochemical detection of intermediate filament proteins in formalin fixed normal and neoplastic canine tissues, *Canadian Journal of Veterinary Research,* **54,** (3), 360-365.

DEPLEWSKI, D. and ROSENFIELD, R.L. (2000) Role of hormones in pilosebaceous unit development, *Endocrine Reviews*, **21,** (4), 363-392.

DOBLER, C. (1969) *Papillarkorper und kapillaren der hundekralle,* schweine- und siegenklaue, **113,** 382-428.

DOWLING, L.M., CREWTHER, W.G. and INGLIS, A.S. *(1986)* The primary structure of component 8c-1, a subunit protein of intermediate filaments in wool keratin. Relationships with proteins from other intermediate filaments, *Biochemistry Journal*, **236**, (3), 695-703.

DYCE, K.M., SACK, W.O. and WENSING, C.J.G. (1987) *Textbook of veterinary anatomy*, London, W.B. Saunders Company.

ECKERT, R.L. and RORKE, E.A. (1989) Molecular biology of keratinocyte differentiation, *Environmental Health Perspectives,* **80,** 109-116.

EICHNER, R., BONITZ, P. and SUN, T.T. (1984) Classification of epidermal keratins according to their immunoreactivity, isoelectric point, and mode of expression, *The Journal of Cell Biology,* **98,** 1388-1396.

EICHNER, R.E., KAHN, M., CAPETOLA, R.J., GENDIMENICO, G.J. and MEZICK, J.A. (1992) Effects of topical retinoids on cytoskeletal proteins:

implications for retinoid effects on epidermal differentiation, *The Journal of Investigative Dermatology,* **98,** (2), 154-161.

ELIAS, P.M. (1981) Epidermal lipids, membranes, and keratinization, *International Journal of Dermatology,* **20,** 1-9.

ERICKSON, A.C. and COUCHMAN, J.R. (2000) Still more complexity in mammalian basement membranes, *The Journal of Histochemistry and Cytochemistry,* **48,** (10), 1291-1306.

FAERGEMANN, J., BERGBRANT, I.-M., DOHSE, M., SCOTT, A. and WESTGATE, G.E. (2001) Seborrhoeic dermatitis and pityrosporum (mallassezia) folliculitis: characterisation of inflammatory cells and mediators in the skin by immunohistochemistry, *British Journal of Dermatology,* **144,** 549-556.

FARREN, L., SHAYLER, S. and ENNOS, A.R. (2004) The fracture properties and mechanical design of human fingernails, *The Journal of Experimental Biology,* **207,** 735-741.

FAVRE, B., FONTAO, L., KOSTER, J., SHAFAATIAN, R., JAUNIN, F., SAURAT, J.H., SONNENBERG, A. and BORRADOR, L. (2001) The hemidesmosomal protein bullous pemphigoid antigen 1 and the integrin beta 4 subunit bind to ERBIN. Molecular cloning of multiple alternative splice variants of ERBIN and analysis of their tissue expression, The *Journal of Biological Chemistry*, **276**, (35), 32427-32436.

FOWLER, M.E. (1980) Hoof, claw and nail problems in nondomestic animals, *Journal of American Veterinary Medical Association*, **177**, (9), 885-893.

FUCHS, E. (1990) Epidermal differentiation: the bare essentials, *The Journal of Cell Biology,* **111,** (6 part 2), 2807-2814.

GALVIN, S., LOOMIS, C., MANABE, M., DHOUAILLY, D. and SUN, T.T. (1989) The major pathways of keratinocyte differentiation as defined by keratin expression: an overview, *Advances in Dermatology,* **4,** 277-300.

GHOHESTANI, R.F., LI, K., ROUSSELLE, P. and UITTO, J. ((2001)) Molecular organization of the cutaneous basement membrane zone, *Clinics in Dermatology,* **19,** 551-562.

GEISELER, N. and WEBER, K. (1982) The amino acid sequence of chicken muscle desmin provides a common structural model for intermediate filament proteins, *The EMBO Journal,* **1,** (12), 1649- 1656.

GIBBS, S., PINTO, A.N.S., MURLI, S., HUBER, M., HOHL, D. and PONEC, M. (2000) Epidermal growth factor and keratinocyte growth factor differentially regulate epidermal migration, growth, and differentiation, *Wound Repair and Regeneration,* **8,** 192-203.

GIMENO, E.J., COSTA, E.F., GOMAR, M.S., MASSONE, A.R. and PORTIANSKY, E.L. (2000) Effects of plant-induced hypervitaminosis D on cutaneous structure, cell differentiation and cell proliferation in cattle, *Journal of Veterinary Medicine,* **47,** 201-211.

GODDARD, D.R. and SCHUBERT, M.P. (1935) The action of iodoethyl alcohol on thiol compounds and on proteins, *Biochemistry Journal,* **29,** (5), 1009-1011.

GROSENBAUGH, A. and HOOD, D.M. (1992) Keratin and associated proteins of the equine hoof wall, *American Journal of Veterinary Research,* **53,** (10), 1859-1863.

GROSENBAUGH, D.A. and HOOD, D.M. (1993) Practical equine hoof wall biochemistry, *Equine Practice,* **15,** (8), 8-14.

GUNARATNAM, P. and WILKINSON, G.T. (1983) A study of normal hair growth in the dog, *Journal of Small Animal Practice,* **24,** 445-453.

HALLMAN, J.R., FANG, D., SETALURI, V. and WHITE, W.L. (2002) Microtubule associated protein (MAP-2) expression defines the companion layer of the anagen hair follicle and an analogous zone in the nail unit, *Journal of Cutaneous Pathology*, **29,** 549-556.

HAMRICK, M.W. (1998) Functional and adaptive significance of primate pads and claws: evidence from new world anthropoids, *American Journal of Physical Anthropology*, **106**, (2), 113-127.

HAMRICK, M.W. (1999) Pattern and process in the evolution of primate nails and claws, *Journal of Human Evolution,* **37,** 293-297.

HAMRICK, M.W. (2001) Development and evolution of the mammalian limb: adaptive diversification of nails, hooves and claws, *Evolution and Development,* **3,** (5), 355-363.

HAMRICK, M.W. (2002) Developmental mechanisms of digit reduction, *Evolution and Development,* **4,** (4), 247-248.

HARDY, M.H. (1992) The secret life of hair, *Trends in Genetics*, **8,** (2), 55-61.

HASHIMOTO, K. (1971) Ultrastructure of the human toenail, *Journal of Ultrastructural Research,* **36,** 391-410.

HASHIMOTO, K. (1988) The structure of human hair, *Clinical Dermatology,* **6,** (4), 7-21.

HATZFIELD, M. and FRANKE, W.W. (1985) Pair formation and promiscuity of cytokeratins: formation in vitro of heterotypic complexes and intermediate-sized filaments by homologous and heterologous recombination of purified polypeptides. *Journal of Cell Biology*, **101**, 1826–1841.

HEID, H.W., WERNER, E. and FRANKE, W.W. (1986) The complement of native alpha-keratin polypeptides of hair-forming cells: a subset of eight polypeptides that differ from epithelial cytokeratins, *Differentiation*, **32**, 101-119.

HEID,H.W., MOLL, I. and FRANKE, W.W. (1988) Patterns of expression of trichocytic and epithelial cytokeratins in mammalian tissues. I. human and bovine hair follicles, *Differentiation*, **37**, (2), 137-157.

HENDRY, K.A.K., MACCALLUM, A.J., KNIGHT, C.H. and WILDE, C.J. (1997) Laminitis in the dairy cow: a cell biological approach, *Journal of Dairy Research*, **64**, 475-486.

HERBERT, F.S. and MATOLSTSY, A.G. (1956) Observations on urea-extractable substance of the human abdominal epidermis, *Journal of Investigative Dermatology*, **27**, (4), 263-270.

HESSE, M., MAGIN, T.M. and WEBER, K. (2001) Genes for intermediate filament proteins and the draft sequence of the human genome: novel keratin genes and a surprisingly high number of pseudogenes related to keratin genes 8 and 18, *Journal of Cell Science*, **114**, (14), 2569-2575.

HSIEH, S.T. and LIN, W.M. (1999) Modulation of keratinocyte proliferation by skin innervation, *The Journal of Investigative Dermatology*, **113**, (4), 579-586.

JARNIK, M., SIMON, M.N. and STEVEN, A.C. (1998) Cornified cell envelope assembly: a model based on electron microscopic determinations of thickness and projected density, *Journal of Cell Science*, **111**, (8), 1051-1060.

JIANG, C.K., MAGNALDO, T., OHTSUKI, M., FREEDBERG, I.M., BERNARD, B.A. and BLUMENBERG, M. (1993) Epidermal growth factor and transforming growth factor alpha specifically induce the activation- and hyperproliferation-associated keratins 6 and 16, *Proceedings from the National Academy of Science*, **90**, (14), 6786-6790.

KALININ, A., MAREKOV, L.N. and STEINERT, P.M. (2001) Assembly of the epidermal cornified cell envelope, *Journal of Cell Science,* **114,** (17), 3069-3070.

KELLER, R.C., SWITONSKI, M., JORG, H., LADON, D., ARNOLD, S. and SCHELLING, C. (1998a) Chromosomal assignment of two putative canine keratin gene clusters, *Animal Genetics,* **29,** 141-143.

KELLER, R.C., SWITONSKI, M., JORG, H., LADON, D., ARNOLD, S. and SCHELLING, C. (1998b) Chromosomal assignment of canine genes for keratin 9 and keratin 2, *Canine Practice,* **23,** (1), 53.

KITAHARA, T. and OGAWA, H. (1991) The extraction and characterization of human nail keratin, *Journal of Dermatological Science,* **2,** 402-406.

KOCH, P.J., MAHONEY, M.G., COSTARELIS, G., ROTHENBERGER, K., LAVKER, R.M. and STANLEY, J.R. (1998) Desmoglein 3 anchors telogen hair in the follicle, *Journal of Cell Science,* **111,** (17), 2529-2537.

KOPAN, R., TRASKA, G. and FUCHS, E. (1987) Retinoids as important regulators of terminal differentiation: examining keratin expression in individual epidermal cells at various stages of keratinisation, *The Journal of Cell Biology,* **105,** 427-440.

KOPAN, R. and FUCHS, E. (1989) A new look into an old problem: keratins as tools to investigate determination, morphogenesis, and differentiation in skin, *Genes and Development,* **3,** (1), 1-15.

KUWANO, A., KATAYAMA, Y., KASASHIMA, Y., OKADA, K. and REILLY, J.D. (2002) A gross and histopathological study of an ectopic white line development in equine laminitis, *Journal of Veterinary Medical Science,* **64,** (10), 893-900.

LANGBEIN, L., ROGERS, M.A., WINTER, H., PRAETZEL, S., BECKHAUS, U., RACKWITZ, H.-R. and SCHWEIZER, J. (1999) The catalog of human hair

keratins I. Expression of the nine type I members in the hair follicle, *The Journal of Cell Biology*, **274**, (28), 19874-19884.

LANGBEIN, L., ROGERS, M.A., WINTER, H., PRAETZEL, S. and SCHWEIZER, J. (2001) The catalog of human hair keratins. II. Expression of the six type II members in the hair follicle and the combined catalog of human type I and II keratins, *Journal of Biological Chemistry*, **276**, (37), 35123-15132.

LANGBEIN, L., ROGERS, M.A., PRAETZEL, S., AOKI, N., WINTER, H. and SCHWEIZER, J. (2002) A novel epithelial keratin, hK6irs1, is expressed differentially in all layers of the inner root sheath, including specialised huxley cells (flugelzellen) of the human hair follicle, *Journal of Investigative Dermatology*, **118**, (5), 789-799.

LANGBEIN, L., ROGERS, M.A., PRAETZEL, S., WINTER, H. and SCHWEIZER, J. (2003) K6irs1, K6irs2, Kirs3, and K6irs4 represent the inner-root-sheath-specific type II epithelial keratins of the human hair follicle, *Journal of Investigative Dermatology*, **120**, 512-522.

LANGBEIN, L., ROGERS, M.A., PRAETZEL, W.S., HELMKE, B. SCHIRMACHER, P. and SCHWEIZER, J. (2006) K25 (K25irs1), K26 (K25irs2, K27 (K25irs3) and K28 (K25irs4) represent the type I inner root sheath keratins of the human hair follicle, *Journal of Investigative Dermatology*, **126**, 2377-2386.

LANGBEIN, L., ROGERS, M.A., PRAETZEL, S., BOCKLER, D., SCHIRMACHER, P. and SCHWEIZER, J. (2007) Novel type I keratins K39 and K40 are the last to be expressed in differentiation of the hair: completion of the human hair catalog, *Journal of Investigative Dermatology*, **127**, (6), 1532-1535.

LANGBEIN, L. and SCHWEIZER, J. (2005) Keratins of the human hair follicle, *International Review of Cytology*, **243**, 1-78.

LANSDOWN, A.B.G. (1985) Morphological variations in keratinising epithelia in the beagle, *Veterinary Record*, **116**, 127-130.

LAUCHAUME, P., HITTE, C., JOUQUAND, S., PRIAT, C. and GALIBERT, F. (1998) Identification and analysis of the dog keratin 9 (KRT9) gene, *Animal Genetics*, **29**, 173-177.

LEACH, D.H. and OLIPHANT, L.W. (1983) Ultrastructure of the equine hoof wall secondary epidermal lamellae, *American Journal of Veterinary Research*, **44**, (8), 1561-1570.

LE GROS CLARK, W.E. (1936) The problem of the claw in primates, Proceedings of the General Meetings for Scientific Business of the Zoological Society of London, 1-24.

LEIGH, I.M., NAVSARIA, H., PURKIS, P.E., McKAY, I.A., BOWDEN, P.E. and RIDDLE, P.N. (1995) Keratins (K16 and K17) as markers of keratinocyte hyperproliferation in psoriasis in vivo and in vitro, *British Journal of Dermatology*, **133**, 501-511.

LI, Z.L., LILIENBAUM, A., BUTLER-BROWNE, G. and PAULIN, D. (1989) Human desmin-coding gene: complete nucleotide sequence, characterization and regulation of expression during myogenesis and development, *Gene*, **78**, (2), 243-254.

LYLE, S., CHRISTOFIDOU-SOLOMIDOU, M., LIU, Y., ELDER, D.E., ALBELDA, S. and COSTARELIS, G. (1999) Human hair follicle bulge cells are biochemically distinct and possess an epithelial stem cell phenotype, *Journal of Investigative Dermatology*, **4**, (3), 296-301.

LYNCH, M.H., O'GUIN, W.M., HARDY, C., MAK, L. and SUN, T.T. (1986) Acidic and basic hair/nail ("hard") keratins: their co-localization in upper cortical and cuticle cells of the human hair follicle and their relationship to "soft" keratins, *The Journal of Cell Biology*, **103**, (6), 2593-2606.

MARSHALL, R.C. (1983) Characterization of the proteins of human hair and nail by electrophoresis, *The Journal of Investigative Dermatology,* **80,** 519-524.

MARSHALL, R.C. and GILLESPIE, J.M. (1982) Comparison of samples of human hair by two-dimensional electrophoresis, *Journal of the Forensic Science Society,* **22,** 377-385.

MARSHALL, R.C., ORWIN, D.F., GILLESPIE, J.M. (1991) Structure and biochemistry of mammalian hard keratin, *Electron Microscopy Reviews*, **4**, 47-83.

MATOLTSY, A.G. (1976) Keratinization, *The Journal of Investigative Dermatology,* **67,** 20-25.

MATTHECK, C. and REUSS, S. (1991) The claw of the tiger: an assessment of its mechanical shape optimization, *Journal of Theoretical Biology,* **150,** 323-328.

MCELWEE, K.J., SILVA, K., BOGGESS, D., BECHTOLD, L., KING, L.E.Jr and SUNDBERG, J.P. (2003) Alopecia areata susceptibility in rodent models, *Journal of Investigative Dermatology Symposium Proceedings*, **8,** (2), 182-187.

MCLEAN, W.H., RUGG, E.L., LUNNY, D.P., MORLEY, S.M., LANE, E.B., SWENSSON, O., DOPPING-HEPENSTAL, P.J., GRIFFITHS, W.A., EADY, R.A. and HIGGINS, C. (1995) Keratin 16 and keratin 17 mutations cause pachyonychia congenita, **9,** (3), 273-278.

MCGOWAN, K.M. and COULOMBE, P.A. (2000) Keratin 17 Expression in the Hard Epithelial Context of the Hair and Nail, and its Relevance for the Pachyonychia Congenita Phenotype, *Journal of Investigative Dermatology,* **114,** (6), 1101-1107.

MCMILLAN, J.R., MCGRATH, J.A., TIDMAN, M.J. and EADY, R.A. (1998) Hemidesmosome show abnormal association with the keratin filament network in junctional forms of epidermolysis bullosa, *Journal of Cell Biology,* **27,** 137-138.

MEYER, W. and TSIKISE, A. (1995) Lectin histochemistry of snout skin and foot pads in the wolf and the domesticated dog (mammalia:canidae), *Annals of Anatomy*, **177**, 39-49.

MILLER, A.B., BREEN, M. and MURPHY, K.E. (1999) Chromosomal localisation of acidic and basic keratin genes of the domestic dog, *Mammalian Genome*, **10**, 371-375.

MINOR, J., DUNSTAN, R., GUYON, R., ANDRE, C., BARNHART, K., and CREDILLE, K. (2005) Comparative sequence analysis and radiation hybrid mapping of the canine keratin 10 gene, *DNA Sequencing*, **16**, (2), 89-95.

MOLL, I., HEID, H.W., FRANKE, W.W. and MOLL, R. (1988) Patterns of expression of trichocytic and epithelial cytokeratins in mammalian tissues. III. Hair and nail formation during human fetal development, *Differentiation*, **39**, (3), 167-184.

MOLL, R., FRANKE, W.W. and SCHILLER, D.L. (1982a) The catalog of human cytokeratins: patterns of expression in normal epithelia, tumors and cultured cells, *Cell*, **31**, 11-24.

MOLL, R., FRANKE, W.W., VOLC-PLATZER, B. and KREPLER, R. (1982b) Different keratin polypeptides in epidermis and other epithelia of human skin: a specific cytokeratin of molecular weight 46,000 in epithelia of the pilosebaceous tract and basal cell epitheliomas, *The Journal of Cell Biology*, **95**, 285-295.

MUELLER, G., KIRK, R. and SCOTT, D. (1989) Small animal dermatology, London, W.B. Saunders.

MUELLER, R.S. (1999) Diagnosis and management of canine claw disease, *Dermatology*, **29**, (6), 1357-1371.

MUELLER, R.S., FRIEND, S., SHIPSTONE, M.A. and BURTON, G. (2000) Diagnosis of canine claw disease- a prospective study of 24 dogs, *Veterinary Dermatology*, **11**, 133-141.

MULLING, C.K.W., BRAGULLA, H.H., REESE, S., BUDRAS, K.D. and STEINBERG, W. (1999) How structure in bovine hoof epidermis are influenced by nutritional factors, *Anatomica Histologica Embryologica*, **28**, 103-108.

O'KEEFE, E.J., HAMILTON, E.H., LEE, S.C. and STEINERT, P. (1993) Trichohyalin: a structural protein of hair, tongue, nail and epidermis, *Journal of Investigative Dermatology*, **101**, (1), 65S-71S.

OLIVERY, T., FINE, J.-D., DUNSTON, S.M., CHASSE, D., TENORIO, A.P., MONTEIRO-RIVIERE, N.A., CHEN, M. and WOODLEY, D.T. (1998) Canine epidermolysis bullosa acquisita: circulating autoantibodies target the amino-terminal non-collagenous (NC1) domain of collagen VII in anchoring fibrils, *Veterinary Dermatology*, **9**, 19-31.

PARAMIO, J.M., CASANOVA, M.L., SEGRELLES, C., MITTNACHT, S., LANE, E.B. and JORCANO, J.L. (1999) Modulation of cell proliferation by cytokeratins K10 and K16, *Molecular and Cellular Biology*, **19**, (4), 3086-3094.

PARRY, D.A.D. and STEINERT, P.M. (1999) Intermediate filaments: molecular architecture, assembly, dynamics and polymorphism, *Quarterly Reviews of Biophysics*, **32**, 99-187.

PATEL, G.K., WILSON, C., HARDING, K.G., FINLAY, A.Y. and BOWDEN, P.E. (2006) Numerous keratinocyte subtypes involved in wound healing re-epithelialization, *Journal of Investigative Dermatology*, **126**, 497-502

PAULING, L. and COREY, R.B. (1953) Compound helical configurations of polypeptide chains: structure of proteins of the alpha-keratin type, *Nature*, **10**, 59-61.

PAUS, R., BOTTGE, J.A., HENZ, B.M. and MAURER, M. (1996) Hair growth control by immunosuppression, *Archives of Dermatological Research*, **288**, (7), 408-410.

PAUS, R. and COTSARELIS, G. (1999) The biology of hair follicles, *The New England Journal of Medicine*, **341**, (7), 491-497.

PAUS, R., MULLER-ROVER, S., VAN DER VEEN, C., MAURER, M., EICHMULLER, S., LING, G., HOFMANN, U., FOITZIK, K., MECKLENBURG, L. and HANDJISKI, B. (1999) A comprehensive guide for the recognition and classification of distinct stages of hair follicle morphogenesis, *Journal of Investigative Dermatology*, **113**, 523-532.

PERRIN, C., LANGBEIN, L. and SCHWEIZER, J. (2004) Expression of hair keratins in the adult nail unit: an immunohistochemical analysis of the onychogenesis in the proximal nail fold, matrix and nail bed, *British Journal of Dermatology*, **151**, (2), 362-371.

PHILPOTT, M.P., GREEN, M.R. and KEALEY, T. (1990) Human hair growth in vitro, *Journal of Cell Science*, **97**, 463-471.

PHILPOTT, M.P. and PAUS, R. (1998) Principles of hair follicle morphogenesis. In Chuong, C-H. (Ed.) *Molecular basis of epithelial appendage morphogenesis*, Texas, Landes Bioscience, 75–110.

POLLITT, C.C. and MOLYNEUX, G.S. (1990) A scanning electron microscopical study of the dermal microcirculation of the equine foot, *Equine Veterinary Journal*, **22**, (2), 79-87.

POLLITT, C.C. (1992) Clinical anatomy and physiology of the normal equine foot, *Equine Veterinary Education*, **4**, (5), 219-224.

POLLITT, C.C. (1995) *Colour atlas of the horse's foot*, Mosby Wolfe, Barcelona.

POLLITT, C.C. (1996) Basement membrane pathology: a feature of acute equine laminitis, *Equine Veterinary Journal,* **28,** (1), 38-46.

POLLITT, C. (1998) The anatomy and physiology of the hoof wall, *The Equine Hoof Supplement: Equine Veterinary Education,* 3-9.

PONEC, M., GIBBS, S., WEERHEIM, A., KEMPENAAR, J., MULDER, A. and MIEKE MOMMAAS, A. (1997) Epidermal growth factor and temperature regulate keratinocyte differentiation, *Archives of Dermatological Research,* **289,** (6), 317 - 326.

POPESCU, N., BOWDEN, P.E. and DIPAOLO, J.A. (1989) Two type II keratin genes are localised on human chromosome 12, *Human Genetics,* **82,** 109-112.

PORTER, R.M., CORDEN, L.D., LUNNY, D.P., SMITH, F.J.D., LANE, E.B. and MCLEAN, W.H.I. (2001) Keratin K6irs is specific to the inner root sheath of hair follicles in mice and humans, *British Journal of Dermatology,* **145,** 558-568.

PORTER, R.M., GHANDHI, M., WILSON, N.J., WOOD, P., MCLEAN, W.H.I. and LANE, E.B. (2004) Functional analysis of keratin components in the mouse hair follicle inner root sheath, *British Journal of Dermatology*, **150**, 195-204.

POWELLL, B.C. and ROGERS, G.E. (1986) Hair keratin: composition, structure and biogenesis. In Bereiter-Hahn J., Matoltsy A.G. and Richards K.S. (Eds.). *Biology of the Integument,* Springer-Verlag, Berlin, 696–721.

POWELL, B., CROCKER, L. and ROGERS, G. (1992) Hair follicle differentiation: expression, structure and evolutionary conservation of the hair type II keratin intermediate filament gene family, *Development*, **114**, (2), 417-433.

PRESLAND, R.B., KUECHLE, M.K., LEWIS, S.P., FLECKMAN, P. and DALE, B.A. (2001) Regulated expression of human filaggrin in keratinocytes results in cytoskeletal disruption, loss of cell-cell adhesion, and cell cycle arrest, *Experimental Cell Research,* **270,** 199-213.

RAO, S.K., BABU, R.K.K. and GUPTA, P.D. (1996) Keratins and skin disorders, *Cell Biology International,* **20,** (4), 261-274.

REARDON, C.M., MCARTHUR, P.A., SURVANA, S.K. and BROTHERSTON, T.M. (1999) The surface anatomy of the germinal matrix of the nail bed in the finger, *Journal of Hand Surgery,* **24B,** (5), 531-533.

REICHELT, J., BUSSOW, H., GRUND, C. and MAGIN, T.M. (2001) Formation of a normal epidermis supported by increased stability of keratins 5 and 14 in keratin 10 null mice, *Molecular Biology of the Cell,* **12,** 1557-1568.

REILLY, J.D., COLLINS, S.N., MARTIN, R. and CUDDEFORD, D. (1996) Tubule density in equine hoof horn, *Biomimetics,* **4,** (1) 23-36.

REILLY, J.D. (1997) The donkey's foot and its care, *The Professional Handbook of the Donkey,* Whittet Books Limited, London.

RICE, R.H., MEHRPOUYAN, M., QUIN, Q. and PHILLIPS, M.A. (1994) Transglutaminase in keratinocytes, *The Keratinocyte Handbook,* Cambridge, Cambridge University Press, 259-274.

ROBBINS, Morphological and macromolecular structure, *Chemical and Physical Behaviour of Human Hair 4th edition,* Chapter 1, Springer.

ROGERS, G.E. (1964) Isolation and properties of inner sheath cells of hair follicles, *Experimental Cell Research,* **33,** 264-276.

ROGER, G.E. and POWELL, B.C. (1993) Organization and expression of hair follicle genes, *Journal of Investigative Dermatology,* **101,** (1), 50S-55S.

ROGERS, G.E., DUNN, S. and POWELL, B.C. (1998) Late events and the regulation of keratinocyte differentiation in hair and feather follicles. In Chuong

C.M. (Ed.), *Molecular Basis of Epithelial Appendages and Morphogenesis*, Texas, Landes Bioscience, 315-338.

ROGERS, M.A., WINTER, H., LANGBEIN, L., KRIEG, T. and SCHWEIZER, J. (1996) Genomic characterisation of the human type I cuticular hair keratin hHa2 and identification of an adjacent novel type I hair keratin gene hHa5, *Journal of Investigative Dermatology*, **107**, 633-638.

ROGERS, M.A., LANGBEIN, L., PRAETZEL, S., MOLL, I., KRIEG, T., WINTER, H. and SCHWEIZER, J. (1997) Sequences and differential expression of three novel human type-II hair keratins, *Differentiation*, **61**, (3), 187-194.

ROGERS, M.A., WINTER, H., WOLF, C. and MARINA, H. (1998) Characterisation of a 190-kilobase pair domain of human type I hair keratin genes, *The Journal of Biological Chemistry*, **273**, (41), 26683-26691.

ROGERS, M.A., WINTER, H., LANGBEIN, L., WOLF, C. and SCHWEIZER, J. (2000) Characterization of a 300 kbp region of human DNA containing the type II hair keratin gene domain, *Journal of Investigative Dermatology*, **114**, (3), 464-472.

ROGERS, M.A., WINTER, H., LANGBEIN, L., BLEILER, R. and SCHWEIZER, J. (2004) The human type I keratin gene family: characterization of new hair follicle specific members and evaluation of the chromosome 17q21.2 gene domain, *Differentiation*, **72**, (9-10), 527-540.

ROGERS, M.A., EDLER, L., WINTER, H., LANGBEIN, L., BECKMANN, I. and SCHWEIZER, J. (2005) Characterization of new members of the human type II keratin gene family and a general evaluation of the keratin gene domain on chromosome 12q13.13, *Journal of Investigative Dermatology*, **124**, (3), 236-544.

ROSENBERG, M., RAYCHAUDHURY, A., SHOWS, T.B., LE BEAU, M.M. and FUCHS, E. (1988) A group of type I keratin genes on human chromosome 17: characterization and expression, *Molecular and Cellualr Biology*, **8**, 722-736.

ROSS, E. and SCHATZ, G. (1973) Assay of protein in the presence of high concentrations of sulfhydryl compounds, *Analytical Biochemistry,* **54,** (1), 304-306.

ROTHNAGEL, J.A. and ROGERS, G.E. (1986) Trichohyalin, an intermediate filament-associated protein of the hair follicle, *Journal of Cell Biology*, **102,** (4), 1419-1429.

ROTHNAGEL, J.A. and ROOP, D.R. (1995) Hair follicle companion layer: re-aquainting an old friend, *Journal of Investigative Dermatology,* **104,** 42SS.

SAGOO, G.S., TAZI-AHNINI, R., BARKER, J.W., ELDER, J.T., NAIR, R.P., SAMUELSSON, L., TRAUPE, H., TREMBATH, R.C., ROBINSON, D.A. and ILES, M.M. (2004) Meta-analysis of genome-wide studies of psoriasis susceptibility reveals linkage to chromosomes 6p21 and 4q28-q31 in Caucasian and Chinese Hans population, *Journal of Investigative Dermatology,* **122,** (6), 1401-1405.

SANDUSKY, G.E., WIGHTMAN, K.A. and CARLTON, W.W. (1991) Immunocytochemical study of tissues from clinically normal dogs and of neoplasms, using keratin monoclonal antibodies, *American Journal of Veterinary Research,* **52,** (4), 613-618.

SCHLEIFER, S.G., VERSTEEG, S.A., VAN OOST, B. and WILLEMSE, T. (2003) Familial foot pad hyperkeratosis and inheritance of keratin 2, keratin 9, and desmoglein 1 in two pedigrees of Irish terriers, *American Journal of Veterinary Research*, **64**, (6), 715-720.

SCHUILENGA-HUT, P.H., SCHEFFER, H., PAS, H.H., NIJENHUIS, M., BUYS, C.H. and JONKMAN, M.F. (2002) Partial revertant mosaicism of keratin 14 in a patient with recessive epidermolysis bullosa simplex, *Journal of Investigative Dermatology,* **118,** (4), 626-30.

SCHUMMER, A., WILKENS, H., VOLLMERHAUS, B. and HABERMEHL, K.H. (1981) The circulatory system, the skin, and the cutaneous organs of the domestic mammals, Berlin, Verlag Paul Parey, 442-449.

SCHWEIZER, J., BOWDEN, P.E., COULOMBE, P.A., LANGBEIN, L., LANE, E.B., MAGIN, T.M., MALTAIS, L., OMARY, M.B., PARRY, D.A., ROGERS, M.A. and WRIGHT, M.W. (2006) New consensus nomenclature for mammalian keratins, *Journal of Cell Biology*, **174**, (2), 169-174.

SCOTT, D.W., ROUSSELLE, S. and MILLER, W.H. (1995) Symmetrical lupoid onychodystrophy in dogs: a retrospective analysis of 18 cases (1989-1993), *Journal of the American Animal Hospital Association*, **31**, 194-201.

SENTER, D.A., SCOTT, D.W., MILLER, W.H. and ERB, H.N. (2002) Inter-corneal vacuoles in skin diseases with parakeratotic hyperkeratosis in the dog: a retrospective light-microscopy study of 111 cases (1973-2000), *Veterinary Dermatology*, **13**, 45-49.

SHIMOMURA, Y., AOKI, N., ROGERS, M.A., LANGBEIN, L., SCHWEIZER, J. and ITO, M. (2002) hKAP1.6 and hKAP1.7, two novel hunab high sulfur keratin-associated proteins are expressed in the hair follicle cortex, *Journal of Investigative Dermatology*, **118**, 226-231.

SIMON, M., HAFTEK, M., SEBBAG, M., MONTEZIN, M., GIRBAL-NEUHAUSSER, E., SCHMITT, D. and SERRE, G. (1996) Evidence that filaggrin is a component of cornified cell enveloped in human plantar epidermis, *Biochemical Journal*, **317**, 173-177.

SMACK, D.P., KORGE, B.P. and JAMES, W.D. (1994) Keratins and keratinisation, *Journal of the American Academy of Dermatology*, **30**, (1), 85-102.

SMITH, F.J., JONKMAN, M.F., VAN GOOR, H., COLEMAN, C.M., COVELLO, S.P., UITTO, J. and MCLEAN, W.H. (1998) A mutation in human

keratin K6b produces a phenocopy of the K17 disorder pachyonychia congenita type 2, *Human Molecular Genetics*, **7**, (7), 1143-1148.

SMOLA, H., STARK, H.J., THIEKOTTER, G., MIRANCEA, N., KREIG, T. and FUSENIG, N.E. (1998) Dynamics of basement membrane formation by keratinocyte-fibroblast interactions in organotypic skin culture, *Experimental Cell Research,* **239,** 399-410.

SOLIGO, C. and MULLER, A.E. (1999) Nails and claws in primate evolution, *Journal of Human Evolution,* **36,** 97-114.

SONNEX, T.S., GRIFFITHS, W.A. and NICOL, W.J. (1991) The nature and significance of the transverse white band of human nails, *Seminars in Dermatology,* **10,** (1), 12-16.

SPEARMAN, R.I.C. (1977) Keratins and keratinization, *Symposium of the Zoological Society of London,* **39,** 335-342.

STARK, H.-J., BREITKREUTZ, D., LIMAT, A., BOWDEN, P.E. and FUSENIG, N.E. (1987) Keratins of the human hair follicle: "hyperproliferative" keratins consistently expressed in outer root sheath cells in vivo and in vitro, *Differentiation,* **35,** 236-248.

STEINERT, P.M. and ROGERS, G.E. (1973) Characterization of the proteins of guinea-pig hair and hair-follicle tissue, *Biochemical Journal*, **135**, (4), 759-771.

STEINERT, P.M. (1990) The two-chain coiled-coil molecule of native epidermal keratin intermediate filaments is a type I-type II heterodimer, *Journal of Biological Chemistry,* **265,** 8766-8774.

STEINERT, P.M. (1991) Organization of coiled-coil molecules in native mouse keratin1/keratin 10 intermediate filaments: evidence for alternating rows of antiparallel in-register and antiparallel staggered molecules, *Journal of Structural Biology*, **107**, (2), 157-174.

STEINERT, P.M., MAREKOV, L.N., FRASER, R.D.B. and PARRY, D.A.D. (1993) Keratin intermediate filament structure cross-linking studies yield quantitative information on molecular dimension and mechanism of assembly, *Journal of Molecular Biology,* **230,** 436-452.

STEINERT, P.M. and PARRY, D.A.D. (1993) The conserved H1 domain of the type II keratin 1 chain plays an essential role in the alignment of the nearest neighbour molecules in mouse and human keratin 1/keratin 10 intermediate filaments at the two- to four-molecule levels of structure, *The Journal of Biochemical Chemistry,* **268,** (4), 2878-2887.

STEINERT, P.M. and MAREKOV, L.N. (1995) The proteins elafin, filaggrin, keratin intermediate filaments, loricrin and small proline rich proteins 1 and 2 are isodipeptide cross-linked components of the human epidermal cornified cell envelope, *The Journal of Biological Chemistry,* **270,** (30), 17702-17711.

STEINERT, P.M. and MAREKOV, L.N. (1997) Direct evidence that involucrin is a major early isopeptide cross-linked component of the keratinocyte cornified cell envelope, *The Journal of Biochemical Chemistry,* **272,** (3), 2021-2030.

STEINERT, P.M. and MAREKOV, L.N. (1999) Initiation of assembly of the cell envelope barrier structure of stratified squamous epithelia, *Molecular Biology of the Cell,* **10,** 4247-4261.

STEINERT, P.M., PARRY, D.A. and MAREKOV, L.N. (2003) Trichohyalin mechanically strengthens the hair follicle: multiple cross-bridging roles in the inner root sheath, *Journal of Biological Chemistry*, **248**, (42), 41409-41419.

STENN, K.S. (1991) Induction of hair follicle growth, *Journal of Investigative Dermatology*, **96**, (5), 80S.

STENN, K.S., COMBATES, N.J., EILERTESEN, K.J., GORDON, J.S., PARDINAS, J.R., PARIMOO, S. and PROUTY, S.M. (1996) Hair follicle growth controls, *Dermatologic Clinics*, **14**, (4), 543-548.

STENN, K.S., PAUS, R. and FILIPPI, M. (1998) Failure of topical estrogen receptor agonists and antagonists to alter murine hair follicle cycling, *Journal of Investigative Dermatology*, **110**, (1), 95.

STENN, K.S., SUNDBERG, J.P. and SPERLING, L.C. (1999) Hair follicle biology, the sebaceous gland, and scarring alopecias, *Archives of Dermatology*, **135**, (8), 973-974.

STEVEN, A.C. and STEINERT, P.M. (1994) Protein Composition of Cornified Cell Envelopes of Epidermal Keratinocytes, *Journal of Cell Science,* **107**, 693-700.

STRELKOV, S.V., HERMANN, H., GEISLER, N., WEDIG, T., ZIMBELMANN, R., AEBI, U. and BURKHARD, P. (2002) Conserved segments 1A and 2B of the intermediate filament dimmer: their atomic structures and role in filament assembly, *The European Molecular Biology Organization Journal*, **21**, (6), 1255-1266.

STURMAN, N., SASSE, B. and FISHER, P.A. (1996) Intermediate filament protein polymerization: molecular analysis of drosophila nuclear lamin head-to-tail binding, *Journal of Structural Biology,* **117**, 1-15.

SUNDBERG, J.P., ERICKSON, A.A., ROOP, D.R. and BINDER, R.L. (1994) Ornithine decarboxylase expression in cutaneous papillomas in sencar mice is associated with altered expression of keratins 1 and 10, *Cancer Research*, **54**, (5), 1344-1351.

SUTER, M.M., CRAMERI, F.M., OLIVERY, T., MUELLER, E., VON TSCHARNER, C. and JENSEN, P.J. (1997) Keratinocyte biology and pathology, *Veterinary Dermatology,* **8**, 67-100.

SWENSSON, O., LANGBEIN, L., MCMILLAN, J.R., STEVENS, H.P., LEIGH, I.M., MCLEAN, W.H.I., LANE, E.B. and EADY, R.A. (1998) Specialized keratin expression pattern in human ridged skin as an adaptation to high physical assault, *British Journal of Dermatology,* **139,** (5), 767-775.

SWITONSKI, M., REIMANN, N., BOSMA, A.A., LONG, S., BARTNITZKE, S., PEINKOWSKA, A., MORENO-MILAN, M.M. and FISCHER, P. (1996) Report on the progress of standardization of the G-banded canine (canis familiaris) karyotype, *Chromosome Research,* **4,** 306-309.

TAYLOR, G., LEHRER, M.S., JENSEN, P.J., SUN, T.-T. and LAVKER, R.M. (2000) Involvement of follicular stem cells in forming not only the follicle but also the epidermis, *Cell,* **102,** 451-461.

TAKAHASHI, H., FOLMER, J. and COULOMBE, P.A. (1994) Increased expression of keratin 16 causes anomalies in cytoarchitecture and keratinization in transgenic mouse skin, *Journal of Cell Biology,* **127,** 505-520.

TAKAHASHI, K., PALADINI, R.D. and COULOMBE, P.A. (1995) Cloning and characterization of multiple human genes and cDNAs encoding highly related type II keratin 6 isoforms, *Journal of Biological Chemistry*, **270**, (31), 18581-18592.

THORNDIKE, E.E. (1968) A microscopic study of the marmoset claw and nail, *American Journal of Physical Anthropology,* **28,** 247-262.

TIMPL, R. (1996) Macromolecular organization of basement membranes, *Current Opinion in Cell Biology,* **8,** 618-624.

TORTORA, G. and GRABOWSKI, S. (2000) *Principles of anatomy and physiology, 9th edition,* New York, John Wiley.

TOWBIN, H., STAEHELIN, T. and GORDON, J. (1979) Electrophoretic transfer of proteins from polyacrylamide gels to nitrocellulose sheets: procedure and some applications, *Proceedings of the National Academy of Sciences of the United States of America*, **76**, (9), 4350-4354.

TYNER, A.L. and FUCHS, E. (1986) Evidence for posttranscriptional regulation of the keratins expressed during hyperproliferation and malignant transformation in human epidermis, *Journal of Cell Biology*, **103**, (5), 1945-1955.

VAN OMMEN, G.J. (2002) The Human Genome Project and the future of diagnostics, treatment and prevention, *Journal of Inheritance and Metabolic Diseases*, **25**, (3), 183-8.

VOS, J.H., VAN DEN INGH, T.S.G.A.M., MISDORP, W., RAMAEKERS, F.C.S., VAN MIL, F.N. and DE NEIJS, M. (1989) Keratin staining of canine epithelial tissues by a polyclonal antiserum, *Journal of Veterinary Medicine*, **36**, 374-385.

WANG, Z., WONG, P., LANGBEIN, L., SCHEWEIZER, J. and COULOMBE, P.A. (2003) Type II epithelial keratin 6hf (K6hf) is expressed in the companion layer, matrix, and medulla in anagen-stage hair follicles, *Journal of Investigative Dermatology*, **121**, (1276-1282).

WASEEM, A., ALEXANDER, C.M., STEEL, J.B. and LANE, E.B. (1990) Embryonic simple epithelia keratins 8 and 18 chromosomal location emphasizes difference from other keratin pairs, *The New Biologist*, **2**, (5), 464-478.

WATT, F.M. (1988a) The epidermal keratinocyte, *BioEssays*, **8**, (5), 163-167.

WATT, F.M. (1988a) Proliferation and terminal differentiation of human epidermal keratinocytes in culture, *Biochemical Society Transactions*, **16**, 666-668.

WATT, F.M. (1989) Terminal differentiation of epidermal keratinocytes, *Current Opinion in Cell Biology,* **1,** (6), 1107-1115.

WATTLE, O. (1998) Cytokeratins of the equine hoof wall, chestnut and skin: bio- and immunohisto-chemistry, *Equine Veterinary Journal,* **S26,** 66-80.

WATTLE, O. (2000) Cytokeratins of the stratum medium and stratum internum of the equine hoof wall in acute laminitis, *Acta Veterinaria Scandanavia,* **41,** 363-379.

WAWERSIK, M.J., MAZZALUPO, S., NGUYEN, D. and COULOMBE, P.A. (2001) Increased levels of keratin 16 alter epithelialisation potential of mouse skin keratinocytes in vivo and ex vivo, *Molecular Biology of the Cell,* **12,** 3439-3450.

WEISS, R.A., EICHNER, R. and SUN, T.T. (1984) Monoclonal antibody analysis of keratin expression in epidermal disease: a 48- and 56 kilodalton keratin as molecular markers for hyperproliferative keratinocytes, *Journal of Cell Biology,* **98,** 1397-1406.

WILKINSON, J.E., LEE, C.S., LILLIE, J.H., SUTER, M.M. and LEWIS, R.M. (1989) Ultrastructure of cultured canine oral keratinocytes, *American Journal of Veterinary Research,* **50,** (7), 1161-1165.

WINTER, H., LANGBEIN, L., PRAETZEL, S., JACOBS, M., ROGERS, M.A., LEIGH, I.M., TIDMAN, M.J. and SCHWEIZER, J. (1998) A novel human type II cytokeratin, K6hf, specifically expressed in the companion layer of the hair follicle, *Journal of Investigative Dermatology,* **111,** 955-962.

WOODCOCK-MITCHELL, J., EICHNER, R., NELSON, W.G. and SUN, T.T. (1982) Immunolocalization of keratin polypeptides in human epidermis using monoclonal antibodies, *The Journal of Cell Biology,* **95,** 580-587.

YOON, K.H., YOON, M., MOIR, R.D., KHUON, S., FLITNEY, F.W. and GOLDMAN, R.D. (2001) Insights into the dynamic properties of keratin

intermediate filaments in living epithelial cells, *The Journal of Cell Biology,* **153,** (3), 503-516.

ZAHN, H. (2002) Progress report on hair keratin research, *International Journal of Cosmetic Science,* **24,** 163-169.

ZOOK, E.G., VAN BEEK, A.L., RUSSELL, R.C. and BEATTY, M.C. (1980) Anatomy and physiology of the perionychium: a review of the literature and anatomic study, *Journal of Hand Surgery,* **5,** 528-536.